Distribution Agreement

In presenting this thesis or dissertation as a partial fulfillment of the requirements for an advanced degree from Emory University, I hereby grant to Emory University and its agents the non-exclusive license to archive, make accessible, and display my thesis or dissertation in whole or in part in all forms of media, now or hereafter known, including display on the world wide web. I understand that I may select some access restrictions as part of the online submission of this thesis or dissertation. I retain all ownership rights to the copyright of the thesis or dissertation. I also retain the right to use in future works (such as articles or books) all or part of this thesis or dissertation.

Signature:

Danielle Clarkson-Townsend

Date

Environmental Light and Circadian Disruption Impact Visual, Metabolic, and Developmental Programming

By Danielle Clarkson-Townsend
Doctor of Philosophy
Environmental Health Sciences

Carmen Marsit, PhD
Advisor

Machelle Pardue, PhD
Advisor

William Michael Caudle, PhD
Committee Member

Michael Iuvone, PhD
Committee Member

Melissa Smarr, PhD
Committee Member

Zhaohui Qin, PhD
Committee Member

Qiang Zhang, MD, PhD
Committee Member

Accepted:

Lisa A. Tedesco, Ph.D.
Dean of the James T. Laney School of Graduate Studies

Date

Environmental Light and Circadian Disruption Impact Visual, Metabolic, and Developmental Programming

By

Danielle Clarkson-Townsend
MPH, Emory University, 2016
BS, Tufts University, 2012

Advisor: Carmen Marsit, PhD
Advisor: Machelle Pardue, PhD

An abstract of
A dissertation submitted to the Faculty of the
James T. Laney School of Graduate Studies of Emory University
in partial fulfillment of the requirements for the degree of
Doctor of Philosophy
in Environmental Health Sciences
2021

Abstract

Environmental Light and Circadian Disruption Impact Visual, Metabolic, and Developmental Programming

By Danielle Clarkson-Townsend

Abstract

Circadian disruption, commonly caused by light exposure out of sync with the body's internal clock system, is a significant stressor affecting human health. This exposure is relevant not only for working adults, but also for infants, children, and adolescents. However, little is known about how circadian disruption at the earliest points of life, including during *in utero*, affects development across the life course. Using data from both a human cohort and a mouse model, this body of work investigated the influence of light and circadian disruption on developmental programming.

Utilizing both a differential expression analysis and cosinor analysis, we uncovered seasonal gene expression in full-term human placenta and characterized placental processes demonstrating season rhythmicity. To examine if shift work, which can lead to circadian disruption, was related to epigenetic variation in the placenta, we conducted an epigenome-wide association study (EWAS) of maternal night shift work and placental DNA methylation. The EWAS revealed differential methylation of genes related to immune system function and neurodevelopment in the placenta of night shift workers.

To examine the developmental impacts of environmental circadian disruption, we utilized a mouse model of developmental chronodisruption and measured placental signaling (embryonic day 15.5) as well as longitudinal visual and metabolic outcomes in adulthood. Embryo count, fetal sex ratio and placental weight did not differ, but developmental chronodisruption caused higher expression of immune markers CD11b and Iba1 and lower gene expression of *Serpinf1*, which encodes a protein that regulates macrophage inflammatory signaling and neuronal differentiation, in the placenta. Likewise, adult offspring developmentally exposed to chronodisruption developed impaired visual function and had increased retinal expression of immune markers.

These findings suggest that circadian disruption can contribute to developmental programming of adult disease, with the placenta as a potential regulator. Furthermore, our results suggest that developmental circadian disruption and light environment are relevant exposures for human health and should be integrated in more studies of environmental public health and Developmental Origins of Health and Disease (DOHaD) research. These results warrant further research to characterize the placental clock system and the mechanisms by which circadian disruption affects placental and fetal development.

Environmental Light and Circadian Disruption Impact Visual, Metabolic, and Developmental Programming

By

Danielle Clarkson-Townsend
MPH, Emory University, 2016
BS, Tufts University, 2012

Advisor: Carmen Marsit, PhD
Advisor: Machelle Pardue, PhD

A dissertation submitted to the
Faculty of the James T. Laney School of Graduate Studies of Emory University
in partial fulfillment of the requirements for the degree of
Doctor of Philosophy
in Environmental Health Sciences
2021

Acknowledgements

First and foremost, I would like to express my deep gratitude and appreciation for my two co-mentors and advisors, Dr. Carmen Marsit and Dr. Machelle Pardue. The political environment of the last four years and the pandemic have been particularly challenging, but your unflagging support, guidance, and kindness have made my PhD experience a happy and rewarding one. I have learned so much from both of you and will be forever grateful that you each took me under your wing. I hope to become as gifted at mentoring others as you.

I would like to sincerely thank my committee members, Dr. Caudle, Dr. Iuvone, Dr. Smarr, Dr. Qin, and Dr. Zhang, for their time, direction, and feedback. I have enjoyed getting to know you all and have had fun working with you.

I would also like to thank the teachers in my life, whose encouragement brought me here.

I want to thank Rollins students and the EHS program; they have been so instrumental in helping me grow as a scientist and public health researcher. Thank you to my friends and classmates, who inspire me every day with their commitment to equity and human health. When I first came to Emory as an MPH student, I felt like I had found my people; I have so much admiration for this community of passionate public health practitioners and count myself lucky to call you my colleagues. I particularly want to thank Molly, Fred, Vrinda, Jiawen, Tyiesha, Jianzhao, Brittney, Aimée, and all EHS students for their camaraderie and support.

Thank you to my lab friends and colleagues, who made science even more fun and who so generously helped me troubleshoot code and experiments; I couldn’t have done it without you. Thank you Amber, Karen, Liz, Fuying, Jesse, Derek, Aimée, Todd, Katie, Andrew, Rachael, Monica, Dillon, Reece, Pooja, Cara, Kyle, and Jenny.

I want to thank my family, especially my mother and father, who supported my naturalist interests from an early age and who have made so many sacrifices for me. I would also like to thank my brother for cheering me on, and my grandmother, who can always make me laugh.

Most importantly, I want to thank my partner, Trip, who, since meeting during my first week of class as a PhD student, has been by my side for this whole journey. Thank you for supporting me, laughing with me, cooking with me, exploring the outdoors with me, and reminding me to not ruin my back with my hunched posture when I’m coding. Time with you is such a gift and I’m so lucky to share it with you.

Table of Contents

Chapter 1: Introduction **1**

Telling time: the core circadian clock 2

Entrainment to zeitgebers 4

The eye as part of the visual system 4

Suprachiasmatic nucleus (SCN), the central clock 6

Night shift work as a “Probable Human Carcinogen” 8

Light as an endocrine disruptor 10

Rhythms and development 15

Figure 1-1 17

Developmental origins of health and disease (DOHaD) 17

Dissertation overview 19

Figure 1-2 20

Chapter 2: Seasonally Variant Gene Expression in Full-Term Human Placenta **23**

Abstract 24

Introduction 24

Materials and methods 26

Figure 2-1 28

Results 31

Table 2-1 32

Figure 2-2 34

Figure 2-3 35

Table 2-2 36

Figure 2-4 37

Figure 2-5 38

Discussion 39

Chapter 2 Supplemental Material 44

Chapter 3: Maternal Circadian Disruption is Associated with Variation in Placental DNA Methylation **51**

Abstract 52

Introduction 53

Materials and methods 54

Results 59

Table 3-1 60

Table 3-2 61

Figure 3-1 64

Table 3-3 65

Discussion 67

Chapter 3 Supplemental Material 71

Chapter 4: Impacts of High Fat Diet on Ocular Outcomes in Rodent Models of Visual Disease 76

Abstract 77

Introduction 78

Methods 80

Figure 4-1 81

HFD treatment 81

Systemic and metabolic effects of HFD 83

Table 4-1 83

HFD models of diet-induced obesity and diabetes 86

STZ with HFD models of Type 1 and Type 2 Diabetes and DR 87

Table 4-2 89

HFD and genetic models of AMD 90

Figure 4-2 91

Table 4-3 92

Effects of HFD on ocular tissues and possible mechanisms 95

Table 4-4 97

Figure 4-3 98

Table 4-5 100

Table 4-6 106

Table 4-7 108

Important considerations in experimental design 112

Summary of findings 115
Chapter 4 Supplemental Material 116

Chapter 5: Light Environment Influences Developmental Programming of the Metabolic and Visual Systems in Mice 118
Abstract 119
Introduction 119
Methods 121
Figure 5-1 122
Figure 5-2 124
Results 129
Figure 5-3 130
Figure 5-4 132
Figure 5-5 134
Figure 5-6 136
Figure 5-7 138
Figure 5-8 140
Discussion 142
Figure 5-9 143
Chapter 5 Supplemental Material 147

Chapter 6: Developmental Circadian Disruption Alters Placental Signaling in Mice 155
Abstract 156
Introduction 156
Materials and methods 158
Results and discussion 163
Figure 6-1 164
Figure 6-2 167
Figure 6-3 171
Chapter 6 Supplemental Material 172

Chapter 7: Summary and conclusions 176

Figure 7-1 181

References 182

Title: Environmental Light and Circadian Disruption Impact Visual, Metabolic, and Developmental Programming

Chapter 1: Introduction

Telling time: the core circadian clock

Light has served as an important stimulus over the course of evolution on Earth, signaling time of day. From sunrise to sunset, light wavelength and intensity changes. Likewise, in non-equatorial regions, the photoperiod, or ratio of daily light to dark exposure, changes seasonally. Organisms developed internal systems to be able to keep track of time by using light as a time cue. With the ability to track time came the binning of other activities, such as reproduction, metabolism, growth, and immune activity, around the 24-hour day/night cycle. These temporal rhythms, termed circadian rhythms if they occur in approximately 24-hour cycles (for “circa”=about, “diem”=day), are highly conserved across eukaryotic organisms and are even present in prokaryotic cyanobacteria(Dvornyk et al., 2003).

On a molecular level, circadian rhythms are endogenously produced via cycles of gene expression generated by oscillating transcription factors. Machinery for the core circadian clock exists in almost every cell in the body; in a simplified version of the genomic clock, core mammalian clock genes such as *CLOCK*, *ARNTL* (*BMAL1*), *PER*, and *CRY* heterodimerize and bind to E-boxes in target genes to regulate transcription of DNA(Buhr and Takahashi, 2013). The CLOCK:BMAL1 heterodimer binds to E-boxes for *PER* and *CRY*, initiating the transcription of *PER* and *CRY* mRNA, which is then shuttled out of the nucleus into the cytosol(Buhr and Takahashi, 2013). The mRNA can undergo post-transcriptional modifications, such as mRNA methylation (m^6A)(Fustin et al.). The *PER* and *CRY* mRNA is translated into PER and CRY proteins, which are transported back into the nucleus and bind to CLOCK:BMAL1 to inhibit further transcription of *PER* and *CRY*, thereby acting as negative autoregulators(Buhr and Takahashi, 2013). Other components such as kinases, phosphatases, and ubiquitin ligases interact with the clock to regulate stability and function by controlling degradation rate and movement.

PER and CRY undergo proteasomal degradation, lifting the inhibition of CLOCK:BMAL1 and allowing the cycle to begin again(Hirano et al., 2016). Thus, CLOCK:BMAL1 forms the positive arm of the feedback loop, while PER and CRY form the negative arm of the feedback loop. The time delay in the negative arm, caused by transport and post-translational mechanisms, is responsible for the oscillatory behavior of this genetic regulatory system(Ueda, 2007).

The circadian system is profoundly important for global gene expression, regulating it on an epigenetic level. In a feedback loop between chromatin structure and gene expression, components of the core circadian clock can both directly and indirectly affect chromatin structure and architecture, which also influences the expression of core clock genes and circadian expressed transcripts. For example, CLOCK itself is a histone acetyltransferase(Doi et al., 2006), altering chromatin accessibility by modifying histones, and CLOCK:BMAL1 alters chromatin accessibility by binding to nucleosomes and replacing histones with the H2A.Z variant to loosen DNA packaging(Menet et al., 2014). Rev-ErbA alpha can promote histone deacetylation and also prevent chromatin looping and transcription by binding to topologically associating domains(Kim et al., 2018). This affects the rhythmic expression of a large number of genes; for example, in a transcriptome analysis of non-human primates, an estimated 80% of all protein-coding genes displayed rhythmicity in expression(Mure et al., 2018), while an analysis of mouse tissue reported approximately 43% exhibiting 24-hour rhythms(Zhang et al., 2014). In this way, circadian patterns of both chromatin structure as well as transcription factor binding elicit rhythmic gene expression(Menet et al., 2014; Panda, 2016; Takahashi, 2016). However, further research is necessary to illuminate how chromatin structure changes over time (termed the ‘4D nucleome’)(Takahashi, 2016).

Entrainment to zeitgebers

These endogenous daily rhythms make up the internal circadian clock. However, the phase of the internal clock can be reset, called “entrainment”, to be in time with environmental *zeitgebers* (“time giver”), such as light; this system presumably evolved to allow organisms to anticipate and prepare for predictable environmental changes in temperature, food availability, etc., that occur coincidentally with changing light patterns, thereby making energy use more efficient. Light is not the only stimulus that can entrain the circadian system, but light is the most salient circadian cue(Duffy and Czeisler, 2009). In the eye, intrinsically-photosensitive retinal ganglion cells (ipRGCs) act as irradiance detectors and are responsible for non-image forming vision(Peirson and Foster, 2006); they relay light and photoperiod information to the brain(Schmidt et al., 2011) via the retinohypothalamic tract(Hattar et al., 2006). The SCN central clock(Berson et al., 2002) plays a central role in entrainment, receiving light-sensing information from the eyes and signaling peripheral “clocks” in other tissues.

The eye as part of the visual system

The eye is a sight organ, which in mammals is shaped like a cup(Lamb, 2013). The outer tissue layer of the eye, the sclera, is made of fibrous and elastic components and provides overall eye shape. While the sclera is opaque and white in color, the cornea is a continuation of the sclera that is transparent in nature; light is able to pass through the cornea due to the absence of blood vessels and the regular organization and thinner diameter of corneal tissue fibers. The cornea also provides the majority of the eye’s refractive power, due to the refraction of light passing from air to a water-based material(DelMonte and Kim, 2011). Light passes through the cornea into the anterior chamber and through the pupil, the hole of the eye framed by the iris and manipulated by pupillary muscles. Light then passes through the posterior chamber and the lens, which further refracts light before it passes into the vitreous chamber. The second layer of the eye is the choroid, whose blood supply provides a main source of gas exchange and nutrients for the high metabolic demands of the retina(Nickla and Wallman, 2010). A layer of pigmented tissue containing melanin, the retinal pigment epithelium, lies between the choroid and retina to absorb scattered light and provide light protection(Fuhrmann et al., 2014). Retinal tissue makes up the third layer of the eye. It is composed of multiple neural cell layers which are responsible for capturing and transmitting the light signal to the brain. The retina is organized "backwards", with incident light passing through the ganglion cell layer and inner retina before reaching the photoreceptive rods and cones(Lamb, 2013). Rods contain rhodopsin and are most active in dim light (able to respond to a single photon), although they can also function at bright light intensities(Tikidji-Hamburyan et al., 2017); cones, on the other hand, contain opsins which, in humans, can respond to short-wavelength (blue), medium-wavelength (green), or long-wavelength (red) light(Lamb, 2013). Rods and cones (first order neurons) have a "dark current", meaning they depolarize in response to darkness; they become hyperpolarized in response to light, triggering release of glutamate to cause depolarization of bipolar cells (second order neurons)(Molday and Moritz, 2015). Bipolar cells, located in the inner retina, transfer the light signal to retinal ganglion cells (RGCs, third order neurons), with possible modulation from horizontal and amacrine cells(Euler et al., 2014). Some RGC subtypes are also capable of detecting light due to their expression of melanopsin and function as irradiance detectors; these RGCs are called intrinsically photosensitive retinal ganglion cells (ipRGCs)(Do and Yau, 2010). These ipRGCs also play important roles in photoentrainment and the circadian system(Ospri et al., 2017).

Suprachiasmatic nucleus (SCN), the central clock

The SCN, located in the hypothalamus above the optic chiasm in the brain, is the central clock that communicates with “peripheral clocks” to entrain internal rhythms to the external environment. The SCN is composed primarily of two parts, the inner ventral “core” and the outer dorsal “shell”(Evans et al., 2015). RGCs project from the retina via the retinohypothalamic tract to synapse directly to neurons in the SCN core, which project to the SCN shell. At synapses with SCN neurons, these RGCs release pituitary adenylate cyclase-activating polypeptide (PACAP) and glutamate, triggering a calcium signaling cascade that activates *PER* genes via cAMP-response element binding protein (CREB)(Astiz et al., 2019; Welsh et al., 2010). This activation allows light exposure to entrain SCN core neurons, which communicate with the SCN shell via gastrin-releasing peptide (GRP) and vasoactive intestinal peptide (VIP). SCN shell neurons project to other regions of the brain and are mostly GABAergic, but also release vasopressin (AVP) and other molecules(Astiz et al., 2019; Patton and Hastings, 2018).

Neurons from the SCN shell synapse onto neurosecretory neurons in the hypothalamus, which signal to peripheral tissues, such as the liver, adipose tissue, the pancreas, and possibly the placenta, via hormones(Saper, 2013). The existence of a peripherally-circulating hormone secreted by the SCN that entrains peripheral oscillators is still debated(Silver et al., 1996); prokineticin-2 (PK2)(Cheng et al., 2002) may be a possible secreted factor. Through this hormonal signaling, peripheral tissues receive phase information from the SCN so that their endogenously generated rhythms are in sync with the external environment and with neighboring cells(Patton and Hastings, 2018).

Though the SCN primarily controls peripheral oscillators through the hypothalamus and hormones, the SCN also connects to the pineal gland, which secretes melatonin in the absence of light to promote sleep, and to the pituitary and paraventricular nucleus of the hypothalamus, which signals to the pituitary to secrete adrenocorticotrophic hormone (ACTH) to promote cortisol release from the adrenal glands(Dumbell et al., 2016). Glucocorticoids are a powerful entraining signal, with dexamethasone able to shift the circadian phase of peripheral tissue; glucocorticoid response elements (GREs) also regulate the expression of core clock genes(Mohawk et al., 2012). Temperature is also an important entraining signal for peripheral tissues(Buhr et al., 2010). The SCN sets the circadian phase of body temperature and is itself insensitive to cyclical temperature fluctuations. Lung, liver, kidney, and other tissues with peripheral oscillations are sensitive to temperature rhythms, possibly through heat shock factor proteins such as HSF1(Buhr et al., 2010; Mohawk et al., 2012).

While the SCN is the “central clock” of the physiological circadian system, many other tissues, such as the liver, gut, pancreas, muscle, and fat, also exhibit circadian rhythms; these “peripheral clocks” rely on cues from the SCN for entrainment(Mohawk et al., 2012). The influence of the central SCN clock on peripheral oscillators has mainly been tested in animals with SCN lesions, transplants, or genetic manipulation of core clock machinery. In rats, lesion of the SCN results in loss of circadian corticosterone rhythmicity in the adrenal glands(Moore and Eichler, 1972), locomotion, and eating and drinking behavior(Stephan and Zucker, 1972). Specific lesions of the SCN core, compared to the SCN shell, had the greatest impact on locomotion, body temperature, and behavior(Kriegsfeld et al., 2004; LeSauter and Silver, 1999). In hamsters made arrhythmic by SCN lesions, transplants of fetal SCN tissue containing circadian neuropeptides re-established locomotor circadian rhythms(Lehman et al., 1987);

however, grafts do not generally restore endocrine rhythms(Meyer-Bernstein et al., 1999). Without the ability to entrain to light, these arrhythmic animals are termed “free-running” because their internal clock is not tethered to external light cues(Aschoff, 1981). While ablation of the SCN prevents photoentrainment, entrainment to other cues, such as food, is still possible(Marchant and Mistlberger, 1997). Internal circadian rhythms can also become desynchronized in relation to the external environment, called circadian disruption. Circadian disruption can occur due to occupation, social behavior, and/or environment. For example, people who work non-day shifts, such as afternoon, evening, or night shifts, are expected to perform work duties during time periods that day workers are sleeping and/or are preparing to sleep. This misalignment between work schedule and light:dark schedule can lead to inflammation and chronic disease(Inokawa et al., 2020; Puttonen et al., 2011).

Night shift work as a “Probable Human Carcinogen”

Shift work, a form of occupational circadian disruption, captured the attention of the International Agency for Research on Cancer (IARC) as a potential carcinogen. IARC, established in 1965, is an organization within the World Health Organization (WHO) and the United Nations (UN) that works to prevent cancer, in part by identifying exposures that are carcinogenic to humans. The IARC Monographs program identifies exposures and evaluates the weight of the evidence as to its carcinogenicity in humans. During evaluation of an exposure, an international group of experts on the topic is called to participate as part of the scientific Working Group; this group consists of researchers with specialties in exposure science, epidemiology, toxicology, and animal model research. Together, they evaluate the quality and weight of the evidence and develop a report on: exposure characterization, evidence for cancer in humans, evidence for cancer in animals, and the mechanistic evidence. Towards the end of this process, they convene as a Working Group and openly discuss the evidence before coming to a consensus as a body. Based on the evidence, the Working Group may designate an exposure as “Not classifiable as to its carcinogenicity to humans (Group 3)”, “Possibly carcinogenic to humans (Group 2B)”, “Probably carcinogenic to humans (Group 2A)”, or “Carcinogenic to humans (Group 1)”.

IARC first evaluated the occupational exposure of shift work in 2007 during the IARC Monographs 98 meeting, titled “Painting, Firefighting, and Shiftwork”(IARC, 2010). Shift work is generally classified as work that takes place outside of the normal working hours of 7AM-6PM. The Working Group assessed the effects of shift work on breast cancer and prostate cancer and concluded that there was limited evidence for carcinogenicity in humans but sufficient evidence for carcinogenicity in experimental animals, which led to the overall evaluation that “shift work that involves circadian disruption is probably carcinogenic to humans (Group 2A)”(IARC, 2010), the second-highest classification. In 2019, shift work was again evaluated by IARC, but the exposure was explicitly confined to night shift work in the IARC Monographs 124 meeting, titled “Night Shift Work”(IARC, 2019). In addition to breast and prostate cancer, this meeting also included cancer of the colon and rectum in their evaluation. After 10 days of deliberation, the Working Group came to the consensus that the evidence for cancer in humans was limited, but there was sufficient evidence for cancer in experimental animals and strong mechanistic evidence in experimental systems; this led to the overall classification of night shift work as “Probably carcinogenic to humans (Group 2A)”(IARC, 2019). While the carcinogenicity classification did not change from the 2007 meeting to the 2019 meeting, an additional cancer was added to the evaluation.

The classification of night shift work as a “Probable” human carcinogen is notable, given the careful selection of agents of concern; of the 1,022 currently classified agents, only 121 are catalogued as Group 1; 89 agents belong to Group 2A, night shift work being one of them(IARC, 2021). With the increasing interest in circadian disruption and greater understanding of the role of the circadian system in metabolic and epigenetic regulation, it is possible that night shift work will be re-evaluated again in a future IARC meeting. In that time, new evidence may have come to light that causes night shift work to be reclassified as a higher (or lower) group.

Because night shift work (and, likewise, circadian disruption) is a relatively common occupational exposure, the classification of night shift work as a Group 1 agent would have enormous implications. For example, it would open the door for class action lawsuits and major litigation for people who were exposed to night shift work as well as major reforms to policy. Tighter regulation and limits to night shift work would also likely have economic implications.

Light is an endocrine disruptor

Environmental pollutants that alter hormonal signaling and/or the endocrine system, such as DDT, are known as endocrine disrupting chemicals (EDCs). The Risk Assessment Forum for the U.S. EPA defined an EDC as: "an exogenous agent that interferes with the synthesis, secretion, transport, binding, action, or elimination of natural hormones in the body that are responsible for the maintenance of homeostasis, reproduction, development and/or behavior"(Sayles, 2002). EDCs can elicit hormonal disruption through many different pathways, such as direct binding to nuclear hormone receptors or indirectly by altering steroid metabolism(Diamanti-Kandarakis et al., 2009). Light can also disrupt hormonal signaling(Russart and Nelson, 2018); many hormones are secreted at specific times of the day and are under control of the circadian clock. For example, secretion of cortisol, a key HPA-axis hormone with wide-ranging activities such as immune and metabolic regulation, peaks in the morning, whereas melatonin, termed the “hormone of darkness”, peaks in the evening. Bright light has been shown to suppress cortisol production(Jung et al., 2010) and light at night dampens the production of melatonin(Gooley et al., 2011). Therefore, based on the EDC definition and the known impacts of light exposure on hormonal signaling, light acts as an EDC.

Extensive research has found that circadian misalignment or shift work, a proxy for light exposure out of sync with the internal timekeeping system, can cause altered hormonal signaling, dyslipidemia, and metabolic disorders(Karlsson et al., 2001; Knutsson et al., 1986; Scheer et al., 2009; Tüchsen et al., 2006). This poses a substantial risk to public health, given that more than 15% of the U.S. work force works outside of the traditional hours of 6AM-6PM, with approximately 7% working the evening shift (2PM-12AM) and 3% working the night shift (9PM-8AM)(McMenamin, 2007). The shift distributions are roughly similar between men and women, with more than 9% of working women and more than 10% of working men employed in an evening or night shift position(McMenamin, 2007).

Night shift work and circadian disruption are strongly linked to development of metabolic disorders. The development and pathophysiology of type 2 diabetes (T2D) is intricately involved with circadian rhythms(Javeed and Matveyenko, 2018), and many studies have found associations with shift work and metabolic syndrome or diabetes(Lin et al., 2009; Pan et al., 2011; Suwazono et al., 2009). Research from the Nurses’ Health Study I and II, large prospective cohort studies of female nurses, found that women with a history of night shift work had a higher risk of developing T2D, with risks increasing as time spent working the night shift increased, suggesting a dose-response relationship(Pan et al., 2011). Interestingly, energy intake and sleep quantity did not account for the relationship between diabetes and night shift work in this study(Pan et al., 2011). Additionally, the researchers evaluated sleep quantity, but it did not account for the relationship between diabetes and night shift work(Pan et al., 2011). However, the relationship was partially mitigated after controlling for body mass index (BMI); increased BMI was also associated with increased time spent working the night shift(Pan et al., 2011). Other prospective studies have found that night shift is associated with increased BMI over time(Fujishiro et al., 2017; Morikawa et al., 2007), and when night shift workers switched to a day shift schedule, their BMI decreased(Morikawa et al., 2007; Zhao et al., 2012); therefore, BMI is likely part of the causal pathway between night shift work and diabetes. These findings provide strong evidence that circadian disruption leads to increased BMI, which suggests that light can act as an obesogen and endocrine disruptor.

However, there are a number of possible confounders that may influence associations between night shift work and metabolic problems, such as sleep. Workers with night shift schedules can take measures to try to adapt to their work schedule, such as using blackout shades and earplugs to sleep during the day and sticking to a consistent sleep schedule. However, getting adequate, quality sleep can be very difficult when working a non-day shift, and many shift workers are regularly sleep-deprived. Shift workers can also develop “shift work sleep disorder”, characterized by excessive sleepiness during work hours and insomnia when trying to fall asleep due to desynchronization of the internal circadian clock(Jehan et al., 2017). Other challenges may include frequently rotating shifts and/or conflicts between sleep schedule and social/family life. Circadian disruption is also a common exposure for pilots and flight attendants who travel across time zones and experience “jet lag”. Likewise, “social jet lag” occurs when one’s social commitments and behavior differs between work days and non-work days, where one may keep a consistent schedule on work days but stay up late and sleep in on days off. While night shift work is an extreme occupational exposure, social jet lag and sleep fragmentation may represent a more common cause of circadian disruption that affects more of the general public.

Experimental and observational studies of circadian disruption have found that circadian disruption is associated with decreased sleep quality and quantity(Bass and Takahashi, 2010; Scheer et al., 2009). Therefore, sleep may be an important confounder or effect modifier in studies of circadian disruption. There may also be an overlapping relationship between sleep fragmentation and circadian disruption, where fragmented sleep causes circadian disruption and vice versa(Arble et al., 2015). To evaluate the contributions of circadian disruption versus sleep deficit in insulin signaling, 26 healthy people were subjected to sleep restriction with or without circadian misalignment in an experimental study(Leproult et al., 2014). Participants were allowed to eat *ad libitum* and meals were provided at similar times across groups; caloric intake and weight gain did not significantly differ between groups, although people in the circadian misaligned group ate more at night(Leproult et al., 2014). Compared to baseline measurements, participants in the circadian misalignment group had significantly higher levels of high sensitivity C-reactive protein, a marker of inflammation(Leproult et al., 2014). Both groups had decreased insulin sensitivity, but those with circadian misalignment had much lower insulin sensitivity and significantly lower disposition index, a marker used to predict diabetes susceptibility where a higher number has a decreased risk for diabetes(Leproult et al., 2014). Thus, circadian disruption appears to cause metabolic dysfunction, independent of sleep.

Insulin signaling plays an important role in the pathophysiology of diabetes, where peripheral insulin resistance or dampened insulin release can lead to increased blood glucose levels. Circadian disruption may cause desynchrony in pancreatic beta cells, which exhibit a 24-

hour rhythm in activity(Perelis et al., 2015), dampening rhythmic insulin release(Rakshit et al., 2015) and leading to elevated blood sugar. In rats, *in utero* circadian disruption caused increased leptin levels, insulin secretion, fat deposition and decreased glucose tolerance of offspring(Varcoe et al., 2011). Mice with systemic knockout of core clock genes display pancreatic beta cell loss, dampened insulin signaling, buildup of fat pads, and insulin resistance of skeletal muscle(Harfmann et al., 2016), which are similar to the human T2D phenotype, and similar vasculopathies as in diabetic retinopathy(Bhatwadekar et al., 2013). Mutations in core clock genes are associated with an increased risk for diabetes(Marcheva et al., 2010; Woon et al., 2007) and pericytes, vascular cells affected by early DR, are sensitive to circadian disruption(Nakazato et al., 2017). It is noteworthy, given the roles of the circadian system in metabolism(Green et al., 2008), that the fat mass and obesity-associated protein (FTO) was recently discovered to be an m^6A demethylase(Jia et al., 2011), linking circadian rhythms with mRNA regulation and T2D. FTO variants are associated with 67% increased risk of BMI and obesity in 13 large human cohort studies, as well as T2D(Frayling et al., 2007). FTO is highly expressed in the hypothalamus and in regions involved in visual processing, such as the SCN and dorsal lateral geniculate nucleus(Fredriksson et al., 2008). Interestingly, bromocriptine, a dopamine D2 receptor agonist, is a treatment option for T2D. It is prescribed to be taken within 2 hours of waking up because it boosts dopamine levels in the hypothalamus, possibly acting on the SCN to reset the circadian system(DeFronzo, 2011). Therefore, just as circadian misalignment can cause T2D, circadian alignment may prevent or slow the progression of T2D and DR.

In addition to the epidemiological findings, the communication between the clock and the metabolic system provides a biological mechanism by which circadian disruption could cause increased BMI. Endocrine disruption is increasingly linked to obesity, and many of the targets of endocrine disrupting chemicals(Grün and Blumberg, 2009), such as the heterodimer of retinoid X receptors (RXR) and peroxisome proliferator activated receptors (PPARs)(Kawai and Rosen, 2010; Schug et al., 2011), are clock-controlled oscillating nuclear receptors. This raises the question of whether endocrine disrupting chemical interactions with these circadian receptors contributes to obesity by dysregulating the circadian system. Because light can cause systemic circadian and endocrine disruption(Bedrosian et al., 2016), light exposure out of sync with the biological clock may also be obesogenic.

Rhythms and development

Pregnancy is a unique circadian state; the development of one complete circadian system is taking place within another. As such, the placenta and fetus may act as a peripheral clock in the early stages of pregnancy, with the fetus developing its own endogenous rhythm as development progresses(Mark et al., 2017). Because the fetus has its own SCN and peripheral oscillators(Lunshof et al., 1997), the placenta may mediate maternal and fetal circadian signals.

The placenta is a transient organ that arises during pregnancy to provide nutrients, gas and waste exchange, immune regulation, and arbitrate signals between the maternal and fetal systems. Humans have a discoid, hemochorial placenta(Maltepe and Fisher, 2015). Placental tissue is derived from the trophectoderm and fetal in origin, establishing itself with cytotrophoblast invasion of the maternal uterine wall to remodel and widen uterine blood vessels to increase blood supply; placental villi branch out into this blood supply to increase surface area and support the metabolic demands of the growing fetus(Maltepe and Fisher, 2015). The placenta plays many roles in addition to nutrient supply to support a healthy pregnancy; for example, the placenta also transports and synthesizes hormones, including neuroendocrine hormones important for brain development and function like serotonin (5-HT), dopamine, VIP, and melatonin(Maltepe and Fisher, 2015; Reis et al., 2001). While the role of the placenta is to support fetal growth and health, it is responsive to maternal cues and can alter function based on environmental signals(Jansson and Powell, 2007).

Unfortunately, the placenta has not been a focus in circadian research. While rhythmic gene expression has been measured in tissues such as the liver, lung, intestines, brain, and fat after sequencing tissue collected at specific time intervals(Christou et al., 2019; Mure et al., 2018; Ruben et al., 2018), no such characterization of the placenta exists. Likewise, epidemiological and animal studies of circadian disruption evaluate a wide range of tissues, but the placenta is almost never included as a tissue of interest. However, it is likely that the placenta functions as a peripheral clock (**Figure 1-1**). It expresses clock genes such as *CLOCK*, *ARNTL* (*BMAL1*), *PER2*, and *CRY1*(Pérez et al., 2015). The placenta responds to circadian-relevant hormones such as glucocorticoids, but also produces and secretes its own hormones, such as melatonin, which could also act as entrainment signals for the fetus. The placenta also plays a vital role in mediating nutrient transfer between the mother and fetus; circadian genes can act as nutrient sensors and are sensitive to metabolic cues(Peek et al., 2012). Interestingly, a study using a luciferase reporter for *Per1* revealed a morphological delineation for *Per1* rhythms in the placenta; the decidua, but not the labyrinth, showed rhythmic *Per1* expression(Akiyama et al., 2010). The decidua is maternally-derived but the labyrinth, made up primarily of trophoblast cells, is fetally-derived, suggesting that maternally-derived tissue in the placenta conveys circadian information to fetal tissues. However, an *in vitro* study using an extravillous trophoblast cell line found rhythmic expression of *Per2*, *Dec1*, and *Dbp* before and after treatment with cobalt(II) chloride (which simulates hypoxia), suggesting that fetally-derived tissue can also exhibit rhythmicity in response to hypoxia(Frigato et al., 2009). Because circadian gene expression varies by tissue, it is also possible that there is diversity in circadian signaling between different zones within the placenta.

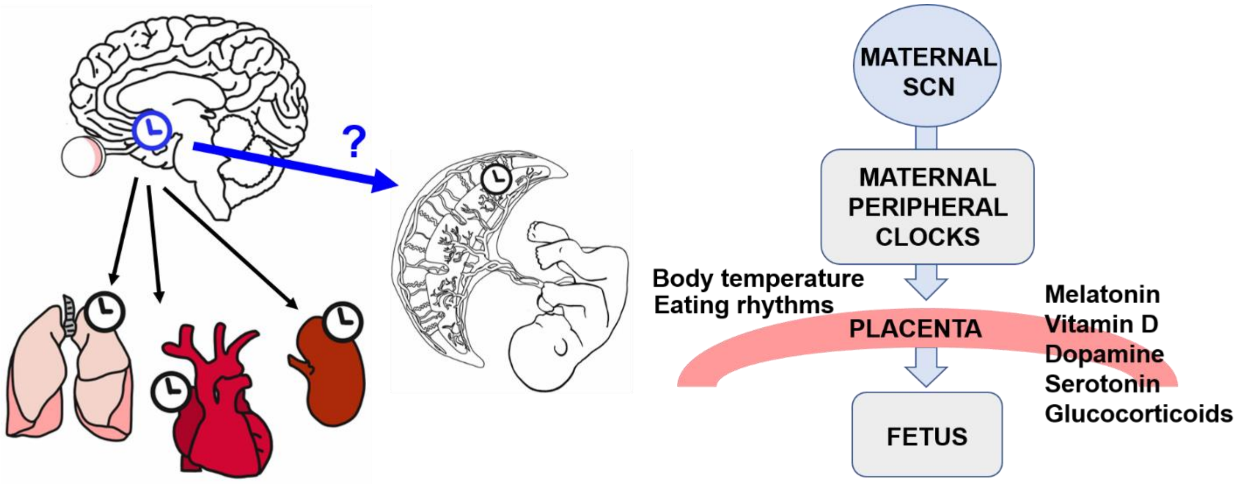
?
MATERNAL SCN
MATERNAL PERIPHERAL CLOCKS
Body temperature
Eating rhythms
PLACENTA
Melatonin
Vitamin D
Dopamine
Serotonin
Glucocorticoids
FETUS

Figure 1-1. *Diagram showing the suprachiasmatic nucleus (SCN) as the central clock communicating with peripheral clocks and the placenta as a possible peripheral clock. Circadian signals may be relayed to the placenta via signaling from the maternal SCN and/or peripheral clocks, maternal eating patterns, body temperature, and/or autonomic nervous signaling. The placenta transports and synthesizes a number of circadian-related hormones and neurotransmitters, such as melatonin and dopamine.*

Developmental origins of health and disease (DOHaD)

The beginning of the developmental origins of health and disease (DOHaD) hypothesis are credited to the 1986 study(Barker and Osmond, 1986) by Barker and Osmond. In this study, they observed that economically depressed areas of England and Wales had higher mortality rates due to cardiovascular disease than other, more prosperous, areas; this was surprising, because they expected rates of cardiovascular disease to be higher in wealthier communities where people were more able to afford indulgent, fatty foods. For each geographic region, they compared historical records of infant mortality and found a strong correlation between infant mortality in 1921-1925 and adult mortality due to ischemic heart disease in 1968-1978. They speculated that suboptimal early life diet conditions primed people to be more vulnerable to chronic disease development when exposed to a rich diet later in life(Barker and Osmond, 1986).

Because low birthweight was (and still is) a main cause of infant mortality, further studies evaluated the relationship between infant birthweight, a proxy for undernutrition *in utero*, and the development of cardiometabolic disease later in life. These studies found that infants born low birthweight or small for their gestational age (SGA) had an increased risk of heart disease and stroke as adults(Barker et al., 1993; Osmond et al., 1993; Rich-Edwards et al., 1997; Tian et al., 2017; Wang et al., 2020). Research of the Dutch Hunger Winter cohort, a cohort of people who were developmentally exposed to famine during WWII, further revealed epigenetic(Heijmans et al., 2008) and transgenerational(Painter et al., 2008) effects of undernutrition *in utero*. With time, DOHaD research grew from nutrition-related exposures to including early life stress and pollutants(Haugen et al., 2015). Likewise, in addition to cardiometabolic diseases, outcomes broadened to include conditions related to neurological and hormonal programming.

Developmental exposures relevant to DOHaD studies focus on pathways related to metabolism and endocrinology. The placenta, as mediator of the fetal and maternal environment, provides nutrients and gas exchange, as well as hormonal regulation, to the developing fetus. Serving as a conduit to the external environment, the placenta plays an important role in shaping fetal development in response to environmental cues. As part of developmental programming, plasticity during development can better prime the fetus for the conditions it is being born into;

however, if postnatal environment significantly differs from uterine conditions, a mismatch occurs between the programmed phenotype and the postnatal environment. Undernutrition *in utero* that programs a “thrifty” phenotype can be maladaptive when confronted with a calorically-dense environment, leading to greater risk of chronic metabolic disease. Likewise, exposures that influence the hormonal and epigenetic milieu during development, such as stressors and pollutants, can also cause maladaptive developmental programming(Almeida et al., 2019; Anway et al., 2005; Egusquiza and Blumberg, 2020; Van den Bergh et al., 2020).

Interestingly, there is much crosstalk between the circadian system and the systems found to be affected in DOHaD studies of developmental programming: metabolism, hormonal signaling, the hypothalamic-pituitary-adrenal (HPA) axis, and epigenetic mechanisms. However, environmental light and maternal chronodisruption have yet to be widely assessed in DOHaD studies.

Dissertation overview

In conclusion, light is an important environmental cue that acts on the circadian system to influence metabolism, hormonal signaling, and other physiologic processes. Light out of sync with the internal circadian system causes circadian disruption and altered hormonal signaling. As such, light can act as an EDC and should be more widely evaluated as an environmental exposure in public health research. The impacts of light and circadian disruption on developmental processes are not well understood, but prior epidemiological studies of shift workers warrant further investigation of these exposures. As light affects the circadian system and can act as an endocrine disruptor, the impacts of light and circadian disruption during pregnancy may affect developmental programming of the metabolic, immune, endocrine, and neurological systems (**Figure 1-2**).

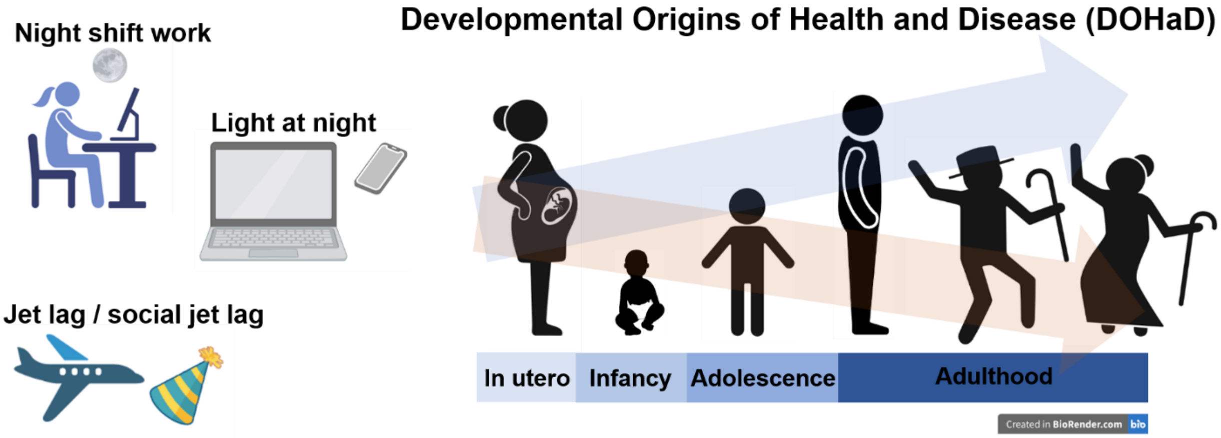
Night shift work
Light at night
Jet lag / social jet lag
Developmental Origins of Health and Disease (DOHaD)
In utero
Infancy
Adolescence
Adulthood
Created in BioRender.com bio

Figure 1-2. *Graphic showing a number of different exposures which can cause circadian disruption, including shift work, exposure to light at night, jet lag, and social jet lag. The modern light environment has changed dramatically over the last century, and may influence disease development. As light can act as an endocrine disruptor, exposure to environmental light during developmental windows may affect health and disease trajectory later in life. (made in ©BioRender - biorender.com)*

This dissertation investigates how environmental light and circadian disruption affect development within a human birth cohort study and a mouse model. The primary aims of this work are:

Aim 1: Investigate the influences of environmental light and circadian disruption on developmental programming by evaluating placental gene expression and methylation in the Rhode Island Child Health Study (RICHS). Hypothesis 1: Placental gene expression differs by season of birth, binned by photoperiod. Hypothesis 2: Maternal night shift work, an occupational proxy for circadian disruption, will be associated with altered placental methylation in an epigenome-wide association study (EWAS).

Aim 2: Test whether developmental circadian disruption affects developmental, visual, and metabolic outcomes in mice. Hypothesis 1: Developmental chronodisruption and later life challenge with HFD will alter visual and metabolic outcomes in adult offspring. Hypothesis 2: Developmental chronodisruption will cause altered placental gene expression and signaling in mice.

These aims are addressed in the following dissertation chapters, some of which have been previously published as stand-alone manuscripts. Chapter 2, previously published in the *FASEB Journal*(Clarkson-Townsend et al., 2020), addresses the first hypothesis of Aim 1 with an analysis of full-term placental gene expression across the seasons in humans. Chapter 3, previously published in *PLOS One*(Clarkson-Townsend et al., 2019), addresses the second hypothesis of Aim 1, with an epigenome-wide association study of maternal night shift work and placental methylation. Chapter 4, previously published in *Experimental Eye Research*(Clarkson-Townsend et al., 2021c), is a review of rodent models of visual disease that utilize a high fat diet (HFD); this chapter introduces many of the techniques and visual science background to provide context for Chapter 5. Chapter 5, previously published *in Investigative Ophthalmology and Visual Science(Clarkson-Townsend et al., 2021b)*, addresses the first hypothesis of Aim 2, with a mouse study of developmental circadian disruption and later life visual and metabolic disease; Chapter 6(Clarkson-Townsend et al., 2021a) addresses the second hypothesis of Aim 2, investigating placental signaling as a potential mediator of the retinal and visual results seen in adult offspring exposed to developmental chronodisruption. Chapter 7 summarizes the research conclusions and discusses future directions.

Chapter 2: Seasonally Variant Gene Expression in Full-Term Human Placenta

Published in a different format as:

Clarkson-Townsend DA, Kennedy E, Everson TM, Deyssenroth MA, Burt AA, Hao K, Chen J, Pardue MT, Marsit CJ. Seasonally variant gene expression in full-term human placenta. *FASEB J*. 2020 Aug;34(8):10431-10442. doi: 10.1096/fj.202000291R. Epub 2020 Jun 23. PMID: 32574425; PMCID: PMC7688493.

Abstract

Seasonal exposures influence human health and development. The placenta, as a mediator of the maternal and fetal systems and a regulator of development, is an ideal tissue to understand the biological pathways underlying relationships between season of birth and later life health outcomes. Here, we conducted a differential expression analysis of season of birth in full-term human placental tissue to evaluate whether the placenta may be influenced by seasonal cues. Of the analyzed transcripts, 583 displayed differential expression between summer and winter births (FDR $q<0.05$); among these, *BHLHE40*, *MIR210HG*, and *HILPDA* had increased expression among winter births (Bonferroni $p<0.05$). Enrichment analyses of the seasonally variant genes between summer and winter births indicated over-representation of transcription factors HIF1A, VDR, and CLOCK, among others, and of GO term pathways related to ribosomal activity and infection. Additionally, a cosinor analysis found rhythmic expression for approximately 11.9% of all 17,664 analyzed placental transcripts. These results suggest that the placenta responds to seasonal cues and add to the growing body of evidence that the placenta acts as a peripheral clock, which may provide a molecular explanation for the extensive associations between season of birth and health outcomes.

Introduction

Seasonal changes in weather(Rashid et al., 2016), pathogens(Lofgren et al., 2007), pollutants(Peng et al., 2005), nutrient contents(Watson and McDonald, 2007), and photoperiod(Stevenson et al., 2015) can influence human health. Associations between season of birth and health outcomes such as autoimmune disease(Disanto et al., 2012), myopia(Mandel et al., 2008), and even lifespan(Doblhammer and Vaupel, 2001), are well-documented(Boland et al., 2015), and developmental photoperiod is one of the proposed mechanisms behind these relationships(Walton et al., 2011). However, annual fluctuations in conception and birthrates can confound associations between season of birth and health outcomes(Currie and Schwandt, 2013; Fiddes et al., 2014). Furthermore, maternal sociodemographic variables, such as maternal education, marital status, and socioeconomic status, are also associated with season of birth(Currie and Schwandt, 2013; Darrow et al., 2009), which may drive some of the seasonal disparities in health outcomes. However, the associations between season of birth and health outcomes may not solely be driven by differences in maternal characteristics; a large study comparing multiple births within mothers (to control for maternal sociodemographic characteristics), found that birth outcomes still displayed a seasonal pattern(Currie and Schwandt, 2013), suggesting an underlying biological effect of environmental factors that vary with season. While photoperiod is almost certainly not the only driver of seasonal differences, the influence of environmental photoperiod on the biological clock may be a key factor in the relationship between seasonality and disease.

Light is a salient *zeitgeber* ("time giver") of the circadian clock, and annual changes (in non-equatorial regions) in photoperiod act as a reliable seasonal cue for the clock(Goldman, 2001; Tackenberg and McMahon, 2018). When light reaches the eye, the light signal is relayed to the suprachiasmatic nucleus of the brain, the central clock, which then entrains other tissues, or peripheral clocks, to the external environment. With the widespread use of indoor lighting, the majority of people in the U.S. are not reliant on outdoor light exposure for illumination; however, the amount of UV light exposure and blood levels of the hormone Vitamin D fluctuate with photoperiod(Klingberg et al., 2015), with a peak in the summer and trough in the winter. Melatonin production also fluctuates seasonally(Wehr, 1997), roughly opposite of Vitamin D with a peak in the winter and trough in the summer. In addition to rhythms in hormone production, rhythmic patterns of gene expression may also underlie season and health relationships(Dopico et al., 2015). Studies in humans and other animals have found seasonal patterns of gene expression in tissues such as blood(Dopico et al., 2015; Ludwig et al., 2019; Morey et al., 2016) and adipose tissue(Dopico et al., 2015; Klingenspor et al., 1996), although some of these differences may also reflect seasonal changes in cell populations(De Jong et al., 2014). These rhythms can vary by tissue type and share pathways with the core circadian clock system(Panda et al., 2002).

The placenta is an important intermediary between maternal photoperiod and fetal development; as a tissue with neuroendocrine properties, the placenta transports and synthesizes hormones related to light exposure, such as melatonin and the active form of vitamin D(Gray et al., 1979; Lanoix et al., 2008; Lanoix et al., 2012). Given these characteristics, we hypothesize that placental gene expression responds to seasonal cues such as photoperiod. To test this hypothesis, we investigated transcriptome-wide placental gene expression from full term (≥37 weeks) pregnancies delivered during different seasonal photoperiods.

Materials and Methods

Placental sequencing

The analysis utilized placental RNA sequencing (RNA-seq) data from the Rhode Island Child Health Study (RICHS) cohort, as previously described(Appleton et al., 2016; Clarkson-Townsend et al., 2019; Deyssenroth et al., 2017). RNA-seq was performed on a subset of placenta samples (n=200) from the RICHS cohort with the Illumina HiSeq 2500 platform to measure gene expression, as previously described(Deyssenroth et al., 2017). These data are available in dbGaP (phs001586.v1.p1). Briefly, FASTQ files were checked for quality and all reads had a phred score > 30. The reads were trimmed using “seqtk” with an error threshold of 0.01 and no minimum length filter. These trimmed FASTQ files were aligned to the human reference genome (Homo sapiens GRCh37.75.gtf version hg19) using STAR(Dobin et al., 2013) v2.4.0g1 with a 15bp minimum overhang and minimum mapped length for chimeric junctions. Counts were mapped from the BAM file using “subread”(Liao et al., 2013) v1.5.0-p1. Of this cohort, 1 sample was removed due to withdrawn consent and 2 samples removed due to mismatched sex, leaving a total of 197 placental samples included in this analysis.

Exposure characterization

Demographic and medical information were provided via structured interviews and standardized medical record abstraction by trained staff. Month of birth was used to characterize the season of birth into one of 4 photoperiod categories: SS (summer solstice), FE (fall equinox), WS (winter solstice), and SE (spring equinox); these categories were based on the midpoints between solstice and equinox dates and rounded to the nearest month to bin by light exposure, where SS included those born from the months of May through July, FE included those born from August through October, WS included those born from November through January, and SE included those born from February through April (**Figure 2-1**), similar to other studies(Day et al., 2015; Lockett et al., 2016). Placenta samples were collected from 2009-2013 during the daytime hospital hours of 8AM to 4PM. Possible confounders were evaluated, including: method of delivery (C-section vs. vaginal), maternal adversity, maternal pre-pregnancy smoking, infant gestational age, infant year of birth, sex of the infant, infant birthweight category, infant birthweight z-score, maternal BMI, maternal weight gain during pregnancy, maternal gestational diabetes, maternal night shift work, maternal age, maternal race, and hour of sample collection. One sample with missing data for the maternal pre-pregnancy smoking variable was recoded to “No”. A cumulative maternal adversity index variable(Clarkson-Townsend et al., 2019) was created to control for multiple maternal sociodemographic characteristics based on maternal education (high school or less = +1), maternal insurance (public, self-pay/ other, or none = +1), maternal support (single and no support = +1), household income adjusted for household size and based on the federal poverty level during the year of birth (below poverty level = +1), and household size (>6 people in same household = +1); this cumulative variable was split into 3 levels (+0, +1, or ≥+2), with higher score indicating greater adversity.

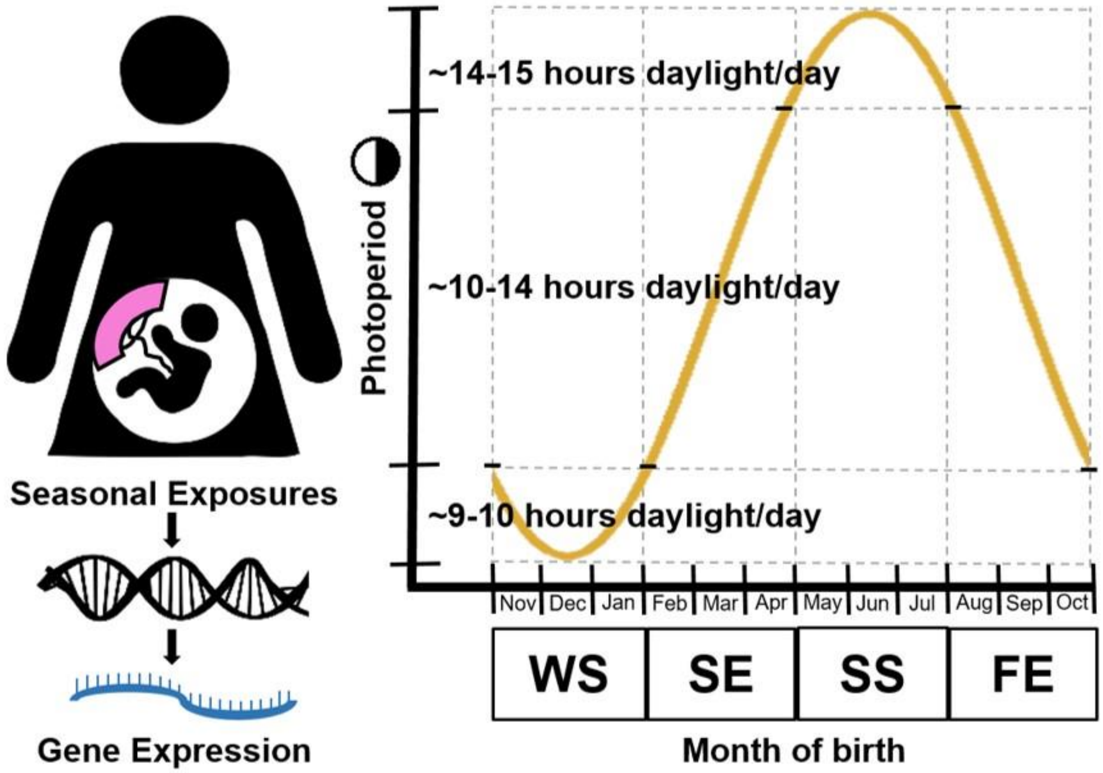
Seasonal Exposures
Gene Expression
Photoperiod
~14-15 hours daylight/day
~10-14 hours daylight/day
~9-10 hours daylight/day
Nov
Dec
Jan
Feb
Mar
Apr
May
Jun
Jul
Aug
Sep
Oct
WS
SE
SS
FE
Month of birth

Figure 2-1. *Illustration of overall study concept and categorization of seasonal exposure groups based on approximate annual photoperiod fluctuations around Providence, Rhode Island, USA (41.81° N, 71.41° W), where the RICHS study enrollment took place.*

Differential expression analysis

RNA-seq count data were read into R and differential expression (DE) analysis was performed using the *DESeq2* package(Love et al., 2014). Before analysis, low count data were filtered from the dataset using a threshold to exclude transcripts with <2 counts for 10% of samples. To control for unwanted heterogeneity due to other batch effects or unmodeled factors and to improve the reproducibility of the results, we also employed surrogate variable analysis(Leek and Storey, 2007) using the *sva* package in R(Leek et al., 2012). To estimate surrogate variables, counts were normalized and the surrogate variables were estimated with the Buja and Eyuboglu ("be") permutation method(Buja and Eyuboglu, 1992) using 200 iterations and then iteratively reweighted in svaseq(Leek, 2014). Normalized gene expression with seasonal photoperiod as the exposure was modeled using *DESeq2*, adjusting for maternal adversity and precision variables that included sex of the infant, method of delivery, gestational age, maternal pre-pregnancy smoking, infant's year of birth, sequencing batch, and the first two estimated surrogate variables. Overall effect of season (across all photoperiod categories) was first evaluated using the likelihood ratio test (LRT) method. Because the primary seasons of interest were those with the longest and shortest photoperiods, the Wald test method was used to compare WS and SS (reference group). However, for visualization of how expression changed across seasons, FE and SE were also compared to SS in subsequent sensitivity analyses. To control for multiple comparisons, we employed the Benjamini and Hochberg (BH) adjustment method(Benjamini and Hochberg, 1995) and the more conservative Bonferroni adjustment method.

Cosinor seasonal rhythmicity analyses

To evaluate whether placental gene expression displayed seasonal rhythmicity, we conducted a cosinor analysis of all placental transcripts that met the count threshold using the *cosinor* package in R(Sachs, 2014; Tong, 1976). A cosinor model was fit to the variance standardized transformation (VST) of gene expression for each transcript using methods laid out by Tong (1976)(Tong, 1976). Briefly, the cosinor function was applied to each transcript with the general formula:

$$Y_{(t)} = M + A\cos\left(\frac{2\pi t}{\tau} - ø\right) + \varepsilon_{(t)}$$

Where the outcome $Y_{(t)}$ is the variance-standardized (VST) gene expression for a gene transcript at time t (birth month), M is the intercept of the fitted curve, A is the amplitude of the curve, τ is the fixed period length (12 months), ø is the acrophase of the curve, and ε is an error term with mean 0. In this way, models with a time period (τ) of 12 were fitted to each transcript to test whether they displayed a significant amplitude and/or acrophase compared to baseline using the consinor.lm function of the *cosinor(Sachs, 2014)* package with the general code:

```
cos.model <- cosinor.lm(transcript ~ time(birth_month), period=12, data=df)
```

To test the fit of the cosinor model compared to the intercept, global F tests were performed and results controlled for multiple comparisons using the BH or Bonferroni method; amplitude or acrophase were considered significant if FDR q<0.05. This same model was also applied to previously generated eigengene values of placental gene network modules(Deyssenroth et al., 2017) to assess rhythmicity of co-regulated placental processes; amplitude or acrophase were considered significant if FDR q<0.05.

Bioinformatic analyses

To identify transcription factors and pathways over-represented amongst the SS and WS photoperiod, representing the longest and shortest photoperiods, DE genes (FDR $q<0.05$) were analyzed for functional enrichment against references gene lists within the ChEA 2016, KEGG 2019, and GO 2018 databases using enrichR(Kuleshov et al., 2016). Enrichment significance was computed using Fisher's exact test and considered significant if resulting FDR $q<0.05$. To identify gene expression correlated with genes of interest, Spearman correlation coefficients were calculated between all transcripts and the transcript of interest and considered significant if resulting Bonferroni-adjusted $p<0.05$.

Results

Of the 197 placental samples included in the analysis, 60 (30%) were delivered during the SS season, 57 (29%) during the FE season, 31 (16%) during the WS season, and 49 (25%) during the SE season (**Table 2-1, Figure 2-1**). Infant birthweight group, infant birthweight z-score, maternal BMI, maternal weight gain during pregnancy, maternal gestational diabetes, maternal night shift work, maternal age, maternal race, and hour of sample collection did not significantly differ by seasonal category (**Table 2-1**, **Supplemental Figure 2-1**). Maternal adversity significantly differed across seasonal categories ($p=0.01$) and was included in the final model. The final DE model adjusted for maternal adversity, sex of the infant, method of delivery, gestational age, maternal pre-pregnancy smoking, infant's year of birth, sequencing batch, and the first two estimated surrogate variables, with season of birth as the exposure of interest and normalized gene expression the outcome of interest (**Table 2-1**).

Table 2-1. *Demographic characteristics evaluated for inclusion in the final model testing differential expression. To evaluate statistical difference of variables across birth categories, 1-way ANOVA was used for continuous variables and chi-square or Fisher's exact tests were used for categorical variables.*

Variable	**Season of birth**				**p-val**
	SS (n=60)	**FE (n=57)**	**WS (n=31)**	**SE (n=49)**	
C-section, n (%)	21 (35.0)	11 (19.3)	9 (29.0)	16 (32.7)	0.264
Maternal adversity, n (%)					0.013
0	30 (50.0)	42 (73.7)	21 (67.7)	38 (77.6)	
1	15 (25.0)	5 (8.8)	7 (22.6)	8 (16.3)	
≥2	15 (25.0)	10 (17.5)	3 (9.7)	3 (6.1)	
Maternal pre-pregnancy smoking, n (%)	6 (10.0)	3 (5.3)	2 (6.5)	5 (10.2)	0.757
Gestational age					0.190
37-38 weeks	15 (25.0)	8 (14.0)	7 (22.6)	10 (20.4)	
39 weeks	34 (56.7)	33 (57.9)	18 (58.1)	20 (40.8)	
40-41 weeks	11 (18.3)	16 (28.1)	6 (19.4)	19 (38.8)	
Year of birth					0.055
2009-2010	34 (56.7)	27 (47.4)	12 (38.7)	13 (26.5)	
2011	13 (21.7)	16 (28.1)	9 (29.0)	14 (28.6)	
2012-2013	13 (21.7)	14 (24.6)	10 (32.3)	22 (44.9)	
Male infant, n (%)	27 (45.0)	30 (52.6)	14 (45.2)	25 (51.0)	0.815
Birthweight Group, n (%)					0.660
Small for gestational age	8 (13.3)	11 (19.3)	7 (22.6)	6 (12.2)	
Average for gestational age	33 (55.0)	30 (52.6)	19 (61.3)	29 (59.2)	
Large for gestational age	19 (31.7)	14 (28.6)	5 (16.1)	14 (28.6)	
Birthweight z-score, mean (SD)	0.24 (1.18)	0.32 (1.34)	-0.20 (1.16)	0.23 (1.24)	0.281
Maternal BMI, mean (SD)	26.67 (6.35)	27.58 (7.44)	24.14 (4.97)	25.89 (5.85)	0.104
Maternal Weight Gain (kg), mean (SD)	15.32 (5.58)	14.11 (6.08)	13.86 (6.61)	14.91 (6.30)	0.622
Maternal Gestational Diabetes (yes), n (%)	5 (8.3)	6 (10.5)	4 (14.3)	4 (8.3)	0.818
Maternal Night Shift Work (yes), n (%)	11 (21.2)	11 (20.8)	6 (20.7)	11 (23.9)	0.980
Maternal Age (yrs)					0.398
18-31	34 (56.7)	24 (42.1)	17 (54.8)	23 (46.9)	
32-40	26 (43.3)	33 (57.9)	14 (45.2)	26 (53.1)	

Maternal Race (white), n (%)	36 (64.3)	45 (81.8)	21 (70.0)	38 (77.6)	0.171
Hour Sample Collection, mean (SD)	11.51 (2.30)	12.35 (2.37)	12.45 (2.23)	11.51 (2.47)	0.083

After applying a threshold to filter out genes with counts <2 for 10% of samples, the number of transcripts modeled in the analysis decreased from the original set of 50,810 transcripts to a filtered set of 17,664 transcripts. In the resulting overall likelihood ratio test analysis of DE across all seasonal categories, 819 transcripts were considered significant after adjusting for multiple comparisons (FDR q<0.05, **Supplemental Table 2-1**), suggesting an overall effect of season. To measure expression differences between the specific seasonal categories of interest, the Wald test comparing the SS and WS groups found DE of 583 transcripts (FDR q<0.05), of which 574 were annotated to genes (**Figure 2-2**, **Supplemental Table 2-2**). Compared to SS, 347 transcripts had increased expression and 236 had decreased expression in WS. While not the primary aim of the study, DE results of the FE and SE seasonal groups compared to SS are also provided (**Supplemental Table 2-2**, **Supplemental Figure 2-2**), as are the effect estimates from the maternal adversity variable (**Supplemental Table 2-3**). As expected, those genes demonstrating associations with adversity did not overlap with seasonal genes.

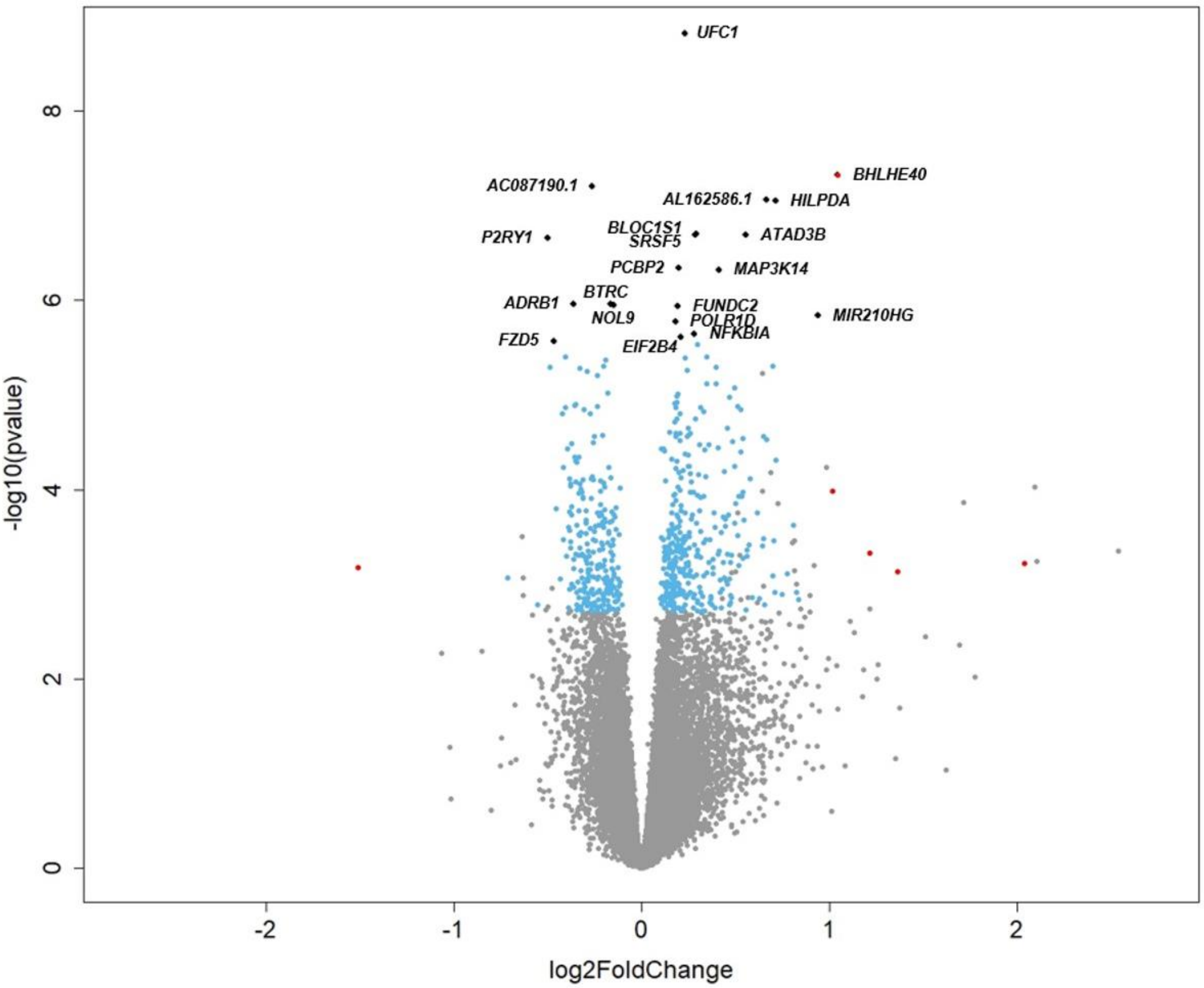

Figure 2-2. *Volcano plot of results from the differential expression analysis of placental gene expression by birth season showing Wald test results comparing winter (WS) to the summer (SS) reference group. Transcripts are plotted by effect size estimate [*Log_2*(Fold Change), x-axis] and statistical significance [-*Log_{10}*(Pvalue), y-axis], with grey dots indicating non-significant FDR q≥0.05, blue dots indicating FDR q<0.05, black dots indicating Bonferroni p<0.05, and red dots indicating absolute* log_2*(fold change)>1 and FDR q<0.05. Labels indicate Bonferroni-significant (p<0.05) genes.*

The cosinor analysis to measure gene expression seasonal rhythmicity by birth month found that of the 17,664 transcripts, 2,109 (11.9%) had significant seasonal amplitude and/or acrophase (FDR q<0.05) (**Figure 2-3**, **Supplemental Table 2-4**). When the more conservative Bonferroni adjustment (p<0.05) was applied to the DE results, 15 genes were found to be significant in both the DE and cosinor analysis: *UFC1*, *BHLHE40*, *HILPDA*, *ATAD3B*, *BLOC1S1*, *P2RY1*, *ADRB1*, *BTRC*, *FUNDC2*, *NOL9*, *MIR210HG*, *POLR1D*, *NFKBIA*, *EIF2B4*, and *FZD5* (**Table 2-2, Figure 2-4**); an additional transcript, ENSG00000260708, was found to be significant in both analyses. Of the placental gene networks previously generated from a weighted gene coexpression network analysis(Deyssenroth et al., 2017), 9 of the modules were seasonally rhythmic when analyzed in the cosinor model (FDR q<0.05, **Figure 2-5**, **Supplemental Table 2-4**).

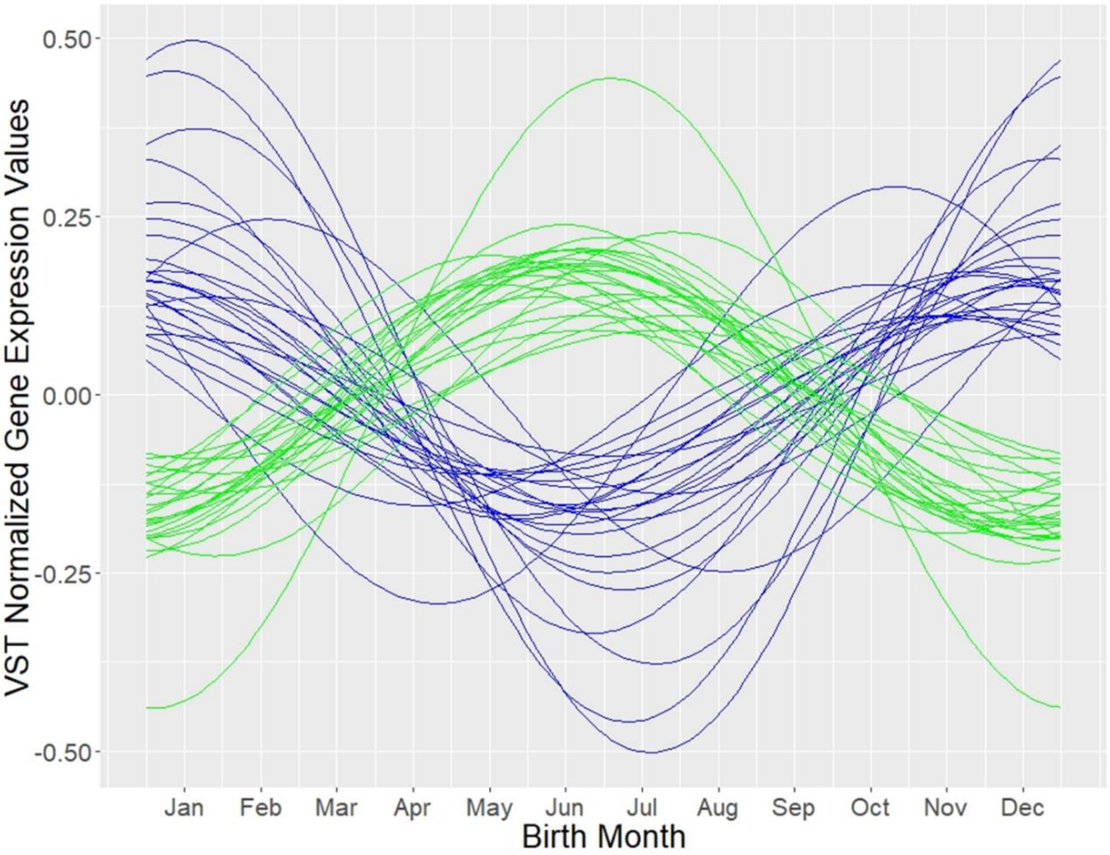

Figure 2-3. *Graph showing the fitted curves of variance standardized expression (normalized to baseline) of the top 25 upregulated and top 25 downregulated genes (FDR q<0.05) in the DE*

analysis comparing winter (WS) births to summer (SS) births when analyzed in the cosinor analysis. The green curves represent transcripts with peak expression in summer and the blue curves represent transcripts with peak expression in winter.

Table 2-2. *List of Bonferroni-significant ($p<0.05$) genes differentially expressed in SS vs WS placenta that also displayed seasonal rhythmicity in the cosinor analysis (FDR $q<0.05$).*

Ensemble ID	**Gene ID**	**Gene description**
ENSG00000143222	*UFC1*	ubiquitin-fold modifier conjugating enzyme 1 [Source:HGNC Symbol;Acc:HGNC:26941]
ENSG00000134107	*BHLHE40*	basic helix-loop-helix family member e40 [Source:HGNC Symbol;Acc:HGNC:1046]
ENSG00000135245	*HILPDA*	hypoxia inducible lipid droplet associated [Source:HGNC Symbol;Acc:HGNC:28859]
ENSG00000160072	*ATAD3B*	ATPase family AAA domain containing 3B [Source:HGNC Symbol;Acc:HGNC:24007]
ENSG00000135441	*BLOC1S1*	biogenesis of lysosomal organelles complex 1 subunit 1 [Source:HGNC Symbol;Acc:HGNC:4200]
ENSG00000169860	*P2RY1*	purinergic receptor P2Y1 [Source:HGNC Symbol;Acc:HGNC:8539]
ENSG00000043591	*ADRB1*	adrenoceptor beta 1 [Source:HGNC Symbol;Acc:HGNC:285]
ENSG00000166167	*BTRC*	beta-transducin repeat containing E3 ubiquitin protein ligase [Source:HGNC Symbol;Acc:HGNC:1144]
ENSG00000165775	*FUNDC2*	FUN14 domain containing 2 [Source:HGNC Symbol;Acc:HGNC:24925]
ENSG00000162408	*NOL9*	nucleolar protein 9 [Source:HGNC Symbol;Acc:HGNC:26265]
ENSG00000247095	*MIR210HG*	MIR210 host gene [Source:HGNC Symbol;Acc:HGNC:39524]
ENSG00000186184	*POLR1D*	RNA polymerase I and III subunit D [Source:HGNC Symbol;Acc:HGNC:20422]
ENSG00000100906	*NFKBIA*	NFKB inhibitor alpha [Source:HGNC Symbol;Acc:HGNC:7797]
ENSG00000115211	*EIF2B4*	eukaryotic translation initiation factor 2B subunit delta [Source:HGNC Symbol;Acc:HGNC:3260]
ENSG00000163251	*FZD5*	frizzled class receptor 5 [Source:HGNC Symbol;Acc:HGNC:4043]

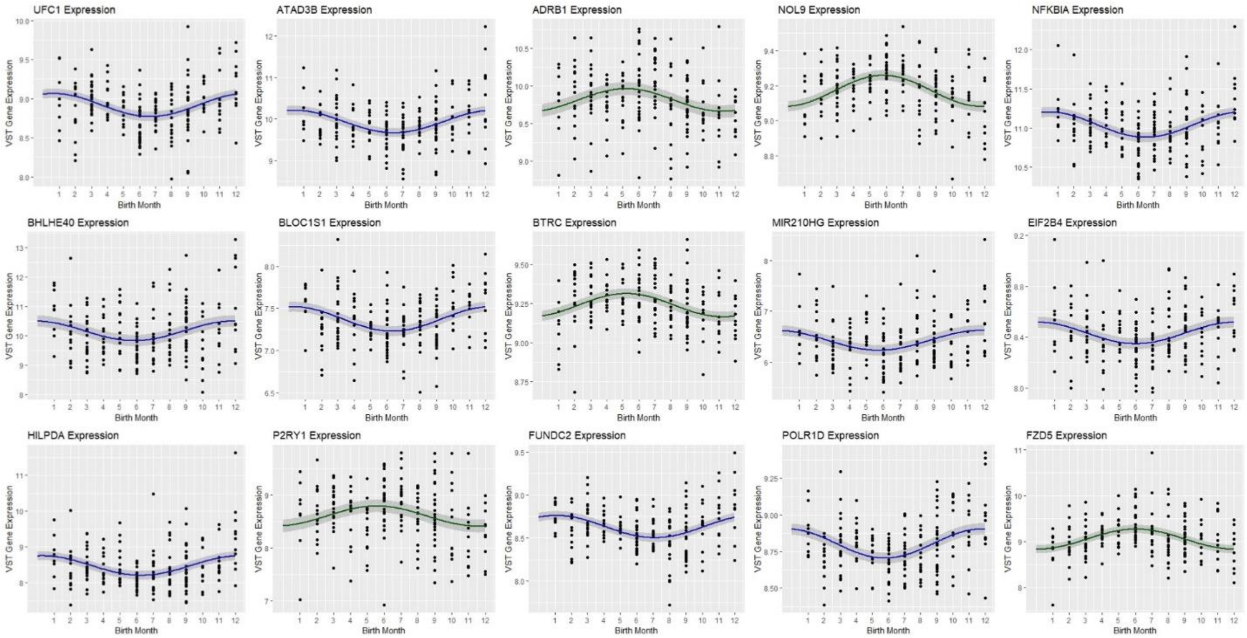

Figure 2-4. *Panel graphs from the genes listed in Table 2 that were significant in the DE (Bon p<0.05) and cosinor (FDR q<0.05) analyses. Each plot shows the variance standardized expression value of a gene (black dots) by birth month with the fitted curve from the cosinor model overlaid; green curves represent genes with peak expression in summer and the blue curves represent genes with peak expression in winter. Blue or green shaded areas around the fitted curve indicate 95% confidence intervals from the cosinor model.*

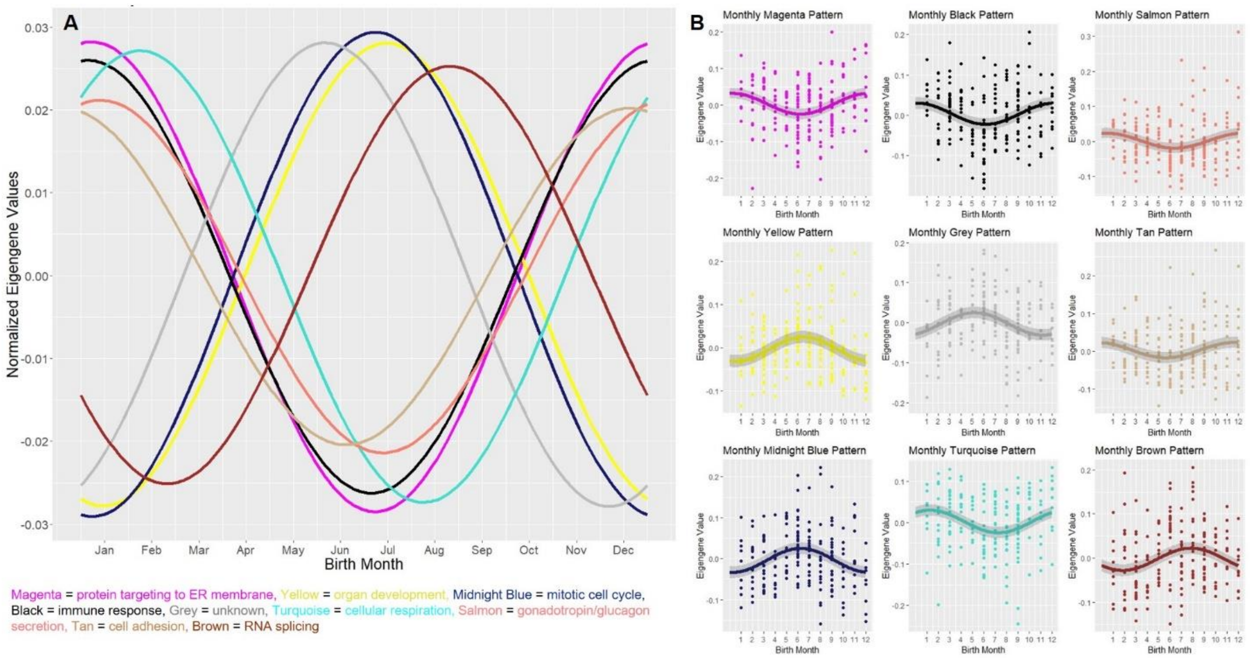

Figure 2-5. *Panel graphs from the cosinor analysis of previously identified placenta gene networks. (A) Graph showing the fitted curves of the normalized eigengene values from the placental gene network modules by birth month that were significantly rhythmic in the cosinor analysis (FDR q<0.05). These modules were previously identified as relating to protein targeting to the ER membrane (magenta), organ development (yellow), mitotic cell cycle (midnight blue), immune response (black), cellular respiration (turquoise), gonadotropin/glucagon secretion (salmon), cell adhesion (tan), and RNA splicing (brown). (B) Panel graphs of the individual network modules with eigengene values and fitted curves with shaded areas to indicate 95% confidence interval from the cosinor analysis.*

Examining the over-representation of transcription factor binding sites amongst the genes demonstrating DE between SS and WS (FDR q<0.05) using the ChEA database highlighted the transcription factors HIF1A, VDR, ELK1, TAL1, ELK3, FOXP1, CLOCK, NUCKS1, DMRT1, SPI1, DCP1A, ZNF217, and XRN2 to be over-represented (FDR q<0.05, **Supplemental Table 2-5**). These DE genes were also over-represented by the KEGG ribosome pathway and GO molecular and biological terms related to ribosomes, RNA processing, viral infection, and protein signaling to the endoplasmic reticulum (FDR q<0.05, **Supplemental Table 2-5**). To identify possible co-regulated genes that may be implicated in circadian regulation of the placenta, correlation analysis revealed 359 transcripts that correlated with *BHLHE40* expression and 2,498 transcripts that correlated with *CLOCK* expression (Bon p<0.05, **Supplemental Table 2-6**).

Discussion

The placenta, a transient organ that develops during pregnancy, plays a vital role in fetal health and development. Positioned at the boundaries of the developed maternal circadian system and the developing fetal circadian system, the placenta likely acts as a peripheral oscillator of the physiological circadian clock system, relaying maternal photic and other cues to the fetus. Our results found placental gene expression associated with seasons of birth, suggesting that the placenta may respond to seasonal cues such as photoperiod. While more studies are necessary, these findings provide support that seasonality of birth has underlying biological characteristics in humans that are separate from maternal demographic characteristics. This study adds to the growing body of evidence that the placenta acts as a peripheral clock(Mark et al., 2017).

Core clock genes such as *PER1*, *PER2*, *ARNTL*, *CLOCK*, *CRY1*, and *CRY2* are expressed in the placenta, but only *CLOCK* and *ARNTL* have so far been found to show rhythmic expression in full-term human placenta(Waddell et al., 2012). While *CLOCK* mRNA expression was not found to be seasonally rhythmic in our analyses, CLOCK was identified in our enrichment analysis. Our results raise the possibility that the clock gene *BHLHE40* (also known as *DEC1*), which encodes a basic helix-loop-helix transcription factor that can bind to E-boxes, also exhibits seasonal rhythmicity in the placenta, as it was one of the top hits in the DE and cosinor analyses. BHLHE40 influences other circadian-related transcription factors such as ARNTL through protein-protein binding or by competing for E-box binding sites(Honma et al., 2002; Kato et al., 2014). ARNTL oscillation in the SCN may encode seasonal photoperiod(Myung et al., 2012), and (in the northern hemisphere) a study found seasonal *ARNTL* expression displaying a trough around January and a peak around July(Dopico et al., 2015); in line with these findings, our analysis found the expression of *BHLHE40* expression peaked around December-January (**Figure 2-4**). Additionally, a SNP in *BHLHE40* was found to be associated with placental abruption in full-term human placenta(Qiu et al., 2016) and an *in vitro* experiment using a trophoblast cell line found rhythmic *BHLHE40* expression that was enhanced during hypoxic stress(Frigato et al., 2009). Many of the genes highly correlated with *BHLHE40* expression are relevant to hypoxic response, such as *C8orf58*(Rytkonen et al., 2020), *NDRG1(Cangul, 2004)*, *ERRFI1* (also known as *MIG-6*)(Zhang and Vande Woude, 2007), and *ANKRD37*(Benita et al., 2009), while some of the genes most highly correlated with CLOCK were related to RNA processing, such as *CNOT6L(Horvat et al., 2018)* and *DICER1*(Song and Rossi, 2017)(**Supplemental Table 2-6**). These results support our findings of *BHLHE40* seasonal rhythmicity in the placenta and a possible role for this circadian clock gene in the placental hypoxia response. Future research in understanding, more completely, the mechanisms underlying placental rhythmicity could build from these observations.

In addition to *BHLHE40*, genes such as *UFC1*, *HILPDA*, *P2RY1*, *ADRB1*, *BTRC*, *MIR210HG*, *POLR1D*, *NFKBIA*, and *FZD5* appear to be seasonally rhythmic in the placenta ($p<0.05$) (**Table 2-2**, **Figure 2-4**). The representation of *BTRC* and *NFKBIA* is possibly due to seasonal inflammation, infection, and/or hypoxia (Lawrence, 2009). BTRC is an F-box protein that ubiquitinates NFKBIA for degradation, which disinhibits the NF-κB complex. In accordance, our results show inverse patterns of *BTRC* and *NFKBIA* expression, with *BTRC* peaking in the summer months and *NKBIA* peaking in the winter months. The representation of *MIR210HG* and *HILPDA* peaking in the winter months could also be due to seasonal hypoxia; HILPDA is involved in the hypoxia response(Kim et al., 2013) and *MIR210HG* is a long non-coding RNA precursor to miRNA-210 that is also activated during hypoxia(Voellenkle et al., 2016). *POLR1D*, an RNA polymerase 1 and RNA polymerase 3 subunit that affects ribosomal synthesis and transcription(Noack Watt et al., 2016), also had peak expression during the winter months. *P2RY1* and *ADRB1* both had peak expression during the summer months and function as G-protein coupled receptors; ADRB1 may play an important role in sleep behavior, with a mutation in *ADRB1* found to decrease self-reported sleep need(Shi et al., 2019).

The results from the cosinor analysis of gene expression by birth month supported the findings of the seasonal DE analysis. When results (FDR q<0.05) from the SS vs WS DE analysis and the cosinor analysis were compared, 316 transcripts were represented in both analyses (**Supplemental Table 2-7**). The analysis of the overall 17,664 placental transcripts found seasonal rhythms for 11.9% of them, suggesting widespread seasonal rhythmicity in placental gene expression (**Supplemental Table 2-4**). Interestingly, many of the placental gene modules, derived from prior work(Deyssenroth et al., 2017) independent of exposure, exhibited significant amplitude or acrophase (FDR q<0.05, **Figure 2-5**, **Supplemental Table 2-4**), suggesting seasonal rhythmicity in placental processes. Notably, networks related to protein targeting to the ER membrane, immune response, cellular respiration, gonadotropin/glucagon secretion, and cell adhesion peaked around December-February, while networks related to the mitotic cell cycle, organ development, and RNA splicing peaked around June-August (FDR q<0.05, **Figure 2-5**, **Supplemental Table 2-4**). Other analyses of seasonal and circadian gene expression have reported approximately 23%-43% of transcripts to be seasonally rhythmic(Dopico et al., 2015; Takahashi, 2016; Zhang et al., 2014), with transcript rhythmicity differing by tissue. There are no other studies of transcriptome-wide human placental seasonal rhythmicity, so more research is necessary to confirm genes with seasonal variation in the placenta.

Enrichment analyses indicated that the transcription factors HIF1A, VDR, ELK1, TAL1, ELK3, FOXP1, CLOCK, NUCKS1, DMRT1, SPI1, DCP1A, ZNF217, and XRN2 were over-represented amongst those genes that are DE between summer (SS) and winter (WS) births (**Supplemental Table 2-5**). Among these, HIF1A, TAL1, and CLOCK are members of the basic helix-loop-helix family of transcription factors and are associated with circadian rhythm regulation. HIF1A can also heterodimerize with ARNTL (also known as BMAL1) and disruption of ARNTL can induce HIF1A activity(Peek et al., 2017). During the early stages of placental development when conditions are hypoxic, HIF1A levels increase to promote trophoblast invasion; during later stages of pregnancy (>10-18 weeks), HIF1A levels decrease and stabilize(Ietta et al., 2006). However, our analysis of full-term (≥37 weeks) placenta found over-representation of HIF1A binding sites associated with photoperiod (SS vs WS), suggesting environmental exposures may influence seasonal patterns in placental hypoxic signaling.

We also identified over-representation of binding sites for VDR, the vitamin D-receptor, lending credence to our results. As outdoor UV light exposure is highest during the summer months (SS) and lowest during the winter months (WS)(Christakos et al., 2016), seasonal differences in genes controlled by this transcription factor are expected. Seasonal decreases in maternal UV light exposure could lead to decreased placental synthesis and transport of active vitamin D, altering VDR activity. VDR also heterodimerizes with RXR, another interactive component of the circadian clock, to bind vitamin D response elements in the genome and induce widespread gene expression.

The KEGG term and many of the GO terms associated with season of birth were related to ribosomes. Because ribosomes are responsible for translating mRNA into proteins, ribosomal abundance can affect rates of cell growth or transcriptional activity. The increased expression of ribosomal genes in winter births suggest that there may be seasonal differences in transcription rates. The GO term results of infection-related pathways possibly reflect the increased exposure to viral pathogens and infections during the winter months or a seasonally programmed ability to respond to infection. The cosinor analysis of placental modules supported and expanded upon these results, displaying a winter peak for immune response and a summer peak for RNA splicing. While these results need to be validated in other cohorts, seasonal rhythms in human development have long been postulated in the scientific literature, and these findings provide possible genetic and molecular pathways that underpin these processes.

There are some limitations to the study and results should be interpreted cautiously. Because temperature and photoperiod are tightly linked, some of our results may be due to temperature (or other seasonally fluctuating exposures) rather than being exclusively driven by photoperiod. The changes in gene expression are possibly due, at least in part, to seasonal changes in underlying placental cell populations. Additionally, while we utilized surrogate variable analysis to control for unknown heterogeneity in samples, there may be false positives and residual confounding from unmodeled factors. While conception rates fluctuate seasonally, this effect may not have a large influence on the results as all samples were from full-term (≥37 weeks), singleton pregnancies free from congenital abnormalities, infant birthweight z-scores did not significantly differ by season, and the model adjusted for maternal sociodemographic characteristics. Strengths of this study include the use of full-term human placenta and the use of cosinor analyses to further confirm and characterize transcript and module rhythmicity by birth month. More research is necessary to elucidate the role of the placenta in circadian signal arbitration between the maternal and developing fetal systems, and we plan to conduct targeted analyses of the placental circadian system in future analyses.

In conclusion, we report seasonal variation in gene expression of human placental tissue from full-term (≥37 weeks) pregnancies. These seasonal variations were associated with the core circadian clock system, which may have implications for human health and provide further evidence for the placenta as a peripheral oscillator. Results also suggested seasonal changes in placental inflammation and hypoxia. The circadian system regulates many biological processes, and seasonal effects on the clock may alter placental function and fetal development. Further study of seasonal and circadian effects on the placenta could shed light on the pathways that influence the associations between season of birth and human health, as well as possible therapeutic targets.

Supplemental Material

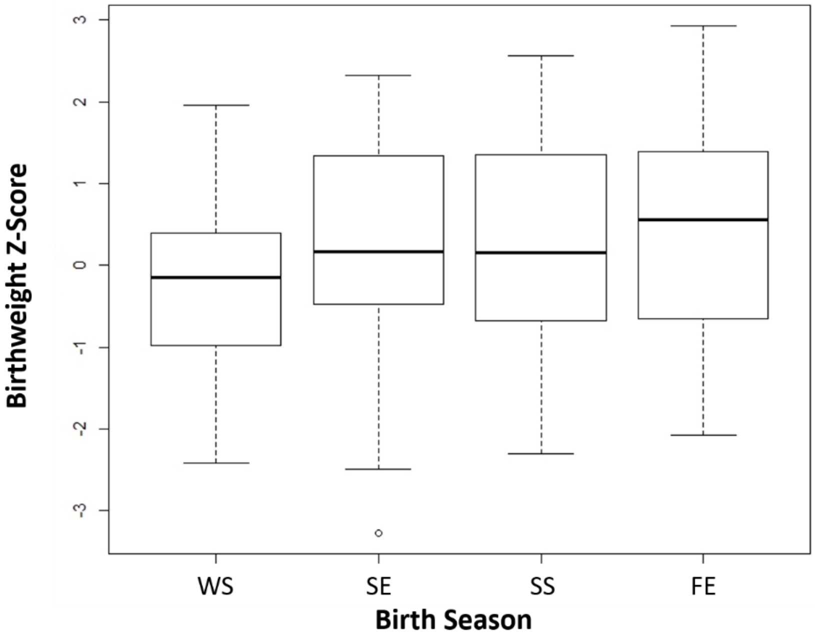

Supplementary Figure 2-1*. Boxplots of infant birthweight z-scores by season of birth. Birthweight z-scores did not significantly differ across seasonal categories (p=0.281, 1-way ANOVA).*

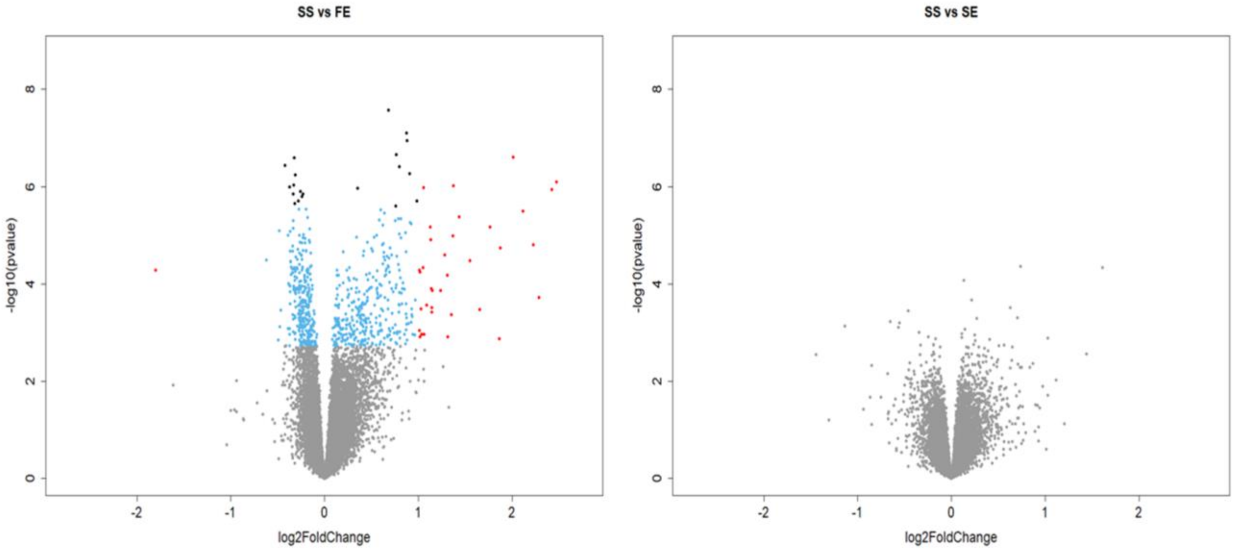

Supplementary Figure 2-2*. Volcano plot of results from the differential expression analysis of placental gene expression by birth season showing Wald test results comparing spring (SE) and* *fall (FE) to the summer (SS) reference group. Transcripts are plotted by effect size estimate [Log_2(Fold Change), x-axis] and statistical significance [-Log_{10}(Pvalue), y-axis], with grey dots indicating non-significant FDR $q \geq 0.05$, blue dots indicating FDR $q < 0.05$, black dots indicating Bonferroni $p < 0.05$, and red dots indicating absolute Log_2(Fold Change)>1 and FDR $q < 0.05$.*

Supplementary Table 2-1. *Likelihood ratio test (LRT) of the DE results comparing all seasonal categories to evaluate the overall effect of season. P-values are adjusted for multiple comparisons using either the Bonferroni or BH adjustment methods. (a portion of the material is provided below; for the full table, see supplemental materials here: https://faseb.onlinelibrary.wiley.com/doi/abs/10.1096/fj.202000291R)*

Ensemble_ID	**Mean**	**log2FC**	**lfcSE**	**stat**	**pval**	**qval**	**Bon_pval**
ENSG00000143222	434.49	0.23	0.04	40.18	9.77E-09	0.0002	0.0002
ENSG00000197111	1154.31	0.20	0.04	36.05	7.30E-08	0.0003	0.0013
ENSG00000186184	394.56	0.18	0.04	35.64	8.92E-08	0.0003	0.0016
ENSG00000135441	117.41	0.29	0.06	35.57	9.21E-08	0.0003	0.0016
ENSG00000043591	892.98	-0.36	0.07	35.32	1.04E-07	0.0003	0.0018
ENSG00000134107	1363.90	1.05	0.19	35.31	1.05E-07	0.0003	0.0019
ENSG00000260349	218.70	-0.26	0.05	35.29	1.06E-07	0.0003	0.0019
ENSG00000204262	2265.50	-0.35	0.08	34.03	1.95E-07	0.0004	0.0034
ENSG00000165775	345.68	0.19	0.04	33.85	2.13E-07	0.0004	0.0038
ENSG00000020181	1111.03	-0.37	0.10	33.15	3.00E-07	0.0005	0.0053
ENSG00000176463	16.70	0.54	0.15	33.07	3.11E-07	0.0005	0.0055
ENSG00000135245	335.70	0.72	0.13	32.90	3.37E-07	0.0005	0.0060
ENSG00000163590	456.67	-0.22	0.06	32.74	3.65E-07	0.0005	0.0064
ENSG00000168421	8.85	0.65	0.20	32.35	4.42E-07	0.0005	0.0078
ENSG00000091409	4057.47	-0.36	0.08	32.32	4.49E-07	0.0005	0.0079
ENSG00000225032	66.56	0.66	0.12	31.63	6.27E-07	0.0006	0.0111
ENSG00000169860	375.16	-0.50	0.10	31.62	6.29E-07	0.0006	0.0111
ENSG00000166167	559.40	-0.16	0.03	31.55	6.53E-07	0.0006	0.0115
ENSG00000144668	348.10	-0.40	0.09	31.42	6.94E-07	0.0006	0.0123
ENSG00000160072	977.85	0.56	0.11	31.37	7.11E-07	0.0006	0.0126
ENSG00000092964	1350.40	-0.21	0.05	31.35	7.19E-07	0.0006	0.0127

ENSG00000118971	1349.97	-0.18	0.10	30.82	9.29E-07	0.0007	0.0164
ENSG00000100034	1257.88	-0.25	0.06	30.74	9.63E-07	0.0007	0.0170
ENSG00000135862	8501.43	-0.26	0.06	30.73	9.68E-07	0.0007	0.0171
ENSG00000087086	5049.21	0.33	0.08	30.28	1.21E-06	0.0008	0.0213
ENSG00000174083	9.38	0.32	0.18	30.21	1.24E-06	0.0008	0.0220
ENSG00000187498	26583.7	-0.33	0.07	30.17	1.27E-06	0.0008	0.0224
ENSG00000144642	733.72	-0.29	0.08	30.14	1.29E-06	0.0008	0.0228
ENSG00000173269	1340.98	-0.29	0.09	30.11	1.31E-06	0.0008	0.0232
ENSG00000134248	315.65	0.22	0.06	30.09	1.32E-06	0.0008	0.0233
ENSG00000260708	12.17	0.81	0.15	30.08	1.33E-06	0.0008	0.0234
ENSG00000130844	686.84	0.40	0.09	29.80	1.52E-06	0.0008	0.0269
ENSG00000147113	863.88	-0.37	0.09	29.69	1.60E-06	0.0008	0.0283
ENSG00000184313	11.22	0.50	0.21	29.66	1.62E-06	0.0008	0.0287
ENSG00000210196	55.51	0.50	0.19	29.27	1.97E-06	0.0010	0.0348
ENSG00000189350	13.65	0.42	0.22	29.08	2.15E-06	0.0010	0.0381
ENSG00000260359	84.45	-0.39	0.09	29.00	2.23E-06	0.0010	0.0395
ENSG00000152268	500.83	-0.23	0.09	28.97	2.27E-06	0.0010	0.0400
ENSG00000178033	247.52	-0.49	0.11	28.96	2.28E-06	0.0010	0.0403
ENSG00000129925	3693.74	-0.21	0.07	28.90	2.35E-06	0.0010	0.0414
ENSG00000177119	2762.77	-0.24	0.05	28.90	2.35E-06	0.0010	0.0415
ENSG00000100650	4494.15	0.29	0.06	28.87	2.39E-06	0.0010	0.0421
ENSG00000113263	14.46	0.73	0.19	28.78	2.49E-06	0.0010	0.0440
ENSG00000168090	403.13	0.23	0.05	28.73	2.55E-06	0.0010	0.0451
ENSG00000143376	1831.03	-0.19	0.04	28.73	2.56E-06	0.0010	0.0452
ENSG00000155850	4316.81	-0.42	0.10	28.72	2.56E-06	0.0010	0.0452

Supplementary Table 2-2. *DE results from the Wald test comparing expression between winter (WS) and summer (SS) births, with SS as the reference. P-values are adjusted for multiple comparisons using either the Bonferroni or BH adjustment methods. Wald test results comparing differential expression between falle (FE) and summer (SS) births or spring (SE) and summer (SS) births are also provided. (please see supplemental materials here: https://faseb.onlinelibrary.wiley.com/doi/abs/10.1096/fj.202000291R)*

Supplementary Table 2-3. *Transcripts associated with comparing low maternal adversity (adv="0", ref) to some maternal adversity (adv="1",) or low maternal adversity (adv="0", ref) to high maternal adversity (adv="≥2") in the final model of differential expression between summer (SS) and winter (WS) births. P-values are adjusted for multiple comparisons using the Benjamini and Hochberg (BH) method or the Bonferroni (Bon) method. (a portion of the material is provided below; for the full table, see supplemental materials here: https://faseb.onlinelibrary.wiley.com/doi/abs/10.1096/fj.202000291R)*

Ensemble_ID	Mean	log2FC	lfcSE	stat	pval	qval	Bon_pval
ENSG00000237973	136.48	2.92	0.42	6.91	4.8E-12	8.4E-08	8.4E-08
ENSG00000114771	11.44	1.31	0.28	4.76	1.9E-06	1.7E-02	3.4E-02
ENSG00000165810	98.23	-1.01	0.23	-4.44	8.9E-06	5.2E-02	1.6E-01
ENSG00000113648	1780.02	0.11	0.03	4.00	6.2E-05	2.7E-01	1.0E+00
ENSG00000137225	8.73	-0.69	0.18	-3.81	1.4E-04	2.7E-01	1.0E+00
ENSG00000125538	68.44	0.56	0.15	3.77	1.6E-04	2.7E-01	1.0E+00
ENSG00000102575	102.19	0.31	0.08	3.77	1.7E-04	2.7E-01	1.0E+00
ENSG00000223478	43.90	0.30	0.08	3.76	1.7E-04	2.7E-01	1.0E+00
ENSG00000146530	29.54	-0.45	0.12	-3.72	2.0E-04	2.7E-01	1.0E+00
ENSG00000148450	198.56	0.19	0.05	3.69	2.2E-04	2.7E-01	1.0E+00
ENSG00000137496	128.22	0.38	0.10	3.68	2.3E-04	2.7E-01	1.0E+00
ENSG00000128268	694.65	-0.35	0.10	-3.68	2.3E-04	2.7E-01	1.0E+00
ENSG00000163975	35.93	0.58	0.16	3.67	2.4E-04	2.7E-01	1.0E+00
ENSG00000188735	149.94	0.22	0.06	3.66	2.5E-04	2.7E-01	1.0E+00
ENSG00000133710	57.36	0.36	0.10	3.64	2.8E-04	2.7E-01	1.0E+00
ENSG00000162729	868.43	-0.34	0.09	-3.63	2.8E-04	2.7E-01	1.0E+00
ENSG00000111405	4547.33	-0.34	0.09	-3.62	2.9E-04	2.7E-01	1.0E+00
ENSG00000047579	121.73	0.19	0.05	3.61	3.0E-04	2.7E-01	1.0E+00
ENSG00000112902	406.49	0.53	0.15	3.61	3.1E-04	2.7E-01	1.0E+00
ENSG00000185721	542.24	0.10	0.03	3.60	3.1E-04	2.7E-01	1.0E+00
ENSG00000066629	677.41	-0.17	0.05	-3.60	3.2E-04	2.7E-01	1.0E+00
ENSG00000115523	43.99	0.93	0.26	3.57	3.5E-04	2.8E-01	1.0E+00
ENSG00000227330	30.02	0.36	0.10	3.48	4.9E-04	3.6E-01	1.0E+00
ENSG00000162552	50.79	0.48	0.14	3.48	5.0E-04	3.6E-01	1.0E+00

Supplementary Table 2-4. *Results from the cosinor analysis. F tests were performed on the cosinor model results and corrected for multipled comparisons using either the Bonferroni or BH adjustment methods. Transcripts with a significant (FDR q<0.05) amplitude or acrophase were considered to be possibly rhythmic. (please see supplemental materials here: https://faseb.onlinelibrary.wiley.com/doi/abs/10.1096/fj.202000291R)*

Supplementary Table 2-5. *Results from the EnrichR analysis of the differentially expressed transcripts between SS and WS placenta (FDR q<0.05). The ChEA 2016, KEGG 2019, and GO 2018 databases were queried for enrichment. (please see supplemental materials here: https://faseb.onlinelibrary.wiley.com/doi/abs/10.1096/fj.202000291R)*

Supplementary Table 2-6. *Spearman correlation coefficients ("Rho") between BHLHE40 expression and all other transcripts and CLOCK expression and all other transcripts. P-values are adjusted for multiple comparisons using the Benjamini and Hochberg (BH) or Bonferroni (Bon) method. (a portion of the material is provided below; for the full table, see supplemental materials here: https://faseb.onlinelibrary.wiley.com/doi/abs/10.1096/fj.202000291R)*

Ensemble_ID	**Pval**	**Rho**	**qval**	**Bon_pval**	**Gene**
ENSG00000134852	0	1	0	0	CLOCK
ENSG00000260110	3.9E-46	8.2E-01	3.4E-42	6.9E-42	
ENSG00000138767	2.7E-41	8.0E-01	1.6E-37	4.7E-37	CNOT6L
ENSG00000100697	2.6E-38	7.8E-01	1.2E-34	4.6E-34	DICER1
ENSG00000188647	7.0E-38	7.8E-01	2.5E-34	1.2E-33	PTAR1
ENSG00000056586	4.9E-37	7.7E-01	1.4E-33	8.6E-33	RC3H2
ENSG00000169967	1.2E-34	7.6E-01	3.1E-31	2.2E-30	MAP3K2

ENSG00000151233	1.5E-34	7.6E-01	3.4E-31	2.7E-30	GXYLT1
ENSG00000080345	1.5E-33	7.5E-01	3.0E-30	2.7E-29	RIF1
ENSG00000205765	1.4E-32	7.4E-01	2.5E-29	2.5E-28	C5orf51
ENSG00000114127	3.5E-32	7.4E-01	5.2E-29	6.3E-28	XRN1
ENSG00000120137	3.5E-32	7.4E-01	5.2E-29	6.3E-28	PANK3
ENSG00000163946	6.3E-32	7.4E-01	8.6E-29	1.1E-27	FAM208A
ENSG00000165417	1.2E-31	7.4E-01	1.5E-28	2.1E-27	GTF2A1
ENSG00000152332	4.8E-30	7.2E-01	5.7E-27	8.6E-26	UHMK1
ENSG00000175387	1.0E-29	7.2E-01	1.1E-26	1.8E-25	SMAD2
ENSG00000118412	5.6E-29	7.1E-01	5.8E-26	9.9E-25	CASP8AP2
ENSG00000196233	6.6E-29	7.1E-01	6.5E-26	1.2E-24	LCOR
ENSG00000067208	8.4E-29	7.1E-01	7.6E-26	1.5E-24	EVI5
ENSG00000163320	8.6E-29	7.1E-01	7.6E-26	1.5E-24	CGGBP1
ENSG00000128585	1.9E-28	7.1E-01	1.6E-25	3.4E-24	MKLN1
ENSG00000128989	6.9E-28	7.0E-01	5.6E-25	1.2E-23	ARPP19
ENSG00000092439	8.2E-28	7.0E-01	6.1E-25	1.5E-23	TRPM7
ENSG00000115808	8.2E-28	7.0E-01	6.1E-25	1.5E-23	STRN

Supplementary Table 2-7*. Transcripts (FDR q<0.05) that overlapped between the differential expression and cosinor analyses. (please see supplemental materials here: https://faseb.onlinelibrary.wiley.com/doi/abs/10.1096/fj.202000291R)*

Chapter 3: Maternal Circadian Disruption is Associated with Variation in Placental DNA Methylation

Published in a different format as:

Clarkson-Townsend DA, Everson TM, Deyssenroth MA, Burt AA, Hermetz KE, Hao K, Chen J, Marsit CJ. Maternal circadian disruption is associated with variation in placental DNA methylation. *PLoS One*. 2019 Apr 26;14(4):e0215745. doi: 10.1371/journal.pone.0215745. PMID: 31026301; PMCID: PMC6485638.

Abstract

Circadian disruption is a common environmental and occupational exposure with public health consequences, but not much is known about whether circadian disruption affects *in utero* development. We investigated whether maternal circadian disruption, using night shift work as a proxy, is associated with variations in DNA methylation patterns of placental tissue in an epigenome-wide association study (EWAS) of night shift work. Here, we compared cytosine-guanosine dinucleotide (CpG) specific methylation genome-wide of placental tissue (measured with the Illumina 450K array) from participants (n=237) in the Rhode Island Child Health Study (RICHS) who did (n=53) and did not (n=184) report working the night shift, using robust linear modeling and adjusting for maternal age, pre-pregnancy smoking, infant sex, maternal adversity, and putative cell mixture. Statistical analyses were adjusted for multiple comparisons and results presented with Bonferroni or Benjamini and Hochberg (BH) adjustment for false discovery rate. Night shift work was associated with differential methylation in placental tissue, including CpG sites in the genes *NAV1*, *SMPD1*, *TAPBP*, *CLEC16A*, *DIP2C*, *FAM172A*, and *PLEKHG6* (Bonferroni-adjusted $p<0.05$). CpG sites within *NAV1*, *MXRA8*, *GABRG1*, *PRDM16*, *WNT5A*, and *FOXG1* exhibited the most hypomethylation, while CpG sites within *TDO2*, *ADAMTSL3*, *DLX2*, and *SERPINA1* exhibited the most hypermethylation (BH $q<0.10$). Functional analysis indicated GO-terms associated with cell-cell adhesion and enriched GWAS results for psoriasis. Night shift work was associated with differential methylation of the placenta, which may have implications for fetal health and development. This is the first study to examine the epigenetic impacts of night shift exposure, as a proxy for circadian disruption, on placental methylation in humans, and, while results should be interpreted with caution, suggests circadian disruption may have epigenetic impacts.

Introduction

Disruption of circadian rhythms is associated with negative health outcomes such as cancer, metabolic disorders, and neurological disorders in epidemiologic(Bass and Lazar, 2016) and animal studies(Opperhuizen et al., 2015); however, the impacts of circadian disruption during pregnancy on fetal development and child health have been largely overlooked. The core circadian clock consists of feedback loops of transcription factors (TF) that generate oscillating cycles of gene transcription and translation. These endogenously generated rhythms rely on cues, such as light, to synchronize patterns of physiological activity with the external environment. Light signals the suprachiasmatic nucleus (SCN) of the hypothalamus, the central clock, to set the body's peripheral clocks(Berson et al., 2002).

There have been numerous studies to evaluate health outcomes associated with night shift work, an occupational proxy for circadian disruption, but it is unknown whether working the night shift before or during pregnancy poses health risks to the mother or child. This understudied exposure may have large public health consequences, as approximately 15% of American employees work outside of the traditional 9AM-5PM work schedule(Straif et al., 2007). While some aspects of the circadian system may return to normal after a regular schedule of night shift work, studies suggest the majority of regular night shift workers (~97%) are not able to fully adapt their endogenous circadian rhythms to their work schedules(Folkard, 2008).

Although there appear to be only small risks of negative reproductive health outcomes associated with shift work(Palmer et al., 2013), not much is known about the impact of light or circadian rhythms in human pregnancy or on long-term fetal programming. The placenta, an organ responsible for mediating the maternal and fetal environment to regulate growth and development, may be affected by circadian disruption; yet, little attention has been paid to the impact of circadian disruption on placental function. Because the placenta is composed of fetal DNA, methylation of placental tissue may reflect fetal exposures and future health effects. Therefore, differences in placental methylation patterns between night shift workers and non-night shift workers may indicate altered fetal development and infant health in response to circadian disruption. In this study, we conducted an epigenome-wide association study (EWAS) to investigate whether night shift work is associated with differences in DNA methylation in the placental epigenome, which can impact long-term health outcomes in the offspring.

Methods

Study population – The Rhode Island Child Health Study (RICHS)

The Rhode Island Child Health Study (RICHS) is a hospital-based cohort study of mothers and infants in Rhode Island, described in detail elsewhere(Appleton et al., 2016). Briefly, from 2009 to 2014, women between the ages of 18-40 and their infants were enrolled at the Women and Infants Hospital of Rhode Island, oversampling for large and small for gestational age infants and matching each to an appropriate for gestational age control by maternal age (± 2 years), sex, and gestational age (± 3 days). RICHS enrolled only full-term (≥37 weeks), singleton deliveries without congenital or chromosomal abnormalities. All participants provided written informed consent under protocols approved by the Institutional Review Boards of Women and Infants Hospital and Emory University.

Demographic information was collected from a questionnaire administered by a trained interviewer and clinical outcome information was obtained from medical records. Information on night shift work was obtained from questionnaire by first asking, “Have you ever worked outside the home? (Yes/No)" and if "Yes", participants were asked "If yes, please list all of the jobs you have had starting with your current job first. Please indicate whether you worked a swing shift or a night shift on any of these jobs". To indicate shift jobs, the questionnaire included check boxes for "Yes" and "No" under a category for "Night Shift". For this analysis, only the most recently reported job history was used and only those who reported "Yes" for night shift work were considered night shift workers; people who reported working a swing shift but not a night shift were not included as night shift workers.

To adjust for socioeconomic factors while avoiding multicollinearity, we used an adversity score index to adjust for household income, maternal education, marital status and partner support. The cumulative risk score ranged from 0 to 4, with 0 representing the lowest level of adversity and 4 representing the highest level of adversity. A higher risk score was given to women whose median household income (adjusting for the number of people in the household) fell below the federal poverty line for the year the infant was born (+1), to women whose household was larger than 6 (+1), to women who were single and did not receive support from a partner (+1) and to women whose highest level of education was high school or less (+1)(Appleton et al., 2013).

Placental sample collection and measurement of DNA methylation

Genome-wide DNA methylation (measured with the Illumina 450k arrays) was obtained on 334 placentae parenchyma samples in RICHS as previously described(Paquette et al., 2016), and of these, data from 237 samples were included in this analysis. The QA/QC process has been described elsewhere(Maccani et al., 2015), including functional normalization, BMIQ, and 'ComBAT' to adjust for technical variations and batch effects in R(Johnson et al., 2007; Paquette et al., 2016). Briefly, we used the ‘minfi’ package in R to convert the raw methylation files to β values, a ratio of methylation ranging from 0 to 1, for analysis. Probes associated with the X or Y chromosomes, single nucleotide polymorphism (SNP)-associated (within 10bp of the target cytosine-guanosine dinucleotide (CpG) site and with minor allele frequency >1%), identified as cross-reactive or polymorphic by Chen et al(Chen et al., 2013), or with poor detection p-values were excluded, yielding 334,692 probes for analysis in this study(Paquette et al., 2016). DNA methylation array data for RICHS can be found in the NCBI Gene Expression Omnibus (GEO) database with the number GSE75248. Women with missing information on pre-pregnancy smoking status (“No”/”Yes”), defined as smoking 3 months prior to pregnancy, or adversity score were not included in the analysis. Women who did not provide an answer for the nightshift variable (n=16) were recoded to “No”. This study included the 237 mother-infant pairs within RICHS for which DNA methylation data and the necessary demographic information were available.

Placental RNA sequencing

Gene expression was measured using the Illumina HiSeq 2500 system in 199 placental samples from RICHS; methods have been previously described (Deyssenroth et al., 2017). After standard QA/QC procedures, final data were normalized to log2 counts per million (logCPM) values. Raw data is available in the NCBI sequence read archive (SRP095910).

Statistical analyses

Because a reference panel for placental cell types does not yet exist, we used a validated reference-free method, the ‘RefFreeEWAS’ package in R, to adjust for heterogeneity in cell-type composition(Houseman et al., 2016; Teschendorff and Zheng, 2017). We implemented the RefFree estimation via the same process described in detail in our lab's prior work(Everson et al., 2017), and identified 8 components to represent the putative cell mixture in our placental samples. We also examined the outlier screening plots of the cell mixture array for extreme outliers. We then conducted an EWAS using robust linear modeling by regressing CpG methylation β-values on night shift work ("No"/"Yes"), adjusting for putative cell mixture, maternal age (years), pre-pregnancy smoking status ("No"/"Yes") adversity score (0-4)(Lam et al., 2012), and sex of the infant ("Female"/"Male"). To adjust for multiple comparisons, we used the Bonferroni method and the Benjamini and Hochberg (BH) false discovery rate (FDR) methods. To evaluate the extent of *in utero* night shift exposure, we compared job and delivery date data. A sensitivity analysis using data from women who provided night shift job information (n=221) without recoding missing to "No" was performed. We also conducted a sensitivity analysis to evaluate gestational diabetes mellitus (GDM) and CpG methylation outcomes, as numerous studies have found an association between night shift work and the development of obesity and metabolic diseases(Froy, 2010; Scheer et al., 2009), as well as GDM and altered methylation(Haertle et al., 2017). While DNA methylation is not expected to change on a day-to-night basis(Reik, 2007), a few recent studies of brain tissue have found diurnal differences in DNA methylation(Coulson et al., 2018; Lim et al., 2017). To assess possible confounding by time of placenta sample collection, we categorized time of sample collection into 3-hour bins (7AM-9AM, 10AM-12PM, 1PM-3PM, and 4PM-5PM) and performed a Fisher's exact test (one of the cells had <5 participants) to compare night shift and non-night shift workers. We also modelled sample collection time as a continuous outcome and night shift work as a categorical exposure (No/Yes).

Additionally, we investigated differentially methylated regions (DMRs) using the ‘Bumphunter’ package in R(Jaffe et al., 2012). We modeled the β-values between non-night shift workers and night shift workers, controlling for the same variables as the individual CpG by CpG site genome-wide analysis. CpG sites within 500 base pairs were clustered together and β-values were modeled against a null distribution generated via bootstrapping; sites with differential methylation of 2% or more were considered to be possible DMRs.

To examine the functional implications of night shift work-associated DNA methylation (BH $q<0.05$), we also conducted an expression quantitative trait (eQTM) analysis using ‘MEAL’ in R to investigate whether methylation was associated with gene expression in the RICHS samples on which both DNA methylation and expression data were available (n=199). Using robust linear modeling, we regressed the expression levels of genes within a 100kb window of the CpG site on methylation β-values ($p<0.05$).

Bioinformatic analyses

To better understand the biological significance of the EWAS results, we performed an enrichment analysis of the top 298 CpG sites (BH $q<0.10$) with GO-terms and KEGG pathways in R using the ‘missMethyl’ package(Phipson et al., 2016). We also evaluated whether the genes (n=45) from overlapping CpG sites with BH $q<0.05$ were listed as rhythmic within the available CircaDB mouse databases(Pizarro et al., 2013). We searched within CIRCA mouse experimental datasets using the JTK filter with a q-value probability cut-off of 0.05 and a JTK phase range of 0-40(Hughes et al., 2010). To investigate whether the CpGs from our EWAS results were within genomic regions that have been linked to traits from previous GWAS findings, windows of the top 298 CpG sites (BH $q<0.10$) and flanking 5kb regions of DNA were compared for overlap with SNP results ($p<1x10^{-8}$) in the GWAS catalog of the National Human Genome Research Institute and the European Bioinformatics Institute (NHGRI-EBI)(MacArthur et al., 2017) using the TraseR package(Chen and Qin, 2016) in R. As background, we only included SNPs that were within 5kb of CpGs that were included in the EWAS study. If more than one top CpG site fell within the same 10kb window, they were clustered together and considered the same region. Only GWAS trait-associated SNP windows that overlapped with 2 or more of the top CpG windows and were statistically significant after Fisher's exact test (BH q <0.05) were considered enriched.

Results

Demographic and medical Information

Demographic information for the women (n=237) and covariates included in the final model for the epigenome-wide analysis are provided in **Table 3-1**. A sensitivity analysis comparing results from women who provided night shift job information (n=221) without recoding missing to "No" did not indicate any large differences in demographic features. Overall, women who reported working the night shift were more likely to be younger, smokers pre-pregnancy, cases of GDM, single and never married, lower household income, and higher adversity (p<0.05). While not statistically significant, women who worked the night shift trended towards a higher BMI and an evening chronotype. Of those included in the analysis, one participant reported taking melatonin and she was not a night shift worker. Additionally, 37 out of the 53 (70%) night shift workers reported working the night shift during pregnancy; time between working the night shift and the birth of the infant ranged from within a week to approximately 4.5 years, with a median value of 10 weeks.

Table 3-1. *Demographic characteristics of participants included in the analysis (n=237) by night shift work status. *Signifies p-value <0.05 (using either $\chi 2$ test, Fisher's exact test or 2-sided t-test) between non-night shift and night shift workers.*

	N	**Non-night shift (n=184)**	**Night shift (n=53)**	**Statistical significance**
Maternal age*, mean ± SD	237	30.7+/- 5.4	28.8+/- 5.1	p<0.05
Pre-pregnancy smoking*, % (n)	237	12% (22)	25% (13)	p<0.05
Sex of the infant (male/female), % (n)	237	48% / 52% (88/96)	53% / 47% (28/25)	p=0.6
Gestational diabetes*, % (n)	234	9% (16)	21% (11)	p<0.05
Marital status*, % (n)	237			p<0.05
Single, never married		24% (44)	43% (23)	
Separated or divorced		3% (6)	4% (2)	
Married		73% (134)	53% (28)	
Household income*, % (n)	229			p<0.01
<$9-14,999		14% (25)	24% (12)	
$15-29,999		9% (17)	20% (10)	
$30-49,999		10% (18)	18% (9)	
$50-99,999		39% (69)	30% (15)	
.>$100,000		28% (50)	8% (4)	
Adversity score*, % (n)	237			p<0.05
0		78% (143)	58% (31)	
1		12% (22)	30% (16)	
2		9% (16)	9% (5)	
3		1% (2)	2% (1)	
4		1% (1)	0% (0)	
Maternal education*, % (n)	237			p<0.01
<11th grade		5% (10)	4% (2)	
High school		15% (28)	26% (14)	
Junior college or equivalent		22% (40)	40% (21)	
College		36% (67)	26% (14)	
Any post-graduate		21% (39)	4% (2)	

Epigenome-wide methylation associations

DNA methylation at 298 CpG sites was found to be significantly different in night shift workers after FDR correction at the BH q<0.10, 57 CpG sites significant at the BH q<0.05 (**Table 3-2**), and 10 CpG sites at the Bonferroni-corrected p<0.05 (**Table 3-2**). CpG sites for the *NAV1*, *SMPD1*, *TAPBP*, *CLEC16A*, *DIP2C*, *FAM172A*, and *PLEKHG6* genes had genome-wide significance after Bonferroni correction (p<0.05). The *ADAMTS10*, *CLEC16A*, *CTBP1*, *EGFL8*, *GNAS, HDAC4, HEATR2, KCNA4, KDELC2, MFHAS1, MXRA8*, *NAV1*, *PLXND1*, *UBR5*, *WNT5A*, and *ZBTB22* genes had multiple CpG sites represented in the results.

Table 3-2. *List of differentially methylated CpG sites in night shift workers compared to non-night shift workers after epigenome-wide analysis (BH q<0.05).*

UCSC Gene Name	Chromosome	Position	Probe ID	β1	SE	P-value	BH q-value	Bonferroni
NAV1	chr1	201708718	cg14168733	-0.04	0.007	2.53E-08	0.003	0.008
NAV1	chr1	201709135	cg14377596	-0.04	0.007	2.98E-08	0.003	0.01
SMPD1	chr11	6412852	cg14814323	-0.016	0.003	2.97E-08	0.003	0.01
NAV1	chr1	201709390	cg01411786	-0.032	0.006	9.91E-08	0.004	0.033
TAPBP	chr6	33273011	cg03190911	-0.014	0.003	9.94E-08	0.004	0.033
	chr6	27390647	cg06667732	-0.023	0.004	9.35E-08	0.004	0.031
CLEC16A	chr16	11073063	cg08082763	-0.023	0.004	7.21E-08	0.004	0.024
DIP2C	chr10	560669	cg21373996	-0.019	0.004	1.06E-07	0.004	0.035
FAM172A	chr5	93076910	cg25342875	-0.024	0.004	9.46E-08	0.004	0.032
PLEKHG6	chr12	6436676	cg14858786	-0.026	0.005	1.42E-07	0.005	0.047
KRT15	chr17	39675154	cg11983245	-0.024	0.005	1.84E-07	0.005	0.062
NAV1	chr1	201709675	cg18539461	-0.036	0.007	1.71E-07	0.005	0.057
RHOT2	chr16	717556	cg04365973	-0.019	0.004	2.58E-07	0.007	0.086
NAV1	chr1	201708888	cg13877974	-0.043	0.009	4.11E-07	0.01	0.137
ERI3	chr1	44716226	cg24373865	-0.024	0.005	5.66E-07	0.013	0.189
PTPN6	chr12	7060187	cg23147227	-0.02	0.004	8.98E-07	0.019	0.301
EGFL8	chr6	32135718	cg08759957	-0.021	0.004	1.22E-06	0.023	0.407
ZBTB22	chr6	33284168	cg14771240	-0.02	0.004	1.18E-06	0.023	0.396

	chr10	22725309	cg01422243	-0.019	0.004	1.51E-06	0.027	0.504
UBR5	chr8	103344822	cg02530407	-0.019	0.004	1.68E-06	0.027	0.561
HDAC4	chr2	240213173	cg23601374	-0.017	0.004	1.64E-06	0.027	0.549
	chr7	25702848	cg03700230	0.048	0.01	1.93E-06	0.029	0.645
CYB5R2	chr11	7694163	cg05919312	-0.018	0.004	2.03E-06	0.03	0.679
RPS6KA4	chr11	64139406	cg07425109	-0.016	0.003	2.15E-06	0.03	0.719
MSI2	chr17	55742491	cg07618409	-0.02	0.004	2.26E-06	0.03	0.755
CDYL2	chr16	80716710	cg16713168	-0.021	0.004	2.33E-06	0.03	0.78
FAM118A	chr22	45705265	cg06575572	-0.02	0.004	2.50E-06	0.03	0.835
LRRC2	chr3	46618325	cg07225641	-0.027	0.006	2.61E-06	0.03	0.875
CLDN9	chr16	3063894	cg10492999	-0.026	0.006	2.70E-06	0.03	0.905
LOC645323	chr5	87955859	cg13982098	-0.028	0.006	2.65E-06	0.03	0.886
C2orf54	chr2	241827789	cg21333033	-0.019	0.004	2.93E-06	0.032	0.981
SLC41A1	chr1	205780033	cg00762738	-0.017	0.004	3.08E-06	0.032	1
MXRA8	chr1	1290712	cg00040588	-0.051	0.011	3.49E-06	0.032	1
EGFL8	chr6	32135715	cg12305588	-0.019	0.004	3.35E-06	0.032	1
BAIAP2	chr17	79022879	cg12472449	-0.016	0.004	3.43E-06	0.032	1
FBXW7	chr4	153437193	cg13536107	-0.022	0.005	3.35E-06	0.032	1
BAT2	chr6	31599646	cg25371129	-0.005	0.001	3.61E-06	0.033	1
MIRLET7A3	chr22	46508563	cg04063235	-0.019	0.004	3.71E-06	0.033	1
HDLBP	chr2	242174625	cg11221200	-0.014	0.003	3.90E-06	0.033	1
	chr11	22454301	cg23181580	-0.031	0.007	4.22E-06	0.035	1
BATF3	chr1	212874153	cg00168835	0.005	0.001	4.42E-06	0.036	1
	chr22	50221949	cg08174792	-0.034	0.007	4.91E-06	0.039	1
MFHAS1	chr8	8749074	cg01022370	-0.023	0.005	5.20E-06	0.04	1
ZNF284	chr19	44575547	cg05333740	-0.023	0.005	5.83E-06	0.042	1
DPEP2	chr16	68027297	cg06866814	0.002	0	5.50E-06	0.042	1
GALNTL4	chr11	11438208	cg16337763	-0.022	0.005	5.67E-06	0.042	1
AZI1	chr17	79184968	cg20296990	-0.02	0.004	5.84E-06	0.042	1
GALNTL1	chr14	69725831	cg00080706	-0.019	0.004	5.99E-06	0.042	1
MFHAS1	chr8	8749278	cg01784220	-0.022	0.005	6.21E-06	0.042	1
C11orf2	chr11	64863151	cg13626866	-0.026	0.006	6.37E-06	0.043	1
BANF1	chr11	65770987	cg17985854	-0.023	0.005	6.49E-06	0.043	1
IQGAP2	chr5	75784957	cg23289545	-0.019	0.004	6.62E-06	0.043	1
	chr17	43222106	cg00625783	-0.025	0.006	7.26E-06	0.045	1
TUBGCP2	chr10	135120640	cg04070692	-0.019	0.004	7.21E-06	0.045	1
BAT1	chr6	31502388	cg10895184	-0.018	0.004	7.53E-06	0.045	1
HAPLN1	chr5	83016779	cg18024167	-0.023	0.005	7.44E-06	0.045	1
PKHD1L1	chr8	110374866	cg19906741	0.018	0.004	7.77E-06	0.046	1

The Manhattan plot of the results indicated a number of differentially methylated sites that distributed across the genome, with some occurring in the same regions (**Figure 3-1A**). There was also an overall trend towards hypomethylation (**Fig 3-1B**). CpG sites for *NAV1*, *MXRA8*, *GABRG1*, *PRDM16*, *WNT5A*, and *FOXG1* were among the 10 sites with the most hypomethylation, while CpG sites for *TDO2*, *ADAMTSL3*, *DLX2*, and *SERPINA1* were among the 10 sites with the most hypermethylation To more rigorously examine the co-located CpG sites associated with night shift work, we employed a 'Bumphunter' analysis and identified 6584 'bumps', with areas of the *NAV1*, *PURA*, *C6orf47*, and *GNAS* genes as DMRs (BH q<0.10)(**Table 3-3**). Of these, CpGs for the *NAV1* and *GNAS* genes were also differentially methylated in the CpG by CpG analysis (**Supplemental Table 3-1**).

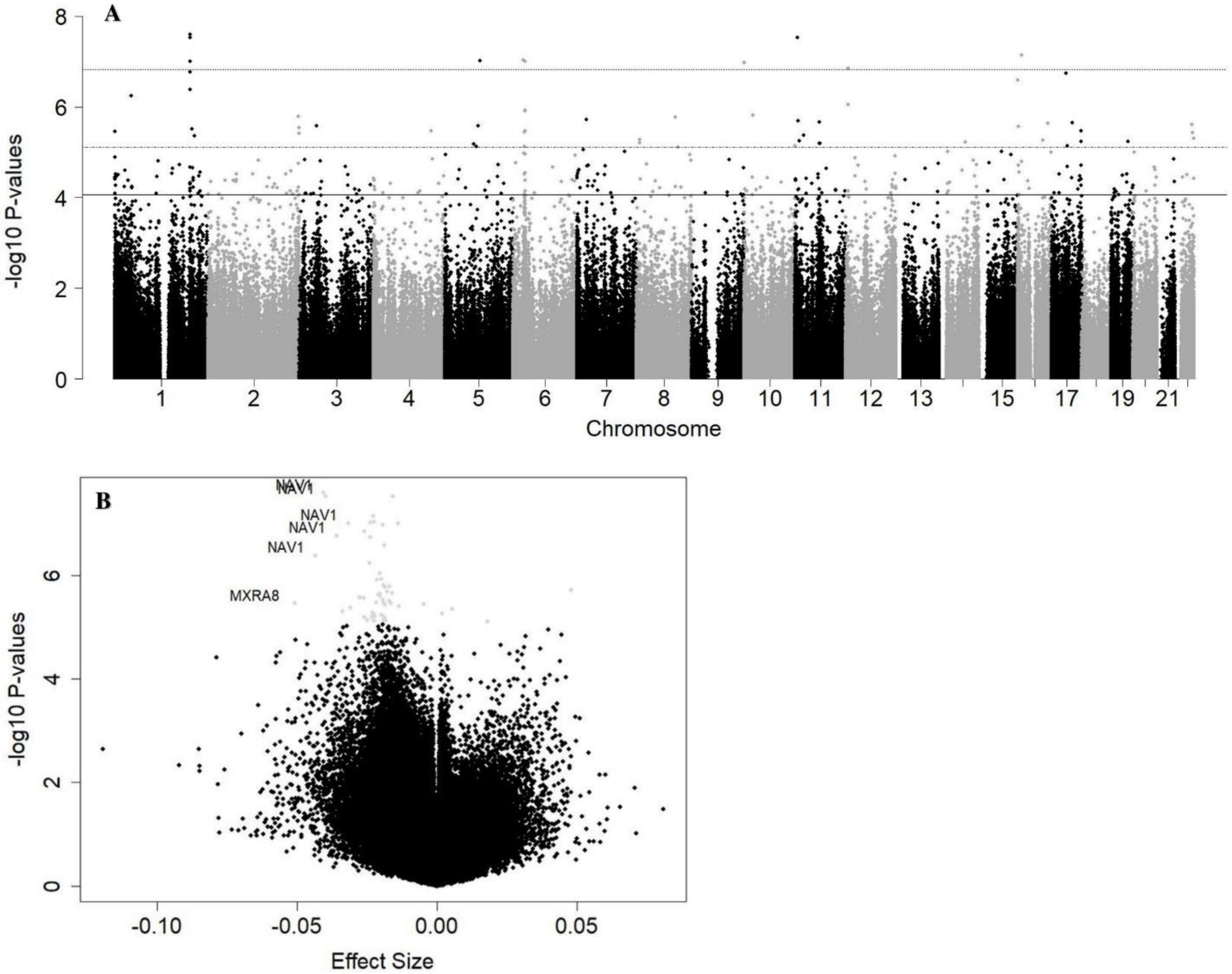

Figure 3-1. *Results of placental DNA methylation and night shift work EWAS.* ***A,*** *Manhattan plot of CpG results, adjusted for maternal age, pre-pregnancy smoking, adversity score, sex of the infant, and estimated cell mixture. The dashed upper boundary line denotes p-value of 1.49x10-7 as the significance threshold after Bonferroni adjustment (p<0.05), the dashed middle boundary line denotes the p-value of 7.7x10-6 as the approximate significance threshold of BH q<0.05, and the solid boundary line at denotes the p-value of 8.8x10-5 as the approximate significance threshold of BH q<0.10.* ***B,*** *Volcano plot of results, adjusted for maternal age, pre-pregnancy smoking, adversity score, sex of the infant, and estimated cell mixture. Gray dots signify CpG sites with BH q<0.05 and CpG sites with both absolute beta coefficients of 0.03 or greater and BH q<0.05 are labelled with UCSC gene names.*

Table 3-3. *'Bumphunter' results of significant DMRs (BH q<0.10).*

Gene	**β1**	**P-value**	**FWER**	**P-value Area**	**FWER Area**	**BH**	**Bon**
NAV1	-0.038	3.29E-05	0.166	1.74E-04	0.606	0.054	0.217
PURA	-0.054	2.54E-05	0.131	6.80E-05	0.31	0.054	0.167
C6orf47	-0.112	3.24E-05	0.163	1.17E-02	1	0.054	0.213
GNAS	-0.034	9.35E-06	0.05	1.31E-04	0.512	0.054	0.062

A sensitivity analysis with GDM included as an additional covariate shared many of the top CpG sites with the primary results, suggesting GDM is not a confounder of these associations. An additional analysis evaluating GDM as the primary exposure shared no top genes with the EWAS results. In comparing time of placenta sample collection, there was no significant difference between the two groups when compared categorically (p=0.547) or continuously (p=0.945), with a mean collection time around 11AM. In another sensitivity analysis comparing the beta coefficients from models that utilized *in utero* night shift work exposure as the independent variable (n=37) to the beta coefficients from models that included all night shift workers (n=53), the differences were small; only 1 CpG site, cg24373865, had an absolute difference in beta coefficients greater than 0.01, at 0.011. We also re-examined our results removing those with missing data on night shift work and the findings were substantially similar.

Functional analyses

Comparing the 298 significant CpG sites (BH q<0.10) to the remaining 334,394 CpG sites, there was a higher frequency of top CpG sites within enhancer regions (χ^2 = 13.48, df = 1, p-value = 0.0002). Because transcription factors (TFs) can bind to enhancer regions to alter gene expression, we assessed whether CpG methylation was associated with expression levels in nearby genes. The eQTM analysis found the expression of 18 genes to be associated with 14 CpG sites ($p<0.05$). Of these, the expression levels of *ACBD4* were associated with methylation in cg00625783 ($\beta1=2.515$, p-value=1.94E-05) and the expression levels of *KRT15* were associated with methylation in cg11983245 ($\beta1=7.895$, p-value=8.04E-05)(**Supplemental Table 3-2**). For both of these genes, increasing methylation of the CpG sites was associated with increased gene expression. The cg00625783 CpG is not annotated to a gene, but is located within an enhancer region, and cg11983245 is annotated to the 5' untranslated region (5'UTR) and 1st exon of the *KRT15* gene. Methylation of cg11983245 was also associated ($p<0.05$) with increased *KRT19* ($\beta1=4.404$, p-value=3.87E-03) and *LINC00974* ($\beta1=6.011$, p-value=3.40E-02) expression levels.

We analyzed the top 298 CpG sites (BH $q<0.10$) for enrichment of KEGG pathways and GO-terms. The GO-terms "cell-cell adhesion", "cell-cell adhesion via plasma-membrane adhesion molecules", and "hemophilic cell adhesion via plasma membrane adhesion molecules" were found to be significant after FDR correction (BH<0.05)(**Supplemental Table 3-3**). The top KEGG pathway results were "valine, leucine and isoleucine biosynthesis", "mucin type O-glycan biosynthesis" and "melanogenesis", but they were not significant after correcting for FDR (**Supplemental Table 3-4**). Surprisingly, *PER1* was the only core circadian gene represented among the 298 CpG sites. However, we evaluated whether the 45 genes of the top 57 CpG sites exhibited circadian rhythmicity within the CircaDB mouse expression database(Pizarro et al., 2013) and found 27 out of the 45 genes (60%) displayed rhythmic expression(Hughes et al., 2010)(**Supplemental Table 3-5**). Of these genes, *BAIAP2*, *GALNTL1*, *HDLBP*, *NAV1*, and *TAPBP* displayed rhythmicity in mouse SCN tissue. We then tested for trait-associated SNP enrichment within 10kb regions surrounding the top 298 CpG sites (BH q<0.05) among GWAS SNPs ($p<1x10^{-8}$) in NHGRI-EBI GWAS catalog(MacArthur et al., 2017) using a Fisher's exact test in TraseR(Chen and Qin, 2016). These regions were significantly enriched (FDR < 5%) for the following traits: Psoriasis, Systemic Lupus Erythematosus, Type 1 Diabetes Mellitus, and Multiple Sclerosis (**Supplemental Table 3-6**).

Discussion

We identified a number of CpG sites exhibiting differential methylation associated with night shift work in newborn placental tissue. While the average absolute differences for the 298 CpG site corresponded to a roughly 1.7% change in methylation, even a small change in methylation may have physiologically-relevant effects, and these magnitudes of association are comparable to others reported for exposures including toxic trace elements and maternal smoking during pregnancy(Breton et al., 2017). The overall trend of hypomethylation with night shift work may be due to increased TF binding to DNA, leading to chromatin changes establishing the hypomethylated state(Martin and Fry, 2016). Because one of the core components of the circadian clock, CLOCK, acts as a histone acetyltransferase(Doi et al., 2006), it is also possible that circadian disruption impacts the epigenetic activity of CLOCK, affecting chromatin state and accessibility. However, there is still much to discover about circadian interactions with methylation and developmental processes.

Light at night and night shift work exposure can cause altered hormonal signaling and endocrine disruption; because hormone receptors can act as TFs, it is possible that circadian disruption causes increased hormonal signaling and increased TF binding. Animal studies of *in utero* circadian disruption suggest that circadian disruption may negatively affect the health and development of offspring(Smarr et al., 2017b). For example, chronic changes in the photoperiod of pregnant rats caused increased leptin levels, insulin secretion, fat deposition, and decreased glucose tolerance of offspring in adulthood(Varcoe et al., 2011). Additionally, mice exposed to a 22-hour light-dark cycle, instead of the normal 24-hour cycle, had altered methylation patterns in the SCN and altered circadian behavior; differential methylation was also found for genes related to axonal migration, synaptogenesis, and neuroendocrine hormones(Azzi et al., 2014).

We identified a DMR and multiple individual CpG sites within and nearby to *NAV1* that were consistently represented among the top results. In general, the functions of NAV1, particularly in the placenta, are not well characterized. *NAV1* is homologous to the *unc-53* gene in *C.elegans*, which plays a role in axonal migration(Maes et al., 2002). The mouse homolog also appears to play a role in neuronal migration; NAV1 is enriched in growth cones and associates with microtubule plus ends(van Haren et al., 2009), and the deficit of *Nav1* causes loss of direction in leading processes(Martinez-Lopez et al., 2005). Research has also found increased embryonic lethality, decreased birthweight, and infertility in female offspring for Nav1$^{-/-}$ mice(Kunert, 2014), suggesting an important role for *Nav1* in fetal development and health. Our mouse tissue query of the CircaDB database revealed that *Nav1* specifically displayed circadian rhythmicity in mouse SCN tissue (**Supplemental Table 3-4**). This suggests NAV1 may play a role in the mammalian SCN. A DMR was also identified in *GNAS*, which is imprinted in the paraventricular nucleus of the hypothalamus and encodes the $G_s\alpha$ G-protein, which regulates cAMP generation and metabolism. *Gnas* is implicated in REM and NREM sleep and the browning of white adipose tissue for thermogenesis(Lassi et al., 2012). Additionally, in a microarray analysis of retina samples from an *rd/rd* mouse model, *Gnas* was implicated in melanopsin signaling(Peirson et al., 2007). Therefore, GNAS may be important in integrating light and metabolic cues.

The top 298 CpG results (BH q<.05) were enriched for traits related to psoriasis, lupus, type 1 diabetes, and multiple sclerosis, all of which involve the immune system and/or inflammation. Interestingly, a large study of night shift workers in the Nurse's Health Study found an increased risk of psoriasis among night shift workers(Li et al., 2013). Another study that analyzed two separate cohorts also found an association between engaging in shift work before 20 years old and multiple sclerosis(Hedström et al., 2011). The skin has circadian rhythms that may affect the development of psoriasis(Ando et al., 2015), during which abnormal activity of keratinocytes and T cells can cause lesions. Because adhesion molecules may play an important role in this process, this GWAS trait may explain the KEGG-pathway and GO-term enrichment analysis, among which "cell-cell adhesion" and "melanogenesis" were some of the top results.

A possible limitation of this analysis is the moderate sample size of night shift workers (n=53). Because placenta samples were only collected during daytime hospital hours (7AM-5PM), we are also limited in our ability to fully evaluate diurnal differences in DNA methylation. Additionally, the adjustment for cell-type heterogeneity is an estimation, so there is a possibility of residual confounding by cell type. On the other hand, the results may be a conservative estimate of the true association, as this analysis occurred in full-term pregnancies and approximately 30% of the women included as night shift workers did not have *in utero* exposure. While a sensitivity analysis of *in utero* night shift work exposure did not find large differences in the magnitudes of association, exposure to circadian disruption at different windows of development could have different magnitudes of effect. Prior research has found that shift workers continue to have chronic health effects even after they switch to a day shift schedule. For example, researchers found that a history of shift work was associated with a decrease in cognitive ability that took 5 years or more after cessation of shift work to recover(Marquié et al., 2015); this suggests recovery from regular shift work may take an extended period of time and a history of shift work may have a prolonged influence on health.

This is the first study to examine the epigenetic impacts of night shift exposure on placental methylation in humans, and results should be interpreted with caution. Methylation of placental tissue, an indicator of the *in utero* epigenetic landscape, reflects functional activities of the placenta, which can impact various aspects of fetal development, including neurodevelopment. The findings that the methylation of *NAV1* differed by night shift work exposure and that *Nav1* is rhythmically expressed in mouse SCN suggests NAV1 may play a role in the human circadian system. Because the circadian system coordinates an array of physiological systems, alterations to circadian system development could affect immune response, sleep patterns, behavior, metabolism, and future health status. We have found night shift work to be associated with variation in methylation of placental tissue, which has implications for fetal development and future health. However, these findings may also be relevant for people who experience circadian disruption due to common exposures such as light at night(Chang et al., 2015a).

In conclusion, night shift work is associated with differential methylation patterns in placental tissue. NAV1 may be an important component in the development of the human circadian system. Night shift work is a complex exposure encompassing altered hormonal signaling, eating and activity patterns, light exposure, and sleep patterns. Therefore, it is difficult to tease apart which aspects of night shift work contribute to which result. However, night shift work is a prevalent exposure in the workforce and, more generally, circadian disruption is a common facet of modern life. Circadian disruption may contribute to immune-mediated and inflammatory disease, but it is still unclear how this exposure may affect fetal development and infant health. These findings warrant further investigation to evaluate the effects of *in utero* circadian disruption and possible impacts on fetal and child health, as well as the role of the circadian system in the function of the placenta.

Supplemental Material

Supplemental Table 3-1. *List of the 298 CpG sites that were differentially methylated in placenta tissue from night shift workers compared to non-night shift workers (BH q<0.10). (Supplemental material provided here:* https://doi.org/10.1371/journal.pone.0215745.s001)

Supplemental Table 3-2. *Table of results from expression quantitative trait methylation (eQTM) analysis of genes within 100kb of CpG sites with BH q<0.05. The data used in this analysis came from RICHS samples that had both methylation and RNAseq data available (n=197).*

CpG site	**Ensemble_ID**	**Gene**	**β1**	**p-val**	**q-val**
cg00625783	ENSG00000181513	ACBD4	2.515	1.94E-05	0.006
cg11983245	ENSG00000171346	KRT15	7.895	8.04E-05	0.012
cg11983245	ENSG00000171345	KRT19	4.404	3.87E-03	0.339
cg25371129	ENSG00000204438	GPANK1	9.243	4.64E-03	0.339
cg21373996	ENSG00000233021	AL669841.1	8.131	6.68E-03	0.39
cg00762738	ENSG00000117280	RAB29	-2.956	1.48E-02	0.506
cg07425109	ENSG00000168071	CCDC88B	3.982	1.56E-02	0.506
cg19906741	ENSG00000250267	LINC00482	-6.082	1.21E-02	0.506
cg20296990	ENSG00000185168	AC021237.1	2.471	1.27E-02	0.506
cg10895184	ENSG00000204516	MICB	5.118	1.78E-02	0.518
cg03190911	ENSG00000237441	SMPD1	1.594	4.80E-02	0.67
cg06667732	ENSG00000096654	CLDN6	-1.16	4.98E-02	0.67

cg10492999	ENSG00000184697	LINC00974	3.458	4.94E-02	0.67
cg11221200	ENSG00000115685	TEPSIN	-2.25	2.66E-02	0.67
cg11221200	ENSG00000146205	PPP1R7	6.327	3.36E-02	0.67
cg11983245	ENSG00000226629	LINC00974	6.011	3.40E-02	0.67
cg14814323	ENSG00000166311	ZNF184	-2.589	4.95E-02	0.67
cg20296990	ENSG00000167302	RGL2	1.351	2.78E-02	0.67

Supplemental Table 3-3. *Table of top results from the GO-term and KEGG pathway analyses of top 298 CpG sites (BH q<0.10). N refers to the overall number of genes annotated to the term or pathway and DE refers to the number of genes from the top CpG sites within that term or pathway.*

GO-term ID	**Term**	**N**	**DE**	**P-val**	**q-val**
GO:0098609	Cell-cell adhesion	744	37	2.45E-08	1.77E-04
GO:0098742	Cell-cell adhesion via plasma-membrane adhesion molecules	221	26	2.14E-12	4.64E-08
GO:0007156	Homophilic cell adhesion via plasma membrane adhesion molecules	150	22	2.36E-11	2.56E-07
KEGG analysis					
KEGG pathway ID	**Pathway**	**N**	**DE**	**P-val**	**q-val**
path:hsa00290	Valine, leucine and isoleucine biosynthesis	4	1	0.044	1
path:hsa00512	Mucin type O-glycan biosynthesis	29	2	0.064	1
path:hsa04916	Melanogenesis	101	4	0.083	1

Supplemental Table 3-4. *Table of results from CircaDB analysis of EWAS gene results (n=45 genes, q<0.05). Gene list was entered and analyzed using a JTK q-value filter with a probability cut-off of 0.05 and JTK phase range of 0-40 of all available CIRCA mouse databases.*

UCSC Gene Name	**Rhythmic expression? (No/Yes)**	**CircaDB expression dataset (JTK q<0.05)**
AZI1	N	
BAIAP2	Y	Mouse 1.OST Brown Adipose, 1.OST Liver, Liver 48 hour Hughes 2009, 1.OST Kidney (Affymetrix), Mouse Wild Type SCN (GNF microarray)
BANF1	Y	Mouse 1.OST Liver, Pituitary 48 hour Hughes 2009 (Affymetrix)
BAT1	N	
BAT2	Y	Mouse Distal Colon 2008 (Affymetrix)
BATF3	Y	Mouse Liver 48 hour Hughes 2009 (Affymetrix)
C11orf2	N	
C2orf54	N	
CDYL2	N	
CLDN9	Y	Mouse Distal Colon 2008 (Affymetrix)
CLEC16A	Y	Mouse Distal Colon 2008 (Affymetrix)
CYB5R2	N	
DIP2C	Y	Mouse 1.OST Heart, 1.OST Kidney, Distal Colon 2008 (Affymetrix)
DPEP2	N	
EGFL8	N	
ERI3	Y	Mouse Distal Colon 2008 (Affymetrix)
FAM118A	N	
FAM172A	Y	Mouse 1.OST Liver, Liver 48 hour Hughes 2009 (Affymetrix)
FBXW7	Y	Mouse Heart LD (Affymetrix), Mouse Wild Type Muscle (GNF microarray)
GALNTL1	Y	Mouse Wild Type SCN (GNF microarray)
GALNTL4	Y	Mouse 1.OST Brown Adipose, 1.OST Lung, 1.OST Heart, Mouse Pituitary 48 hour Hughes 2009 (Affymetrix)
HAPLN1	Y	Mouse 1.OST Liver, Liver 48 hour Hughes 2009, 1.OST Adrenal Gland, 1.OST Aorta, Distal Colon 2008 (Affymetrix)
HDAC4	Y	Mouse 1.OST Heart, 1.OST Lung (Affymetrix)

HDLBP	Y	Mouse Liver 48 hour Hughes 2009, Distal Colon 2008, Mouse SCN MAS4 Panda 2002 (Affymetrix)
IQGAP2	Y	Mouse Liver 48 hour Hughes 2009 (Affymetrix), Mouse NIH 3T3 Immortilized Cell Line 48 hour Hughes 2009 (Affymetrix)
KRT15	N	
LOC645323	N	
LRRC2	Y	Mouse 1.OST Brown Adipose, Distal Colon 2008 (Affymetrix)
MFHAS1	Y	Mouse 1.OST Liver, 1.OST Lung (Affymetrix)
MIRLET7A3	N	
MSI2	Y	Mouse Liver 48 hour Hughes 2009, 1.OST Liver, 1.OST Kidney, Distal Colon 2008 (Affymetrix)
MXRA8	N	
NAV1	Y	Mouse 1.OST SCN 2014, Distal Colon 2008, 1.OST Heart (Affymetrix)
PKHD1L1	N	
PLEKHG6	N	
PTPN6	Y	Mouse Liver 48 hour Hughes 2009, 1.OST Lung (Affymetrix)
RHOT2	N	
RPS6KA4	Y	Mouse Distal Colon 2008, 1.OST Lung (Affymetrix)
SLC41A1	Y	Mouse 1.OST Brown Adipose, 1.OST Kidney, 1.OST Lung (Affymetrix)
SMPD1	Y	Mouse 1.OST Lung (Affymetrix)
TAPBP	Y	Mouse SCN MAS4 Panda 2002, SCN gcrma Panda 2002, 1.OST Adrenal Gland, 1.OST Lung, Mouse Aorta Rudic 2004, Distal Colon 2008 (Affymetrix), Mouse Wild Type Muscle (GNF microarray),
TUBGCP2	Y	Mouse 1.OST Hypothalamus, Mouse Liver 48 hour Hughes 2009 (Affymetrix)
UBR5	N	
ZBTB22	Y	Mouse Liver 48 hour Hughes 2009, 1.OST Liver (Affymetrix)

ZNF284	N	

Supplemental Table 3-5. *Trait-associated SNP enrichment within 10kb regions surrounding the top 298 CpG sites (BH q<0.05) among GWAS SNPs in NHGRI-EBI GWAS catalog that yielded trait-associations at p<1x10-8.*

Trait	**P-Value**	**BH q-value**	**taSNP Hits**	**Total taSNPs**
Psoriasis	4.24444E-13	7.1E-11	6	67
Lupus Erythematosus, Systemic	9.10157E-11	1.0E-08	5	73
Diabetes Mellitus, Type 1	7.66872E-08	6.4E-06	4	112
Multiple Sclerosis	3.92525E-05	1.2E-03	2	70

Chapter 4: Impacts of High Fat Diet on Ocular Outcomes in Rodent Models of Visual Disease

Published in a different format as:

Clarkson-Townsend DA, Douglass AJ, Singh A, Allen RS, Uwaifo IN, Pardue MT. Impacts of high fat diet on ocular outcomes in rodent models of visual disease. *Exp Eye Res*. 2021 Mar;204:108440. doi: 10.1016/j.exer.2021.108440. Epub 2021 Jan 11. PMID: 33444582; PMCID: PMC7946735.

Abstract

High fat diets (HFD) have been utilized in rodent models of visual disease for over 50 years to model the effects of lipids, metabolic dysfunction, and diet-induced obesity on vision and ocular health. HFD treatment can recapitulate the pathologies of some of the leading causes of blindness, such as age-related macular degeneration (AMD) and diabetic retinopathy (DR) in rodent models of visual disease. However, there are many important factors to consider when using and interpreting these models. To synthesize our current understanding of the importance of lipid signaling, metabolism, and inflammation in HFD-driven visual disease processes, we systematically review the use of HFD in mouse and rat models of visual disease. The resulting literature is grouped into three clusters: models that solely focus on HFD treatment, models of diabetes that utilize both HFD and streptozotocin (STZ), and models of AMD that utilize both HFD and genetic models and/or other exposures. Our findings show that HFD profoundly affects vision, retinal function, many different ocular tissues, and multiple cell types through a variety of mechanisms. We delineate how HFD affects the cornea, lens, uvea, vitreous humor, retina, retinal pigmented epithelium (RPE), and Bruch's membrane (BM). Furthermore, we highlight how HFD impairs several retinal cell types, including glia (microglia), retinal ganglion cells, bipolar cells, photoreceptors, and vascular support cells (endothelial cells and pericytes). However, there are a number of gaps, limitations, and biases in the current literature. We highlight these gaps and discuss experimental design to help guide future studies. Very little is known about how HFD impacts the lens, ciliary bodies, and specific neuronal populations, such as rods, cones, bipolar cells, amacrine cells, and retinal ganglion cells. Additionally, sex bias is an important limitation in the current literature, with few HFD studies utilizing female rodents. Future studies should use ingredient-matched control diets (IMCD), include both sexes in

experiments to evaluate sex-specific outcomes, conduct longitudinal metabolic and visual measurements, and capture acute outcomes. In conclusion, HFD is a systemic exposure with profound systemic effects, and rodent models are invaluable in understanding the impacts on visual and ocular disease.

Introduction

Diets high in fat, specifically saturated fats, are a common exposure with significant public health implications. High fat diets (HFD) are associated with metabolic disease(Feskens et al., 1995), cancer(Carroll et al., 1986), and neurological disease(Kalmijn et al., 1997). Total fat and saturated fat consumption is associated with the development of Type II diabetes(Risérus et al., 2009), which can lead to serious complications such as DR and blindness. Additionally, dietary fat is considered an important contributing factor in the global obesity epidemic(Hall, 2018; James et al., 2001). The global prevalence of obesity in the adult population is approximately 12%, numbering more than 600 million adults(Collaborators, 2017) and expected to continue growing. These trends are promoted by lifestyle factors such as diet and reduced physical activity that cause inflammation and weight gain, leading to obesity and metabolic diseases such as diabetes(Collaborators, 2017). Likewise, approximately 9% of the global population, 463 million people, are living with diabetes and this number is expected to rise to 578 million people by 2030(Saeedi et al., 2019).

Dietary fat is a well-known modulator of neurological health and disease. Consuming unhealthy trans and saturated fats is associated with dementia, cognitive disorders(Freeman et al., 2014), and Alzheimer’s Disease(Bayer-Carter et al., 2011). HFD consumption also exacerbates outcomes in animal models of brain injury(Shaito et al., 2020) and neurodegenerative disorders(Kothari et al., 2017; Nam et al., 2017). HFD drives these outcomes via immune activation and inflammation, atherosclerosis and vascular dysfunction, and altered hormonal and cell signaling cascades.

As part of the brain, the eye is also impacted by HFD, particularly in ocular diseases such as diabetic retinopathy (DR) and age-related macular degeneration (AMD). The epidemiological evidence linking fat consumption to DR development is mixed(Alcubierre et al., 2016; Dow et al., 2018), but when stratified by diabetes control, saturated fat intake increased the odds of DR development among people with well-controlled diabetes(Sasaki et al., 2015). Additionally, total and saturated fat consumption worsen DR risk factors, which improve with decreased saturated fat consumption(Cundiff and Nigg, 2005). AMD is also associated with altered lipid signaling and may be exacerbated or ameliorated by dietary fat(Chapman et al., 2019; Dighe et al., 2020; Merle et al., 2015; van Leeuwen et al., 2018). Lipid homeostasis is a significant driver in the development and progression of AMD, and polymorphisms in genes related to cholesterol metabolism and lipoproteins, such as *ABCA1* and *APOE*(Fritsche et al., 2016), as well as the complement system and *CFH*(Fritsche et al., 2016; Klein et al., 2005), are implicated in AMD. Likewise, consumption of saturated fatty acids and trans fats may contribute to AMD, but epidemiological studies are mixed(van Leeuwen et al., 2018).

Animal models are invaluable in understanding the impacts of HFD on DR and AMD disease mechanisms. Surprisingly, while the HFD model has been used in visual research for over 50 years, there are no comprehensive reviews summarizing the use of HFD in models of visual disease. Therefore, we systematically review and synthesize the scientific literature on the use of HFD in mouse and rat models of ocular disease. Additionally, we discuss current gaps and limitations in the literature to guide future research directions.

Methods for systematic review and results

In conducting this literature review, Pubmed, Web of Science, and ScienceDirect databases were systematically searched for peer-reviewed literature using the following search keywords: (high fat diet OR HFD OR western diet OR high fat) AND (retina OR eye OR ocular OR visual) AND (mouse OR mice OR rat). The search was performed for all years up to the last search date of July 18, 2020 and results de-duplicated prior to sorting.

Results were considered eligible for inclusion if they utilized a high fat diet (approximately 25-60% kcal fat), had an outcome that involved the eye or retina, and utilized a mouse or rat model. Results were excluded if they were published in a language other than English, only used qualitative methodology, were published as a conference abstract or non-peer reviewed journal, did not include relevant visual health outcomes (for example, non-rapid eye movement), did not include HFD or an appropriate description of the HFD model with brand information or diet breakdown, did not include appropriate control groups that allowed for the evaluation of the impact of HFD or the interaction of HFD on ocular outcomes, or were otherwise considered irrelevant to the topic. Additionally, duplicates or studies where the full text was unavailable were also excluded from the review.

The initial search resulted in 806 studies after de-duplication. Of these, 695 studies were considered irrelevant after initial abstract screening, leaving 111 studies considered for eligibility in full-text screening. On further inspection, 45 of these studies were excluded, yielding a total of 66 studies remaining for inclusion in this review (**Figure 4-1, Supplemental Table 4-1**). The references cited in the included studies were combed for additional articles that were not found in the original search but met eligibility requirements, producing 1 of the total 66 studies included in this review.

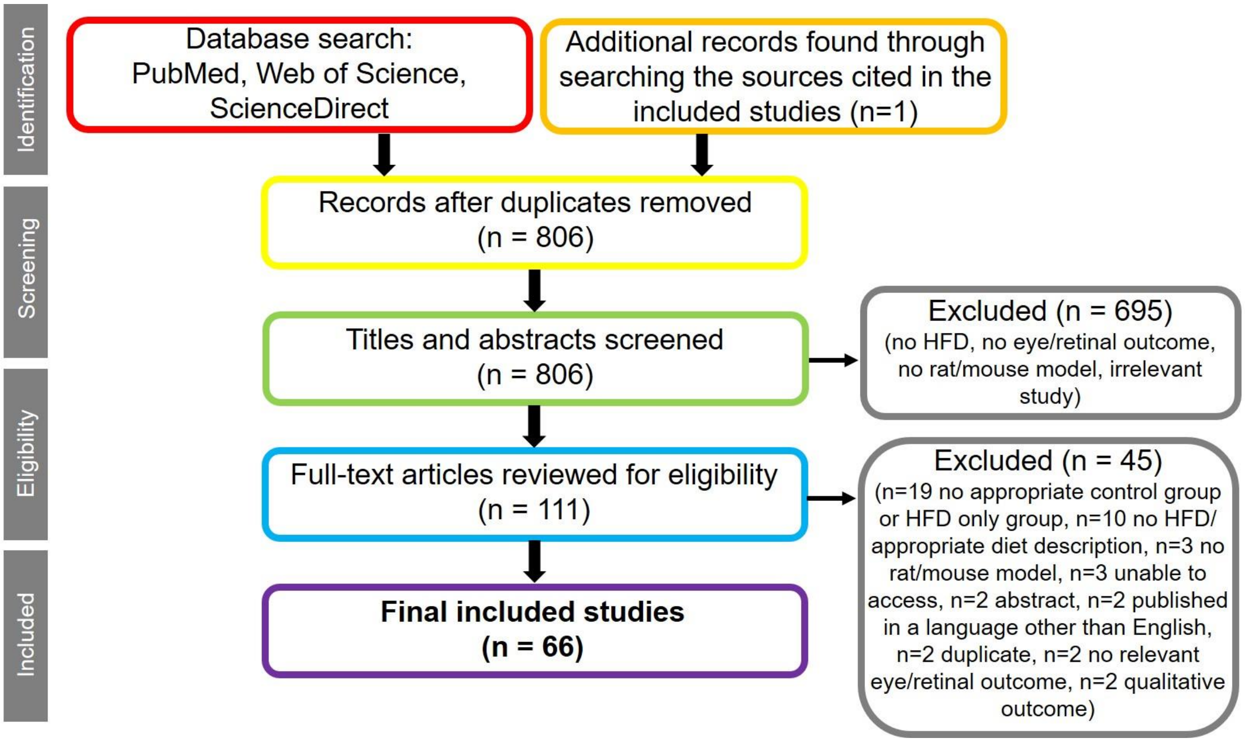
Identification
Screening
Eligibility
Included
Database search: PubMed, Web of Science, ScienceDirect
Additional records found through searching the sources cited in the included studies (n=1)
Records after duplicates removed (n = 806)
Titles and abstracts screened (n = 806)
Excluded (n = 695)
(no HFD, no eye/retinal outcome, no rat/mouse model, irrelevant study)
Full-text articles reviewed for eligibility (n = 111)
Excluded (n = 45)
(n=19 no appropriate control group or HFD only group, n=10 no HFD/ appropriate diet description, n=3 no rat/mouse model, n=3 unable to access, n=2 abstract, n=2 published in a language other than English, n=2 duplicate, n=2 no relevant eye/retinal outcome, n=2 qualitative outcome)
Final included studies (n = 66)

Figure 4-1. *Flow-chart of study identification, screening, eligibility criteria, and final studies included for the review.*

Characteristics of the reviews, such as diet composition and sex, were extracted and graphs created using R (data and code available on GitHub: https://github.com/dclarktown/HFD_review/tree/v1 DOI: 10.5281/zenodo.4003038).

HFD treatment

HFD rodent models have been used in research since at least the 1940’s(Samuels et al., 1942) and have only become more commonly used as the prevalence of obesity and metabolic diseases has increased(Blüher, 2019). Metabolic syndrome and diabetes are complex, systemic endocrine diseases that are growing public health crises. While societal and infrastructural change is necessary to slow and reverse these trends(Blüher, 2019), prevention and treatment approaches such as diet and lifestyle changes and medicines such as insulin and metformin, an oral hypoglycemic, are often prescribed for patients. Because these diseases are so prevalent, and only expected to keep rising(Saeedi et al., 2019), it is imperative to understand the mechanisms and impacts of these diseases and find new treatment options.

In animal models of diabetes and similar disorders, HFD treatment can induce metabolic disruption and diet-induced obesity. HFD perturbs metabolism and drives disease through multiple mechanisms, leading to chronic inflammation and inflammatory processes. HFD consumption also increases the absorption and signaling of free fatty acids (FFAs), which can directly exert inflammatory effects and promote insulin resistance by binding to Toll-like receptors(Könner and Brüning, 2011; Lee et al., 2015). The gut microbiome may also be an important mediator in the initial and chronic inflammatory response of HFD, as germ-free mice are protected from HFD-induced obesity(Bäckhed et al., 2007) and HFD consumption alters microbiota composition and increases intestinal permeability(Murphy et al., 2015; Sanmiguel et al., 2015). HFD research has been paradigm-shifting in many ways and has helped us gain a broader understanding of the roles of lipids in neurodegeneration, developmental metabolic programming, and the role of the immune system in metabolism.

In addition to the large body of research on HFD and development, metabolism, the microbiome, cardiovascular disease, and neurological disease, HFD is useful in modelling and understanding the influence of metabolic disease on ocular tissues and visual outcomes. The eye is a window to the brain(London et al., 2013), and as such, it is not only an easily-accessible visual organ, but serves as a biomarker of neurologic and systemic health(London et al., 2013).

This is very useful in clinical applications, as non-invasive or minimally invasive biomarkers can allow for earlier detection(Safi et al., 2018) and treatment of disease, improving patient outcomes and preserving vision.

Systemic and metabolic effects of HFD

HFD treatment affects systemic metabolic processes and energy balance. The most commonly reported outcomes of HFD treatment are diet-induced obesity and increased body weight (**Table 4-1**). Other common outcomes include impaired glucose tolerance, decreased insulin sensitivity, increased fat mass or percentage, increased serum cholesterol levels, and increased free fatty acid levels. Some outcomes, such as blood glucose and serum triglyceride levels, are very mixed. Differences in outcomes may be due to duration of diet, age of diet induction, strain, measurement error, and/or diet model used. However, approximately half of all the reviewed HFD studies provided information on body weight or systemic metabolic outcomes, which future studies should strive to include.

Table 4-1. *Summary of systemic and metabolic findings from reviewed studies.*

Outcome	Direction(s)	Reference(s)
Body weight	Increased	(Agardh et al., 2000; Alamri et al., 2019; Albouery et al., 2020; Asare-Bediako et al., 2020; Barakat et al., 2019; Bu et al., 2020; Chang et al., 2015b; Collins et al., 2018; Coppey et al., 2020; Coppey et al., 2018a; Coppey et al., 2018b; Dai et al., 2018a; Datilo et al., 2018; Davidson et al., 2014; Fink et al., 2020; Fujihara et al., 2009; Katsumata, 1970; Kim et al., 2017; Kneer et al., 2018; Lee et al., 2015; Marcal et al., 2013; Mohamed et al., 2020; Muhammad et al., 2019; Mykkanen et al., 2012; Nakazawa

		et al., 2019; Provost et al., 2009; Rajagopal et al., 2016; Shi et al., 2016; Shu et al., 2019; Wu et al., 2020; Yorek et al., 2015; Zhu et al., 2018)
	No change	(Chrysostomou et al., 2017; Dai et al., 2018b; Miceli et al., 2000; Miller et al., 2017)
Fat % or mass	Increased	(Albouery et al., 2020; Asare-Bediako et al., 2020; Chang et al., 2015b; Collins et al., 2018; Marcal et al., 2013; Rajagopal et al., 2016)
Steatosis	Increased	(Coppey et al., 2018b; Yorek et al., 2015)
Liver weight	Increased	(Miceli et al., 2000)
Blood pressure	Increased	(Mykkanen et al., 2012)
Blood glucose	Hyperglycemia	(Agardh et al., 2000; Albouery et al., 2020; Chang et al., 2015b; Datilo et al., 2018; Kim et al., 2017; Marcal et al., 2013; Mohamed et al., 2020; Muhammad et al., 2019; Mykkanen et al., 2012; Shi et al., 2016; Shu et al., 2019; Tuzcu et al., 2017)
	No change	(Alamri et al., 2019; Barakat et al., 2019; Chrysostomou et al., 2017; Coppey et al., 2020; Coppey et al., 2018a; Dai et al., 2018a; Dai et al., 2018b; Davidson et al., 2014; Fink et al., 2020; Miller et al., 2017; Yorek et al., 2015)
Glucose tolerance (GTT)	Decreased	(Chang et al., 2015b; Coppey et al., 2020; Datilo et al., 2018; Davidson et al., 2014; Katsumata, 1970; Kim et al., 2017; Kneer et al., 2018; Lee et al., 2015; Marcal et al., 2013; Rajagopal et al., 2016; Yorek et al., 2015; Zhu et al., 2018)
	No change	(Asare-Bediako et al., 2020)
Insulin sensitivity (ITT)	Decreased	(Asare-Bediako et al., 2020; Chang et al., 2015b; Datilo et al., 2018; Lee et al., 2015; Rajagopal et al., 2016; Zhu et al., 2018)

Serum insulin	Increased	(Agardh et al., 2000; Marcal et al., 2013; Rajagopal et al., 2016; Shu et al., 2019; Tuzcu et al., 2017; Zhu et al., 2018)
Serum triglycerides	Increased	(Barakat et al., 2019; Marcal et al., 2013; Nakazawa et al., 2019; Provost et al., 2009; Tuzcu et al., 2017; Zhu et al., 2018)
	No change	(Albouery et al., 2020; Coppey et al., 2018a; Fujihara et al., 2009; Schmidt-Erfurth et al., 2008; Yorek et al., 2015)
Serum cholesterol	Increased	(Asare-Bediako et al., 2020; Barakat et al., 2019; Bu et al., 2020; Coppey et al., 2020; Coppey et al., 2018b; Dithmar et al., 2001; Fujihara et al., 2009; Marcal et al., 2013; Nakazawa et al., 2019; Provost et al., 2009; Schmidt-Erfurth et al., 2008; Stanton et al., 2017; Tuzcu et al., 2017; Yorek et al., 2015)
	No change	(Albouery et al., 2020; Coppey et al., 2018a)
Low-density lipoprotein (LDL)	Increased	(Albouery et al., 2020)
	No change	(Marcal et al., 2013)
High-density lipoprotein (HDL)	Increased	(Marcal et al., 2013)
	No change	(Albouery et al., 2020; Provost et al., 2009; Schmidt-Erfurth et al., 2008)
Free Fatty Acids	Increased	(Coppey et al., 2018a; Mykkanen et al., 2012; Tuzcu et al., 2017; Zhu et al., 2018)
	No change	(Barakat et al., 2019; Fujihara et al., 2009; Yorek et al., 2015)
Hemoglobin A1C (HbA1c)	Increased	(Davidson et al., 2014)
	No change	(Asare-Bediako et al., 2020; Barakat et al., 2019; Yorek et al., 2015)

HFD studies tend to evaluate outcomes after chronic (≥2 months) exposure to HFD. While most studies reported weight and metabolic changes after a few months of HFD treatment, some have reported significant differences in body weight after only 1(Kim et al., 2017) or

2(Barakat et al., 2019) weeks of HFD treatment. However, the sparsity of studies with acute measurements leave a gap in the current literature.

Overall, because measurements of systemic outcomes are useful, future studies of HFD in models of visual disease should include longitudinal measures of (non-endpoint) metabolic impacts and/or biomarkers of disease. These longitudinal outcomes could also be utilized to evaluate correlations with ocular outcomes, possibly providing insight for improved early detection methods in human disease. Future studies should also evaluate acute (hours, days, weeks) effects of HFD on ocular outcomes.

HFD models of diet-induced obesity and diabetes

Models of obesity, diabetes, and DR generally employ HFD treatment to cause significant weight gain and metabolic disturbance. These models are utilized in vision research to better understand the visual and ocular impacts of metabolic dysregulation and hyperglycemia. Diabetes is a chronic metabolic disease characterized by problems in glucose homeostasis and can be elicited in animal models with chronic (≥2-5 months) HFD treatment, when fasting blood glucose levels typically rise above 250 mg/dL(Heydemann, 2016). This HFD model is useful in tracking the progression of metabolic dysfunction and in identifying early biomarkers of disease. There are a number of forms of diabetes, but the most common are Type 1 diabetes (approximately 5-10% of cases) and Type 2 diabetes (approximately 90-95% of cases). Type 2 diabetes generally begins with tissues becoming less responsive to insulin over time, driving a feedback loop of hyperglycemia, oxidative stress, damage to pancreatic beta cells, and decreased insulin output(Stumvoll et al., 2005). Unlike Type 1 diabetes, which is generally considered an autoimmune disease, Type 2 diabetes is most associated with metabolic dysfunction driven by obesity and diet(Hu et al., 2001; Taylor, 2013).

Hyperglycemia is modeled in rodents by damaging pancreatic beta cells, HFD feeding, utilizing specific strains or genetic knockouts, or a combination of these approaches. Of the studies that induce metabolic dysfunction solely through HFD feeding, there are a number of HFD models. Generally, HFD treatment consists of feeding a diet 25%-60% kcal from fat. There are some variations, such as the "Western diet" HFD model, which is generally composed of 40-45% kcal from fat and has an enriched amount of saturated fat. Other variants are the high fat-high sucrose (HFHS) and high fat-high fructose models, which incorporate high levels of sucrose or fructose as part of the carbohydrate portion of the HFD. While not included in this review, the ketogenic diet, a diet that is low in carbohydrates and very high in fat (~75%+ kcal from fat), has gained renewed interest among researchers. The specific impacts of HFD on ocular tissues and outcomes are described in detail in the ocular tissue sections.

STZ with HFD Models of Type 1 and Type 2 Diabetes and DR

In addition to HFD feeding, diabetes is also modelled in rodents using a combination of HFD and high or low-dose streptozotocin (STZ), a beta cell toxin. Type 1 diabetes is characterized by autoimmune loss of the insulin-producing beta cells of the pancreas, causing blood glucose levels to rise because of decreased insulin output(Belle et al., 2011). The streptozotocin (STZ) model is a well-characterized animal model of Type 1 diabetes and it is commonly utilized in models of diabetic retinopathy (DR) and diabetic neuropathy(Furman, 2015). Originally isolated from soil bacteria, STZ has antibiotic properties and inhibits DNA synthesis. As a toxic analog of glucose, it is preferentially taken up by pancreatic beta cells via glucose 2 transporters, where it causes cell death through methylation, oxidative stress, and other mechanisms(Eleazu et al., 2013); however, it is also taken up by other tissues that express this transporter and have high glucose absorption, such as the liver, kidneys, and brain(Eleazu et al., 2013), an important consideration when utilizing the STZ model.

To induce diabetes, STZ is given intraperitoneally to the mouse or rat, usually parceled out in a few low-dose injections in the mouse model or as a single injection in the rat model(Furman, 2015). The effectiveness of STZ in causing beta-cell loss and hyperglycemia is strain and sex-dependent, with females generally showing less overt hyperglycemia than males(Furman, 2015; Kolb, 1987), possibly due to the protective and antidiabetic effects of estradiol(Le May et al., 2006). In addition to using STZ as a Type 1 model of diabetes, low-dose STZ treatment is also sometimes combined with HFD feeding to model Type 2 diabetes. These models are also utilized in vision research to model DR. While mouse and rat models do not adequately model the later stages of DR (for example, retinal neovascularization), they do recapitulate many characteristics of the disease, such as inflammation, decreased retinal function, visual function, pericyte loss, and vascular leakage(Robinson et al., 2012).

In this review, the studies that modelled Type 1 or Type 2 diabetes and DR using a combination of STZ and HFD treatment equally utilized mouse and rat models (**Figure 4-2A, Supplemental Table 4-1**). However, the majority used males, with only 1 study(Coppey et al., 2018b) reporting the inclusion of female animals (perhaps partly due to the sex differences in responsiveness to STZ). All studies initiated HFD feeding at 1-3 months of age and most (90%) fed a HFD containing 40-60% calories from fat (**Figures 4-2B-C**). A majority of these studies focused on corneal outcomes (60%) while the remaining focused on retinal and RPE outcomes. Corneal defects included decreased corneal sensitivity(Coppey et al., 2020; Davidson et al., 2014; Fink et al., 2020), decreased corneal nerve fiber density(Alamri et al., 2019; Coppey et al., 2020; Coppey et al., 2018b; Davidson et al., 2014; Yorek et al., 2015), and decreased corneal nerve fiber length(Coppey et al., 2020; Coppey et al., 2018b; Davidson et al., 2014) (**Table 4-2**). HFD in combination with STZ was also found to heighten immune activation and inflammatory processes(Barakat et al., 2019; Jo et al., 2019; Mancini et al., 2013), but not all studies include appropriate control groups to allow assessment of the interactions between HFD and STZ treatment.

Table 4-2. *Summary of outcomes from studies that utilized a model of HFD and STZ.*

Treatment Group	**Outcomes**	**Reference(s)**
HFD, HFD + STZ	Decreased corneal nerve fiber density and/or nerve fiber length	(Alamri et al., 2019; Coppey et al., 2020; Coppey et al., 2018b; Davidson et al., 2014; Yorek et al., 2015)
	Decreased corneal sensitivity	(Coppey et al., 2020; Davidson et al., 2014; Fink et al., 2020)
HFD + STZ	Increased leukocyte adhesion, increased endothelial cell injury and death	(Barakat et al., 2019)
	Reduced RGC survival	(Shanab et al., 2012)
	Increased markers of inflammatory and immune response, reduced number of pericytes, increased number of acellular capillaries, decreased retinal thickness and number of retinal ganglion cells	(Mancini et al., 2013)
	Increased microglial recruitment to RPE	(Jo et al., 2019)

HFD and Genetic Models of AMD

AMD, one of the most common causes of blindness, is caused by retinal degeneration that leads to gradual visual field loss. Pathological features of AMD include deposition of membranous debris containing proteins, lipids, and/or complement proteins(Curcio et al., 2001; Curcio et al., 2005; Mitchell et al., 2018; van Lookeren Campagne et al., 2014) and basal laminar deposits, made up of thickened extracellular matrix material between the retinal pigment epithelium (RPE) and Bruch's membrane (BM)(Mitchell et al., 2018; Sarks et al., 2007; Sura et al., 2020). HFD alone or with exposures such as cigarette smoke promote basal laminar deposit growth and alter BM and RPE morphology(Espinosa-Heidmann et al., 2006; Roddy et al., 2019).

With age the RPE becomes less efficient at clearing waste products, leading to buildup of cellular debris and lipids and causing inflammation and cell death(Ebrahimi and Handa, 2011; van Lookeren Campagne et al., 2014). Risk factors for AMD development include age (>50 years), having a history of smoking, and certain genetic polymorphisms(Chakravarthy et al., 2010). AMD is more prevalent among females, possibly because AMD is highly age-related and women tend to live longer than men(Owen et al., 2012). Because of these risk factors, rodent models of AMD sometimes use aged female rodents(Cousins et al., 2003; Espinosa-Heidmann et al., 2006; Schmidt-Erfurth et al., 2008), as well as genetically modified strains fed a HFD (**Figure 4-2**).

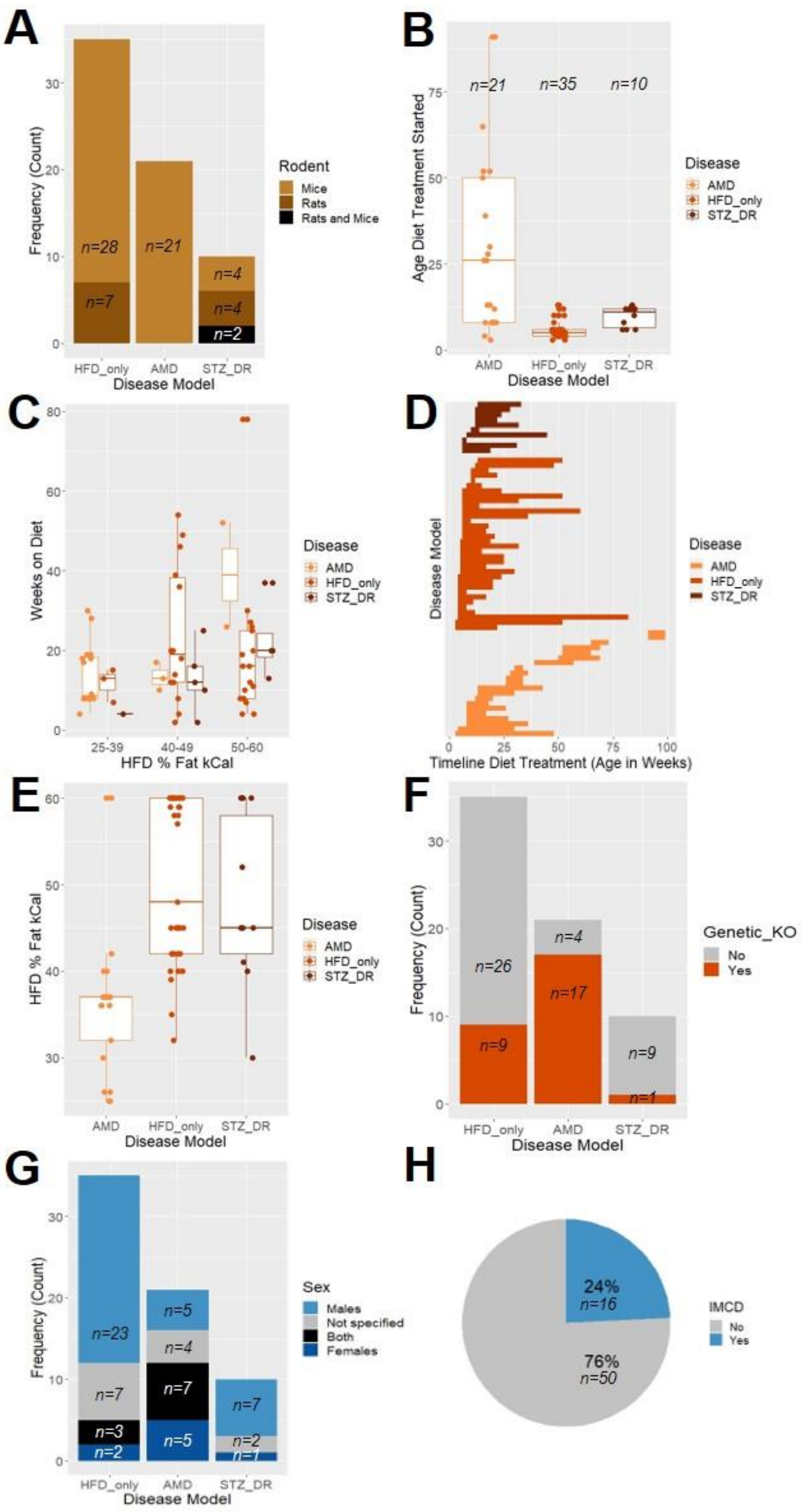

Figure 4-2. *Characteristics of the studies included in the review.* ***A****) The number of studies that utilize mice, rat, or mice and rat models in the experiment, separated by HFD model.* ***B****) Age*

(weeks) at which HFD treatment started, separated by HFD model; some studies used mice or rats of varying ages, in which case the youngest age at which diet treatment was started was used. ***C****) Number of weeks rodents were treated with HFD, separated by model.* ***D****) Timeline of start age (weeks) to end age (weeks) of HFD treatment, separated by model.* ***E****) HFD fat % used, separated by model.* ***F****) Number of studies that utilized a genetic knockout or knock-in strain, separated by HFD model.* ***G****) Number of studies by sex specification of rodents used, separated by model.* ***H****) Breakdown of the number of studies that did and did not utilize an ingredient-matched control diet (IMCD).*

The AMD HFD models reliably produce sub-RPE deposits, particularly in aged rodents. As lipid metabolism and complement factor signaling are implicated as the primary genetic(Fritsche et al., 2016) and pathological drivers of AMD, AMD models commonly utilize strains with genetically manipulated complement factor proteins or lipoproteins(Pennesi et al., 2012). Other drivers of AMD include oxidative stress and aging processes(Beatty et al., 2000), which may act in concert with the complement system. Therefore, exposure to cigarette smoke or blue light is also sometimes utilized in animal models to recapitulate the human disease (**Table 4-3**).

Table 4-3*. Summary of systemic and metabolic findings from reviewed studies.*

Treatment Group	Outcome(s)	Reference(s)
HFD	Thicker BM	(Dithmar et al., 2001; Roddy et al., 2019)
	No change BM thickness	(Schmidt-Erfurth et al., 2008)
	Increased basal laminar deposits, loss of RPE cells	(Roddy et al., 2019)

	Increased lipofuscin area, decreased number of fenestrations	(Zhang et al., 2018)
	Increased lesions in RPE	(Zhao et al., 2014)
HFD + blue light	Basal laminar deposits	(Cousins et al., 2002; Cousins et al., 2003; Espinosa-Heidmann et al., 2006)
HFD + cigarette smoke	Sub-RPE deposits	(Espinosa-Heidmann et al., 2006; Stanton et al., 2017)
	Thicker BM	(Espinosa-Heidmann et al., 2006)
HFD + *APOE*	Thicker BM	(Ding et al., 2011; Picard et al., 2010)
	Increased complement activation, Aβ deposition	(Ding et al., 2011)
	Increased lipid accumulation in RPE	(Lee et al., 2007)
	Decreased ERG b-wave amplitude	(Ding et al., 2011)
HFD + *APOE2/3/4*	RPE vacuolization (E2, E3), mottled RPE (E2), thicker BM (E4), hypo and hyperpigmentation of RPE and atrophy (E4), sub-RPE deposits (E4), neovascularization positive for VEGF and Aβ (E4)	(Malek et al., 2005)
HFD + *Cfh*	Decreased ERG b-wave amplitude, increased number of multinucleated RPE cells	(Landowski et al., 2019; Toomey et al., 2015; Toomey et al., 2018)
	Increased complement activation	(Landowski et al., 2019)
	Increased sub-RPE deposit height	(Toomey et al., 2015; Toomey et al., 2018)
	Increased expression of inflammatory genes, increased leukocytes and monocytes in peripheral blood	(Toomey et al., 2018)

HFD + *Pgc1α*$^{-/-}$	Decreased IS and OS thickness, increased expression of genes related to lipid deposition, increased lipofuscin area, decreased number of fenestrations	(Zhang et al., 2018)
HFD + *Nrf2*$^{-/-}$	Increased sub-retinal deposits, increased lesion progression, increased sub-RPE cells, increased lesions in RPE	(Zhao et al., 2014)
HFD + *SR-BI*$^{-/-}$	Thicker BM, sub-RPE deposits, increased VEGF staining	(Provost et al., 2009)
HFD + *Ldlr*$^{-/-}$, *Ldlr*$^{-/-}$	Increased VEGF expression	(Rudolf et al., 2005; Schmidt-Erfurth et al., 2008)
	Thicker BM, decreased fenestrations, decreased luminal vessel diameter, decreased RPE height	(Schmidt-Erfurth et al., 2008)
	Increased BM deposits	(Rudolf et al., 2005)
HFD + *Igf-II/Ldlr-/-ApoB100*, *Igf-II/Ldlr-/-ApoB100*	No change in retinal vasculature, altered retinal morphology	(Kinnunen et al., 2013)
HFD + *Abca1/g1*$^{F/F}$ and *Abca1/g1*$^{-rod/-rod}$	Lipid accumulation, accelerated degeneration of photoreceptor outer segments, decreased ERG b-wave amplitudes (*Abca1*/*g1*$^{-rod/-rod}$)	(Ban et al., 2018)
HFD + *ApoB100*	Increased basal deposits	(Fujihara et al., 2009)
	decreased WNT signaling in RPE	(Ebrahimi et al., 2018)
HFD + *ApoB100* + cigarette smoke	Increased RPE atrophy, decreased OS and IS thickness, decreased ONL thickness	(Ebrahimi et al., 2018)
HFD + *ApoB100* + blue light	Increased basal lamina deposits	(Espinosa-Heidmann et al., 2004)

All reviewed studies modelling AMD or sub-retinal lipid deposition utilized mouse models (**Figure 4-2A**, **Supplemental Table 4-1**). The majority of these studies fed a HFD with 25-39% fat kcal (78%), initiated HFD feeding at or after 3-6 months of age (61%), utilized a genetically modified strain (78%), and used female animals (56%)(**Figures 4-2B-G**). Many of the reviewed studies utilized genetically manipulated strains to better model the known genetic risk factors identified in human population studies (**Table 4-3**). Among these, Apolipoprotein E

(*APOE*)(Huang and Mahley, 2014), peroxisome proliferator-activated receptor-γ coactivator 1-α (*Pgc1α*)(Zhang et al., 2004), scavenger receptor class B type 1 (*SR-BI*)(Rhainds and Brissette, 2004), low density lipoprotein receptor (*LDLr*)(Go and Mani, 2012), ATP binding cassette subfamily A member 1 (*ABCA1*)(Phillips, 2018), and apolipoprotein B-100 (*ApoB100*)(Olofsson and Borén, 2005) play roles in lipid metabolism while Complement factor H (*Cfh*)(Ferreira et al., 2010) and Nuclear factor erythroid 2-related factor 2 (*Nrf2*)(Itoh et al., 2004) mediate immune and inflammatory responses. These genetic models are useful in understanding the contributions and interactions of genetic and environmental impacts on AMD development(Pennesi et al., 2012).

Across some of the reviewed studies, HFD alone increased thickness and lipid deposition of BM(Dithmar et al., 2001; Roddy et al., 2019; Zhang et al., 2018) and impaired retinal pigment epithelium (RPE) integrity(Zhao et al., 2014) (**Table 4-3**). HFD in combination with blue light or cigarette smoke, exposures that cause oxidative stress, led to increased lipid deposition(Cousins et al., 2002; Cousins et al., 2003; Espinosa-Heidmann et al., 2006) (**Table 4-3**). Results from studies that utilized HFD in combination with a genetically manipulated strain were dependent on the targeted gene, but overall tended to increase sub-RPE deposition and alter RPE morphology and/or signaling(Ding et al., 2011; Lee et al., 2007; Toomey et al., 2015; Toomey et al., 2018; Zhang et al., 2018; Zhao et al., 2014) (**Table 4-3**).

Effects of HFD on ocular tissues and possible mechanisms

As HFD treatment is a systemic exposure, it impacts many different ocular tissues – an important consideration when designing studies and evaluating results. Here, we discuss how HFD treatment impacts different ocular tissues. Tissue sections are organized starting from the front of the eye and moving towards the back of the eye and grouped according to the focus of the reviewed literature.

Cornea, lens, uvea, and vitreous humor

The impacts of HFD on the cornea have been evaluated primarily in the context of diabetes and diabetic neuropathy. This tissue not only makes up the majority of the eye's total refractive power, but also acts as a defensive barrier, producing tear film with lubricating and anti-microbial properties(Blackburn et al., 2019; Dartt and Willcox, 2013). Well-organized unidirectional collagen fibers make the cornea transparent and allow light to pass through corneal tissue into the eye chamber, unlike the irregular fibers of the opaque sclera. Because of the cornea's role in vision, it is important to understand how diabetes and metabolic disturbance may impair corneal integrity and function.

There are reports of HFD altering corneal morphology and structure (**Table 4-4**). While no differences were found in thickness of the corneal epithelia, the stromal layer was found to be thicker after HFD(Kneer et al., 2018). HFD exposure also decreased corneal endothelial cell density and hexagonal cell number, possibly due to disrupted tight junctions between corneal epithelial cells, increased oxidative stress(Bu et al., 2020), and increased keratinization and matrix metalloprotease expression(Wu et al., 2020). Additionally, HFD may influence the development of dry eye symptoms and impair the integrity of the corneal surface; HFD treatment increased corneal permeability, decreased tear production, and decreased the number of goblet cells(Wu et al., 2020) responsible for producing mucins for ocular tear film and eye lubrication (**Figure 4-3**).

Table 4-4. *Summary table of reviewed corneal, vitreous, and lens outcomes after HFD treatment.*

Tissue	**Outcome(s)**	**Direction(s)**	**Reference(s)**
Cornea	Corneal endothelial cell density	Decreased	(Bu et al., 2020)
	Epithelial thickness	No change	(Kneer et al., 2018)
	Stromal thickness	Decreased	(Kneer et al., 2018)
	Goblet cell number	Decreased	(Wu et al., 2020)
	Tear production	Decreased	(Wu et al., 2020)
	Palmitate concentration in aqueous humor	Increased	(Bu et al., 2020)
	Lipid droplets	Increased	(Bu et al., 2020)
	Expression of tight junction proteins	Decreased	(Bu et al., 2020)
	Corneal permeability	Increased	(Wu et al., 2020)
	Corneal nerve fiber density and/or nerve fiber length	Decreased	(Alamri et al., 2019; Coppey et al., 2020; Coppey et al., 2018a; Coppey et al., 2018b; Davidson et al., 2014; Yorek et al., 2015)
	Corneal sensitivity	Decreased	(Coppey et al., 2020; Davidson et al., 2014; Fink et al., 2020)
	Corneal whorl integrity	Decreased	(Kneer et al., 2018)
Lens	Markers of oxidative stress	Increased	(Jayaratne et al., 2017)
	Glutathione concentration, ascorbic acid concentration	Decreased	(Nakazawa et al., 2019)
Uvea	Uveitis	Increased	(Muhammad et al., 2019)
Vitreous humor	Inflammatory markers	Increased	(Collins et al., 2018)

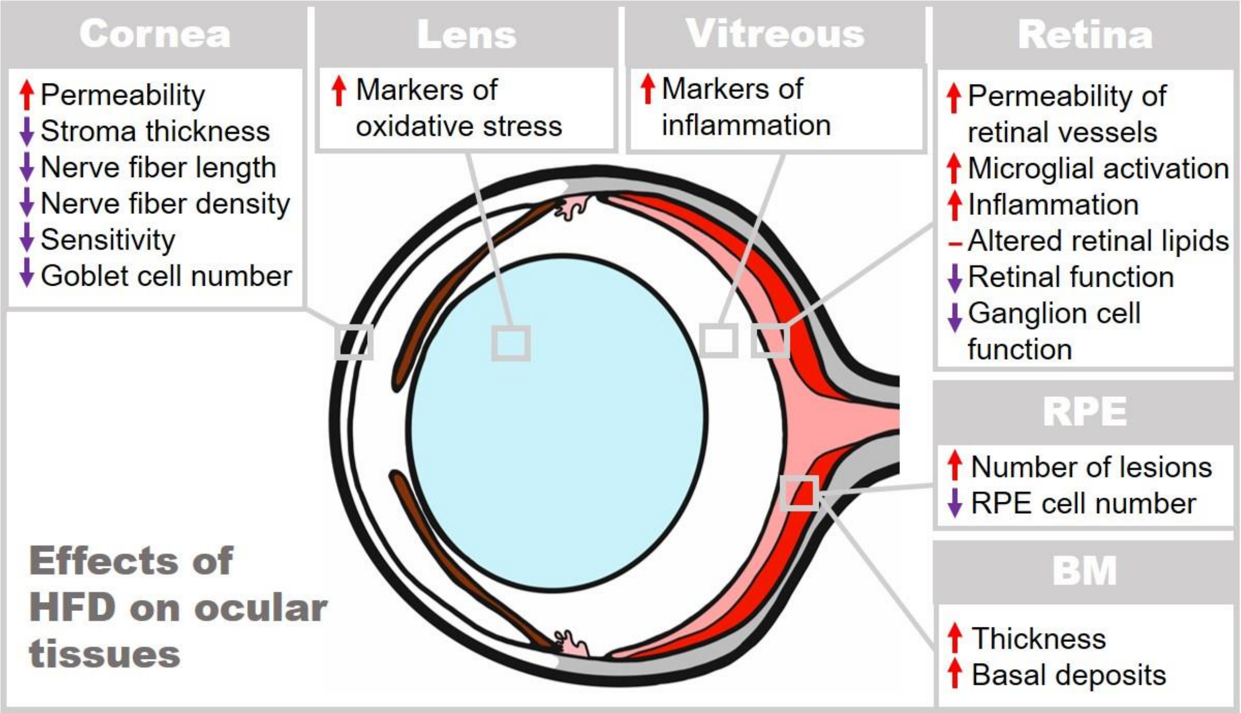
Cornea
↑ Permeability
↓ Stroma thickness
↓ Nerve fiber length
↓ Nerve fiber density
↓ Sensitivity
↓ Goblet cell number
Lens
↑ Markers of oxidative stress
Vitreous
↑ Markers of inflammation
Retina
↑ Permeability of retinal vessels
↑ Microglial activation
↑ Inflammation
– Altered retinal lipids
↓ Retinal function
↓ Ganglion cell function
RPE
↑ Number of lesions
↓ RPE cell number
BM
↑ Thickness
↑ Basal deposits
Effects of HFD on ocular tissues

Figure 4-3. *Diagram of a mouse / rat eye and how HFD affects different parts of the eye. RPE signifies retinal pigment epithelium and BM signifies Bruch's membrane*.

Particular attention has been paid to the impact of HFD on corneal nerve integrity and response, as the cornea is one of the body's most highly innervated tissues(Bonini et al., 2003). It impairs corneal sensitivity(Coppey et al., 2020; Davidson et al., 2014; Fink et al., 2020) and corneal nerve fiber density and length(Alamri et al., 2019; Coppey et al., 2020; Coppey et al., 2018a; Coppey et al., 2018b; Davidson et al., 2014; Yorek et al., 2015) in the central region of the cornea(Alamri et al., 2019), where nerve length is longest, and in the inferior whorl(Davidson et al., 2014), an innervated area of the cornea located inferior and nasal to the corneal center. The structure of the corneal whorl is also disrupted by HFD(Kneer et al., 2018). Additionally, peripheral and central corneal cold thermoreceptors populations (as labelled by TRPM8), but not corneal nociceptor populations (as labelled by TRPV1), appear to be vulnerable to HFD(Alamri et al., 2019). Because corneal nerves are responsible for sensing stimuli as well as stimulating tear production and the blinking reflex, damage to them can impair tear film production and corneal integrity.

Research on how HFD impacts the lens and vitreous is sparse (**Table 4-4**). The lens is a tissue with a layered life history, with the core developing *in utero* and the outer cortex developing postnatally. While the lens is a continually-growing tissue, embryonic lens cells are preserved in the central core with cells layered postnatally in the outer cortex(Augusteyn, 2010). As a tissue with both embryonic and adult components, the lens can be useful in investigating the impacts of prenatal and postnatal exposures, such as nutrition. A developmental study found that prenatally undernourished rats (males and females) developed significantly more markers of oxidative stress in the lens core and cortex when postnatally fed a HFD(Jayaratne et al., 2017). When the control group (not prenatally undernourished) were fed a HFD, males (but not females) had increased markers of oxidative stress in the lens cortex(Jayaratne et al., 2017). HFD feeding has also been found to decrease levels of the antioxidants glutathione and ascorbic acid in the lens(Nakazawa et al., 2019). Metabolic disturbance such as diabetes can cause cataract formation(Javadi and Zarei-Ghanavati, 2008) and has been reported in a rat model of diabetes, but the HFD only group did not show signs of cataract(Su et al., 2014). These findings support the idea that the lens can serve as a biomarker for exposures across the lifespan, but more research is necessary to understand the relationship between the lens and visual outcomes in HFD models.

The uvea comprises the choroid, ciliary body, and iris. It plays important roles in metabolic support, light regulation, and accommodation. HFD treatment was found to exacerbate outcomes in an experimental model of autoimmune uveitis(Muhammad et al., 2019), suggesting it can worsen immune-related outcomes. The vitreous humor, encapsulated by the vitreous membrane, is a gel-like substance filling the space between the lens and the retina. HFD treatment has been found to increase the expression of inflammatory markers such as IL-1B, IL-6, IL-13, IL-17, and IL-18 in the vitreous humor of rats fed a HFHS diet(Collins et al., 2018). These inflammatory markers were also significantly correlated with body fat, suggesting that diet-induced obesity may increase ocular inflammation and influence the development of ocular disease with inflammatory components, such as DR and uveitis(Collins et al., 2018).

Retina

The majority of HFD research in ocular disease models focuses on retinal outcomes (**Table 4-5**). For its size, the retina is one of the most metabolically active tissue in the body(Arden et al., 2005). This thin layer of tissue draws from the retinal and choroidal blood supply and its own rich fatty acid stores to support energy demands. Because it is so metabolically active, it has many mechanisms to scavenge and quench reactive oxygen species; however, it is still vulnerable to oxidative stress(Saccà et al., 2018). Additionally, the rich stores of polyunsaturated fatty acids in the retina are susceptible to oxidation(Stone et al., 1979). As disruption of retinal nutrient supply can lead to pathologies such as abnormal angiogenesis and photoreceptor degeneration(Sun and Smith, 2018), it is reasonable to assume that HFD-induced metabolic disruption would negatively affect retinal health.

Table 4-5. *Summary table of reviewed retinal outcomes after HFD treatment.*

Retinal Tissue	Outcome(s)	Direction(s)	Reference(s)
Retinal neuronal morphology	Retinal thickness	No change	(Atawia et al., 2020; Chang et al., 2015b; Rajagopal et al., 2016)
		Decreased	(Marcal et al., 2013)
	Axonal thickness	Decreased	(Zhu et al., 2018)

	Ganglion cell function	Decreased	(Shu et al., 2019; Zhu et al., 2018)
	Synaptophysin expression	Decreased	(Shu et al., 2019; Zhu et al., 2018)
Retinal vasculature	Acellular capillaries	Increased	(Mohamed et al., 2014; Mohamed et al., 2020)
		No change	(Asare-Bediako et al., 2020; Rajagopal et al., 2016)
	Endothelial cell:pericyte ratio	No change	(Agardh et al., 2000)
	Vascular density	Decreased	(Asare-Bediako et al., 2020)
	Vascular leakage / permeability	Increased	(Asare-Bediako et al., 2020; Mohamed et al., 2020; Rajagopal et al., 2016)
		No change	(Zhu et al., 2018)
	Vessel branching	Decreased	(Mohamed et al., 2020)
	Vessel bleeding	Increased	(Katsumata, 1970)
	Vascular lesions	No change	(Shu et al., 2019)
	Vascular eNOS and nNOS	Decreased	(Marcal et al., 2013)
Inflammatory signaling	Microglial activation	Increased	(Atawia et al., 2020; Lee et al., 2015)
	Adherent leukocytes / signaling	Increased	(Mohamed et al., 2020; Tuzcu et al., 2017)
	Immune cells	Increased	(Lee et al., 2015)
	iNOS expression	Increased	(Tuzcu et al., 2017)
	NF-κB signaling	Increased	(Lee et al., 2015; Tuzcu et al., 2017)
	Markers of inflammation	Increased	(Chang et al., 2015b; Marcal et al., 2013)
	Cytokines	Increased	(Kim et al., 2017; Lee et al., 2015)
	Glutathione and cysteine levels	No change	(Agardh et al., 2000)
	miR150 expression	Decreased	(Shi et al., 2016)
Retinal lipids	Spots on fundus imaging	Increased	(Asare-Bediako et al., 2020; Barathi et al., 2014)
	Lipid levels	Altered	(Albouery et al., 2020; Dai et al., 2018a)

	Lipid peroxidases	Increased	(Mohamed et al., 2014)
Other signaling	Glycolytic processes	Altered	(Katsumata, 1970)
	Protein O-GlcNAcylation	Increased	(Dai et al., 2018b)
	Abnormal tau phosphorylation	Increased	(Zhu et al., 2018)
	Akt/JNK signaling	Altered	(Dai et al., 2018a; Miller et al., 2017)
	AKT_1 expression	Decreased	(Marcal et al., 2013)
	HIF1α expression	Increased	(Asare-Bediako et al., 2020)
	LXRβ expression	Decreased	(Asare-Bediako et al., 2020)
	Crystallin expression	Increased	(Mykkanen et al., 2012)
	GLP-1 expression	Decreased	(Shu et al., 2019)
	GLUT4 expression	Decreased	(Chang et al., 2015b)

The effects of HFD on retinal morphology are mixed, with some authors reporting no differences in retinal layer thickness(Atawia et al., 2020; Chang et al., 2015b) and others reporting axonal(Zhu et al., 2018) and retinal thinning(Marcal et al., 2013), possibly due to increased retinal cell death(Dai et al., 2018a)(**Figure 4-3, Table 4-5**). When comparing these studies for sources of variability, the strains, age at which diet began, and diet duration were similar, but dietary fat ratio was different. Those that reported no differences used a 59-60% fat kcal diet, while those that did report differences used a 39-45% fat kcal diet. Alternatively, the variability may be due to measurement sensitivity and error.

HFD induces vascular changes in the retina, causing retinal vascular endothelial cell injury, increased expression of adhesion markers such as ICAM-1 in retinal vessels(Barakat et al., 2019), and increased acellular capillaries(Mohamed et al., 2014), a hallmark of DR. However, others report no difference in ratio of endothelial cells to pericytes after HFD treatment(Agardh et al., 2000), although this could be due to decreases in both endothelial cells and pericytes. HFD also increases the permeability of retinal vessels(Rajagopal et al., 2016; Zhu et al., 2018) and can even lead to bleeding in retinal vessels(Katsumata, 1970), one of the mechanisms that leads to abnormal angiogenesis and neovascularization in the eye. However, while disorders such as DR are often viewed as vascular in nature, it is now understood that neuronal dysfunction in the retina often precedes vascular symptoms(Lynch and Abràmoff, 2017; Simó et al., 2018), highlighting the need for neuronal assessments.

Feeding a diet high in fat may also alter the lipid composition of the retina (fats comprise approximately 20% of the retina’s dry weight (Fliesler and Anderson, 1983)), influencing the retina’s vulnerability to oxidative stress, energy availability, and altering retinal signaling. Lipids act as ligands and signaling molecules and mediate vesicle secretion and fusion(Wymann and Schneiter, 2008). It has been shown that HFD treatment alters retinal fat composition, decreasing levels of tetracosanoic acid, palmitoleic acid, and vaccenic acid, and increasing ratios of linoleic acid:alpha-linolenic acid(Albouery et al., 2020) and retinal sphingolipids(Dai et al., 2018a), including ceramide, which is implicated in retinal and neurodegenerative disease(Simón et al., 2019). Therefore, these HFD-induced changes in retinal lipid composition could be an important component of retinal disease.

While the retina has robust systems in place to neutralize oxidative stress, it is nevertheless vulnerable to fatty acid oxidation and metabolic disturbance. HFD increases retinal lipid peroxidases(Mohamed et al., 2014) and disrupts retinal glycolytic processes(Katsumata, 1970). This metabolic dysregulation can cause inflammation. HFD has been shown to activate retinal microglia(Atawia et al., 2020; Lee et al., 2015), potentially via TLR4, which may be responsible for the increased inflammatory markers(Chang et al., 2015b), cytokines(Kim et al., 2017; Lee et al., 2015), and immune cells(Lee et al., 2015) also found following HFD treatment. Insulin resistance, glucose intolerance, and microglial activation appear to occur simultaneously in the retina(Lee et al., 2015). HFD also increased expression(Tuzcu et al., 2017) and phosphorylation(Lee et al., 2015) of NF-κB and decreased retinal Nrf-2(Tuzcu et al., 2017), well-known regulators of inflammatory signaling. Interestingly, HFD-fed mice with astrocyte-specific conditional deletion of *IKKβ*, part of the NF-κB pathway, had improved glucose tolerance(Douglass et al., 2017). All together, these studies suggest that the immune system is an important mediator in the metabolic responses to HFD and modulating it may ameliorate some of the impacts of HFD.

A number of other signaling mechanisms have been implicated in the retinal effects of HFD (**Table 4-5**). HFD may influence retinal metabolic dysfunction by increasing protein O-GlcNAcylation(Dai et al., 2018b), altering retinal Akt/JNK signaling(Dai et al., 2018a; Miller et al., 2017), and decreasing AKT_1(Marcal et al., 2013) and GLP-1 expression(Shu et al., 2019), a proglucagon peptide that decreases blood glucose by increasing insulin secretion. Decreased expression of the *GLUT4* glucose transporter in the retina(Chang et al., 2015b) suggests altered retinal glucose trafficking after HFD treatment. Increased iNOS(Tuzcu et al., 2017) and decreased eNOS and nNOS(Marcal et al., 2013) may also be mediators or symptoms of the noted vascular pathology, as iNOS is produced during inflammation and eNOS and nNOS promote vasodilation(Förstermann and Sessa, 2012). Additionally, the decrease in miR-150 following HFD(Shi et al., 2016) may underlie some of the vascular pathologies, as miR-150 suppresses ocular vascularization(Liu et al., 2015). The axonal changes in the retina may be a cause or effect of decreased synaptophysin expression after HFD exposure(Shu et al., 2019; Zhu et al., 2018). Other perturbations driven by HFD include decreased LXRβ and HIF1α(Asare-Bediako et al., 2020), increased expression of crystallins(Mykkanen et al., 2012), VEGF, ICAM-1(Tuzcu et al., 2017), and abnormal tau phosphorylation(Zhu et al., 2018) in the retina.

Clearly the retina is negatively impacted by HFD, similar to other HFD studies of neural tissue(Arnold et al., 2014; Dutheil et al., 2016). However, because it is easier to access and measure non-invasively than brain tissue, the retina is ideal for measuring the longitudinal effects of metabolic perturbation on neural function. While much research exists on HFD and the retina, more research is needed on the effects of HFD on specific retinal neuron types (for example, retinal ganglion cells).

Retinal pigment epithelium and Bruch's membrane

The RPE and BM lie between the metabolically demanding photoreceptors and the energy-providing choriocapillaris. The RPE is a richly pigmented, monolayered tissue in intimate contact with the rod and cone photoreceptors, engulfing and phagocytosing photoreceptor discs during regular disc shedding(Kevany and Palczewski, 2010). The melanin pigments within the RPE prevent light scattering and sharpen image quality by absorbing light and also provide a photoprotective role against excess reactive oxygen species(Seagle et al., 2005). The RPE transports nutrients from the choriocapillaris and is responsible for regenerating 11-*cis*-retinal from all-*trans*-retinol, thereby sustaining the visual cycle(Kevany and Palczewski, 2010). Likewise, the collagen-rich BM plays an important role in mediating nutrient and waste exchange between the choriocapillaris and retina, as well as providing structural support for the RPE(Booij et al., 2010).

HFD alters the morphology of the RPE and BM (**Table 4-6**), causing RPE lesions(Zhao et al., 2014), RPE cell death(Roddy et al., 2019), increased RPE vacuoles(Barathi et al., 2014), BM thickening(Dithmar et al., 2001; Roddy et al., 2019), and decreased fenestrations(Zhang et al., 2018). One of the most pronounced changes in morphology is pathological lipid deposition in the RPE and BM(Roddy et al., 2019; Zhang et al., 2018). These lipid deposits may act as a barrier for nutrient transfer, impairing the function of the RPE and BM(van Leeuwen et al., 2018). Because they perform vital roles in maintaining the health of photoreceptors, impairment to the RPE and BM can lead to damage and degeneration of photoreceptors, eventually causing vision loss(Sparrow et al., 2010). Likewise, HFD treatment can cause lipid deposition and altered morphology of the BM/choriocapillaris interface(Barathi et al., 2014; Cousins et al., 2003; Miceli et al., 2000), which could ultimately lead to retinal degeneration(Picard et al., 2010; Schmidt-Erfurth et al., 2008).

Table 4-6. *Summary table of reviewed RPE and BM outcomes after HFD treatment.*

Tissue	**Outcome**	**Direction(s)**	**Reference(s)**
Retinal Pigment Epithelium (RPE)	Number of lesions	Increased	(Zhao et al., 2014)
	Number of RPE cells	Decreased	(Roddy et al., 2019)
	Vacuoles	Increased	(Barathi et al., 2014; Schmidt-Erfurth et al., 2008)
Bruch's Membrane (BM)	Thickness	Increased	(Barathi et al., 2014; Dithmar et al., 2001; Roddy et al., 2019)
		No change	(Schmidt-Erfurth et al., 2008)
	Basal laminar deposits	Increased	(Barathi et al., 2014; Roddy et al., 2019)
		No change	(Stanton et al., 2017; Toomey et al., 2015)
	Lipofuscin / autofluorescence of what appears to be lipofuscin	Increased	(Miceli et al., 2000; Zhang et al., 2018)

	Number of fenestrations in choriocapillaris endothelium	Decreased	(Zhang et al., 2018)
		No change	(Schmidt-Erfurth et al., 2008)

The RPE and BM appear to be specifically vulnerable to HFD and dyslipidemia, perhaps because they are responsible for transporting lipids to the retina and maintaining cholesterol homeostasis. Treatments that specifically target the RPE and BM to provide protection against the effects of dyslipidemia are needed.

Retinal and visual function outcomes of HFD

HFD affects a variety of retinal function measures including electroretinography (ERG), visual evoked potential (VEP), and pattern electroretinography (P-ERG). ERG is a useful, non-invasive tool to measure retinal function. The foundational work of Ragnar Granit in isolating components of the ERG waveform(Granit, 1933) provided the foundation for the later discoveries that the a-wave is generated by rod and cone photoreceptors while the b-wave is generated by bipolar cells(Brown and Wiesel, 1961; Bush and Sieving, 1996; Hood and Birch, 1996; Penn and Hagins, 1969; Robson and Frishman, 1995; Robson and Frishman, 1996; Sieving et al., 1994; Tomita, 1950). Oscillatory potentials (OPs) are believed to originate from amacrine cells, with each OP possibly representing a different cell type(Wachtmeister and Dowling, 1978). ERGs are useful in assessing ocular diseases such as DR, retinitis pigmentosa, and AMD. For example, declines in cognitive and motor function that can occur in diabetes often correlate with retinal dysfunction, with retinal deficiencies occurring prior to other symptoms(Allen et al., 2019; Aung et al., 2013; Motz et al., 2020; Pardue et al., 2014; Shirao and Kawasaki, 1998). The amplitude and timing of ERG waveforms reflect the response of the retina, neural tissue, to a light stimulus. Therefore, any changes to ERG amplitude or timing suggests altered retinal function. Because of these connections between retinal function, cognition, vascular health, and disease, ERGs and similar measurements can be useful in early identification and intervention of disease processes.

When measured with ERG, HFD exposure has varying impacts on retinal function (**Table 4-7**). Decreases in a-wave amplitudes and/or decreases in b-wave amplitudes were found after 2-3(Chang et al., 2015b; Kim et al., 2017) and 6-7(Asare-Bediako et al., 2020; Barathi et al., 2014; Shi et al., 2016) months of HFD. However, other studies found no differences in a-wave or b-wave amplitudes after 1(Chrysostomou et al., 2017; Kim et al., 2017), 2(Qu et al., 2020), 3-4(Datilo et al., 2018; Rajagopal et al., 2016), 6(Rajagopal et al., 2016), or 12(Asare-Bediako et al., 2020; Rajagopal et al., 2016) months of HFD treatment. Conversely, another study found increased b-wave and c-wave amplitudes after 4 months of HFHS diet(Atawia et al., 2020), although this could be due to the ERG protocol and/or the HFHS treatment. In another study, after 6 weeks HFHS there were no baseline differences in intraocular pressure (IOP) or positive scotopic threshold response (pSTR)(Chrysostomou et al., 2017), a measure of ganglion cells(Bui and Fortune, 2004). However, in this same study, pSTR amplitudes were significantly lower in HFHS group compared to the control diet after injury by brief IOP increase; these deficits suggest that HFHS diet hinders recovery of ganglion cells after injury, possibly through mitochondrial impairment(Chrysostomou et al., 2017). When measured with VEP and P-ERG, retinal ganglion cell response was also impaired after 5 months of HFD exposure(Shu et al., 2019; Zhu et al., 2018).

Table 4-7. *Summary table of reviewed retinal function outcomes after HFD treatment.*

ERG Outcome	Direction(s)	Reference(s)

a-wave amplitudes	Decreased	(Asare-Bediako et al., 2020; Barathi et al., 2014; Chang et al., 2015b; Kim et al., 2017; Shi et al., 2016)
	No change	(Asare-Bediako et al., 2020; Atawia et al., 2020; Chrysostomou et al., 2017; Datilo et al., 2018; Qu et al., 2020; Rajagopal et al., 2016)
a-wave implicit times	Delayed	(Chang et al., 2015b; Kim et al., 2017)
	No change	(Chrysostomou et al., 2017)
b-wave amplitudes	Increased	(Atawia et al., 2020)
	Decreased	(Asare-Bediako et al., 2020; Barathi et al., 2014; Chang et al., 2015b; Kim et al., 2017; Shi et al., 2016)
	No change	(Asare-Bediako et al., 2020; Chrysostomou et al., 2017; Datilo et al., 2018; Qu et al., 2020; Rajagopal et al., 2016)
b-wave implicit times	Delayed	(Chang et al., 2015b; Kim et al., 2017)
	No change	(Chrysostomou et al., 2017)
c-wave amplitudes	Increased	(Atawia et al., 2020)
	No change	(Datilo et al., 2018)
pSTR amplitude	No change	(Chrysostomou et al., 2017)
Oscillatory potential amplitudes	Decreased	(Datilo et al., 2018; Kim et al., 2017; Shi et al., 2016)
Oscillatory potential implicit times	Delayed	(Kim et al., 2017; Rajagopal et al., 2016)
VEP and/or P-ERG amplitudes	Decreased	(Shu et al., 2019; Zhu et al., 2018)

Timing is also an important component of ERG waves, and delayed implicit times are associated with retinal disease(Aung et al., 2013; Bronson-Castain et al., 2007; Fortune et al., 1999; Parisi, 2003). For example, delays in the timing of oscillatory potentials have been found to be an early indicator of DR(Aung et al., 2013; Fortune et al., 1999). Thus, differences in implicit times may indicate dysfunction. Delays in a-wave and b-wave implicit times have been reported after 1(Kim et al., 2017) and 3(Chang et al., 2015b) months of HFD (**Table 4-7**). Additionally, decreased oscillatory potential amplitudes were reported after 1-2(Kim et al., 2017), 4(Datilo et al., 2018) and 7(Shi et al., 2016) months of HFD, with delays in oscillatory potential implicit times after 1-2(Kim et al., 2017) and 6-12(Rajagopal et al., 2016) months HFD treatment.

While some do not report retinal function changes in wildtype mice after HFD treatment(Landowski et al., 2019; Toomey et al., 2015), AMD models of mutant mice show decreased b-wave amplitudes after HFD treatment with(Ding et al., 2011; Landowski et al., 2019; Toomey et al., 2015; Toomey et al., 2018) and without (Ban et al., 2018) cholesterol enrichment. HFD treatment in genetic *APOE4*(Ding et al., 2011), *CFH*(Toomey et al., 2015; Toomey et al., 2018), *CFH-H*/*H*(Landowski et al., 2019), and *ABCA1*(Ban et al., 2018) strains caused ERG deficits (**Table 4-3**), suggesting that lipid metabolism, complement signaling, and/or morphological changes seen in these models also impair retinal function. An AMD model with *ABCA1*/*ABCG1* mutant mice also found lipid accumulation in RPE, photoreceptor degeneration, and ERG deficits without HFD feeding(Storti et al., 2019), which both suggests that impaired lipid metabolism can cause retinal function deficits and that the addition of HFD in genetic AMD models may act to speed up the emergence of deficits caused by genetic background.

To evaluate whether differences in experimental design could account for this variability in ERG outcomes, methods were compared across studies. Among the studies that found no difference in amplitudes in wildtype mice, one utilized a HFHS diet that did not cause body weight or blood glucose changes(Chrysostomou et al., 2017), one utilized a HFC diet in aged mice(Toomey et al., 2015), and another utilized male Swiss mice(Datilo et al., 2018), a strain that shows less susceptibility to some of the metabolic effects of HFD(Anderson et al., 2014; Marei et al., 2020). Of the studies that did not find differences, four used the Espion Diagnosys system(Chrysostomou et al., 2017; Landowski et al., 2019; Qu et al., 2020; Toomey et al., 2015) and one appears to have built their own system(Atawia et al., 2020). One study did not find decreased amplitudes at 1 month but did find decreases at 2 months(Kim et al., 2017), while another found decreased amplitudes at 6 months but no difference at 12 months(Asare-Bediako et al., 2020). Other possible reasons for variability include retinal circuit differences, compensation with disease, and altered signaling of neurotransmitters such as dopamine. However, the numerous reports of impaired ERG outcomes suggest that HFD treatment impairs retinal function and retinal cell types such as photoreceptors, bipolar cells, amacrine cells, and retinal ganglion cells.

While 17 of the reviewed studies evaluated retinal function (physiological assessments), only one evaluated visual function (behavioral assessments). A study of HFHS diet did not find any changes in spatial frequency thresholds as measured by optomotor response (OMR) in male C57Bl/6J mice(Atawia et al., 2020). As this study also found no difference in ERG outcomes and used a HFHS diet model, the impact of HFD on visual function is an open question. Additionally, only three of the reviewed studies conducted longitudinal ERG measurements(Asare-Bediako et al., 2020; Kim et al., 2017; Rajagopal et al., 2016); because ERGs and OMRs are non-invasive, non-terminal procedures, future HFD studies should strive to conduct longitudinal assessments of both retinal and visual function.

It is surprising that little research has been done in the area of HFD and retinal and visual function. Future studies should further evaluate outcomes of retinal function, including direct recording to assess single retinal cell electrophysiology. It would be useful to evaluate whether specific cell types, such as rods and retinal ganglion cells, are more vulnerable to HFD. Additionally, HFD studies of visual function, such as optomotor or optokinetic response, are missing and should be a focus of future studies. The visual effects of HFD are difficult to evaluate in epidemiological studies, but animal models of HFD exposure represent a way to close this gap.

Important considerations in experimental design

HFD is commonly utilized in animal models to better understand and treat human diseases, but epidemiological studies of dietary fat and ocular outcomes are mixed, muddying the translation between human and animal studies. Epidemiological nutrition research has a number of strengths and limitations. For example, diet studies generally rely on food frequency questionnaire data to derive approximate macronutrient and micronutrient components, but this data can be prone to recall bias and/or capture a small window of time, making it difficult to extrapolate to lifelong dietary patterns and capture dietary complexity(Shim et al., 2014). Other considerations are the variety of fats and the interactions between dietary components within the dietary milieu(Spector and Gardner, 2020), which may not be accurately estimated from questionnaire data. On the other hand, epidemiological studies measure real-world exposures, whereas animal models of HFD exposure utilize refined diets that may not fully reflect the diversity of human exposures. Therefore, both epidemiological and animal studies have strengths and limitations, and animal models of diet-induced visual disease are invaluable in understanding mechanisms of disease.

However, research in animal models has its own biases and limitations. One of the major biases in the current literature is the overwhelming use of male animals in HFD research, leading to a paucity of data on female outcomes. In the clinical population, metabolic syndrome(Bentley-Lewis et al., 2007) and diabetes(Wild et al., 2004) are equally prevalent among men and women; however, the incidence of diabetes by age group and the development of complications, such as diabetic retinopathy, may differ by sex(Ozawa et al., 2015).

Of the 66 studies included in this review (**Figure 4-1, Supplemental Table 4-1**), only 18 (27%) used female rodents (**Figure 4-2G**). While sex bias towards utilizing males in scientific research is not new(Beery and Zucker, 2011; Holdcroft, 2007; Lee, 2018), this scarcity of data on female outcomes is a loss of knowledge for the scientific community. While the National Institutes of Health has developed a policy to address sex as a biological variable in research(Clayton, 2018), more work needs to be done to ensure that female animals are included in HFD studies. There are a number of reasons why female rodents may not be included in HFD studies. There are valid reasons to use one sex in a study, such as a female model to understand the role of menopause in a disease outcome, but rationale for doing so should be provided. Female rodents may not be included because of assumptions of hormonal variability in response compared to male rodents(Beery, 2018), although this might not always be the case(Prendergast et al., 2014). HFD outcomes, such as dietary-induced obesity or glucose intolerance, may have different timelines or phenotypes in females compared to males(Hong et al., 2009; Parks et al., 2015; Yang et al., 2014). Likewise, in STZ models with HFD, the use of males over females may be preferred because of sex differences in STZ response. Additionally, to ensure standardized delivery, STZ is often injected in rats via the penile vein (although it is also possible to deliver via the tail vein)(Deeds et al., 2011). To assess sex-specific results, sex-equitable research may require a larger number of animals to maintain statistical power when treatment effects differ by sex, which can be prohibitively expensive. However, because of these differences in outcomes, the use of female animals is arguably even more important in HFD research because sex-specific effects can lead to a deeper understanding of biological mechanisms and, ultimately, successful treatment options(Tannenbaum et al., 2019).

Another common limitation in HFD research is the lack of detailed diet description and/or the lack of a proper control diet. The majority of studies utilize a high fat diet (~35-60% kcal, **Figure 4-2E**) with fat derived from lard, vegetable oil, and/or milk fat, but use standard rodent chow as the control diet. While standard rodent chow is low in fat (~10% kcal), it is made of different ingredients and contains additional phytonutrients and plant-based fiber, thereby providing phytoestrogens(Thigpen et al., 2004) and/or other components not present in the HFD. Because of these ingredient differences, outcomes that occur during HFD treatments are possibly confounded(Warden and Fisler, 2008). These issues can be minimized by choosing an appropriate ingredient-matched control diet, used by 24% of the reviewed studies (**Figure 4-2H**), and allow for better standardization across studies. In studies that do not use ingredient-matched control diets but use HFD to investigate the effects of metabolic disease on visual health, results could be validated with other models of metabolic disease (such as with an STZ model for modeling diabetes) or by treating the metabolic disease after inception (such as with insulin or metformin).

Fat percentage of the HFD is another important consideration in study design. Some models use diets on the lower end of HFD range, with approximately 25-35% fat kcal, but include higher amounts of cholesterol to induce atherosclerosis. The more common models of “western diet” exposure generally contain approximately 40-45% fat kcal, while other high fat diets contain approximately 45-60% fat kcal. Both can cause diet-induced obesity in certain rodent strains, but diets with a higher percentage of energy from fat may lead to more rapid weight gain. Additionally, if the goal is to model human disease, another important consideration is which diet is most comparable to human diets; a rodent diet with 40-45% fat kcal (**Figure 4-2**) may more closely model human exposures(Speakman, 2019). Another practical consideration is that the diet texture may change to a more liquid consistency near the 60% fat kcal range. This should also be considered in experimental design, as a higher fat diet may require special food containers and other accommodations.

Other aspects of experimental design, such as the mouse or rat strain used, age of HFD exposure, and experimental timeline are important to consider. For example, some strains are somewhat resistant to diet-induced obesity and other metabolic outcomes(Funkat et al., 2004). Duration of diet and age at exposure are also important considerations (**Figure 4-2**), as short experimental timelines (a few days or weeks) of HFD exposure capture an adaptive or acute response, whereas longer (2+ months) timelines of HFD exposure can be used to model chronic outcomes(Heydemann, 2016; Ji et al., 2012; Khazen et al., 2019; London et al., 2017; Williams et al., 2014). Most of the reviewed studies focused on chronic outcomes, but transient or rapid adaptive responses may occur in the first hours, days, and weeks of HFD challenge. Characterizing these initial responses could help us understand disease mechanisms as well as the cumulative effects of repeated, acute dietary exposures.

Summary of findings

Overall, HFD affects a multitude of ocular tissues, altering morphology, signaling, and function. Among the common mechanisms identified, oxidative stress, inflammation, and lipid homeostasis were a common thread across HFD studies of ocular disease. Ocular tissues affected include cornea, lens, uvea, vitreous humor, retina, RPE, and Bruch’s membrane. Retinal cell types affected include glia (microglia), neurons (retinal ganglion cells, bipolar cells, amacrine cells, photoreceptors), and vascular support cells (endothelial cells and pericytes). The combination of so many different tissues, mechanisms, and cells types involved implies that

HFD has profound effects on ocular health and vision. A greater understanding of the ocular effects of HFD as well as the development of treatments and interventions that target these effects is urgently needed.

This review also identified common limitations of HFD studies and current gaps in knowledge. Factors such as experimental control groups, age at diet start, and diet composition are also important to consider when attempting to model human disease. Due to the sex bias towards the use of male animals, future studies should aim to address sex-specific and female ocular outcomes in HFD research. Studies should also strive to report systemic metabolic outcomes and longitudinal measures of retinal and visual function. The bulk of the literature focuses on corneal, retinal, and RPE or BM outcomes, but the impacts of HFD on other ocular tissues is not well explored. Likewise, more work needs to be done to tease apart the effects of HFD on specific neuronal populations. Additionally, few studies have tested the acute effects (hours, days, weeks) of HFD on retinal function, visual function, and tissue outcomes, which should be a focus for future studies.

In conclusion, HFD models of visual disease are invaluable. These models are used to recapitulate human disease processes such as AMD and DR, leading causes of blindness. In understanding the mechanisms and pathophysiology of the impacts of HFD on ocular outcomes, we can develop improved treatment strategies to preserve vision and prevent blindness.

Supplemental Materials

Supplemental Table 4-1. *Studies included in the review with extracted information. Diet description gives the approximated diet percentage of kcal from fat; if dietary fat was provided in percent by weight, percentage of kcal from fat was estimated by converting to percent by* *energy for approximate fat % kcal. In cases where age at start diet was variable, the youngest age was used. Title, authors, and year published are listed. "Sex" refers to the sex of the rodents used in the study, "Disease model" refers to whether the study was grouped as an AMD study, an STZ/diabetic retinopathy study, or a study that mainly evaluated the impacts of HFD alone. "Tissue main" refers to the main tissue(s) of interest in the study. "Diet description kcal fat percentage" is the provided or estimated % fat by kilocalories of the HFD. "Ingredient matched control diet" indicates whether and ingredient matched control diet was used, and the diet information/brand is provided in "HFD brand" and "Control diet brand". "Age start weeks" is the (youngest) age at which rodents started being fed the HFD, and "Age end" is the (youngest) age at which the study ended and/or the end time of HFD feeding. "Varied ages" indicates whether rodents of varying ages were used and "Age start HFD" and "Age end HFD" given ages and age ranges of HFD treatment. "Time outcome measured" indicates how long after HFD treatment (and age) that main outcomes were measured and "Diet time" indicates how long rodents were fed HFD. (separate tab) Studies that were reviewed but did not meet the criteria and were excluded from the review. "Reason for exclusion" indicates what exclusion category the paper fit into and "Comments" provides more details as to why the study was excluded. (Supplementary Table available here: https://www.sciencedirect.com/science/article/pii/S0014483521000051)*

Chapter 5: Light Environment Influences Developmental Programming of the Metabolic and Visual Systems in Mice

Published in a different format as:

Clarkson-Townsend DA, Bales KL, Marsit CJ, Pardue MT. Light Environment Influences Developmental Programming of the Metabolic and Visual Systems in Mice. Invest Ophthalmol Vis Sci. 2021 Apr 1;62(4):22. doi: 10.1167/iovs.62.4.22. PMID: 33861321.

Abstract

Purpose: Light is a salient cue that can influence neurodevelopment and the immune system. Light exposure out of sync with the endogenous clock causes circadian disruption and chronic disease. Environmental light exposure may contribute to developmental programming of metabolic and neurological systems but has been largely overlooked in Developmental Origins of Health and Disease (DOHaD) research. Here, we investigated whether developmental light exposure altered programming of visual and metabolic systems.

Methods: Pregnant mice and pups were exposed to control light (12:12LD) or weekly light cycle inversions (CD) until weaning, after which male and female offspring were housed in control light and longitudinally measured to evaluate differences in growth (weight), glucose tolerance, visual function (optomotor response), and retinal function (electroretinogram), with and without high fat diet (HFD) challenge. Retinal microglia and macrophages were quantified by positive Iba1 and CD11b immunofluorescence.

Results: CD exposure caused impaired visual function and increased retinal immune cell expression in adult offspring. When challenged with HFD, CD offspring also exhibited altered retinal function and sex-specific impairments in glucose tolerance.

Conclusions: Overall, these findings suggest that the light environment contributes to developmental programming of the metabolic and visual systems, potentially promoting a pro-inflammatory milieu in the retina and increasing the risk of visual disease later in life.

Introduction

The Developmental Origins of Health and Disease (DOHaD) hypothesis posits that early life exposures affect disease risk later in life(Barker, 2004). The DOHaD framework began with epidemiological studies of nutrition which found that mismatch between developmental and later life environment, such as undernutrition *in utero* and rich postnatal diet, increased diseases such as hypertension and diabetes(McMillen and Robinson, 2005). Like nutrition, light is a salient biological cue and can prime metabolic, immune, endocrine, and neurological systems to alter the trajectory of health and disease(Ciarleglio et al., 2011; Fonken and Nelson, 2016; Jackson et al., 2014; Smarr et al., 2017a; Varcoe et al., 2018).

Light exerts many effects via the circadian system, molecular and physiological “clocks” that regulate biochemical and signaling processes(Panda, 2016). Light acts as a “*zeitgeber*”, or “time giver”, to synchronize the body’s central and peripheral clocks, and is the most powerful entraining cue. Given the crosstalk between the circadian system, metabolism, neurological function, and the immune system, circadian disruption can cause dyslipidemia(Reutrakul and Knutson, 2015), glucose intolerance(Morris et al., 2015; Shimba et al., 2011), cognitive impairment(Chellappa et al., 2019; Karatsoreos et al., 2011; Rouch et al., 2005), and altered immune function(Hergenhan et al., 2020; Loef et al., 2019; Loef et al., 2018; Mohren et al., 2002) in both epidemiological and animal studies(Castanon-Cervantes et al., 2010). Shift work, an occupational cause of circadian disruption, increases the risk of diabetes and cardiometabolic disease(Kecklund and Axelsson, 2016; Leproult et al., 2014); likewise, rodents developmentally exposed to chronodisruption develop glucose intolerance as adults(Varcoe et al., 2018; Varcoe et al., 2011).

A window to the brain, the retina can serve as a marker of neurological health(London et al., 2013). Circadian clocks function in ocular tissues and regulate processes such as retinal differentiation, intraocular pressure, photoreceptor disc shedding, and visual processing (Felder-Schmittbuhl et al., 2018; McMahon et al., 2014; Tosini et al., 2008), the dysregulation of which can lead to visual impairment and blindness(Baba et al., 2018b). Similar to the brain, the retina has high metabolic demands and is affected by metabolic disorders such as diabetes. Unfortunately, environmental light exposure has been largely overlooked in studies of DOHaD and developmental programming.

Given the rapid rise in technologies and behavior that contributes to circadian disruption, the question of how our modern light environment relates to human development and disease is important(Hatori et al., 2017; Lunn et al., 2017). DOHaD studies evaluate disease trajectories after a developmental insult in the mother, followed by a challenge to the offspring, termed the “first hit/second hit” framework(Winett et al., 2016). The “second hit” can expose existing vulnerabilities that may not be obvious at baseline. Therefore, to investigate the impacts of developmental light environment on metabolic and neurological programming, mice were exposed to developmental circadian disruption and challenged with high fat diet (HFD) later in life.

Methods

Animals and developmental light treatment

All experimental procedures were approved by the Institutional Animal Care and Use Committee of the Atlanta Veterans Affairs Healthcare System and conducted in accordance with the Association for Research in Vision and Ophthalmology Statement for the Use of Animals in Ophthalmic and Vision Research. The C57BL/6J offspring used in this study were bred in-house from C57BL/6J mice obtained from Jackson Laboratories (Bar Harbor, ME, USA). Male breeders were singly housed in standard conditions (*ad libitum* chow, 12:12 lighting) and female breeders were randomized and housed in large, wire-top cages. Naïve female breeders acclimated for 2 weeks in standard (12:12 light:dark) light conditions before randomization to either control treatment lighting (CL, n=12) conditions (12:12 light:dark) or circadian disruption (CD, n=13) lighting conditions where light cycle was inverted every 3-4 days (**Figure 5-1A**), similar to other developmental studies(Mendez et al., 2016; Varcoe et al., 2011). White LED light composition was measured with an Exemplar Smart CCD Spectrometer (B&W Tek, Newark, DE, USA) and spectra validated to be characteristic of neutral white LED light, with a peak at 450nm and rounded peak around 575nm. Lux levels were tested and calibrated to be equal between the two light treatment groups and ranged between ~50-400 lux, depending on the position and depth of the lux meter (Dual-range light meter 3151CC, Traceable, Webster, TX, USA) in the cage; lux measurements at the wire-top neared 400 lux due to proximity to the light source, while lux measurements taken from the cage floor underneath the food holder were around 50 lux. Mice from CL and CD groups were housed in the same cage type and set-up, so luminance ranges were equal between groups.

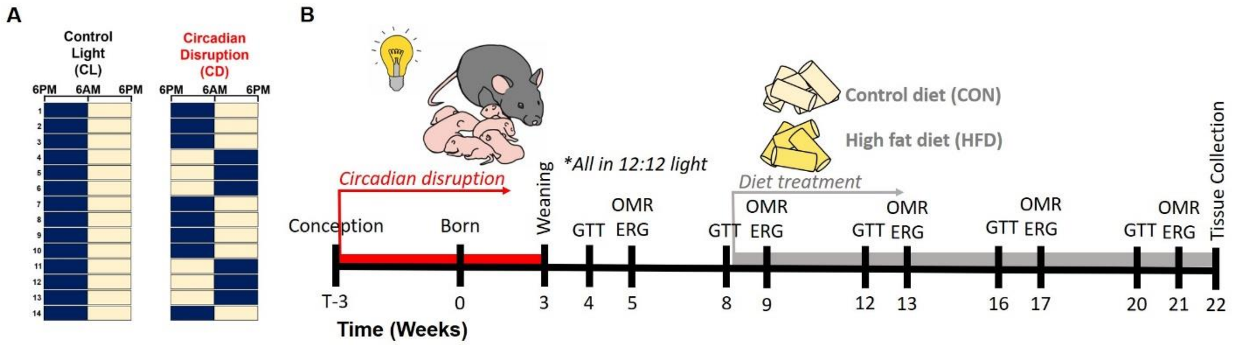
A
Control Light (CL)
Circadian Disruption (CD)
6PM 6AM 6PM
6PM 6AM 6PM
1
2
3
4
5
6
7
8
9
10
11
12
13
14
B
Control diet (CON)
High fat diet (HFD)
*All in 12:12 light
Circadian disruption
Weaning
Diet treatment
Conception
Born
GTT
OMR ERG
GTT
OMR ERG
GTT
OMR ERG
GTT
OMR ERG
GTT
OMR ERG
Tissue Collection
T-3
0
3
4
5
8
9
12
13
16
17
20
21
22
Time (Weeks)

Figure 5-1. *Overall experimental design and timeline. (**A**) Dams and offspring (both sexes) were developmentally exposed to control light (CL) treatment (12:12 lights on at 6AM, off at 6PM) or circadian disruption (CD) treatment (inversion of photoperiod every 3-4 days). The navy blue and yellow boxes each represent a time period of 12 hours, with navy representing lights off and yellow representing lights on; each row is a new day. (**B**) Diagram of the experimental timeline.*

Female breeders and their pups were exposed to CL or CD light conditions during development, as represented by the lightbulb symbol and female with pups. At weaning (3 weeks age), offspring were all housed in control light conditions and fed standard rodent chow ad libitum. At 8 weeks of age, immediately following glucose tolerance test, offspring were fed with either high fat diet (HFD) or ingredient-matched control diet (CON) ad libitum, represented by the pale yellow and bright yellow cylinders. Glucose tolerance testing (GTT), visual function using optomotor response (OMR), and retinal function using electroretinogram (ERG) were longitudinally tested from 4-21 weeks of age. Tissues were collected for analysis at 22 weeks of age.

After four weeks of light treatment, two females, one from each light treatment group, were placed in a male’s cage for two days for timed breeding during concordant light schedules before being returned to their home cages. Females were checked for vaginal plugs after pairings and weighed to confirm pregnancy. Non-pregnant females were re-paired with the same male. Dams and pups remained in CD or CL light treatments until weaning at three weeks of age (**Figure 5-1B**). Developmental light treatment and dam ID were recorded for each pup and kept masked for the duration of the experiment.

From weaning onwards, offspring were housed in standard lighting conditions (12:12 light:dark). Offspring were fed standard rodent chow (Teklad Rodent Diet 2018 irradiated 2918, Envigo Tekland, Madison, WI, USA) *ad libitum* from weaning until 8 weeks of age. Immediately following the glucose tolerance test (GTT) at 8 weeks of age, mice were randomized to receive either Western-style high fat diet (HFD, 42% calories from fat, TD.88137, Envigo Tekland, Madison, WI, USA) or ingredient-matched control diet (CON, 13% calories from fat, TD.08485, Envigo Tekland, Madison, WI, USA) *ad libitum* for the duration of the experiment (**Figure 5-1B**). At 22 weeks of age, adult offspring were sacrificed between 10AM-12PM (zeitgeber time (ZT) ZT4-ZT6) and tissue samples collected and flash frozen or preserved for cryosectioning and stored at -80°C until further analysis.

Actigraphy

Activity patterns of female mice exposed to CL or CD were measured using custom-built Arduino-based passive infrared motion detectors (PIRs, **Figure 5-2A**)(Brown et al., 2017) that collected activity data every 10 seconds. Actigraphy data from PIRs was further validated with running wheels (ENV-047, Med Associates Inc., St. Albans, VT, USA). Actograms from PIRs and running wheels were created in ImageJ using the ActogramJ plugin(Schmid et al., 2011). Measures of intradaily stability, intradaily variability, and relative amplitude were calculated using the nparACT package in R(Blume et al., 2016).

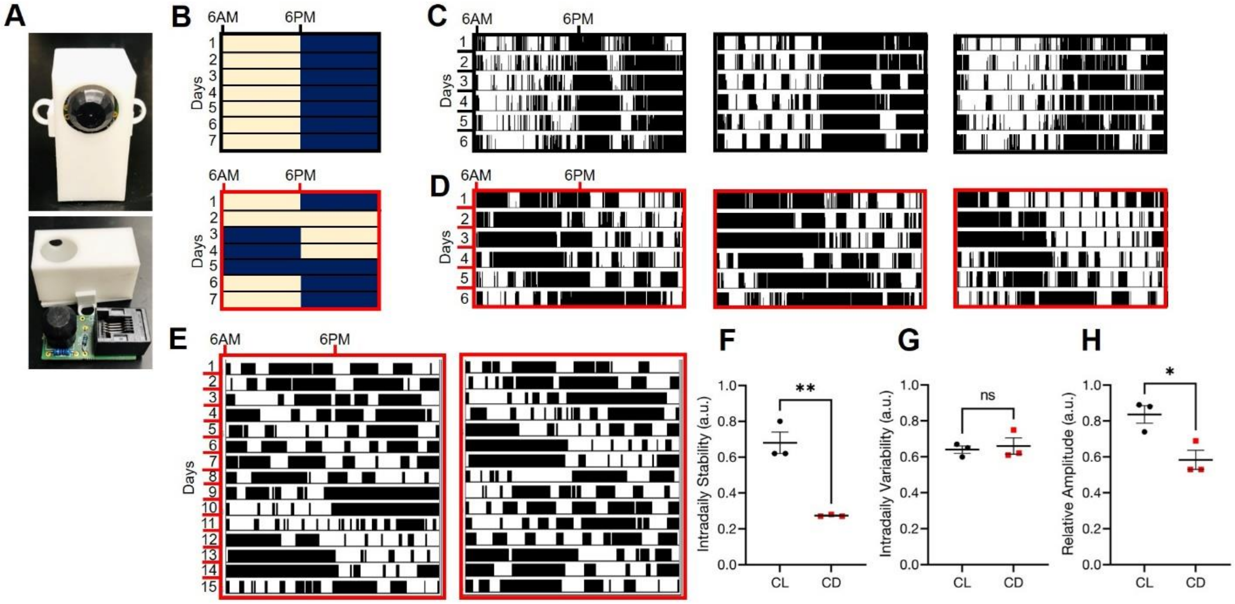

Figure 5-2. *Mice exposed to circadian disruption (CD) light conditions have altered activity rhythms. (**A**) Picture of the custom-built infrared motion sensor (PIR), showing (above) the sensor as encased in a 3D-printed plastic shell and (below) removed from the case showing the*

*circuit board and components. (**B**) Representative control light (CL) cycle (black outline), with lights on (pale yellow shading) at 6AM and lights off (navy blue shading) at 6PM, and CD light cycle (red outline), with light inversions twice weekly (note that this is the same schedule as shown in Figure 1, but plotted with different start time). (**C**) Representative single-plotted actograms from 3 cages of female mice exposed to CL over a 6-day period, with vertical black lines indicating activity and each row representing a 24-hour period. (**D**) Representative single-plotted actograms from 3 cages of female mice exposed to CD over a 6-day period, with black lines indicating activity and each row a 24-hour period. (**E**) Representative actograms from running wheels of females exposed to CD over a 15-day period, with black lines indicating activity and each row a 24-hour period. (**F**) Intradaily stability (t=6.77, df=4, p=0.003), (**G**) intradaily variability (t=0.40, df=4, p=0.71), and (**H**) relative amplitude (t=3.52, df=4, p=0.025) as calculated from the representative actograms in (**C**) and (**D**), presented as mean ± SEM and analyzed with student's 2-tailed unpaired t-tests, *p<0.05, **p<0.01.*

Serum lipids and glucose panel

Dams were sacrificed at weaning between 9AM-11AM (ZT3-ZT5) during concordant light schedules. Serum was collected [1.1mL Z-gel microtube, Sarstedt, Germany] and stored at -80°C. Serum samples were analyzed for lipids, glucose, and free fatty acids (FFAs) on a Beckman Coulter AU480 chemistry autoanalyzer (Brea, CA, USA) using Sekisui Diagnostics (Burlington, MA, USA) reagents and calibrators.

Weekly weight and blood glucose

Mice were measured weekly for body weight and blood glucose (mg/dL) using a handheld glucometer (FreeStyle Lite, Abbott Diabetes Care, Alameda, CA, USA). Prior to glucose recording, the tail was gently cleaned to remove any debris, lightly pricked with an insulin needle (BD insulin syringe #32946), and a drop of blood collected on the glucometer strip.

Glucose tolerance testing (GTT)

Intraperitoneal (IP) GTT was performed at 4, 8, 12, 16, and 20 weeks of age. On the day of the test, food was removed at 7AM (ZT1) and mice fasted for 6 hours. At 1PM (ZT7), baseline blood glucose (mg/dL) of mice was measured just prior to IP injection of glucose solution (D+ glucose in dH_2O, 2g/kg)(Andrikopoulos et al., 2008) and ensuing blood glucose (mg/dL) levels recorded at 15, 30, 60, and 120 minutes post-injection using a handheld glucometer (FreeStyle Lite, Abbott Diabetes Care, Alameda, CA, USA). To summarize the hyperglycemia response, area under the curve (AUC) was calculated for each mouse using the trapezoidal method(Sakaguchi et al., 2015).

Optomotor response testing

Visual function was measured with optomotor response (OMR) testing at 5, 9, 13, 17, and 21 weeks of age, as previously described(Aung et al., 2013; Gudapati et al., 2020; Mui et al., 2018) using the OptoMotry system (Cerebral Mechanics, USA)(Prusky et al., 2004). Briefly, a mouse was placed on a central pedestal in an enclosed chamber of monitors which display rotating vertical sine wave gratings of varying spatial frequency (with contrast set at 100%) or varying grating contrast (with spatial frequency set at 0.103 cycles/degree). A trained observer marked when the characteristic head tracking movement occurred (or did not occur) through a programmed staircase method to calculate the visual threshold. Measurements from the left and right eye were averaged for a combined visual threshold score. Contrast threshold results were converted to Michelson contrast values(Prusky et al., 2006).

Electroretinography

Retinal function was measured using electroretinography (ERGs) at 5, 9, 13, 17, and 21 weeks of age, following OMR testing. Mice were dark-adapted overnight, anesthetized with an IP injection of ketamine (80 mg/kg) and xylazine (16 mg/kg), placed on a heating pad (37°C to maintain body temperature), and given corneal numbing drops (0.5% tetracaine hydrochloride, Bausch and Lomb) and drops for pupil dilation (1.0% tropicamide solution, Sandoz, Alcon) under dim red light. Anesthetized mice were placed on a heated platform (37°C to maintain body temperature) and ground and reference electrodes inserted into the tail and each cheek (Natus neurology Genuine Grass Platinum Subdermal Electrodes #F-E2-48). Custom-made gold loop recording electrodes were gently placed on each cornea and methylcellulose drops (1% carboxyl methylcellulose, Refresh Celluvisc, Allergan) applied after placement to prevent eye dryness and maintain electrode connection. Post-measurement, mice were given an IP injection of atipamezole (1 mg/kg) (Antisedan, Zoetis, Parsippany, NJ, USA) to counteract effects of anesthesia(Turner and Albassam, 2005), saline eye drops, and allowed to recover on a heating pad (37°C) before being returned to housing.

ERGs were performed using a 6-step protocol comprised of 5 scotopic stimuli of increasing luminance (-2.5, -1.9, -0.6, 0.8, and 1.9 log cd s/m^2) followed by a 10-minute light adaptation step (1.5 log cd s/m^2) and final flicker photopic stimulus (1.4 log cd s/m^2 at 6.1 Hz)(Allen et al., 2019; Aung et al., 2014); this protocol measured the rod-dominated, mixed, and cone-dominated retinal responses. For the ERGs performed at 21 weeks of age, an additional photopic step was included to measure blue/green cone (M-opsin) response using a green LED flash (530nm, 0.1 log cd s/m^2) following the photopic flicker step. Retinal responses were recorded, oscillatory potentials (OPs) extracted (75-500 Hz), and signals averaged using the LKC software (UTAS BigShot, LKC Technologies, Gaithersburg, MD, USA); waveforms were marked in MATLAB (Mathworks, Natick, MA, USA). For each mouse, the waveform from the eye with the highest b-wave amplitudes from the brightest dark-adapted step (flash stimulus = 1.9 log cd s/m^2) was used for analysis.

Retinal immunofluorescence microscopy

Fresh whole eyes were fixed in 10% neutral buffered formalin and cryoprotected in 30% sucrose. Tissues were embedded and frozen in optimal cutting temperature compound and sliced into 10-µm-thick sections. Blocking (with 0.1% Triton X-100) and primary antibody incubations on retinal sections were in 5% normal donkey serum in PBS and washed with PBS. Primary antibody incubations using Iba1 (ab178847; 1:100; Abcam) and CD11b (14-0112-82; 1:100; Invitrogen) were performed for 16-24 hours at 4°C. Secondary antibody incubations using Alexa Fluor 488 Donkey anti-mouse IgG (A-21202; 1:500) and Alexa Fluor 647-conjugated Donkey anti-rabbit IgG (A-31573; 1:500) and tissue nuclei visualized with nuclear stain 4′,6-diamidino-2-phenylindole (DAPI, 62247; Thermo Fisher Scientific). Coverslips were mounted using Prolong Gold (P36934; Thermo Fisher Scientific). Retinal tissue (n=4-7 mice/group; 2-3 images per sample) images were taken on an Olympus Fluoview1000 confocal microscope (Center Valley, PA) with a 20x objective and a Lumenera INFINITY 1-3C USB 2.0 Color Microscope camera (Spectra Services, Ontario, NY) by a researcher masked to treatment group. All images were compiled and quantified using ImageJ software. Fluorescence for each image was quantified by dividing the mean fluorescence by the imaging area; mean fluorescence across images was then averaged for each sample for statistical analysis.

Statistical analysis and data availability

Longitudinal metabolic and visual measures were analyzed using 2-way ANOVA or mixed models (in the case of missing data) with post-hoc Dunnett tests to compare treatment groups to the CL+CON control group, correcting for multiple comparisons. Non-longitudinal data was measured using a 1-way ANOVA with post-hoc Dunnett tests to compare treatment groups to the CL+CON control group, correcting for multiple comparisons. Dam serum results, intradaily stability, intradaily variability, and relative amplitude were analyzed with Student's unpaired 2-tailed t-tests. Data are displayed as mean ± SEM and results were considered significant if $p<0.05$. Statistical analyses were performed using GraphPad Prism version 9.0.0 and R version 3.2. Data and R code are available at: https://github.com/dclarktown/Light_mice (DOI: 10.5281/zenodo.4536522).

Results

Circadian disruption during development alters activity patterns

Actigraphy data confirmed that, compared to CL (**Figures 5-2B-C**), CD treatment altered activity patterns (**Figures 5-2B, 5-2D**), similar to other studies using the same light paradigm(Mendez et al., 2016; Varcoe et al., 2013); results were validated with running wheels (**Figure 5-2E**). Disrupted mice had decreased intradaily stability and relative amplitude, suggesting weaker coupling to zeitgebers (e.g. light) and dampening of circadian rhythms in CD mice; however, there was no difference in intradaily variability, a marker of activity fragmentation (**Figures 5-2F-H**).

Circadian disruption alters maternal serum glucose

At weaning, CD dams had significantly higher serum glucose (**Figure 5-3A**, Student's unpaired t-test, (t=2.892, df=7), p=0.023) than CL dams. Serum FFAs, triglycerides, total cholesterol, and high density lipoproteins (HDLc) did not differ between groups (**Figure 5-3B-E**).

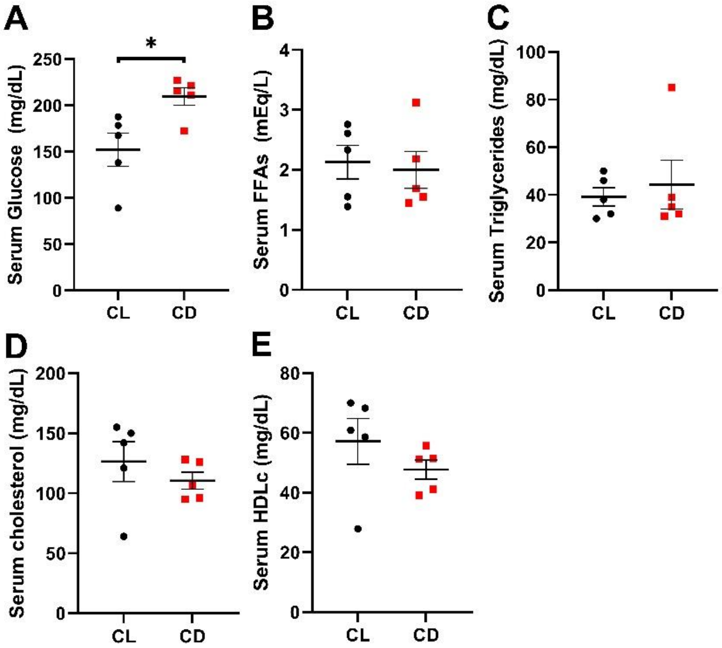

Figure 5-3. *Circadian disruption increases serum glucose levels. At weaning, dams in the CD group had higher serum (**A**) glucose (t=2.836, df=8, p=0.022) but similar levels of (**B**) free fatty acids (FFAs)(t=0.3135, df=8, 0.762), (**C**) triglycerides (t=0.4747, df=8, p=0.648), (**D**) cholesterol (t=0.8841, df=8, p=0.402), and (**E**) high density lipoprotein (HDLc)(t=1.141, df=8, p=0.287) compared to dams in the CL group. Data are presented as mean ± SEM and analyzed with Student's 2-tailed unpaired t-tests, *p<0.05, n=5 per group.*

HFD has sex-specific influences on body weight and blood glucose

Male mice fed HFD developed higher body weight over time (**Figure 5-4A**). Irrespective of developmental light treatment, male HFD groups were significantly heavier than the control groups (mixed-effects, group*time: F(51, 559) = 22.77, $p < 0.0001$), starting just 1 week after diet treatment (9 weeks of age, $p<0.05$) and continuing until the end of the experiment (21 weeks of age, $p<0.001$). While the interaction was significant (mixed-effects, group*time: F(51, 549) = 3.280, $p < 0.0001$), female mice fed HFD did not significantly differ in body weight in post-hoc analyses (**Figure 5-4B**).

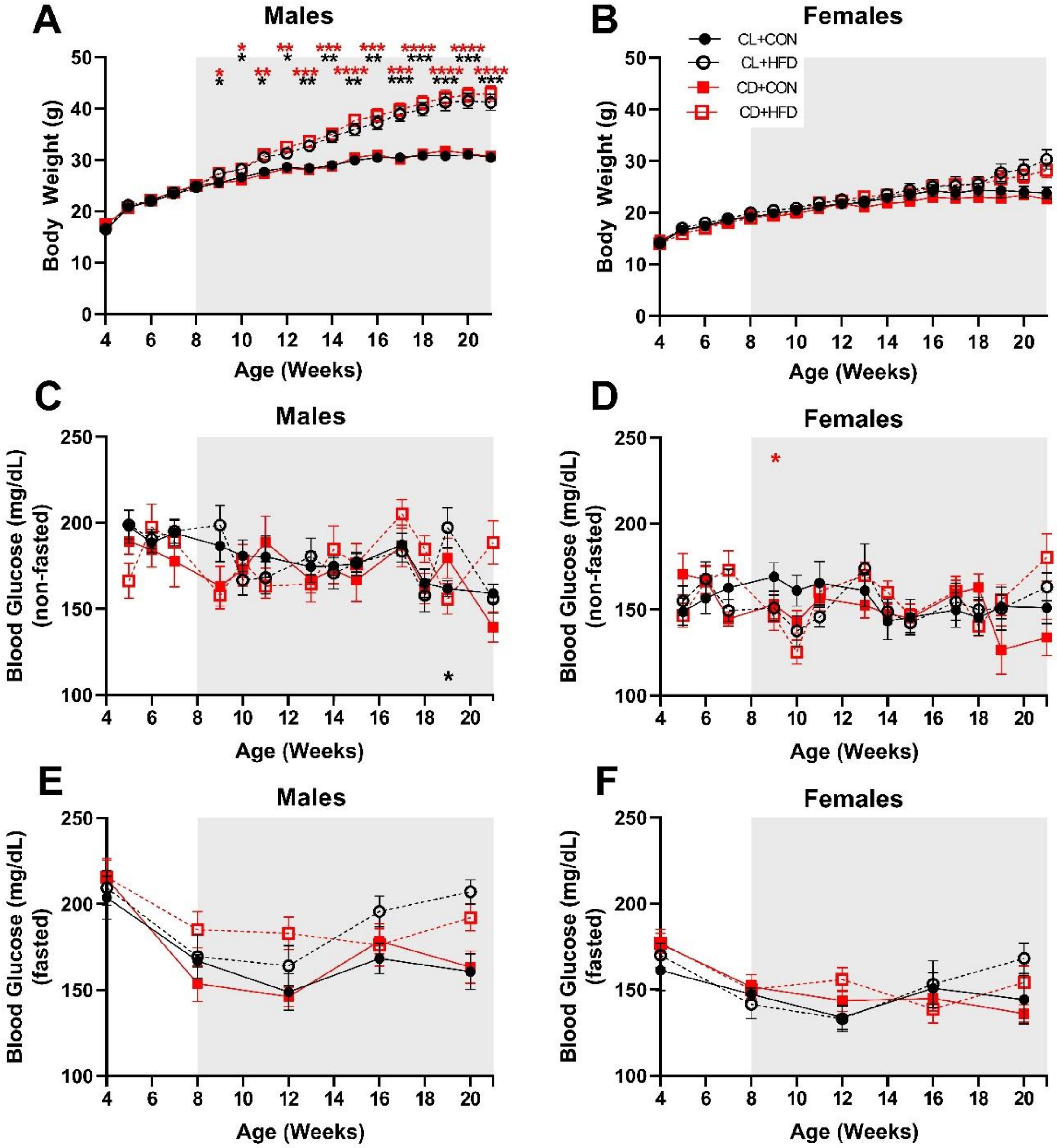

Figure 5-4. *Only male mice gained weight after HFD exposure. (**A**) Male HFD groups developed significantly higher body weight starting at 9 weeks, 1 week after start of diet treatment (mixed-effects analysis, F(51, 559) = 22.77, p<0.0001). (**B**) Female mice showed an interaction between time and treatment (mixed-effects analysis, F (51, 549) = 3.28, p<0.0001), but no significant differences between treatment groups. (**C**) CL+HFD males had significantly higher blood glucose (non-fasted) at 19 weeks (mixed-effects analysis, F (36, 386) = 1.74,*

*p=0.006). (**D**) CD+HFD females had significantly lower blood glucose (non-fasted) at 10 weeks (mixed-effects analysis, F (36, 385) = 1.63, p=0.015). There were no differences between groups in blood glucose levels after fasting for 6hr (prior to GTT) in (**E**) males (mixed-effects analysis, F (12, 132) = 1.56, p=0.11) or (**F**) females (mixed-effects analysis, F (12, 128) = 1.35, p=0.20). Data are presented as mean ± SEM and analyzed by mixed models with post-hoc Dunnett tests. *p<0.05 **p<0.01 ***p<0.001 ****p<0.0001 vs CL+CON group. Black asterisks indicate CL+HFD group and red asterisks indicate CD+HFD group. Grey shading indicates period of diet treatment. For males, CL+CON n=8-10, CL+HFD n=9-10, CD+CON n=7-9, CD+HFD n=8-10 at each timepoint; for females, CL+CON n=8-9, CL+HFD n=5-9, CD+CON n=9-10, CD+HFD n=7-11 at each timepoint.*

Weekly blood glucose measurements varied considerably; male mice fed HFD with developmental circadian disruption had significantly higher non-fasted blood glucose levels (mixed-effects, group*time: F(36, 386)= 1.742, p=0.006) at 19 weeks of age compared to the control group (p<0.05, **Figure 5-4C**). Female mice fed HFD with developmental circadian disruption had slightly lower non-fasted blood glucose levels at 10 weeks of age compared to the control group (mixed-effects, group*time: F(36, 385) = 1.629, p=0.0146, p<0.05, **Figure 5-4D**). There were no differences in fasted blood glucose levels between groups (**Figures 5-4E, 5-4F**).

HFD and developmental disruption impair glucose tolerance

There were no differences in glucose tolerance between groups at 4 or 8 weeks of age (**Figure 5-5**, **Supplemental Figure 5-1**), prior to diet treatment. However, at 12 and 16 weeks of age, there were significant interactions between sex and treatment (2-way ANOVA, sex*diet: p<0.01), with HFD males displaying impaired glucose tolerance after 1 month of diet treatment.

CD+HFD males also developed elevated blood glucose more rapidly post-injection compared to CL+CON (mixed-effects, group*time: F(12, 132) = 4.130, p=0.0001, p<0.05, **Supplemental Figure 5-1E**). This trend of worsened glucose tolerance in the male CD+HFD and CL+HFD groups continued at 16 and 20 weeks of age (p<0.05, **Figure 5-5A, Supplemental Figure 5-1G,I**), whereas females did not differ in glucose tolerance until CD+HFD females developed elevated glucose at 20 weeks of age (mixed-effects, group*time: F(12, 126) = 3.069, p=0.0008, p<0.05, **Figure 5-5B**, **Supplemental Figure 5-1J**).

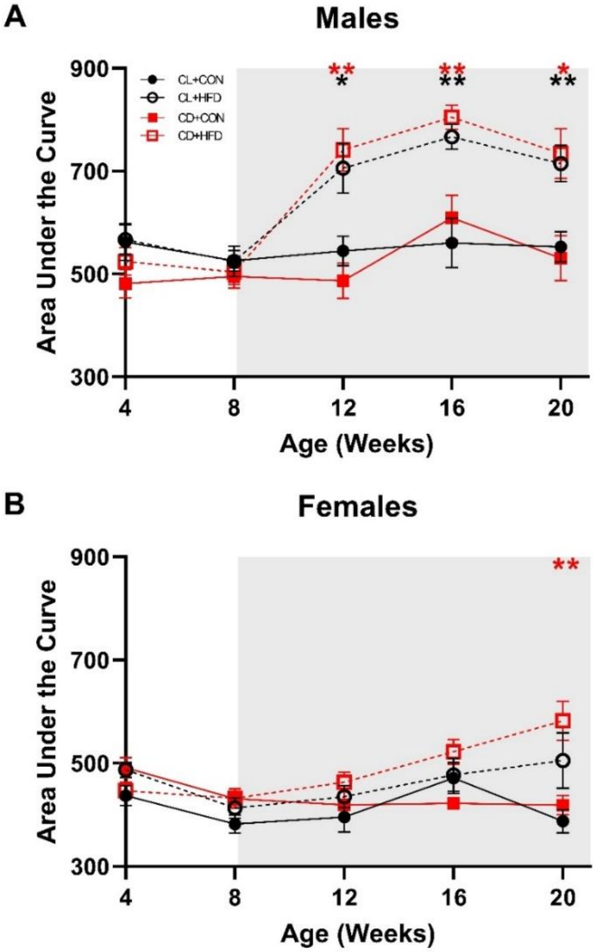

Figure 5-5. *Males on HFD have higher area under the curve (AUC) values of glucose tolerance testing and at earlier timepoints than females. (**A**) Male AUC values; CD+HFD and CL+HFD groups had higher AUC values at 12, 16, and 20 weeks of age compared to the CL+CON group*

*(mixed-effects, group*time: F(12, 132) = 4.13, p<0.0001, p<0.05). (**B**) Female AUC values; CD+HFD group had higher AUC values at 20 weeks of age compared to the CL+CON group (mixed-effects, group*time: F(12, 126) = 3.07, p<0.001, p<0.05). Data are presented as mean ± SEM and analyzed by mixed models with Dunnett tests. *p<0.05 **p<0.01 ***p<0.001 ****p<0.0001 vs CL+CON group. Black asterisks indicate CL+HFD group and red asterisks indicate CD+HFD group. Grey shading indicates period of diet treatment. For males, CL+CON n=9-10, CL+HFD n=9-10, CD+CON n=8-9, CD+HFD n=9-10 at each timepoint; for females, CL+CON n=8-9, CL+HFD n=6-9, CD+CON n=7-10, CD+HFD n=7-11 at each timepoint.*

Developmental circadian disruption and HFD reduce visual function

OMR results did not differ at baseline, but by 9 weeks of age (1 week after diet start), CD+HFD mice exhibited decreased spatial frequency (mixed-effects, group*time: F(12, 275) = 14.33, p<0.0001, p<0.001, **Figure 5-6A**); at 13, 17, and 20 weeks of age, CD+HFD and CL+HFD had decreased spatial frequency, and at 20 weeks of age CD+CON had decreased spatial frequency compared to CL+CON (p<0.01, **Figure 5-6A**). Likewise, CD+HFD and CL+HFD exhibited decreased contrast sensitivity at 9 and 13 weeks of age, and all groups had decreased contrast sensitivity at 17 and 20 weeks of age compared to CL+CON (mixed-effects, group*time: F(12, 275) = 8.233, p<0.0001, p<0.05, **Figure 5-6B**). While there were no significant interactions between sex and treatment, sex as a main effect was significant for frequency at 5, 9 and 13 weeks and for contrast at all time points, with males having slightly higher visual acuity(van Alphen et al., 2009).

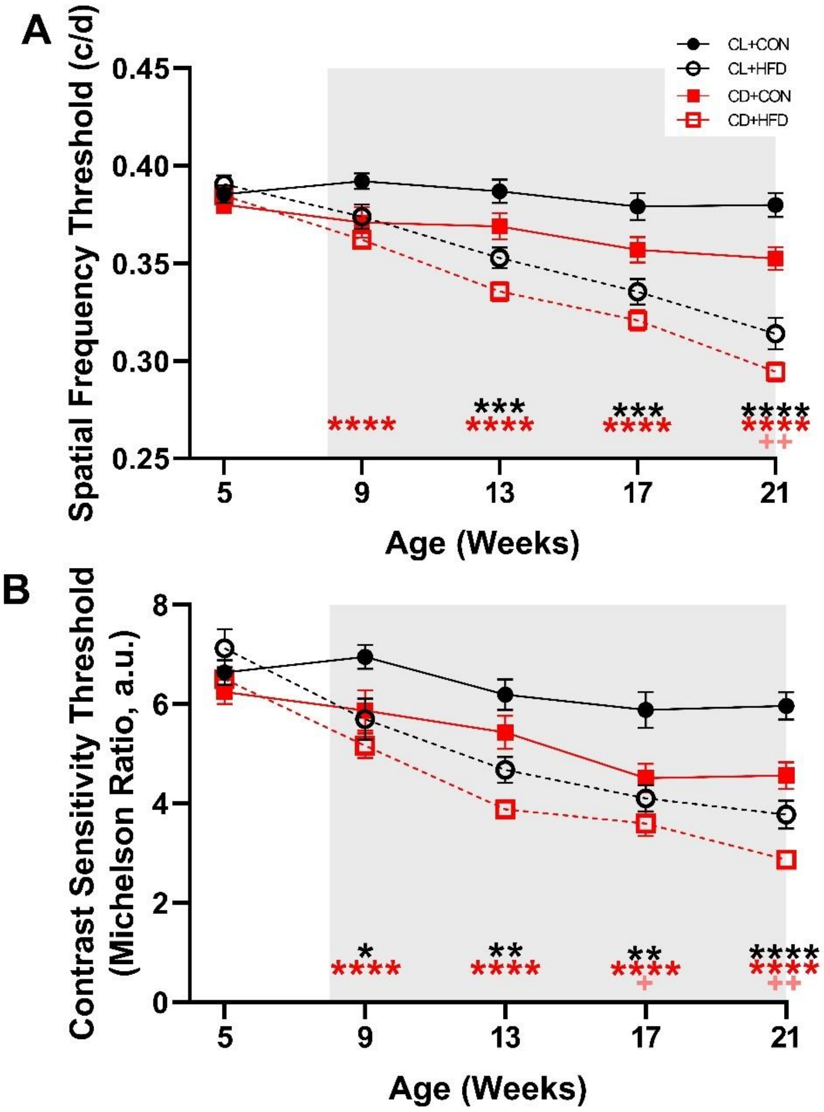

Figure 5-6. *HFD and developmental circadian disruption reduced visual function. (**A**) Spatial frequency thresholds decreased after the induction of HFD (mixed-effects, group*time: F(12, 275) = 14.33, p<0.0001) in the CD+HFD group (p<0.05), while the CL+HFD group developed decreased spatial frequency slightly later (p<0.05) and the CD+CON group had decreased visual frequency at 20 weeks of age (p<0.05). (**B**) Contrast sensitivity thresholds decreased after exposure to HFD (mixed-effects, group*time: F(12, 275) = 8.23, p<0.0001) in the CD+HFD and CL+HFD groups (p<0.05), while the CD+CON group had decreased contrast sensitivity at*

*17 and 21 weeks of age compared to the CL+CON group(p<0.05). Data are presented as mean ± SEM and analyzed by mixed models with Dunnett tests. *p<0.05 **p<0.01 ***p<0.001 ****p<0.0001 vs CL+CON group. Black asterisks indicate CL+HFD group, red asterisks indicate CD+HFD group, and pink crosses indicate CD+CON group. Grey shading indicates period of diet treatment. For each timepoint, CL+CON n=17-19, CL+HFD n=14-19, CD+CON n=17-19, CD+HFD n=16-21.*

Developmental disruption alters retinal function in response to HFD

Results of scotopic full-field ERGs revealed retinal function deficits. Representative scotopic (**Figure 5-7A**) and photopic flicker (**Figure 5-7B**) waveforms visibly show amplitude differences at 9 weeks of age, after 1 week of HFD. As shown in the intensity response curve, the CL+HFD group had lower a-wave (2-way ANOVA, F(6, 140) = 4.025, p<0.001, p<0.05 **Figure 5-7C)** and b-wave (2-way ANOVA, F(12, 280) = 2.519, p<0.01, p<0.05 **Figure 5-7D)** amplitudes**.** When analyzed over time, a-wave amplitudes did not significantly differ (mixed-effects, group*time: F(12, 260) = 1.686, p=0.069, **Figure 5-7E**), but a-wave implicit times (ITs) did differ (mixed-effects, group*time: F(12, 260) = 1.957, p<0.05, **Figure 5-7F**), with the CL+HFD group showing delayed ITs at 9 and 13 weeks (p<0.05) and CD+HFD at 13 weeks (p<0.05). There were also deficits in b-wave amplitudes over time (mixed-effects, group*time: F(12, 260) = 1.957, p<0.05, **Figure 5-7G**) in the CL+HFD group at 9 (p<0.001) and 13 (p<0.01) weeks of age. However, there were no differences in flicker b-wave amplitudes over time (mixed-effects, group*time: F(12, 255) = 1.699, p=0.067, **Figure 5-7H**) or in green cone b-wave amplitude when measured at 21 weeks of age (1-way ANOVA, F(3, 47) = 1.465, p=0.236, **Supplemental Figure 5-2**).

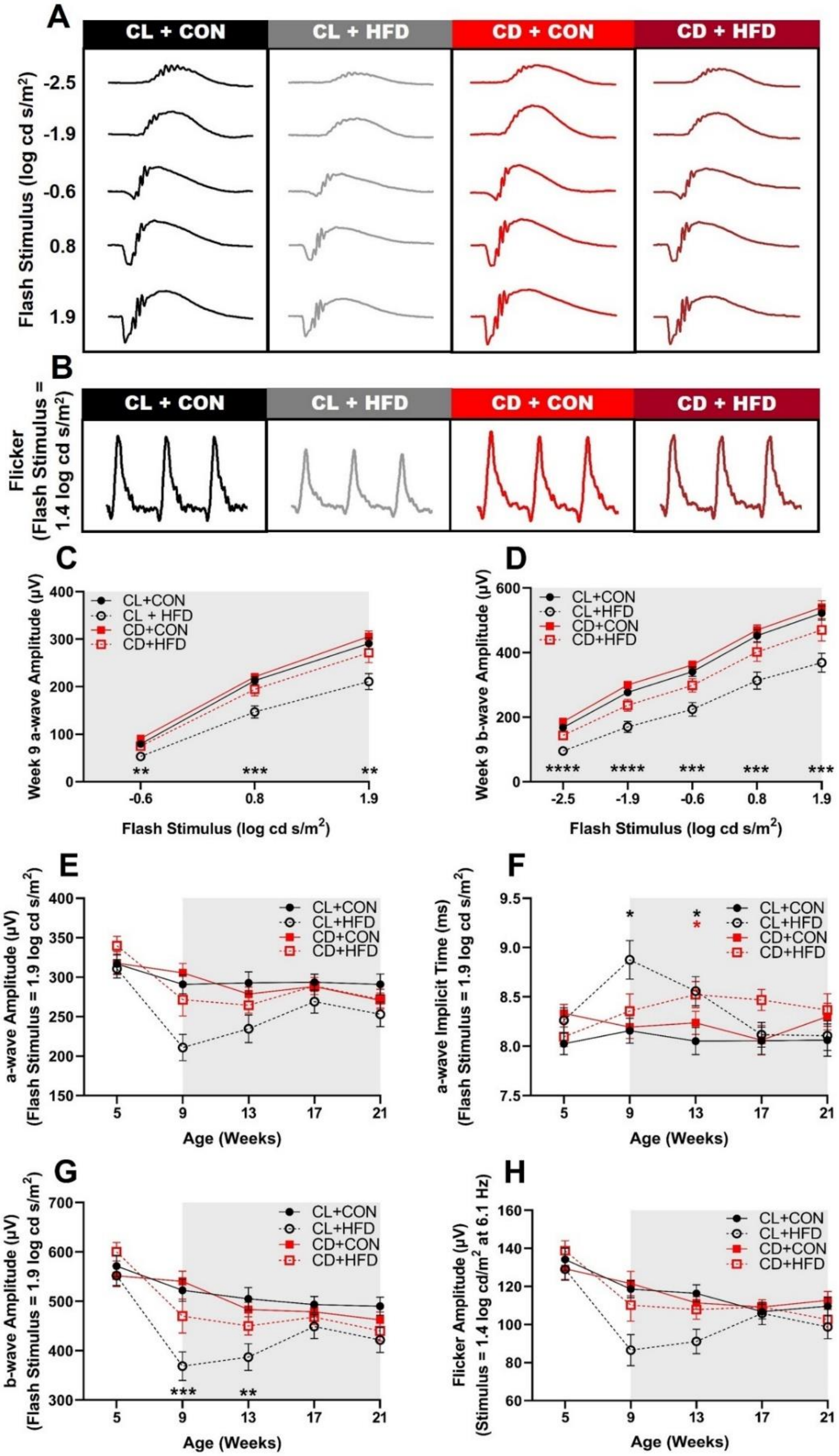

Figure 5-7. *Transient deficits in retinal function after acute HFD treatment. Representative ERG waveforms at 9 weeks of age (1 week after HFD) in response to (**A**) a series of scotopic stimuli*

*and (**B**) photopic flicker stimuli showing visible amplitude deficits in the CL+HFD group. (**C**) Intensity response curve of a-wave amplitudes at 9 weeks of age (2-way ANOVA, F (6, 140) = 4.03, p<0.001) show decreased amplitudes in the CL+HFD group. (**D**) Intensity response curve of b-wave amplitudes at 9 weeks of age (2-way ANOVA, F (12, 280) = 2.52, p<0.005) shows decreased amplitudes in the CL+HFD group. (**E**) a-wave amplitudes (mixed-effects, group*time: F (12, 260) = 1.69, p=0.069) over time and (**F**) implicit times (mixed-effects, group*time: F (12, 260) = 1.96, p<0.05) with delays in the CL+HFD and CD+HFD groups. (**G**) b-wave scotopic (-2.5, -1.9, -0.6, 0.8, and 1.9 log cd s/m*^{2}*) amplitudes (mixed-effects, group*time: F (12, 260) = 2.32, p<0.01) and (**H**) flicker amplitudes (mixed-effects, group*time: F (12, 255) = 1.70, p=0.067) over time. Data are presented as mean ± SEM and analyzed by 2-way ANOVAs or mixed models with Dunnett tests. *p<0.05 **p<0.01 ***p<0.001 ****p<0.0001 vs CL+CON. Black asterisks indicate the CL+HFD group and red asterisks indicate the CD+HFD group. Grey shading indicates period of diet treatment. For each timepoint, CL+CON n=16-19, CL+HFD n=14-19, CD+CON n=15-19, CD+HFD n=15-21.*

OPs, generated by amacrine cells in the inner retina(Wachtmeister, 1998b), were also affected by HFD treatment (**Supplemental Figure 5-3**). Amplitude deficits in OP2 (mixed-effects, group*time: F(12, 260) = 2.436, p<0.01), but not OP4, occurred in the CL+HFD group at 9, 13, and 21 weeks (p<0.05) and in the CD+HFD group at 21 weeks of age (p<0.05). These results suggest HFD-induced impairment in ON-pathway and rod activity (OP2) but not in OFF-pathway and cone signaling (OP4)(Wachtmeister, 1998a).

Increased retinal microglia and macrophage expression in response to altered developmental light environment and HFD

Retinal inflammatory response increased significantly within CD+CON, CL+HFD and CD+HFD groups (**Figure 5-8**). CD11b-positive and Iba1-positive cells (labeling microglia and macrophages) were not only observed within the inner retinal layers, where they typically reside (ganglion cell layer (GCL), inner plexiform layer (IPL) and outer plexiform layer (OPL)), but were also found in the inner nuclear layer (INL) and reached the outer nuclear layer (ONL, **Supplemental Figure 5-4**), where the cell bodies of rods and cones reside.

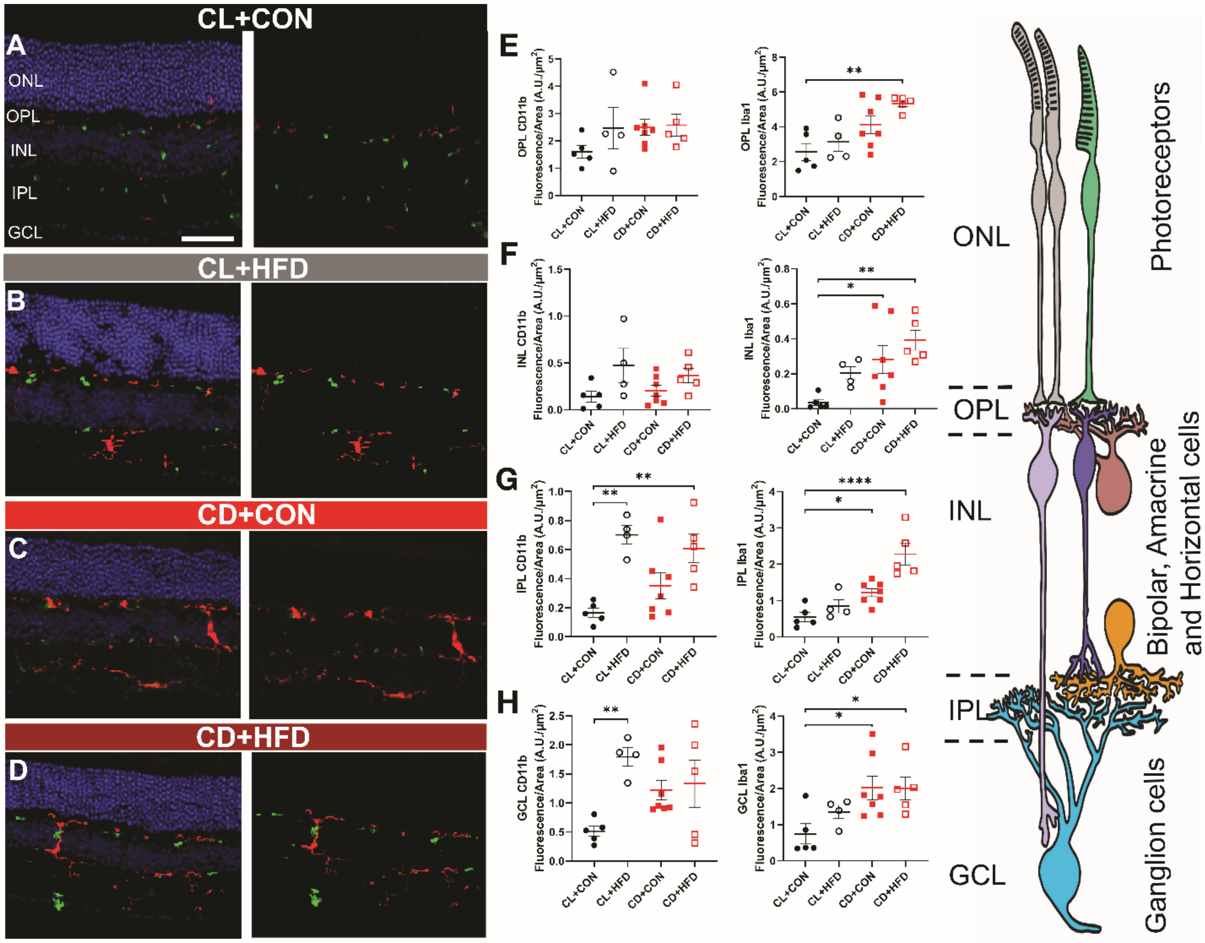

Figure 5-8. Both CD and HFD cause increased retinal immune activation, as measured by CD11b (green) and Iba1 (red). Representative retinal immunofluorescence microscopy results,

*with (left) and without (right) DAPI staining (blue), showing retinal layers of the (**A**) CL+CON group, the (**B**) CL+HFD group, the (**C**) CD+CON group, and the (**D**) CD+HFD group show increased retinal expression of CD11b in CL+HFD, CD+CON, and CD+HFD groups and increased retinal expression of Iba1 in the CD+CON and CD+HFD groups. Measured fluorescence by retinal layer, showing no difference in (**E**) CD11b staining in the OPL (1-way ANOVA, F (3, 17) = 1.23, p=0.33) but increased Iba1 staining in the OPL (1-way ANOVA, F (3, 17) = 6.25, p=0.0047) in the CD+HFD group. (**F**) In the INL, there was also no difference in CD11b expression (1-way ANOVA, F (3, 17) = 2.52, p=0.092), but Iba1 expression was increased (1-way ANOVA, F (3, 17) = 5.36, p=0.022) in the CD+CON and CD+HFD groups. In the IPL, (**G**) CD11b increased (1-way ANOVA, F (3, 17) = 8.06, p=0.0015) in both HFD groups while Iba1 increased (1-way ANOVA, F (3, 17) = 15.87, p<0.0001) in both CD groups. Likewise, in the GCL, (**H**) CD11b was increased (1-way ANOVA, F (3, 17) = 4.34, p=0.019) in the CL+HFD group and Iba1 was increased (1-way ANOVA, F (3, 17) = 3.89, p=0.023) in both CD groups. (**I**) Drawing representing the retinal layers. Images from the CL+CON group (n=5 mice), CL+HFD group (n=4 mice), CD+CON group (n=7 mice), and CD+HFD group (n=5 mice) include both sexes. Data are presented as mean ± SEM and analyzed by 1-way ANOVAs with Dunnett tests. *p<0.05 **p<0.01 ***p<0.001 ****p<0.0001 vs CL+CON group. Scale bar = 12µm.*

Imaging found no difference in CD11b staining in the OPL (**Figure 5-8E**, 1-way ANOVA, F (3, 17) = 1.23, p=0.33) or INL (1-way ANOVA, F (3, 17) = 1.49, p=0.09); conversely, Iba1 staining was increased in the OPL (1-way ANOVA, F (3, 17) = 6.25, p=0.0047) in the CD+HFD group. Comparatively, in the INL (**Figure 5-8F**) Iba1 expression was greater (1-

way ANOVA, F (3, 17) = 9.67, p=0.02) in the CD+CON and CD+HFD groups. In the IPL, (**Figure 5-8G**) CD11b increased (1-way ANOVA, F (3, 17) = 8.06, p=0.0015) in both HFD groups while Iba1 increased (1-way ANOVA, F (3, 17) = 15.87, p<0.0001) in both CD groups. Likewise, in the GCL, (**Figure 5-8H**) CD11b was increased (1-way ANOVA, F (3, 17) = 4.34, p=0.019) in the CL+HFD group and Iba1 was increased (1-way ANOVA, F (3, 17) = 3.89, p=0.028) in both CD groups.

Discussion

We investigated the influence of light environment on developmental programming of metabolic and visual outcomes. Developmental chronodisruption during a vulnerable window (E0 – 3wks) reduced visual function, altered retinal function, increased retinal microglial/macrophage activation, and impaired glucose tolerance in offspring (**Figure 5-9**), with differences exacerbated after metabolic challenge with HFD. The findings of increased expression of retinal microglial and macrophage markers supports a role for immune system activation in mediating the visual function results(Gupta et al., 2003; Rashid et al., 2019; Zhao et al., 2015). Overall, the findings support environmental light as a relevant exposure for developmental programming and DOHaD.

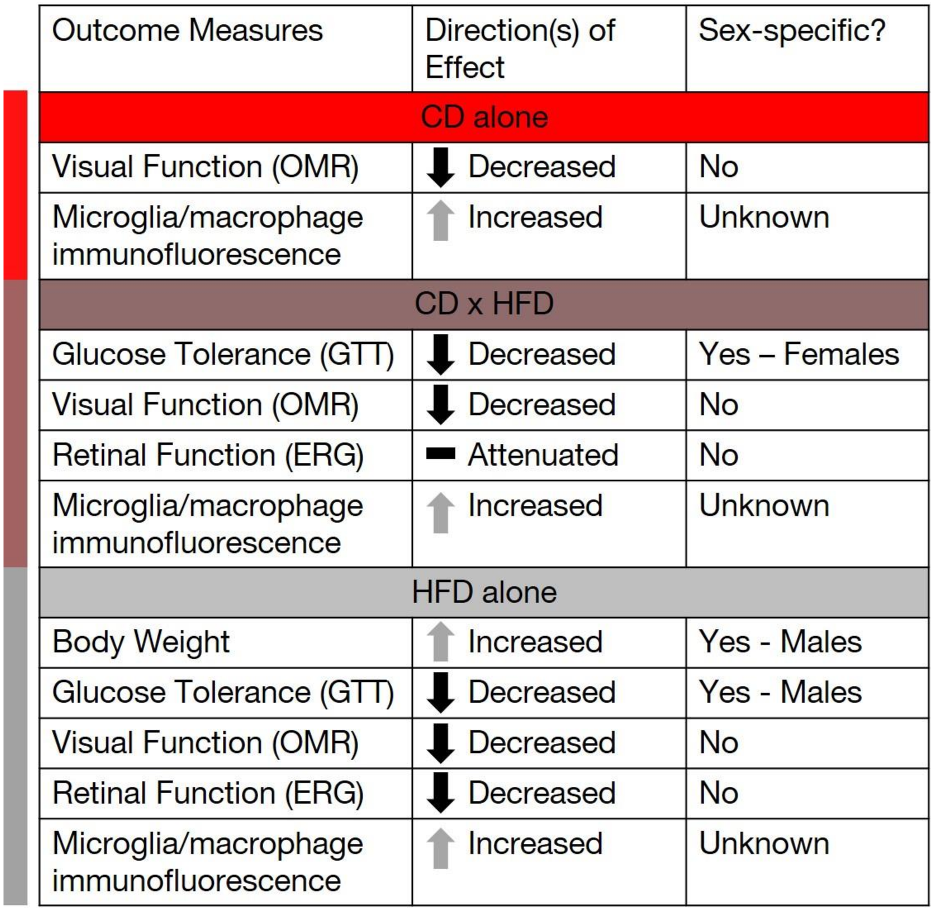

Outcome Measures	Direction(s) of Effect	Sex-specific?
CD alone		
Visual Function (OMR)	⬇ Decreased	No
Microglia/macrophage immunofluorescence	⬆ Increased	Unknown
CD x HFD		
Glucose Tolerance (GTT)	⬇ Decreased	Yes – Females
Visual Function (OMR)	⬇ Decreased	No
Retinal Function (ERG)	▬ Attenuated	No
Microglia/macrophage immunofluorescence	⬆ Increased	Unknown
HFD alone		
Body Weight	⬆ Increased	Yes - Males
Glucose Tolerance (GTT)	⬇ Decreased	Yes - Males
Visual Function (OMR)	⬇ Decreased	No
Retinal Function (ERG)	⬇ Decreased	No
Microglia/macrophage immunofluorescence	⬆ Increased	Unknown

Figure 5-9. *Summary figure highlighting the influence of developmental light treatment and/or later HFD treatment on visual and metabolic outcomes and whether outcomes differed by sex.*

While previous research using genetic knockouts has been useful in understanding the contribution of specific clock genes to development, the use of environmental light to cause circadian disruption is relevant in modeling human exposure and disease. Prior studies have found that developmental chronodisruption dampens maternal rhythms in corticosterone, FFAs, cholesterol, and triglycerides(Varcoe et al., 2013), and alters activity rhythms(Mendez et al., 2016; Varcoe et al., 2013). Likewise, we report altered activity (**Figure 5-2**) and increased serum glucose in CD dams (**Figure 5-3**), although the glucose results may be due to disruption and timing of sample collection rather than mean differences since we did not take multiple measurements at specific time intervals. In offspring, maternal environmental circadian disruption causes increased adiposity, hyperleptinemia(Varcoe et al., 2011), altered glucose handling(Mendez et al., 2016; Varcoe et al., 2011), anxiety-like behavior(Smarr et al., 2017a), and increased blood pressure(Mendez et al., 2016; Mendez et al., 2019); however, previous studies have not characterized effects on the visual system.

In this study, metabolic outcomes exhibited clear sex differences (**Figures 5-4, 5-5, Supplemental Figure 5-1**), as previously reported(Hong et al., 2009; Le May et al., 2006; Parks et al., 2015; Yang et al., 2014). While all males fed HFD developed worse glucose tolerance, notably, only the CD+HFD females developed impaired glucose tolerance, suggesting a sex-specific interaction between developmental light environment and later nutritional challenge. These glucose tolerance results align with previous findings of altered glucose homeostasis and metabolism in offspring following developmental circadian disruption(Mendez et al., 2016; Varcoe et al., 2011) and suggest that developmental chronodisruption enacts sex-specific effects on metabolic programming(Maniu et al., 2016; Zhu et al., 2015).

Developmental chronodisruption led to decreased visual function, the pace of which was quickened by HFD (**Figure 5-6**). HFD alone also impaired visual function, the impact of which has not been well-studied(Clarkson-Townsend et al., 2021c); a previous study utilizing a high-fat, high-sucrose diet reported no differences(Atawia et al., 2020) while another reported decreased OMR responses after 2 months of HFD (Douglass, AJ et al. IOVS 2020;61:ARVO E-Abstract 2245). However, an OCTA study uncovered rapid neurovascular decoupling after sugary beverage consumption(Kwan et al., 2020), suggesting clinical relevance for acute nutritional challenge. OMR measures the accessory optic system reflex in the retina from velocity-selective and direction-selective ON retinal ganglion cells(Giolli et al., 2006; Schiller, 2010). The increased retinal expression of retinal microglial and macrophage markers in the GCL layer of CD and CD+HFD mice supports a potential role for immune system activation in driving the visual function results.

Developmental light treatment altered retinal function responses to HFD challenge (**Figure 5-7**). The largest ERG a-wave and b-wave amplitude deficits occurred acutely in the CL+HFD group, with partial recovery. The retina has high energy needs, is sensitive to metabolic perturbations(Kowluru and Chan, 2007), and utilizes both glucose and lipids as fuel(Joyal et al., 2016); acute metabolic imbalance due to increased dietary fat may have caused ERG amplitude deficits. Surprisingly, ERG amplitude deficits were attenuated in the CD+HFD group. Developmental CD may have influenced retinal response to metabolic challenge.

Inflammasome activation is a well-known contributor to retinal disease pathology. Our study is novel in its investigation of the effects of developmental CD with later life HFD challenge in regards to retinal inflammation (**Figure 5-8**). Several studies have described increased retinal inflammation associated with HFD, primarily in regards to its role in diabetes(Atawia et al., 2020; Clarkson-Townsend et al., 2021c; Collins et al., 2018; Lee et al., 2015; Mancini et al., 2013; Rajagopal et al., 2016; Tuzcu et al., 2017). In the retina, HFD induces toll-like receptor 4 (TLR4) dependent macrophages and microglial activation, a signaling pathway involved in chronic inflammation and insulin resistance(Lee et al., 2015). Likewise, retinal CD11b microglia and/or macrophages activation is observed in patients with diabetes and in diabetic animal models(Ibrahim et al., 2011; Krady et al., 2005; Zeng et al., 2008). In CD and HFD-treated mice, we found upregulation of Iba-1 positive cells (microglia) and CD11b-positive cells (microglia and macrophages) within inner retinal layers (GCL, IPL and OPL), as well as upregulation of Iba1 in the INL. Our results support that CD+HFD elicits a chronic inflammatory response within the inner retina. The circadian system regulates immune signaling(Oishi et al., 2017; Orozco-Solis and Aguilar-Arnal, 2020; Scheiermann et al., 2018), and increased microglial activation and astrogliosis occurs in mice with circadian clock gene knockout *Rev-erbα*(Griffin et al., 2019) and *Arntl* (*Bmal1)*(Musiek et al., 2013). As such, the upregulation in retinal inflammatory markers in CD mice may be due to lingering effects of developmental circadian disruption, aggravated by HFD. This retinal inflammation correlates with the visual impairment and altered retinal function we found in CD-exposed offspring.

Several limitations should be kept in mind when interpreting our findings. As the C57BL/6J mouse strain is melatonin-deficient, these outcomes are independent of melatonin, a key circadian hormone and antioxidant; as untimely light exposure can disrupt melatonin production and rhythms in humans, the relevance of these results to human health requires further characterization of developmental circadian disruption in melatonin-proficient strains. Additionally, while the greatest difference in visual function from baseline was an approximately 0.1 unit decrease in spatial frequency in the CD+HFD group, it is unclear whether this change would affect fitness and how it would translate to human vision. In assessing the results, the 95% confidence intervals for the ERG and GTT AUC results were wider compared to the other outcomes, which suggests that a larger sample size may have provided more robust measures. Environmental light and circadian disruption are ubiquitous exposures with great public health relevance. As genetic or environmental perturbation of the circadian system can affect retinal differentiation and neuronal development(Baba et al., 2018a; Noda et al., 2019; Rao et al., 2013; Sawant et al., 2017; Sawant et al., 2019), and ipRGCs(Lo Giudice et al., 2019) and opsins are active early in retinal development, the timing of light exposure during windows of early neuronal tissue development may impact later life vision outcomes. Our findings demonstrate reduced visual function, altered retinal function, impaired glucose tolerance, and upregulated retinal microglial and macrophage markers in mice developmentally chronodisrupted via environmental light. Likewise, environmental light programming may make offspring more vulnerable to developing metabolic and immune-mediated disease, such as diabetes and diabetic retinopathy. Further studies are also necessary to fully characterize the inflammatory responses associated with CD and HFD. Overall, these findings extend the prior research and collectively support environmental light as a relevant exposure(Varcoe, 2018; Varcoe et al., 2018) for developmental programming and DOHaD research.

Supplemental Material

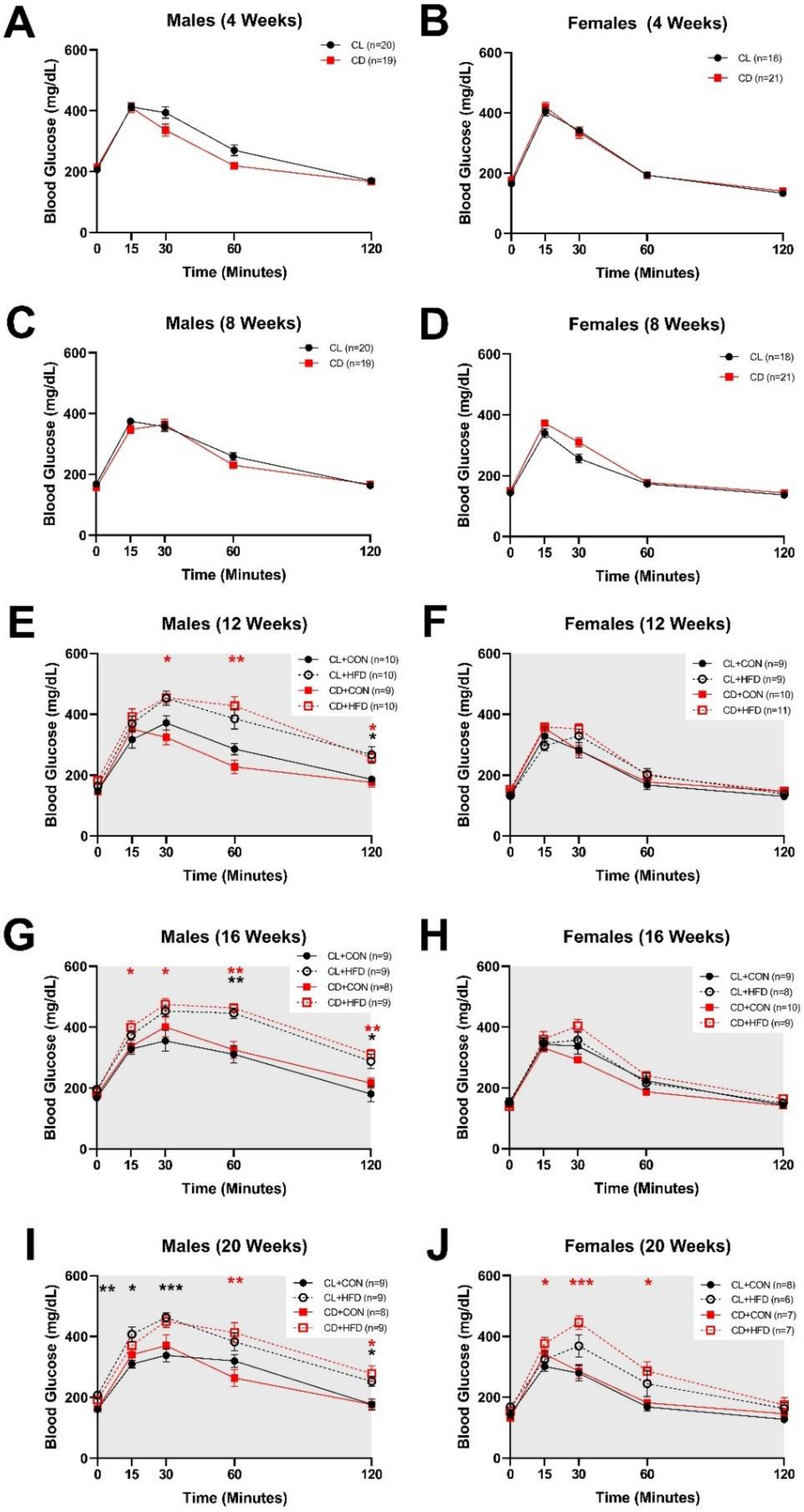
A
Males (4 Weeks)
CL (n=20)
CD (n=19)
B
Females (4 Weeks)
CL (n=18)
CD (n=21)
C
Males (8 Weeks)
CL (n=20)
CD (n=19)
D
Females (8 Weeks)
CL (n=18)
CD (n=21)
E
Males (12 Weeks)
CL+CON (n=10)
CL+HFD (n=10)
CD+CON (n=9)
CD+HFD (n=10)
F
Females (12 Weeks)
CL+CON (n=9)
CL+HFD (n=9)
CD+CON (n=10)
CD+HFD (n=11)
G
Males (16 Weeks)
CL+CON (n=9)
CL+HFD (n=9)
CD+CON (n=8)
CD+HFD (n=9)
H
Females (16 Weeks)
CL+CON (n=9)
CL+HFD (n=8)
CD+CON (n=10)
CD+HFD (n=9)
I
Males (20 Weeks)
** * ***
**
CL+CON (n=9)
CL+HFD (n=9)
CD+CON (n=8)
CD+HFD (n=9)
J
Females (20 Weeks)
* *** *
CL+CON (n=8)
CL+HFD (n=6)
CD+CON (n=7)
CD+HFD (n=7)
Blood Glucose (mg/dL)
0
200
400
600
Time (Minutes)
0
15
30
60
120

Supplemental Figure 5-1. *Males on HFD have abnormal glucose tolerance earlier than females. Male and female glucose tolerance at (**A-B**) 4 weeks of age and (**C-D**) 8 weeks of age, prior to diet treatment. (**E-F**) Male and female glucose tolerance at 12 weeks of age; CD+HFD males developed hyperglycemia by 15 minutes and remained elevated while CL+HFD males didn't show significantly increased blood glucose until 120 minutes ($p<0.05$). (**G-H**) Male and female glucose tolerance at 16 weeks of age; CD+HFD males developed hyperglycemia by 15 minutes and remained elevated compared to CL+HFD males which wasn't significantly elevated until 60 minutes ($p<0.05$). (**I-J**) Male and female glucose tolerance at 20 weeks of age; CD+HFD males developed hyperglycemia by 60 minutes and CL+HFD males by baseline ($p<0.05$); CD+HFD females had hyperglycemia by 15 minutes and remained elevated ($p<0.05$). Data are presented as mean ± SEM and analyzed by 2-way ANOVAs with Dunnett tests. *$p<0.05$ **$p<0.01$ ***$p<0.001$ ****$p<0.0001$ vs CL+CON group. Black asterisks indicate CL+HFD group and red asterisks indicate CD+HFD groups. Grey shading indicates period of diet treatment. For males, CL+CON n=9-10, CL+HFD n=9-10, CD+CON n=8-9, CD+HFD n=9-10 at each timepoint; for females, CL+CON n=8-9, CL+HFD n=6-9, CD+CON n=7-10, CD+HFD n=7-11 at each timepoint.*

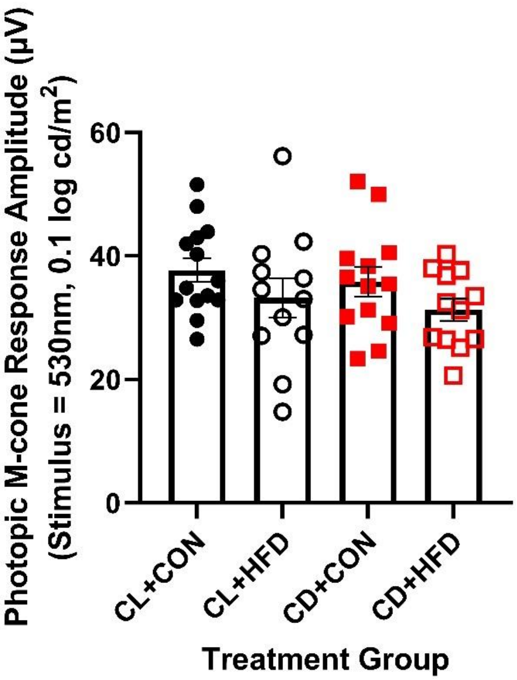

***Supplemental Figure 5-2**. There are no differences in response to photopic green light stimuli after developmental circadian disruption or diet treatment. Graph showing b-wave amplitude of photopic M-cone response to green light (530nm, flash stimulus = 0.1 log cd s/m^2 after 10-minute light adaptation at 1.5 log cd s/m^2) at 21 weeks of age (1-way ANOVA, F (3, 47) = 1.47, p=0.24), CL+CON n=14, CL+HFD n=12, CD+CON n=13, CD+HFD n=12.*

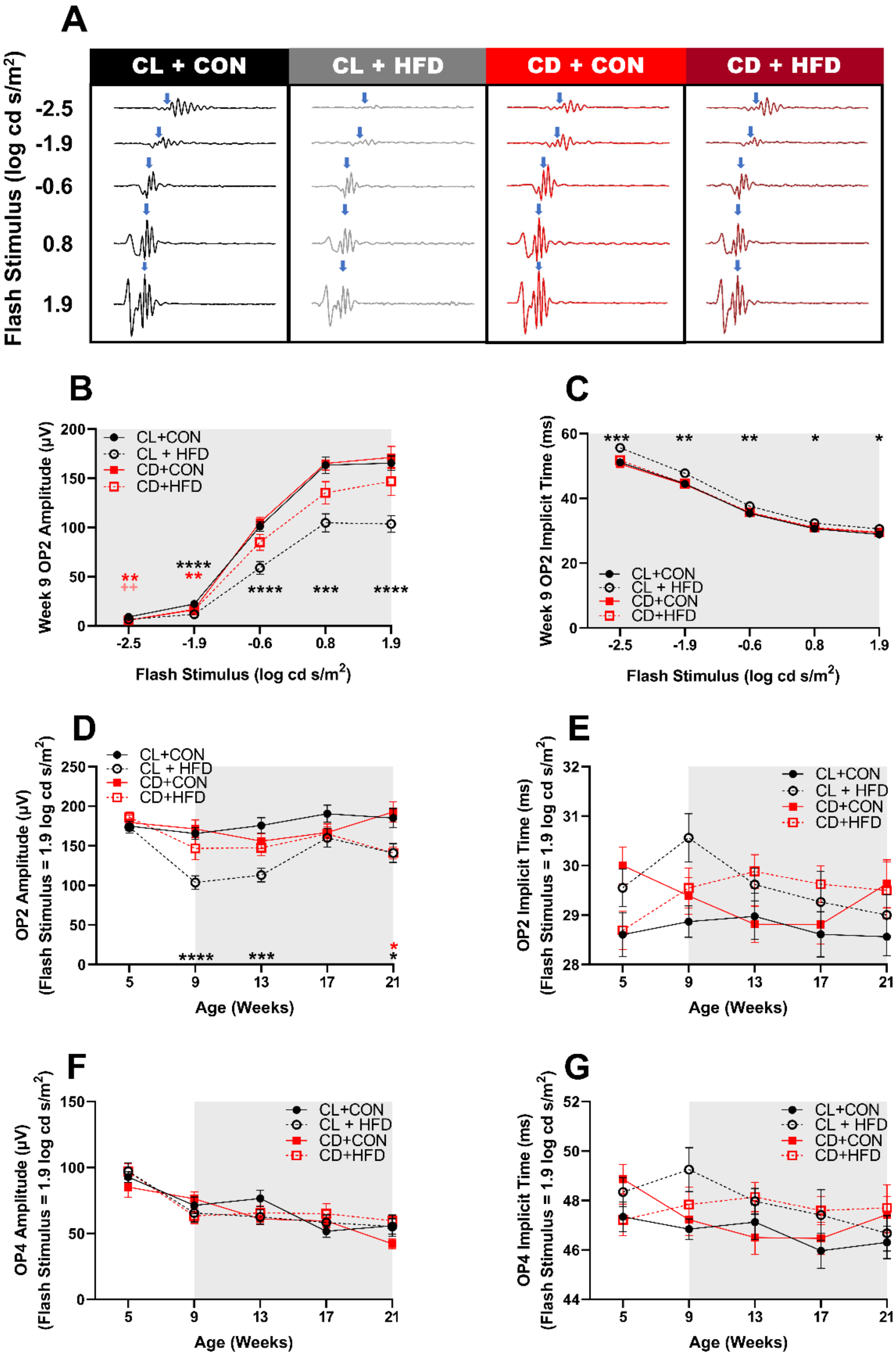

***Supplemental Figure 5-3**. HFD treatment and developmental circadian disruption impair ERG oscillatory potential (OP) amplitudes. (**A**) OP waveforms representative of OP2 at 9 weeks of* *age (1 week after HFD) in response to scotopic stimuli show visible amplitude deficits in the CL+HFD group. Blue arrows indicate the peak for the OP2 wave. (**B**) At 9 weeks of age, the CL+HFD group had both decreased OP2 amplitudes (2-way ANOVA, group*step: F (12, 280) = 6.33, p<0.0001) and (**C**) delayed OP2 implicit times (2-way ANOVA, group*step: F (12, 280) = 5.62, p<0.0001), as shown in the intensity response curves. Over time, the CL+HFD group had decreased (**D**) OP2 amplitudes (mixed-effects, group*time: F (12, 260) = 2.44, p=0.005) at 9, 13, and 21 weeks of age; the CD+HFD group also developed OP2 deficits at 21 weeks. There were no differences in (**E**) OP2 implicit times (mixed-effects, group*time: F (12, 260) = 1.54, p=0.11), (**F**) OP4 amplitudes (mixed-effects, group*time: F (12, 260) = 1.38, p=0.18), or (**G**) OP4 implicit times (mixed-effects, group*time: F (12, 260) = 1.24, p=0.26). Data are presented as mean ± SEM and analyzed by 2-way ANOVAs or mixed models with Dunnett tests. *p<0.05 **p<0.01 ***p<0.001 ****p<0.0001 vs CL+CON group. Black asterisks indicate CL+HFD group, red asterisks indicate CD+HFD, and pink crosses indicate CD+CON group. Grey shading indicates period of diet treatment. For each timepoint, CL+CON n=16-19, CL+HFD n=14-19, CD+CON n=15-19, CD+HFD n=15-21.*

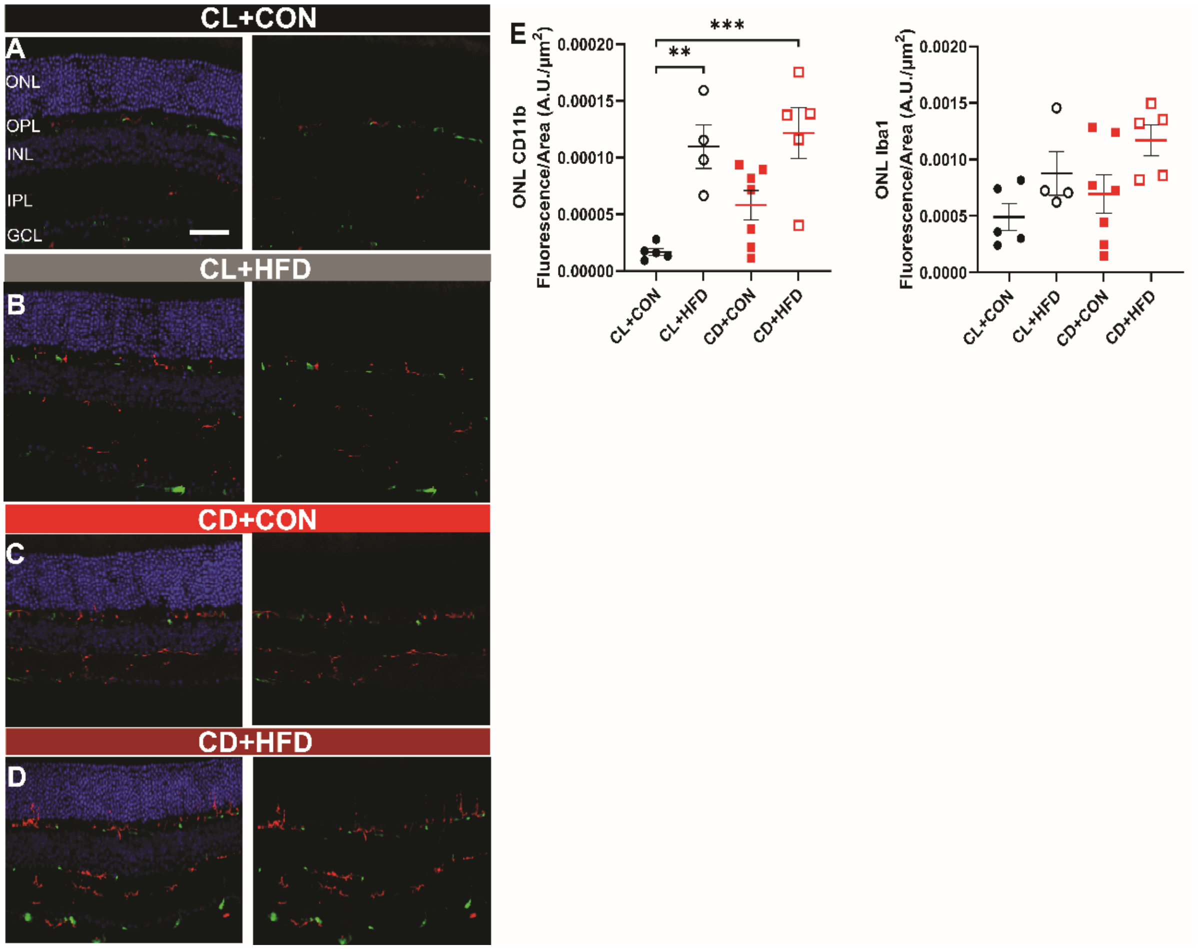
CL+CON
A
ONL
OPL
INL
IPL
GCL
CL+HFD
B
CD+CON
C
CD+HFD
D
E
***
**
ONL CD11b
Fluorescence/Area (A.U./µm²)
0.00020
0.00015
0.00010
0.00005
0.00000
CL+CON
CL+HFD
CD+CON
CD+HFD
ONL Iba1
Fluorescence/Area (A.U./µm²)
0.0020
0.0015
0.0010
0.0005
0.0000
CL+CON
CL+HFD
CD+CON
CD+HFD

Supplemental Figure 5-4. *HFD cause increased CD11b (green) and Iba1 (red) expression in the ONL. Representative retinal immunofluorescence microscopy results, with (left) and without (right) DAPI staining (blue), showing retinal layers of the (**A**) CL+CON group, the (**B**) CL+HFD group, the (**C**) CD+CON group, and the (**D**) CD+HFD group. Measured fluorescence in the ONL, showing (**E**) CD11b+ increased (1-way ANOVA, F (3, 17) = 8.955, p=0.0009) in both HFD groups while Iba1 increased in the CD+HFD group while ONL Iba1 did not significantly differ between groups (1-way ANOVA, F (3, 17) = 3.061, p=0.056). Images from the CL+CON group (n=5 mice), CL+HFD group (n=4 mice), CD+CON group (n=7 mice), and CD+HFD group (n=5 mice) include both sexes. Data are presented as mean ± SEM and* *analyzed by 1-way ANOVAs with Dunnett tests. *$p<0.05$, **$p<0.01$, ***$p<0.001$ vs CL+CON group. Scale bar = 12µm.*

Chapter 6: Developmental Circadian Disruption Alters Placental Signaling in Mice

Under review at time of dissertation submission. Pre-print posted and available here: https://www.biorxiv.org/content/10.1101/2021.04.21.440521v1

Danielle A. Clarkson-Townsend, Katie L. Bales, Karen E. Hermetz, Amber A. Burt, Machelle T. Pardue, Carmen J. Marsit. bioRxiv 2021.04.21.440521; doi: https://doi.org/10.1101/2021.04.21.440521

Abstract

Circadian disruption has been largely overlooked as a developmental exposure. The placenta, a conduit between the maternal and fetal environments, may relay circadian cues to the fetus. We have previously shown that developmental chronodisruption causes visual impairment and increased retinal microglial and macrophage marker expression. Here, we investigated the impacts of environmental circadian disruption on fetal and placental outcomes in a C57BL/6J mouse (Mus musculus) model. Developmental chronodisruption had no effect on embryo count, placental weight, or fetal sex ratio. When measured with RNAseq, mice exposed to developmental circadian disruption (CD) had differential placental expression of several transcripts including Serpinf1, which encodes pigment-epithelium derived factor (PEDF). Immunofluorescence of microglia/macrophage markers, Iba1 and CD11b, also revealed significant upregulation of immune cell markers in CD-exposed placenta. Our results suggest that in utero circadian disruption enhances placental immune cell expression, potentially programming a pro-inflammatory tissue environment that increases the risk of chronic disease in adulthood.

Introduction

Environmental light exposure has changed rapidly within the last century with the introduction of electric lighting. One of the consequences of the modern light environment is circadian disruption, or misalignment between the internal temporal system and external cues(Lunn et al., 2017). Circadian disruption causes chronic disease, such as diabetes and dyslipidemia(Karatsoreos et al., 2011; Morris et al., 2015; Reutrakul and Knutson, 2015; Shimba et al., 2011); night shift work is even categorized by the International Agency for Research on

Cancer as a Group 2A carcinogen, “probably carcinogenic to humans”(IARC, 2019). However, little is known how circadian disruption affects fetal development.

The Developmental Origin of Health and Disease (DOHaD) hypothesis grew out of research on *in utero* undernutrition and later life risk of cardiometabolic disease(Barker and Osmond, 1986; Barker, 2004). These studies found that infants born with low birthweight or small for their gestational age (SGA) had an increased risk of heart disease and stroke as adults(Barker et al., 1993; Osmond et al., 1993; Rich-Edwards et al., 1997; Tian et al., 2017; Wang et al., 2020). Later, the Dutch Hunger Winter cohort revealed epigenetic(Heijmans et al., 2008) and transgenerational(Painter et al., 2008) effects of *in utero* exposure to famine on offspring. DOHaD research has grown to encompass exposure to early life stress and pollutants(Haugen et al., 2015), such as endocrine disrupting compounds, and outcomes related to neurological and hormonal programming. Light can also act as an endocrine disruptor(Russart and Nelson, 2018); however, the influence of light exposure on developmental programming has not yet been widely assessed in DOHaD studies.

We have previously shown that developmental chronodisruption in mice (via environmental light) from embryonic day 0 until weaning at 3 weeks of age has lasting effects on visual and metabolic outcomes of adult offspring; in particular, mice exposed to developmental circadian disruption have increased expression of retinal microglia and macrophage markers accompanied with impaired visual function(Clarkson-Townsend et al., 2021b). The placenta, a neuroendocrine organ, regulates *in utero* growth, including fetal neuronal growth. Communication between the placenta and fetal brain, termed the placenta-brain axis(Rosenfeld, 2021), influences neurodevelopment. The immune system plays an important role in the placenta-brain axis, and activation of placental immune signals can influence development of fetal immune cells, such as microglia, in the fetal brain(Edlow et al., 2019; Prins et al., 2018). Therefore, we investigated the impacts of developmental circadian disruption on overall gene expression and immune cell phenotypes in the placenta. To do this, we exposed pregnant mice to developmental chronodisruption and measured fetal and placenta outcomes (count, weight, sex ratio), placental gene expression (RNAseq), and placental expression of immune cell markers CD11b and Iba1 (immunofluorescence).

Materials and methods

Ethical approval

All experimental procedures were approved by the Institutional Animal Care and Use Committee of the Atlanta Veterans Affairs Healthcare System in facilities that are accredited by the Association for the Assessment and Accreditation of Laboratory Animal Care International (AAALAC).

Animal handling and experimental design

Wildtype female (~3-4 weeks old) C57BL/6J mice (*Mus musculus*) were ordered from Jackson Laboratories (Bar Harbor, ME, USA); wildtype male C57BL/6J mice were ordered or bred in-house from mice from Jackson Laboratories. Males for breeding were singly housed whereas female breeders were co-housed in large (6”x9”x18”) wire-top shoebox cages in standard conditions (*ad libitum* chow (Teklad Rodent Diet 2018 irradiated 2918, Envigo Teklad, Madison, WI, USA), 12:12 lighting) and checked daily for well-being. After a 2 week acclimation period, naïve females were randomized to either control light (CL, 12:12 light:dark) or a chronodisruption (CD) light paradigm, consisting of weekly inversions of the photoperiod(Clarkson-Townsend et al., 2021b; Mendez et al., 2016; Varcoe et al., 2011). Light intensity was standardized across groups to be ~50-400 lux (Dual-range light meter 3151CC, Traceable, Webster, TX, USA), with darkest areas at the bottom of the cage under the food holder and brightest areas near the top of the cage. Females were exposed to light treatments for 4 weeks prior to timed breeding; during aligned light schedules, representative females from each light treatment group were introduced to the male's cage in the afternoon; females were checked for plugs and returned to their home cages after 2 days. Females were weighed several days later to confirm pregnancy; if not pregnant, they were placed with the same male the following week for further rounds of pairing for up to 4 more weeks of pre-pregnancy light treatment. Dams remained in CD or CL light treatments until tissue collection at gestational day 15.5 (E15.5). While placental tissue collection was timed to be the estimated E15.5 date and mouse pairings occurred in a restricted time window, we did not evaluate vaginal cytology or use *in vitro* fertilization, and it is therefore possible that embryonic age varied by a day.

Tissue collection

Pregnant mice (E15.5) were sacrificed with compressed CO_2 gas anesthesia, followed by cervical dislocation and rapid decapitation for truncal blood collection between 9AM-11AM (ZT3-5); within this range, tissue collection time did not substantially differ between CL and CD groups. Position of each placental sample within the uterine horns, placental wet weight, and reabsorptions were recorded and placentae immediately dissected out after removing uterine tissue. Placental tissue samples were snap-frozen in liquid nitrogen and stored at -80°C until further processing for RNA isolation or preserved in 10% neutral buffered formalin for histological and immunohistochemical analyses. Fetal tail samples were also collected, snap frozen, and stored at -80°C until later use for sex determination. Samples from 3 dams, all from the CD group, were excluded due to noted quality issues during collection; for example, in 2 mice, all of the embryos in a uterine horn exhibited blood clots and discoloration. Samples from a total of 12 dams, 6 CL and 6 CD, were included in the analysis.

RNA isolation, sequencing, alignment, and generation of count data

Prior to placental RNA isolation, all fetal tail tissue samples were lysed and RNA extracted using the Qiagen Allprep DNA/RNA Mini Kit according to manufacturer's instructions and *Sry* gene expression measured via PCR to determine sex (SryFWD: 5' – TGG GAC TGG TGA CAA TTG TG -3' and SryREV : 5' – GAG TAC AGG TGT GCA GCT CT-3'). Samples with faint bands were re-run. For RNA sequencing, placental samples without any noted collection quality issues were randomly selected and matched on sex when possible (quality samples of both sexes were not available for each dam). Two samples from each dam were chosen, for a total of 24 placenta samples, 12 from each light treatment group, and DNA and RNA isolated using the Qiagen Allprep DNA/RNA Mini Kit according to manufacturer's instructions. RNA quality was measured using the Agilent 2100 Bioanalyzer with Agilent RNA 6000 Nano kit (cat# 5067-1511) following manufacturer's instructions and RNA concentrations measured with a Thermo Scientific NanoDrop spectrophotometer. All samples had RIN scores $\geq$ 9. Placental RNA samples (n=24) were sent to the Emory Genomics core for PolyA RNA sequencing performed at 30M read depth. FastQC was performed to check read quality and fastq files aligned to the C57 mouse genome (Ensemble assembly GRCm38.p6) with STAR v2.7 using default settings. Read counts were derived using the "quantmode" command in STAR. Raw sequencing data FastQ files, processed gene count data, and sample information have been deposited in GEO (accession number GSE169266). Code for sample alignment and processing, as well as gene count data, are available at: https://github.com/dclarktown/CD_mice_placenta (DOI: 10.5281/zenodo.4536522).

Differential expression (DE) analysis

Count data were read into R (version 3.2) and analyzed for differential expression (DE) using DESeq2(Love et al., 2014). The original 53,801 transcripts measured were limited to transcripts that had at least 1 count in 10% of samples, leaving a total of 14,739 transcripts for analysis. To confirm sex of samples, samples were also evaluated for high expression of *Xist* mRNA, indicative of female sex. Of the 24 samples, 1 sample was mismatched for sex (sample #9, 1009) and edited to the correct sex. After 1 sample was found to be an outlier driving many of the DE results (sample #12, 1012), it was dropped from the analysis. The DE analysis of the remaining 23 samples adjusted for sex and the first surrogate variable, with developmental light treatment group as the main exposure. The first surrogate variable was computed using the *sva* package(Leek et al., 2012) and "be" method with 200 iterations. Results were adjusted for false discovery rate using the Benjamini and Hochberg (BH) method and considered significant if $q<0.05$.

Pathway analysis

Transcript enrichment for differentially expressed genes was performed using EnrichR(Kuleshov et al., 2016) among the Mouse Gene Atlas, ChEA 2016, KEGG 2019 Mouse, and GO 2018 (Biological Process, Molecular Function, Cellular Component) databases. Results were adjusted for multiple comparisons using the Benjamini-Hochberg (BH) method and considered significant if $q<0.05$.

Placental immunofluorescence measurement and quantification

Fresh placenta samples were fixed in 10% neutral buffered formalin overnight at 4°C and then cryoprotected the following day in 30% sucrose after washing with 1x PBS. Samples were embedded and frozen in optimal cutting temperature compound and sliced into 7-µm-thick sections. Placental sections were blocked (with 0.1% Triton X-100) and incubated with primary antibodies in 5% normal donkey serum in PBS before washing with PBS. Primary antibody incubations using Iba1 (ab178847; 1:100; Abcam) and CD11b (14-0112-82; 1:100; Invitrogen) were performed for 16-24 hours at 4°C and secondary antibody incubations were performed for 1 hour at room temperature using Alexa Fluor 488 Donkey anti-mouse IgG (A-21202; 1:500) and Alexa Fluor 647-conjugated Donkey anti-rabbit IgG (A-31573; 1:500). Tissue nuclei were visualized with nuclear stain 4′,6-diamidino-2-phenylindole (DAPI, 62247; Thermo Fisher Scientific). Coverslips were mounted using Prolong Gold (P36934; Thermo Fisher Scientific). Placental tissue (n=4-6 mice/group; 3 images per sample, averaged for the analysis) was imaged with an Olympus Fluoview1000 confocal microscope (Center Valley, PA) using a 20x objective and a Lumenera INFINITY 1-3C USB 2.0 Color Microscope camera (Spectra Services, Ontario, NY). All images were processed and quantified using ImageJ software by a researcher masked to treatment group.

Statistical analysis and data availability

Unless otherwise noted, weight, embryo number, placental weight, sex ratio, and immunofluorescence data were all analyzed with Student’s 2-tailed unpaired t-tests and considered significant if $p<0.05$. Statistical tests were performed in Prism version 9.0.0. Statistics for placental gene expression analyses are described in the previous sections. All data and code used for the analyses are available at: https://github.com/dclarktown/CD_mice_placenta (DOI: 10.5281/zenodo.4536522), except for the raw sequencing data which has been deposited in GEO (accession number GSE169266).

Results and discussion

Here, we investigated whether circadian disruption led to functional and immunologic changes in the placenta. We have previously shown that developmental CD light treatment alters programming of the visual system in offspring(Clarkson-Townsend et al., 2021b). CD females did not differ in pre-pregnancy weight (Student's unpaired 2-tailed t-test, t=0.83, df=10, p=0.43, **Figure 6-1A**) or pregnancy weight at tissue collection (Student's unpaired 2-tailed t-test, t=0.72, df=10, p=0.49, **Figure 6-1B**) compared to CL females. There were also no differences in embryo count, fetal sex ratio, and placental weight (**Figure 6-1C-F**), consistent with previous findings(Varcoe et al., 2013) in a rat model that additionally found no change in fetal weight or placental:fetal weight ratio. Genetic models of developmental circadian disruption have found similar null results; knockout of *Bmal1* (*Arntl*), a core circadian clock gene, in fetal tissue does not alter embryo number or fetal or placental weight(Varcoe et al., 2018), whereas knockout in parental male or female tissue causes infertility(Alvarez et al., 2008). However, the exclusion of 2 CD dams from the analysis due to discoloration and blood clots throughout one uterine horn may have biased results towards a more conservative measure of effect.

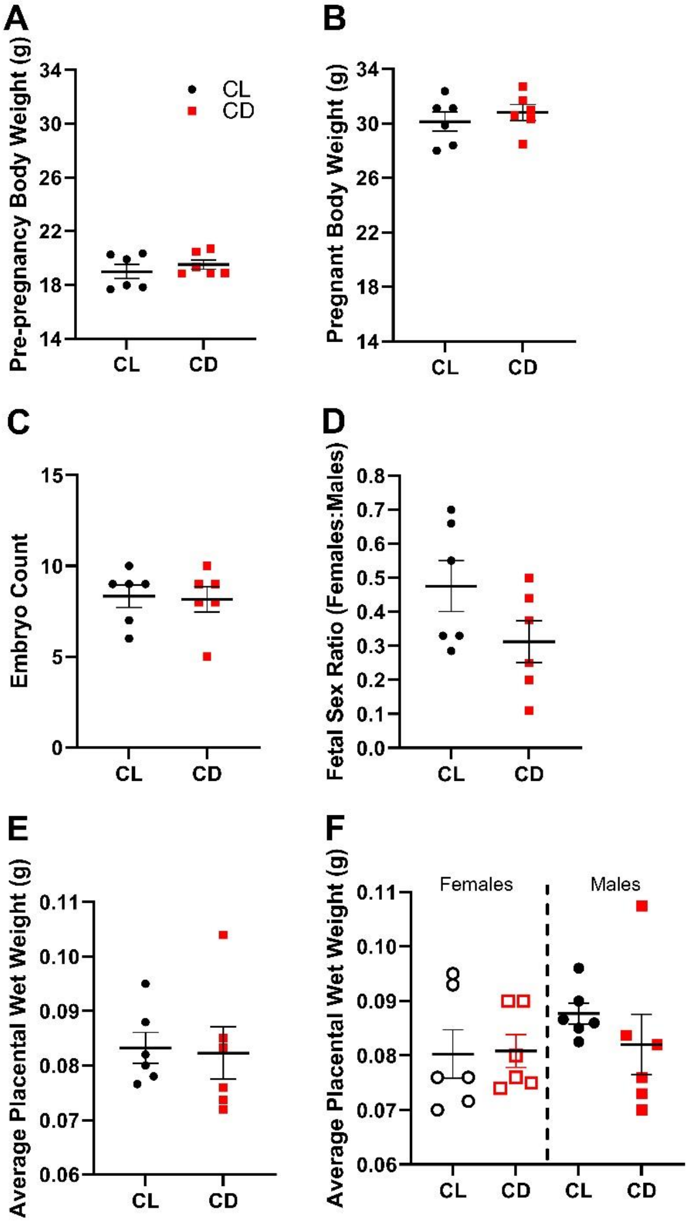

Figure 6-1. Light treatment did not alter dam or fetal outcomes. *Body weight (grams) of female mice (CL n=6, CD n=6) from which placental samples were collected (**A**) just prior to pairing for timed breeding (Student's unpaired 2-tailed t-test, t=0.83, df=10, p=0.43) and (**B**) when pregnant at E15.5 just prior to tissue collection (Student's unpaired 2-tailed t-test, t=0.72, df=10, p=0.49). (**C**) Number of viable embryos per dam counted within the uterine horns (Student's 2-tailed unpaired t-test, t=0.18, df=10, p=0.86). (**D**) Sex ratio of viable embryos per*

*dam, as determined by PCR of fetal tail snip and subset confirmed by RNA sequencing (Student's 2-tailed unpaired t-test, t=1.67, df=10, p=0.12). (**E**) Average placental wet weight (grams) per dame (Student's 2-tailed unpaired t-test, t=0.16, df=10, p=0.87). (**F**) Average placental wet weight (grams) per dam, stratified by sex (1-way ANOVA, F (3, 20) = 0.73, p=0.55). All data are presented as mean ± SEM.*

Placentas were collected at the late stage of pregnancy and sequenced for gene expression. Among the most highly expressed transcripts across all placenta samples (regardless of exposure) were *Tpbpa*, *Prl3b1*, *Tpbpb*, *Psg21*, *Prl8a9*, and *Psg23*, gene expression typical of trophoblasts. The EnrichR pathway analysis of the top 100 most highly expressed placental genes indicated enrichment for mouse placental tissue (q<0.05, **Supplemental File 6-1**) in the Mouse Gene Atlas database, as expected, and, interestingly, for the CLOCK, NELFA, and HSF1 transcription factors in the ChEA database. CLOCK is a core component of the circadian clock, and as mediator of the maternal and fetal environments, the placenta may function as a peripheral oscillator; we have previously shown that placental gene expression varies seasonally(Clarkson-Townsend et al., 2020), which suggests sensitivity to seasonal environmental exposures such as light and temperature. Top KEGG pathways were: "antigen processing and presentation", "protein processing in endoplasmic reticulum", "lysosome" and "HIF-1 signaling pathway"; likewise, top GO pathways were related to immune signaling and protein processing, with terms such as "ATF6-mediated unfolded protein response", "neutrophil degranulation", "collagen binding", "secretory granule lumen", and "focal adhesion" (**Supplemental File 6-1**).

Principle component analysis of the placental samples revealed relative overlap between the CL and CD groups (**Figure 6-2A**). This pattern was not explained by sample position within uterine horn, sample collection time, sex ratio, or RNA quality, and samples from the same dam did not necessarily cluster together. The DE analysis between male and female placental tissue (adjusting for light treatment) resulted in 77 sex-specific placental transcripts ($q<0.05$, **Figure 6-2B, Supplemental File 6-2**). A number of these genes were strikingly different; *Xist*, a non-coding RNA that silences the extra X-chromosome in females and can be used to identify fetal sex(Hoch et al., 2020), was highly expressed in female placenta. *Ddx3y*, *Eif2s3y*, *Kdm5d*, and *Uty* were all highly expressed in male placenta and have previously been reported as male-specific placental genes(Gabory et al., 2012; Lee et al., 2017); these genes could arguably also be used to identify fetal sex. Sex-specific placental gene expression ($n=113$ $q<0.1$) also displayed enrichment for pathways related to lipid, retinoid, and cholesterol metabolism in the KEGG and GO term databases, suggesting sex-specific regulation of these processes in the placenta (**Supplemental File 6-3**). Interestingly, studies of maternal malnutrition and high fat diet exposure have uncovered sex-specific placental(Gallou-Kabani et al., 2010; Lin et al., 2019; Mao et al., 2010) and phenotypic outcomes in the offspring(Howie et al., 2012; Nguyen et al., 2017). These results support investigation of these pathways in sex-specific development in future studies.

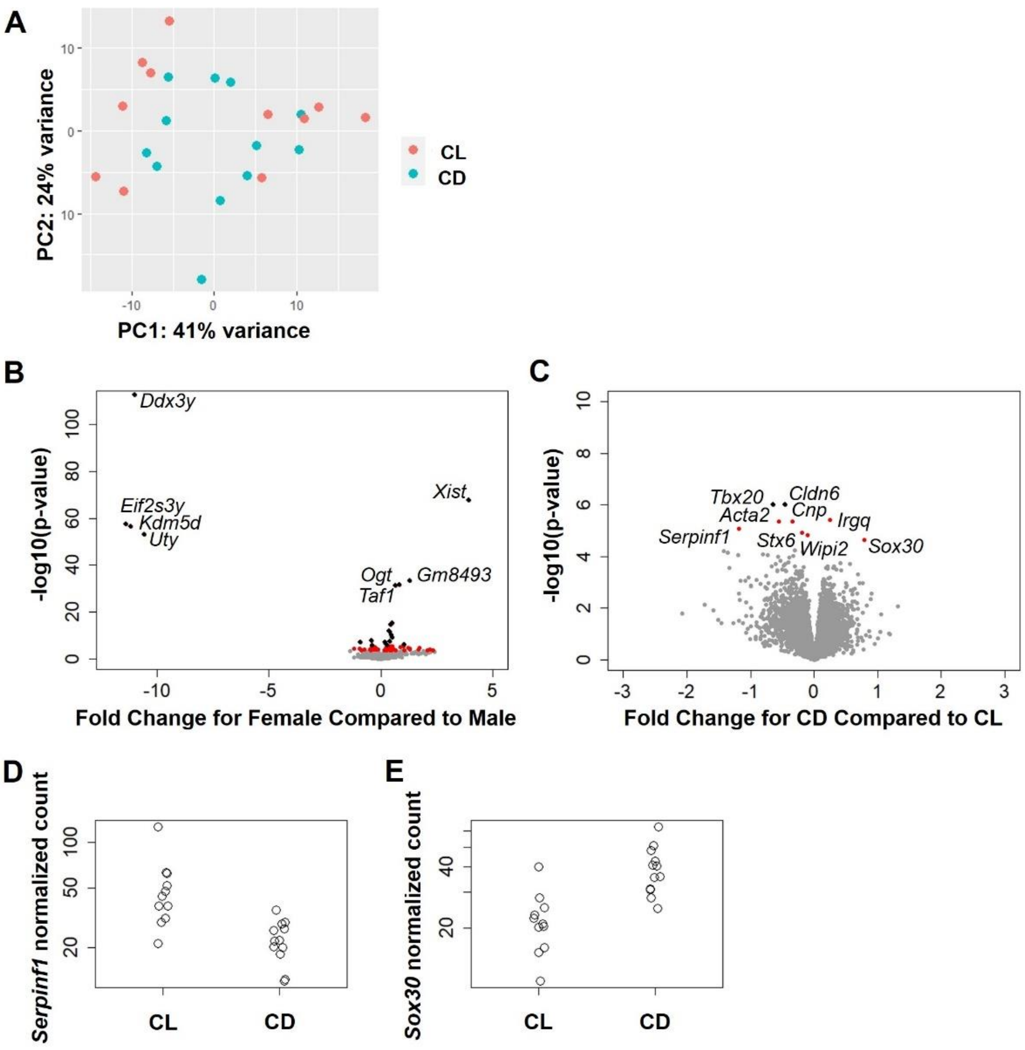

Figure 6-2. Placental gene expression varies by sex and light treatment group. *(**A**) PCA plot of first 2 principal components comparing treatment groups shows general overlap between CL and CD groups. (**B**) Volcano plot of differential placental gene expression by sex (adjusting for light treatment group and first surrogate variable). Male is the reference group, so transcripts with decreased expression in females (or, conversely, increased expression in males) are located to the left of 0, while transcripts with increased expression in females (or, conversely, decreased expression in males) are located to the right of the 0. Black dots denote Bonferroni-significant transcripts (n=22 p<0.05), red dots denote BH-significant transcripts (n=77 q<0.05), and grey dots denote non-significant transcripts. The top differentially expressed genes are plotted with*

*their respective gene names. (**C**) Volcano plot of differential placental gene expression by treatment (adjusting for sex and first surrogate variable). CL is the reference group, so transcripts with decreased expression in CD (or, conversely, increased expression in CL) are located to the left of the 0, while transcripts with increased expression in CD (or, conversely, decreased expression in CL) are located to the right of the 0. Black dots denote Bonferroni-significant transcripts (n=2 p<0.05), red dots denote BH-significant transcripts (n=9 q<0.05) and grey dots denote non-significant transcripts. Plots of raw normalized count data for (**D**) Serpinf1 and (**E**) Sox30 by treatment group.*

Few transcripts exhibited large differences between light treatment groups (**Figure 6-2C**). However, of the differentially expressed genes (n=9 q<0.05, **Supplemental File 6-4**), *Serpinf1*, *Tbx20*, *Acta2*, *Cldn6*, *Cnp*, *Stx6*, and *Wipi2* had decreased expression while *Sox30* and *Irgq* had increased expression in CD placenta (**Figure 6-2C-E**). Pathway analysis revealed that differentially expressed genes were similar to gene expression in osteoblasts in the Mouse Gene Atlas database (**Supplemental File 6-5**). While there was no enrichment for specific transcription factors within the ChEA database, differentially expressed genes were enriched for “cholesterol metabolism” in the KEGG database and terms related to tissue development, adhesion, and cytoplasmic projection in the GO databases. It is perhaps surprising that we did not uncover large differences in placental gene expression between light treatment groups. However, it is possible the small sample size limited the ability to measure more subtle differences in gene expression, especially if such differences occurred in placental cell subpopulations, such as immune cells.

Placenta from CD-exposed dams revealed significantly increased expression of Iba1 and CD11b microglial/macrophage markers than placenta from dams housed in CL conditions (p=0.027 and p=0.038, respectively, **Figure 6-3**). These results align with the finding of decreased *Serpinf1* (which encodes pigment epithelium-derived factor (PEDF)) expression in CD placenta. PEDF inhibits macrophage inflammatory processes(Zamiri et al., 2006), which may have contributed to this observation of increased CD11b and Iba1 marker expression in CD placenta. These data also coincide with our recent previous findings of an increased retinal inflammatory response and reduced visual function within mice developmentally exposed to CD(Clarkson-Townsend et al., 2021b). The immune system and inflammation govern many of the health outcomes caused by chronic circadian disruption(Castanon-Cervantes et al., 2010; Comas et al., 2017; Inokawa et al., 2020). Night shift workers were found to have greater amounts of immune cells, such as T cells and monocytes, than non-shift workers(Loef et al., 2019); likewise, we previously reported hypomethylation in immune-related genes, such as *CLEC16A*, *SMPD1*, and *TAPBP*, in the placentas of infants whose mothers worked the night shift(Clarkson-Townsend et al., 2019). Animal studies have found chronic circadian disruption increased macrophages and "pro-tumor" CD11b+ MHCII cells(Hadadi et al., 2020), altered inflammatory response in the brain(Ramsey et al., 2020), and primed the innate immune response to be more pro-inflammatory(Castanon-Cervantes et al., 2010). The placenta is the only organ formed by the interaction of both fetal/embryonic and maternal tissues and acts as the interface between both circulatory systems(Astiz and Oster, 2020). Previous research has found a strong correlation between placental CD11b expression and fetal brain microglial activation(Edlow et al., 2019). In mice and humans, brain and placental macrophages and microglia originally derive from the same source: the fetal yolk sac(Godin and Cumano, 2002; Stremmel et al., 2018). These progenitor macrophage and microglial cells migrate from the yolk sac to embryonic tissues, where they set up residence; once settled, they are long-lived and able to replenish themselves(Ginhoux et al., 2016; Sieweke and Allen, 2013). Our results suggest that developmental light environment affects programming of the placental and fetal immune systems, laying the groundwork for a pro-inflammatory setting later in life. These findings provide novel evidence linking CD with increased placental inflammatory response and highlight the need to evaluate the influence of the light environment on health and disease outcomes in DOHaD studies.

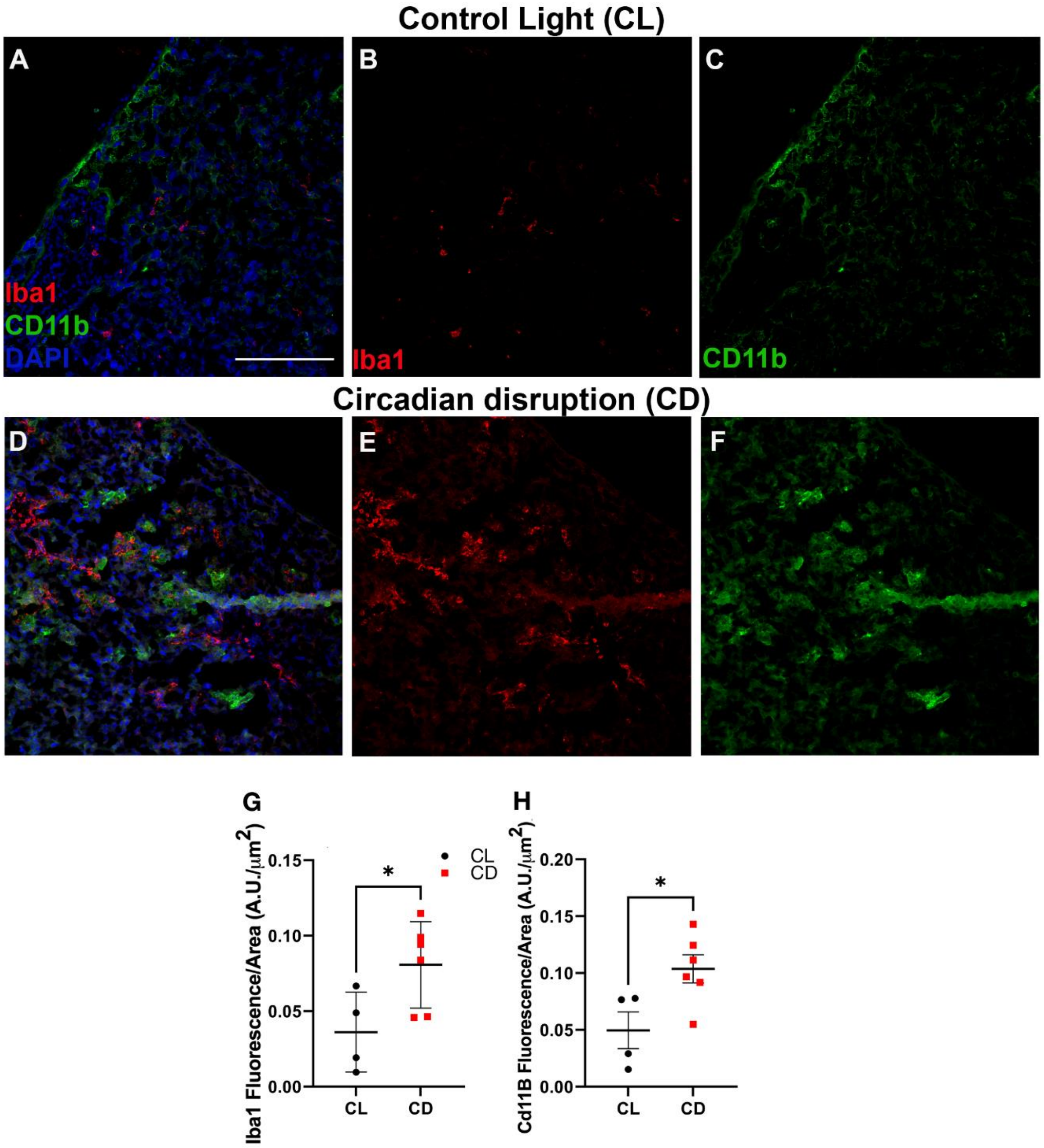
Control Light (CL)
A
Iba1
CD11b
DAPI
B
Iba1
C
CD11b
Circadian disruption (CD)
D
E
F
G
Iba1 Fluorescence/Area (A.U./μm²)
0.15
0.10
0.05
0.00
CL
CD
*
● CL
■ CD
H
Cd11B Fluorescence/Area (A.U./μm²)
0.20
0.15
0.10
0.05
0.00
CL
CD
*

Figure 6-3. Chronodisruption causes increased macrophage and microglial signaling in the placenta. *Placentas from (**A-C**) control light (CL) and mice exposed to (**D-F**) developmental circadian disruption (CD) were labeled for inflammatory markers labeling microglia and macrophages. In placenta from CD mice increased placental (**G**) Iba1 fluorescence (Student's 2-*

tailed unpaired t-test, t=2.49, df=8, p=0.038) and increased placental ***(H)*** *CD11b fluorescence (Student's 2-tailed unpaired t-test, t=2.70, df=8, p=0.027) were detected. CL=4 placenta from different dams, 3 images each; CD=6 placenta from different dams, 3 images each. All data are presented as mean ± SEM, scale bar = 20 microns, and *=p<0.05.*

Supplemental Material

Supplemental File 6-1*. Gene list of the gene IDs of the most highly expressed placental transcripts entered in the EnrichR pathway analysis. (please see supplemental materials here:* https://www.biorxiv.org/content/10.1101/2021.04.21.440521v1.supplementary-material*)*

Supplemental File 6-2 *Sex-specific results of the DESeq2 differential expression analysis of mouse placental tissue show sex-specific expression after adjusting for developmental light treatment and first surrogate variable. Male placenta tissue is the reference, so results show genes that are upregulated (postive log2FC) or downregulated (negative log2FC) in female placenta tissue. To control for false discovery rate, p-values are adjusted using the Benjamini and Hochberg (BH, q-value) method (qval); the more conservative bonferroni-adjusted p-values are also provided (bon_pval). (portion of results provided below; for full results please see supplemental materials here:* https://www.biorxiv.org/content/10.1101/2021.04.21.440521v1.supplementary-material*)*

Ensemble_ID	Mean	log2FC	lfcSE	stat	pval	qval	Bon_pval
ENSMUSG00000069045	1221.48	-10.98	0.49	-22.63	2.10E-113	3.1E-109	3.1E-109
ENSMUSG00000086503	14309.25	3.93	0.22	17.47	2.59E-68	1.9E-64	3.8E-64

ENSMUSG00000069049	492.44	-11.38	0.71	-16.08	3.45E-58	1.7E-54	5.1E-54
ENSMUSG00000056673	338.67	-11.17	0.70	-15.96	2.42E-57	8.9E-54	3.6E-53
ENSMUSG00000068457	334.68	-10.57	0.68	-15.45	7.68E-54	2.3E-50	1.1E-49
ENSMUSG00000106028	138.81	1.30	0.11	12.13	7.01E-34	1.7E-30	1.0E-29
ENSMUSG00000034160	7054.21	0.83	0.07	11.85	2.04E-32	4.3E-29	3.0E-28
ENSMUSG00000031314	1458.47	0.65	0.05	11.80	4.04E-32	7.4E-29	6.0E-28
ENSMUSG00000035150	2717.10	0.51	0.06	8.08	6.61E-16	1.1E-12	9.7E-12
ENSMUSG00000025332	3620.59	0.46	0.06	7.95	1.91E-15	2.8E-12	2.8E-11
ENSMUSG00000016409	669.71	0.37	0.05	7.07	1.54E-12	2.1E-09	2.3E-08
ENSMUSG00000014361	819.74	0.39	0.06	7.01	2.31E-12	2.8E-09	3.4E-08
ENSMUSG00000079480	314.08	0.49	0.08	6.48	9.00E-11	1.0E-07	1.3E-06
ENSMUSG00000087174	227.28	0.50	0.08	6.20	5.76E-10	6.1E-07	8.5E-06
ENSMUSG00000095687	1460.26	-0.41	0.07	-5.63	1.83E-08	1.8E-05	0.000
ENSMUSG00000031226	765.75	0.39	0.07	5.51	3.58E-08	3.3E-05	0.001
ENSMUSG00000028766	3956.46	0.20	0.04	5.38	7.40E-08	6.4E-05	0.001
ENSMUSG00000024868	214.23	-0.92	0.17	-5.32	1.05E-07	8.6E-05	0.002
ENSMUSG00000037369	1332.50	0.24	0.05	5.02	5.14E-07	0.0004	0.008
ENSMUSG00000006538	36.36	1.04	0.21	4.89	1.01E-06	0.0007	0.015
ENSMUSG00000036256	5309.53	-0.38	0.08	-4.81	1.47E-06	0.0010	0.022
ENSMUSG00000063785	266.85	0.31	0.07	4.75	2.07E-06	0.0014	0.031

Supplemental File 6-3. Gene list of the gene IDs of the DE sex-specific analysis entered in the EnrichR pathway analysis and results from the EnrichR pathway analysis of the top sex-specific genes when searched in the ChEA 2016, KEGG 2019 Mouse, and GO 2018 databases. *(please see supplemental materials here:* https://www.biorxiv.org/content/10.1101/2021.04.21.440521v1.supplementary-material*)*

Supplemental File 6-4. *Results of the DESeq2 differential expression analysis of mouse placental tissue show differential expression between control light (CL) and circadian disruption (CD) treament groups after adjusting for sex and first surrogate variable. CL placenta tissue is the reference, so results show genes that are upregulated (postive log2FC) or downregulated (negative log2FC) in CD-exposed placenta tissue. To control for false discovery rate, p-values are adjusted using the Benjamini and Hochberg (BH, q-value) method (qval). (portion of results provided below; for full results, please see supplemental materials here:* https://www.biorxiv.org/content/10.1101/2021.04.21.440521v1.supplementary-material*)*

Ensemble_ID	Mean	log2FC	lfcSE	stat	pval	qval	Gene_ID
ENSMUSG00000031965	95.03842	-0.6384	0.130513	-4.89143	1.00E-06	0.007377	Tbx20
ENSMUSG00000023906	268.7227	-0.45842	0.093699	-4.89248	9.96E-07	0.007377	Cldn6
ENSMUSG00000035783	1244.689	-0.55324	0.120433	-4.59379	4.35E-06	0.012933	Acta2
ENSMUSG00000006782	157.0644	-0.33874	0.073765	-4.59214	4.39E-06	0.012933	Cnp
ENSMUSG00000041037	961.1614	0.250019	0.054067	4.6242	3.76E-06	0.012933	Irgq

ENSMUSG00000000753	35.58648	-1.18002	0.26495	-4.45376	8.44E-06	0.020727	Serpinf1
ENSMUSG00000026470	1882.058	-0.19088	0.04361	-4.37696	1.20E-05	0.02534	Stx6
ENSMUSG00000029578	3404.169	-0.09779	0.022594	-4.32802	1.50E-05	0.02772	Wipi2
ENSMUSG00000040489	30.54977	0.791863	0.186969	4.235267	2.28E-05	0.037385	Sox30

Supplemental File 6-5. Gene list of the gene IDs of the DE light treatment analysis entered in the EnrichR pathway analysis and results from the EnrichR pathway analysis of the top sex-specific genes when searched in the ChEA 2016, KEGG 2019 Mouse, and GO 2018 databases. *(please see supplemental materials here:* https://www.biorxiv.org/content/10.1101/2021.04.21.440521v1.supplementary-material*)*

Chapter 7: Summary and Conclusions

As the health effects of circadian disruption become more and more apparent, it is an increasingly significant exposure for public health research. Epidemiological studies of shift workers have highlighted the dangers of circadian disruption as an occupational exposure; however, the general public also widely experiences circadian disruption due to social behaviors, use of light-emitting devices, and light pollution. Sleep fragmentation, irregular sleep schedules, and sleep disruption could be another driver of circadian disruption in the general population(Huang et al., 2020; Huang and Redline, 2019). Circadian disruption is an exposure that is relevant not only for working adults, but also for infants, children, and adolescents. Very little is known how circadian disruption affects development across the life course, particularly at early developmental stages. However, sleep issues during pregnancy are common, with approximately 46% of people reporting decreased sleep quality during pregnancy(Sedov et al., 2018; Silvestri and Aricò, 2019), and may represent another driver of circadian disruption during development.

Using a variety of approaches, this body of work investigated the influence of light and circadian disruption on developmental programming; our results suggest that they are relevant exposures for *in utero* development and DOHaD research.

In Chapter 2, our novel analysis of seasonal gene expression in the placenta unifies knowledge across seasonality in infant outcomes and seasonal biology. While associations between season of birth and disease have long been made, we uncovered, for the first time, seasonal biological pathways that may underlie these relationships. Intriguingly, one of the top seasonal genes was *BHLHE40* (*DEC1*), a core circadian clock gene, which suggests a role for circadian clock genes in seasonal placental processes. Additionally, our results highlighted how processes in the placenta also show seasonal rhythmicity. Overall, these findings unveiled seasonal biological processes in the placenta, which holds many implications for human development and seasonality of disease.

In Chapter 3, we also evaluated whether maternal history of night shift work was associated with DNA methylation in an epigenome-wide association study of full-term placenta. Our analysis revealed night shift work was associated with overall placental hypomethylation, as well as altered methylation for genes related to neuronal development and immune system function. While prior studies have measured shift work and reproductive and birth outcomes, this was the first study to evaluate impacts on the molecular profile of the placenta. *NAV1*, the gene demonstrating the most robust variation in DNA methylation associated with night shift work from our analysis, encodes a protein that associates with microtubules and is important for neuronal migration. In addition to *NAV1*, *GNAS*, a gene that is imprinted in the hypothalamus and is important in regulating sleep and brown fat development was found to be a differentially methylated region with hypomethylation. In summary, these findings show that maternal night shift work is associated with altered methylation in the placenta and should be investigated in future developmental and DOHaD studies.

In Chapter 5, we utilized a mouse model of circadian disruption and longitudinally followed developmentally-exposed mice for visual and metabolic outcomes to test whether developmental chronodisruption can influence later life health and disease. Our experiments showed that developmental chronodisruption leads to enhanced immune markers in the retina, suggesting a pro-inflammatory environment, and visual impairment in adult offspring. Likewise, these outcomes are exacerbated when offspring are challenged with high fat diet; this diet challenge also exposed altered retinal function and female-specific glucose intolerance in mice exposed to developmental chronodisruption. While prior research has linked developmental circadian disruption to metabolic and neurological alterations in the offspring, this experiment was innovative in measuring visual and retinal immune outcomes. These outcomes suggest that developmental circadian disruption, as caused by environmental light exposure, can alter the trajectory of later life health and disease and interact with adult nutritional environment.

Our investigation of human placental outcomes and mouse visual outcomes led us to question whether placental signaling was responsible for mediating the adult mouse outcomes. Therefore, using the same mouse model, in Chapter 6 we measured placental and fetal outcomes at E15.5. Just as was found in retinal tissue of adults, placental tissue of pregnant females exposed to developmental circadian disruption had greater expression of immune markers, suggesting a more pro-inflammatory placental milieu. Likewise, placenta from pregnant females exposed to chronodisruption had lower levels of *Serpinf1*, a gene that encodes PEDF and regulates macrophage inflammatory signaling. No differences in embryo count or placenta weight were noted, consistent with a prior study, but sex ratio did appear to trend towards male fetuses in the disrupted mice. Overall, this study supports the visual outcomes and suggests that the light environment can prime neurodevelopment via placental signaling, particularly the placental immune system.

Evaluation of circadian disruption and light exposure should be integrated in studies of environmental public health and DOHaD. Circadian biology is relevant to public health research because most tissues exhibit rhythmic processes, and therefore, timing of measurements and seasonality of exposures and outcomes are potential sources of bias. Additionally, circadian misalignment could cause disrupted or dampened tissue rhythms, affecting measurements and outcomes in studies that have not taken circadian rhythms into consideration. When considering environmental public health research, there is also substantial crosstalk between the circadian system, detoxification mechanisms, and metabolism; measurements of biomarkers, pollutants, and metabolites that don’t also take rhythmicity and misalignment into account may result in spurious findings. In the world of exposome research, circadian rhythms can influence practically all omics levels, including the epigenome, the transcriptome, the proteome, the metabolome, and the phenome. It is evident that circadian rhythm biology is applicable and pertinent to environmental public health research.

In conclusion, we have shown that environmental light and circadian disruption contributes to developmental programming (**Figure 7-1**). In epidemiological analyses of a prospective birth cohort, we found altered placental methylation in women who worked the night shift and seasonal rhythms in placental gene expression. In a mouse model of developmental circadian disruption, we found that developmental disruption caused altered placental signaling, impaired visual function and increased expression of retinal microglia/macrophages in adult offspring; challenge with high fat diet also uncovered altered retinal function and impaired glucose tolerance in offspring exposed to developmental chronodisruption. These findings suggest that the placenta functions as a peripheral clock and circadian disruption can contribute to developmental programming of adult disease. These results warrant further research to characterize the placental clock system and the mechanisms by which circadian disruption affects placental and fetal development.

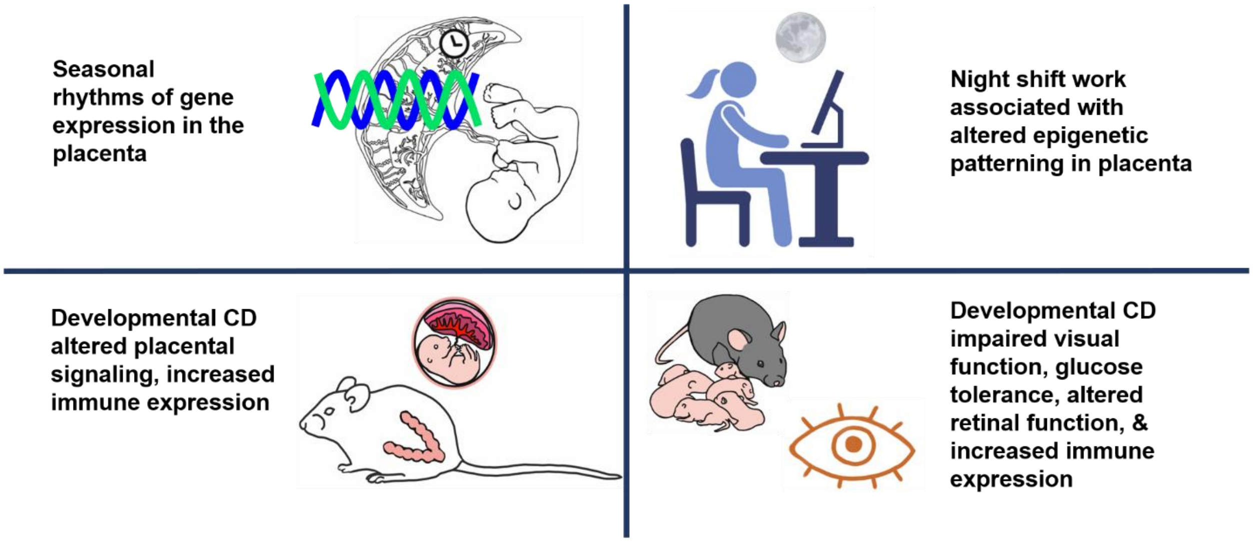
Seasonal rhythms of gene expression in the placenta
Night shift work associated with altered epigenetic patterning in placenta
Developmental CD altered placental signaling, increased immune expression
Developmental CD impaired visual function, glucose tolerance, altered retinal function, & increased immune expression

Figure 7-1*. Graphic summary of the main findings presented in the dissertation. Analyses of human placenta uncovered seasonal gene expression in the placenta and altered methylation in placenta of mothers who worked the night shift. A mouse model of developmental circadian disruption (CD) illustrated altered placenta signaling and increased expression of immune markers in the placenta, as well as impaired visual function, impaired glucose tolerance (in females), altered retinal function, and increased expression of immune markers in retina of adult offspring. (part of image made in ©BioRender - biorender.com)*

References

BIBLIOGRAPHY AND REFERENCES CITED

Agardh, C. D., Agardh, E., Hultberg, B. and Ahrén, B. (2000). Long-standing hyperglycemia in C57BL/6J mice does not affect retinal glutathione levels or endothelial/pericyte ratio in retinal capillaries. *Journal of Diabetes and Its Complications* **14**, 146-53.

Akiyama, S., Ohta, H., Watanabe, S., Moriya, T., Hariu, A., Nakahata, N., Chisaka, H., Matsuda, T., Kimura, Y., Tsuchiya, S. et al. (2010). The uterus sustains stable biological clock during pregnancy. *Tohoku J Exp Med* **221**, 287-98.

Alamri, A. S., Brock, J. A., Herath, C. B., Rajapaksha, I. G., Angus, P. W. and Ivanusic, J. J. (2019). The Effects of Diabetes and High-Fat Diet on Polymodal Nociceptor and Cold Thermoreceptor Nerve Terminal Endings in the Corneal Epithelium. *Investigative Ophthalmology & Visual Science* **60**, 209-217.

Albouery, M., Buteau, B., Grégoire, S., Martine, L., Gambert, S., Bron, A. M., Acar, N., Chassaing, B. and Bringer, M. A. (2020). Impact of a high-fat diet on the fatty acid composition of the retina. *Exp Eye Res* **196**, 108059.

Alcubierre, N., Navarrete-Muñoz, E. M., Rubinat, E., Falguera, M., Valls, J., Traveset, A., Vilanova, M. B., Marsal, J. R., Hernandez, M., Granado-Casas, M. et al. (2016). Association of low oleic acid intake with diabetic retinopathy in type 2 diabetic patients: a case-control study. *Nutr Metab (Lond)* **13**, 40.

Allen, R. S., Feola, A., Motz, C. T., Ottensmeyer, A. L., Chesler, K. C., Dunn, R., Thulé, P. M. and Pardue, M. T. (2019). Retinal Deficits Precede Cognitive and Motor Deficits in a Rat Model of Type II Diabetes. *Invest Ophthalmol Vis Sci* **60**, 123-133.

Almeida, D. L., Pavanello, A., Saavedra, L. P., Pereira, T. S., de Castro-Prado, M. A. A. and de Freitas Mathias, P. C. (2019). Environmental monitoring and the developmental origins of health and disease. *Journal of developmental origins of health and disease* **10**, 608-615.

Alvarez, J. D., Hansen, A., Ord, T., Bebas, P., Chappell, P. E., Giebultowicz, J. M., Williams, C., Moss, S. and Sehgal, A. (2008). The circadian clock protein BMAL1 is necessary for fertility and proper testosterone production in mice. *J Biol Rhythms* **23**, 26-36.

Anderson, N. J., King, M. R., Delbruck, L. and Jolivalt, C. G. (2014). Role of insulin signaling impairment, adiponectin and dyslipidemia in peripheral and central neuropathy in mice. *Dis Model Mech* **7**, 625-33.

Ando, N., Nakamura, Y., Aoki, R., Ishimaru, K., Ogawa, H., Okumura, K., Shibata, S., Shimada, S. and Nakao, A. (2015). Circadian Gene Clock Regulates Psoriasis-Like Skin Inflammation in Mice. *J Invest Dermatol* **135**, 3001-3008.

Andrikopoulos, S., Blair, A. R., Deluca, N., Fam, B. C. and Proietto, J. (2008). Evaluating the glucose tolerance test in mice. *Am J Physiol Endocrinol Metab* **295**, E1323-32.

Anway, M. D., Cupp, A. S., Uzumcu, M. and Skinner, M. K. (2005). Epigenetic transgenerational actions of endocrine disruptors and male fertility. *Science (New York, N.Y.)* **308**, 1466-9.

Appleton, A. A., Armstrong, D. A., Lesseur, C., Lee, J., Padbury, J. F., Lester, B. M. and Marsit, C. J. (2013). Patterning in Placental 11-B Hydroxysteroid Dehydrogenase Methylation According to Prenatal Socioeconomic Adversity. *PLoS One* **8**, e74691.

Appleton, A. A., Murphy, M. A., Koestler, D. C., Lesseur, C., Paquette, A. G., Padbury, J. F., Lester, B. M. and Marsit, C. J. (2016). Prenatal Programming of Infant Neurobehaviour in a Healthy Population. *Paediatr Perinat Epidemiol* **30**, 367-75.

Arble, D. M., Bass, J., Behn, C. D., Butler, M. P., Challet, E., Czeisler, C., Depner, C. M., Elmquist, J., Franken, P., Grandner, M. A. et al. (2015). Impact of Sleep and Circadian Disruption on Energy Balance and Diabetes: A Summary of Workshop Discussions. *Sleep* **38**, 1849-60.

Arden, G. B., Sidman, R. L., Arap, W. and Schlingemann, R. O. (2005). Spare the rod and spoil the eye. *The British journal of ophthalmology* **89**, 764-769.

Arnold, S. E., Lucki, I., Brookshire, B. R., Carlson, G. C., Browne, C. A., Kazi, H., Bang, S., Choi, B.-R., Chen, Y., McMullen, M. F. et al. (2014). High fat diet produces brain insulin resistance, synaptodendritic abnormalities and altered behavior in mice. *Neurobiology of Disease* **67**, 79-87.

Asare-Bediako, B., Noothi, S. K., Li Calzi, S., Athmanathan, B., Vieira, C. P., Adu-Agyeiwaah, Y., Dupont, M., Jones, B. A., Wang, X. X., Chakraborty, D. et al. (2020). Characterizing the Retinal Phenotype in the High-Fat Diet and Western Diet Mouse Models of Prediabetes. *Cells* **9**.

Aschoff, J. (1981). Freerunning and Entrained Circadian Rhythms. In *Biological Rhythms*, (ed. J. Aschoff), pp. 81-93. Boston, MA: Springer US.

Astiz, M., Heyde, I. and Oster, H. (2019). Mechanisms of Communication in the Mammalian Circadian Timing System. *International journal of molecular sciences* **20**, 343.

Astiz, M. and Oster, H. (2020). Feto-Maternal Crosstalk in the Development of the Circadian Clock System. *Front Neurosci* **14**, 631687.

Atawia, R. T., Bunch, K. L., Fouda, A. Y., Lemtalsi, T., Eldahshan, W., Xu, Z. M., Saul, A., Elmasry, K., Al-Shabrawey, M., Caldwell, R. B. et al. (2020). Role of Arginase 2 in Murine Retinopathy Associated with Western Diet-Induced Obesity. *Journal of Clinical Medicine* **9**.

Augusteyn, R. C. (2010). On the growth and internal structure of the human lens. *Experimental Eye Research* **90**, 643-654.

Aung, M. H., Kim, M. K., Olson, D. E., Thule, P. M. and Pardue, M. T. (2013). Early visual deficits in streptozotocin-induced diabetic long evans rats. *Invest Ophthalmol Vis Sci* **54**, 1370-7.

Aung, M. H., Park, H. N., Han, M. K., Obertone, T. S., Abey, J., Aseem, F., Thule, P. M., Iuvone, P. M. and Pardue, M. T. (2014). Dopamine deficiency contributes to early visual dysfunction in a rodent model of type 1 diabetes. *The Journal of neuroscience : the official journal of the Society for Neuroscience* **34**, 726-736.

Azzi, A., Dallmann, R., Casserly, A., Rehrauer, H., Patrignani, A., Maier, B., Kramer, A. and Brown, S. A. (2014). Circadian behavior is light-reprogrammed by plastic DNA methylation. *Nature neuroscience* **17**, 377-382.

Baba, K., Piano, I., Lyuboslavsky, P., Chrenek, M. A., Sellers, J. T., Zhang, S., Gargini, C., He, L., Tosini, G. and Iuvone, P. M. (2018a). Removal of clock gene Bmal1 from the retina affects retinal development and accelerates cone photoreceptor degeneration during aging. *Proceedings of the National Academy of Sciences* **115**, 13099-13104.

Baba, K., Ribelayga, C. P., Michael Iuvone, P. and Tosini, G. (2018b). The Retinal Circadian Clock and Photoreceptor Viability. *Adv Exp Med Biol* **1074**, 345-350.

Bäckhed, F., Manchester, J. K., Semenkovich, C. F. and Gordon, J. I. (2007). Mechanisms underlying the resistance to diet-induced obesity in germ-free mice. *Proc Natl Acad Sci U S A* **104**, 979-84.

Ban, N., Lee, T. J., Sene, A., Dong, Z., Santeford, A., Lin, J. B., Ory, D. S. and Apte, R. S. (2018). Disrupted cholesterol metabolism promotes age-related photoreceptor neurodegeneration. *J Lipid Res* **59**, 1414-1423.

Barakat, A., Nakao, S., Zandi, S., Sun, D., Schmidt-Ullrich, R., Hayes, K. C. and Hafezi-Moghadam, A. (2019). In contrast to Western diet, a plant-based, high-fat, low-sugar diet does not exacerbate retinal endothelial injury in streptozotocin-induced diabetes. *Faseb j* **33**, 10327-10338.

Barathi, V. A., Yeo, S. W., Guymer, R. H., Wong, T. Y. and Luu, C. D. (2014). Effects of Simvastatin on Retinal Structure and Function of a High-Fat Atherogenic Mouse Model of Thickened Bruch's Membrane. *Investigative Ophthalmology & Visual Science* **55**, 460-468.

Barker, D. J., Gluckman, P. D., Godfrey, K. M., Harding, J. E., Owens, J. A. and Robinson, J. S. (1993). Fetal nutrition and cardiovascular disease in adult life. *Lancet* **341**, 938-41.

Barker, D. J. and Osmond, C. (1986). Infant mortality, childhood nutrition, and ischaemic heart disease in England and Wales. *Lancet* **1**, 1077-81.

Barker, D. J. P. (2004). The Developmental Origins of Adult Disease. *Journal of the American College of Nutrition* **23**, 588S-595S.

Bass, J. and Lazar, M. A. (2016). Circadian time signatures of fitness and disease. *Science (New York, N.Y.)* **354**, 994-999.

Bass, J. and Takahashi, J. S. (2010). Circadian integration of metabolism and energetics. *Science* **330**, 1349-54.

Bayer-Carter, J. L., Green, P. S., Montine, T. J., VanFossen, B., Baker, L. D., Watson, S., Bonner, L. M., Callaghan, M., Leverenz, J. B., Walter, B. K. et al. (2011). Diet Intervention and Cerebrospinal Fluid Biomarkers in Amnestic Mild Cognitive Impairment. *Archives of Neurology* **68**, 743-752.

Beatty, S., Koh, H., Phil, M., Henson, D. and Boulton, M. (2000). The role of oxidative stress in the pathogenesis of age-related macular degeneration. *Surv Ophthalmol* **45**, 115-34.

Bedrosian, T. A., Fonken, L. K. and Nelson, R. J. (2016). Endocrine Effects of Circadian Disruption. *Annu Rev Physiol* **78**, 109-31.

Beery, A. K. (2018). Inclusion of females does not increase variability in rodent research studies. *Current Opinion in Behavioral Sciences* **23**, 143-149.

Beery, A. K. and Zucker, I. (2011). Sex bias in neuroscience and biomedical research. *Neurosci Biobehav Rev* **35**, 565-72.

Belle, T. L. V., Coppieters, K. T. and Herrath, M. G. V. (2011). Type 1 Diabetes: Etiology, Immunology, and Therapeutic Strategies. *Physiological Reviews* **91**, 79-118.

Benita, Y., Kikuchi, H., Smith, A. D., Zhang, M. Q., Chung, D. C. and Xavier, R. J. (2009). An integrative genomics approach identifies Hypoxia Inducible Factor-1 (HIF-1)-target genes that form the core response to hypoxia. *Nucleic acids research* **37**, 4587-602.

Benjamini, Y. and Hochberg, Y. (1995). Controlling the False Discovery Rate: A Practical and Powerful Approach to Multiple Testing. *Journal of the Royal Statistical Society. Series B (Methodological)* **57**, 289-300.

Bentley-Lewis, R., Koruda, K. and Seely, E. W. (2007). The metabolic syndrome in women. *Nature clinical practice. Endocrinology & metabolism* **3**, 696-704.

Berson, D. M., Dunn, F. A. and Takao, M. (2002). Phototransduction by retinal ganglion cells that set the circadian clock. *Science (New York, N.Y.)* **295**, 1070-1073.

Bhatwadekar, A. D., Yan, Y. Q., Qi, X. P., Thinschmidt, J. S., Neu, M. B., Calzi, S. L., Shaw, L. C., Dominiguez, J. M., Busik, J. V., Lee, C. et al. (2013). Per2 Mutation Recapitulates the Vascular Phenotype of Diabetes in the Retina and Bone Marrow. *Diabetes* **62**, 273-282.

Blackburn, B. J., Jenkins, M. W., Rollins, A. M. and Dupps, W. J. (2019). A Review of Structural and Biomechanical Changes in the Cornea in Aging, Disease, and Photochemical Crosslinking. *Frontiers in Bioengineering and Biotechnology* **7**.

Blüher, M. (2019). Obesity: global epidemiology and pathogenesis. *Nature Reviews Endocrinology* **15**, 288-298.

Blume, C., Santhi, N. and Schabus, M. (2016). 'nparACT' package for R: A free software tool for the non-parametric analysis of actigraphy data. *MethodsX* **3**, 430-5.

Boland, M. R., Shahn, Z., Madigan, D., Hripcsak, G. and Tatonetti, N. P. (2015). Birth month affects lifetime disease risk: a phenome-wide method. *Journal of the American Medical Informatics Association* **22**, 1042-1053.

Bonini, S., Rama, P., Olzi, D. and Lambiase, A. (2003). Neurotrophic keratitis. *Eye* **17**, 989-995.

Booij, J. C., Baas, D. C., Beisekeeva, J., Gorgels, T. G. and Bergen, A. A. (2010). The dynamic nature of Bruch's membrane. *Prog Retin Eye Res* **29**, 1-18.

Breton, C. V., Marsit, C. J., Faustman, E., Nadeau, K., Goodrich, J. M., Dolinoy, D. C., Herbstman, J., Holland, N., LaSalle, J. M., Schmidt, R. et al. (2017). Small-Magnitude Effect Sizes in Epigenetic End Points are Important in Children’s Environmental Health Studies: The Children’s Environmental Health and Disease Prevention Research Center’s Epigenetics Working Group. *Environ Health Perspect* **125**, 511-526.

Bronson-Castain, K. W., Bearse, M. A., Jr, Han, Y., Schneck, M. E., Barez, S. and Adams, A. J. (2007). Association between Multifocal ERG Implicit Time Delays and Adaptation in Patients with Diabetes. *Investigative Ophthalmology & Visual Science* **48**, 5250-5256.

Brown, K. T. and Wiesel, T. N. (1961). Localization of origins of electroretinogram components by intraretinal recording in the intact cat eye. *J Physiol* **158**, 257-80.

Brown, L. A., Hasan, S., Foster, R. G. and Peirson, S. N. (2017). COMPASS: Continuous Open Mouse Phenotyping of Activity and Sleep Status. *Wellcome open research* **1**, 2-2.

Bu, J. H., Yu, J. W., Wu, Y., Cai, X. X., Li, K. C., Tang, L. Y., Jiang, N., Jeyalatha, M. V., Zhang, M. J., Sun, H. M. et al. (2020). Hyperlipidemia Affects Tight Junctions and Pump Function in the Corneal Endothelium. *American Journal of Pathology* **190**, 563-576.

Buhr, E. D. and Takahashi, J. S. (2013). Molecular components of the Mammalian circadian clock. *Handbook of experimental pharmacology*, 3-27.

Buhr, E. D., Yoo, S.-H. and Takahashi, J. S. (2010). Temperature as a universal resetting cue for mammalian circadian oscillators. *Science (New York, N.Y.)* **330**, 379-385.

Bui, B. V. and Fortune, B. (2004). Ganglion cell contributions to the rat full-field electroretinogram. *J Physiol* **555**, 153-73.

Buja, A. and Eyuboglu, N. (1992). Remarks on Parallel Analysis. *Multivariate Behav Res* **27**, 509-40.

Bush, R. A. and Sieving, P. A. (1996). Inner retinal contributions to the primate photopic fast flicker electroretinogram. *Journal of the Optical Society of America A* **13**, 557-565.

Cangul, H. (2004). Hypoxia upregulates the expression of the NDRG1 gene leading to its overexpression in various human cancers. *BMC Genet* **5**, 27.

Carroll, K. K., Braden, L. M., Bell, J. A. and Kalamegham, R. (1986). Fat and cancer. *Cancer* **58**, 1818-1825.

Castanon-Cervantes, O., Wu, M., Ehlen, J. C., Paul, K., Gamble, K. L., Johnson, R. L., Besing, R. C., Menaker, M., Gewirtz, A. T. and Davidson, A. J. (2010). Dysregulation of inflammatory responses by chronic circadian disruption. *J Immunol* **185**, 5796-805.

Chakravarthy, U., Wong, T. Y., Fletcher, A., Piault, E., Evans, C., Zlateva, G., Buggage, R., Pleil, A. and Mitchell, P. (2010). Clinical risk factors for age-related macular degeneration: a systematic review and meta-analysis. *BMC Ophthalmol* **10**, 31.

Chang, A. M., Aeschbach, D., Duffy, J. F. and Czeisler, C. A. (2015a). Evening use of light-emitting eReaders negatively affects sleep, circadian timing, and next-morning alertness. *Proceedings of the National Academy of Sciences of the United States of America* **112**, 1232-1237.

Chang, R. C. A., Shi, L. H., Huang, C. C. Y., Kim, A. J., Ko, M. L., Zhou, B. Y. and Ko, G. Y. P. (2015b). High-Fat Diet-Induced Retinal Dysfunction. *Investigative Ophthalmology & Visual Science* **56**, 2367-2380.

Chapman, N. A., Jacobs, R. J. and Braakhuis, A. J. (2019). Role of diet and food intake in age-related macular degeneration: a systematic review. *Clin Exp Ophthalmol* **47**, 106-127.

Chellappa, S. L., Morris, C. J. and Scheer, F. A. J. L. (2019). Effects of circadian misalignment on cognition in chronic shift workers. *Scientific Reports* **9**, 699.

Chen, L. and Qin, Z. S. (2016). traseR: an R package for performing trait-associated SNP enrichment analysis in genomic intervals. *Bioinformatics* **32**, 1214-6.

Chen, Y. A., Lemire, M., Choufani, S., Butcher, D. T., Grafodatskaya, D., Zanke, B. W., Gallinger, S., Hudson, T. J. and Weksberg, R. (2013). Discovery of cross-reactive probes and polymorphic CpGs in the Illumina Infinium HumanMethylation450 microarray. *Epigenetics* **8**, 203-9.

Cheng, M. Y., Bullock, C. M., Li, C., Lee, A. G., Bermak, J. C., Belluzzi, J., Weaver, D. R., Leslie, F. M. and Zhou, Q. Y. (2002). Prokineticin 2 transmits the behavioural circadian rhythm of the suprachiasmatic nucleus. *Nature* **417**, 405-10.

Christakos, S., Dhawan, P., Verstuyf, A., Verlinden, L. and Carmeliet, G. (2016). Vitamin D: Metabolism, Molecular Mechanism of Action, and Pleiotropic Effects. *Physiological Reviews* **96**, 365-408.

Christou, S., Wehrens, S. M. T., Isherwood, C., Möller-Levet, C. S., Wu, H., Revell, V. L., Bucca, G., Skene, D. J., Laing, E. E., Archer, S. N. et al. (2019). Circadian regulation in human white adipose tissue revealed by transcriptome and metabolic network analysis. *Scientific Reports* **9**, 2641.

Chrysostomou, V., van Wijngaarden, P., Steinberg, G. R. and Crowston, J. G. (2017). A short term high-fat high-sucrose diet in mice impairs optic nerve recovery after injury and this is not reversed by exercise. *Experimental Eye Research* **162**, 104-109.

Ciarleglio, C. M., Axley, J. C., Strauss, B. R., Gamble, K. L. and McMahon, D. G. (2011). Perinatal photoperiod imprints the circadian clock. *Nature neuroscience* **14**, 25-27.

Clarkson-Townsend, D. A., Bales, K. L., Hermetz, K. E., Burt, A. A., Pardue, M. T. and Marsit, C. J. (2021a). Developmental Circadian Disruption Alters Placental Signaling in Mice. *bioRxiv*, 2021.04.21.440521.

Clarkson-Townsend, D. A., Bales, K. L., Marsit, C. J. and Pardue, M. T. (2021b). Light Environment Influences Developmental Programming of the Metabolic and Visual Systems in Mice. *Investigative Ophthalmology & Visual Science* **62**, 22-22.

Clarkson-Townsend, D. A., Douglass, A. J., Singh, A., Allen, R. S., Uwaifo, I. N. and Pardue, M. T. (2021c). Impacts of high fat diet on ocular outcomes in rodent models of visual disease. *Experimental Eye Research* **204**, 108440.

Clarkson-Townsend, D. A., Everson, T. M., Deyssenroth, M. A., Burt, A. A., Hermetz, K. E., Hao, K., Chen, J. and Marsit, C. J. (2019). Maternal circadian disruption is associated with variation in placental DNA methylation. *PLoS One* **14**, e0215745.

Clarkson-Townsend, D. A., Kennedy, E., Everson, T. M., Deyssenroth, M. A., Burt, A. A., Hao, K., Chen, J., Pardue, M. T. and Marsit, C. J. (2020). Seasonally variant gene expression in full-term human placenta. *Faseb j* **34**, 10431-10442.

Clayton, J. A. (2018). Applying the new SABV (sex as a biological variable) policy to research and clinical care. *Physiology & Behavior* **187**, 2-5.

Collaborators, T. G. O. (2017). Health Effects of Overweight and Obesity in 195 Countries over 25 Years. *New England Journal of Medicine* **377**, 13-27.

Collins, K. H., Herzog, W., Reimer, R. A., Reno, C. R., Heard, B. J. and Hart, D. A. (2018). Diet-induced obesity leads to pro-inflammatory alterations to the vitreous humour of the eye in a rat model. *Inflammation Research* **67**, 139-146.

Comas, M., Gordon, C. J., Oliver, B. G., Stow, N. W., King, G., Sharma, P., Ammit, A. J., Grunstein, R. R. and Phillips, C. L. (2017). A circadian based inflammatory response – implications for respiratory disease and treatment. *Sleep Science and Practice* **1**, 18.

Coppey, L., Davidson, E., Shevalye, H., Obrosov, A., Torres, M. and Yorek, M. A. (2020). Progressive Loss of Corneal Nerve Fibers and Sensitivity in Rats Modeling Obesity and Type 2 Diabetes Is Reversible with Omega-3 Fatty Acid Intervention: Supporting Cornea Analyses as a Marker for Peripheral Neuropathy and Treatment. *Diabetes Metab Syndr Obes* **13**, 1367-1384.

Coppey, L., Davidson, E., Shevalye, H., Torres, M. E. and Yorek, M. A. (2018a). Effect of dietary oils on peripheral neuropathy-related endpoints in dietary obese rats. *Diabetes Metab Syndr Obes* **11**, 117-127.

Coppey, L. J., Shevalye, H., Obrosov, A., Davidson, E. P. and Yorek, M. A. (2018b). Determination of peripheral neuropathy in high-fat diet fed low-dose streptozotocin-treated female C57Bl/6J mice and Sprague-Dawley rats. *J Diabetes Investig* **9**, 1033-1040.

Coulson, R. L., Yasui, D. H., Dunaway, K. W., Laufer, B. I., Vogel Ciernia, A., Zhu, Y., Mordaunt, C. E., Totah, T. S. and LaSalle, J. M. (2018). Snord116-dependent diurnal rhythm of DNA methylation in mouse cortex. *Nature Communications* **9**, 1616.

Cousins, S. W., Espinosa-Heidmann, D. G., Alexandriou, A., Sall, J., Dubovy, S. and Csaky, K. (2002). The role of aging, high fat diet and blue light exposure in an experimental mouse model for basal laminar deposit formation. *Experimental Eye Research* **75**, 543-553.

Cousins, S. W., Marin-Castano, M. E., Espinosa-Heidmann, D. G., Alexandridou, A., Striker, L. and Elliot, S. (2003). Female gender, estrogen loss, and sub-RPE deposit formation in aged mice. *Investigative Ophthalmology & Visual Science* **44**, 1221-1229.

Cundiff, D. K. and Nigg, C. R. (2005). Diet and diabetic retinopathy: insights from the Diabetes Control and Complications Trial (DCCT). *MedGenMed : Medscape general medicine* **7**, 3-3.

Curcio, C. A., Millican, C. L., Bailey, T. and Kruth, H. S. (2001). Accumulation of Cholesterol with Age in Human Bruch's Membrane. *Investigative Ophthalmology & Visual Science* **42**, 265-274.

Curcio, C. A., Presley, J. B., Millican, C. L. and Medeiros, N. E. (2005). Basal deposits and drusen in eyes with age-related maculopathy: evidence for solid lipid particles. *Exp Eye Res* **80**, 761-75.

Currie, J. and Schwandt, H. (2013). Within-mother analysis of seasonal patterns in health at birth. *Proceedings of the National Academy of Sciences*, 201307582.

Dai, W., Miller, W. P., Toro, A. L., Black, A. J., Dierschke, S. K., Feehan, R. P., Kimball, S. R. and Dennis, M. D. (2018a). Deletion of the stress-response protein REDD1 promotes ceramide-induced retinal cell death and JNK activation. *Faseb j* **32**, 6883-6897.

Dai, W. W., Dierschke, S. K., Toro, A. L. and Dennis, M. D. (2018b). Consumption of a high fat diet promotes protein O-GlcNAcylation in mouse retina via NR4A1-dependent GFAT2 expression. *Biochimica Et Biophysica Acta-Molecular Basis of Disease* **1864**, 3568-3576.

Darrow, L. A., Strickland, M. J., Klein, M., Waller, L. A., Flanders, W. D., Correa, A., Marcus, M. and Tolbert, P. E. (2009). Seasonality of birth and implications for temporal studies of preterm birth. *Epidemiology* **20**, 699-706.

Dartt, D. A. and Willcox, M. D. P. (2013). Complexity of the tear film: importance in homeostasis and dysfunction during disease. *Experimental Eye Research* **117**, 1-3.

Datilo, M. N., Sant'Ana, M. R., Formigari, G. P., Rodrigues, P. B., de Moura, L. P., da Silva, A. S. R., Ropelle, E. R., Pauli, J. R. and Cintra, D. E. (2018). Omega-3 from Flaxseed Oil Protects Obese Mice Against Diabetic Retinopathy Through GPR120 Receptor. *Scientific Reports* **8**.

Davidson, E. P., Coppey, L. J., Kardon, R. H. and Yorek, M. A. (2014). Differences and similarities in development of corneal nerve damage and peripheral neuropathy and in diet-induced obesity and type 2 diabetic rats. *Invest Ophthalmol Vis Sci* **55**, 1222-30.

Day, F. R., Forouhi, N. G., Ong, K. K. and Perry, J. R. B. (2015). Season of birth is associated with birth weight, pubertal timing, adult body size and educational attainment: a UK Biobank study. *Heliyon* **1**, e00031-e00031.

De Jong, S., Neeleman, M., Luykx, J. J., Ten Berg, M. J., Strengman, E., Den Breeijen, H. H., Stijvers, L. C., Buizer-Voskamp, J. E., Bakker, S. C., Kahn, R. S. et al. (2014). Seasonal changes in gene expression represent cell-type composition in whole blood. *Hum Mol Genet* **23**, 2721-2728.

Deeds, M. C., Anderson, J. M., Armstrong, A. S., Gastineau, D. A., Hiddinga, H. J., Jahangir, A., Eberhardt, N. L. and Kudva, Y. C. (2011). Single dose streptozotocin-induced diabetes: considerations for study design in islet transplantation models. *Laboratory animals* **45**, 131-140.

DeFronzo, R. A. (2011). Bromocriptine: A Sympatholytic, D2-Dopamine Agonist for the Treatment of Type 2 Diabetes. *Diabetes Care* **34**, 789-794.

DelMonte, D. W. and Kim, T. (2011). Anatomy and physiology of the cornea. *J Cataract Refract Surg* **37**, 588-98.

Deyssenroth, M. A., Peng, S., Hao, K., Lambertini, L., Marsit, C. J. and Chen, J. (2017). Whole-transcriptome analysis delineates the human placenta gene network and its associations with fetal growth. *BMC Genomics* **18**, 520-520.

Diamanti-Kandarakis, E., Bourguignon, J.-P., Giudice, L. C., Hauser, R., Prins, G. S., Soto, A. M., Zoeller, R. T. and Gore, A. C. (2009). Endocrine-disrupting chemicals: an Endocrine Society scientific statement. *Endocrine Reviews* **30**, 293-342.

Dighe, S., Zhao, J., Steffen, L., Mares, J. A., Meuer, S. M., Klein, B. E. K., Klein, R. and Millen, A. E. (2020). Diet patterns and the incidence of age-related macular degeneration in the Atherosclerosis Risk in Communities (ARIC) study. *Br J Ophthalmol* **104**, 1070-1076.

Ding, J. D., Johnson, L. V., Herrmann, R., Farsiu, S., Smith, S. G., Groelle, M., Mace, B. E., Sullivan, P., Jamison, J. A., Kelly, U. et al. (2011). Anti-amyloid therapy protects against retinal pigmented epithelium damage and vision loss in a model of age-related macular degeneration. *Proc Natl Acad Sci U S A* **108**, E279-87.

Disanto, G., Chaplin, G., Morahan, J. M., Giovannoni, G., Hyppönen, E., Ebers, G. C. and Ramagopalan, S. V. (2012). Month of birth, vitamin D and risk of immune-mediated disease: a case control study. *BMC Medicine* **10**, 69.

Dithmar, S., Sharara, N. A., Curcio, C. A., Le, N. A., Zhang, Y., Brown, S. and Grossniklaus, H. E. (2001). Murine high-fat diet and laser photochemical model of basal deposits in Bruch membrane. *Archives of Ophthalmology* **119**, 1643-9.

Do, M. T. H. and Yau, K.-W. (2010). Intrinsically photosensitive retinal ganglion cells. *Physiological Reviews* **90**, 1547-1581.

Dobin, A., Davis, C. A., Schlesinger, F., Drenkow, J., Zaleski, C., Jha, S., Batut, P., Chaisson, M. and Gingeras, T. R. (2013). STAR: ultrafast universal RNA-seq aligner. *Bioinformatics (Oxford, England)* **29**, 15-21.

Doblhammer, G. and Vaupel, J. W. (2001). Lifespan depends on month of birth. *Proceedings of the National Academy of Sciences* **98**, 2934-2939.

Doi, M., Hirayama, J. and Sassone-Corsi, P. (2006). Circadian Regulator CLOCK Is a Histone Acetyltransferase. *Cell* **125**, 497-508.

Dopico, X. C., Evangelou, M., Ferreira, R. C., Guo, H., Pekalski, M. L., Smyth, D. J., Cooper, N., Burren, O. S., Fulford, A. J., Hennig, B. J. et al. (2015). Widespread seasonal gene expression reveals annual differences in human immunity and physiology. *Nat Commun* **6**, 7000.

Douglass, J. D., Dorfman, M. D., Fasnacht, R., Shaffer, L. D. and Thaler, J. P. (2017). Astrocyte IKKβ/NF-κB signaling is required for diet-induced obesity and hypothalamic inflammation. *Molecular Metabolism* **6**, 366-373.

Dow, C., Mancini, F., Rajaobelina, K., Boutron-Ruault, M.-C., Balkau, B., Bonnet, F. and Fagherazzi, G. (2018). Diet and risk of diabetic retinopathy: a systematic review. *European Journal of Epidemiology* **33**, 141-156.

Duffy, J. F. and Czeisler, C. A. (2009). Effect of Light on Human Circadian Physiology. *Sleep medicine clinics* **4**, 165-177.

Dumbell, R., Matveeva, O. and Oster, H. (2016). Circadian Clocks, Stress, and Immunity. *Front Endocrinol (Lausanne)* **7**.

Dutheil, S., Ota, K. T., Wohleb, E. S., Rasmussen, K. and Duman, R. S. (2016). High-Fat Diet Induced Anxiety and Anhedonia: Impact on Brain Homeostasis and Inflammation. *Neuropsychopharmacology* **41**, 1874-1887.

Dvornyk, V., Vinogradova, O. and Nevo, E. (2003). Origin and evolution of circadian clock genes in prokaryotes. *Proceedings of the National Academy of Sciences* **100**, 2495-2500.

Ebrahimi, K. B., Cano, M., Rhee, J., Datta, S., Wang, L. and Handa, J. T. (2018). Oxidative Stress Induces an Interactive Decline in Wnt and Nrf2 Signaling in Degenerating Retinal Pigment Epithelium. *Antioxid Redox Signal* **29**, 389-407.

Ebrahimi, K. B. and Handa, J. T. (2011). Lipids, Lipoproteins, and Age-Related Macular Degeneration. *Journal of Lipids* **2011**, 802059.

Edlow, A. G., Glass, R. M., Smith, C. J., Tran, P. K., James, K. and Bilbo, S. (2019). Placental Macrophages: A Window Into Fetal Microglial Function in Maternal Obesity. *International Journal of Developmental Neuroscience* **77**, 60-68.

Egusquiza, R. J. and Blumberg, B. (2020). Environmental Obesogens and Their Impact on Susceptibility to Obesity: New Mechanisms and Chemicals. *Endocrinology* **161**.

Eleazu, C. O., Eleazu, K. C., Chukwuma, S. and Essien, U. N. (2013). Review of the mechanism of cell death resulting from streptozotocin challenge in experimental animals, its practical use and potential risk to humans. *Journal of diabetes and metabolic disorders* **12**, 60-60.

Espinosa-Heidmann, D. G., Sall, J., Hernandez, E. P. and Cousins, S. W. (2004). Basal laminar deposit formation in APO B100 transgenic mice: Complex interactions between dietary fat, blue light, and vitamin E. *Investigative Ophthalmology & Visual Science* **45**, 260-266.

Espinosa-Heidmann, D. G., Suner, I. J., Catanuto, P., Hernandez, E. P., Marin-Castano, M. E. and Cousins, S. W. (2006). Cigarette smoke-related oxidants and the development of sub-RPE deposits in an experimental animal model of dry AMD. *Investigative Ophthalmology & Visual Science* **47**, 729-737.

Euler, T., Haverkamp, S., Schubert, T. and Baden, T. (2014). Retinal bipolar cells: elementary building blocks of vision. *Nature Reviews Neuroscience* **15**, 507-519.

Evans, J. A., Suen, T.-C., Callif, B. L., Mitchell, A. S., Castanon-Cervantes, O., Baker, K. M., Kloehn, I., Baba, K., Teubner, B. J. W., Ehlen, J. C. et al. (2015). Shell neurons of the master circadian clock coordinate the phase of tissue clocks throughout the brain and body. *BMC biology* **13**, 43-43.

Everson, T. M., Punshon, T., Jackson, B. P., Hao, K., Lambertini, L., Chen, J., Karagas, M. R. and Marsit, C. J. (2017). Cadmium-associated differential methylation throughout the placental genome: epigenome-wide association study of two US birth cohorts. *bioRxiv*.

Felder-Schmittbuhl, M.-P., Buhr, E. D., Dkhissi-Benyahya, O., Hicks, D., Peirson, S. N., Ribelayga, C. P., Sandu, C., Spessert, R. and Tosini, G. (2018). Ocular Clocks: Adapting Mechanisms for Eye Functions and Health. *Investigative Ophthalmology & Visual Science* **59**, 4856-4870.

Ferreira, V. P., Pangburn, M. K. and Cortés, C. (2010). Complement control protein factor H: the good, the bad, and the inadequate. *Molecular immunology* **47**, 2187-2197.

Feskens, E. J., Virtanen, S. M., Räsänen, L., Tuomilehto, J., Stengård, J., Pekkanen, J., Nissinen, A. and Kromhout, D. (1995). Dietary Factors Determining Diabetes and Impaired Glucose Tolerance: A 20-year follow-up of the Finnish and Dutch cohorts of the Seven Countries Study. *Diabetes Care* **18**, 1104-1112.

Fiddes, B., Wason, J. and Sawcer, S. (2014). Confounding in association studies: month of birth and multiple sclerosis. *Journal of neurology* **261**, 1851-1856.

Fink, B., Coppey, L., Davidson, E., Shevalye, H., Obrosov, A., Chheda, P. R., Kerns, R., Sivitz, W. and Yorek, M. (2020). Effect of mitoquinone (Mito-Q) on neuropathic endpoints in an obese and type 2 diabetic rat model. *Free Radic Res* **54**, 311-318.

Fliesler, S. J. and Anderson, R. E. (1983). Chemistry and metabolism of lipids in the vertebrate retina. *Prog Lipid Res* **22**, 79-131.

Folkard, S. (2008). Do permanent night workers show circadian adjustment? A review based on the endogenous melatonin rhythm. *Chronobiology International* **25**, 215-224.

Fonken, L. K. and Nelson, R. J. (2016). Effects of light exposure at night during development. *Current Opinion in Behavioral Sciences* **7**, 33-39.

Förstermann, U. and Sessa, W. C. (2012). Nitric oxide synthases: regulation and function. *European heart journal* **33**, 829-837d.

Fortune, B., Schneck, M. E. and Adams, A. J. (1999). Multifocal electroretinogram delays reveal local retinal dysfunction in early diabetic retinopathy. *Invest Ophthalmol Vis Sci* **40**, 2638-51.

Frayling, T. M., Timpson, N. J., Weedon, M. N., Zeggini, E., Freathy, R. M., Lindgren, C. M., Perry, J. R. B., Elliott, K. S., Lango, H., Rayner, N. W. et al. (2007). A Common Variant in the FTO Gene Is Associated with Body Mass Index and Predisposes to Childhood and Adult Obesity. *Science* **316**, 889-894.

Fredriksson, R., Hägglund, M., Olszewski, P. K., Stephansson, O., Jacobsson, J. A., Olszewska, A. M., Levine, A. S., Lindblom, J. and Schiöth, H. B. (2008). The Obesity Gene, FTO, Is of Ancient Origin, Up-Regulated during Food Deprivation and Expressed in Neurons of Feeding-Related Nuclei of the Brain. *Endocrinology* **149**, 2062-2071.

Freeman, L. R., Haley-Zitlin, V., Rosenberger, D. S. and Granholm, A.-C. (2014). Damaging effects of a high-fat diet to the brain and cognition: a review of proposed mechanisms. *Nutritional Neuroscience* **17**, 241-251.

Frigato, E., Lunghi, L., Ferretti, M. E., Biondi, C. and Bertolucci, C. (2009). Evidence for circadian rhythms in human trophoblast cell line that persist in hypoxia. *Biochem Biophys Res Commun* **378**, 108-11.

Fritsche, L. G. Igl, W. Bailey, J. N. C. Grassmann, F. Sengupta, S. Bragg-Gresham, J. L. Burdon, K. P. Hebbring, S. J. Wen, C. Gorski, M. et al. (2016). A large genome-wide association study of age-related macular degeneration highlights contributions of rare and common variants. *Nature genetics* **48**, 134-143.

Froy, O. (2010). Metabolism and Circadian Rhythms—Implications for Obesity. *Endocrine Reviews* **31**, 1-24.

Fuhrmann, S., Zou, C. and Levine, E. M. (2014). Retinal pigment epithelium development, plasticity, and tissue homeostasis. *Exp Eye Res* **123**, 141-50.

Fujihara, M., Bartels, E., Nielsen, L. B. and Handa, J. T. (2009). A human apoB100 transgenic mouse expresses human apoB100 in the RPE and develops features of early AMD. *Exp Eye Res* **88**, 1115-23.

Fujishiro, K., Lividoti Hibert, E., Schernhammer, E. and Rich-Edwards, J. W. (2017). Shift work, job strain and changes in the body mass index among women: a prospective study. *Occupational and Environmental Medicine* **74**, 410.

Funkat, A., Massa, C. M., Jovanovska, V., Proietto, J. and Andrikopoulos, S. (2004). Metabolic Adaptations of Three Inbred Strains of Mice (C57BL/6, DBA/2, and 129T2) in Response to a High-Fat Diet. *The Journal of Nutrition* **134**, 3264-3269.

Furman, B. L. (2015). Streptozotocin-Induced Diabetic Models in Mice and Rats. *Current Protocols in Pharmacology* **70**, 5.47.1-5.47.20.

Fustin, J.-M., Doi, M., Yamaguchi, Y., Hida, H., Nishimura, S., Yoshida, M., Isagawa, T., Morioka, Masaki S., Kakeya, H., Manabe, I. et al. RNA-Methylation-Dependent RNA Processing Controls the Speed of the Circadian Clock. *Cell* **155**, 793-806.

Gabory, A., Ferry, L., Fajardy, I., Jouneau, L., Gothié, J.-D., Vigé, A., Fleur, C., Mayeur, S., Gallou-Kabani, C., Gross, M.-S. et al. (2012). Maternal diets trigger sex-specific divergent trajectories of gene expression and epigenetic systems in mouse placenta. *PLoS One* **7**, e47986-e47986.

Gallou-Kabani, C., Gabory, A., Tost, J., Karimi, M., Mayeur, S., Lesage, J., Boudadi, E., Gross, M.-S., Taurelle, J., Vigé, A. et al. (2010). Sex- and Diet-Specific Changes of Imprinted Gene Expression and DNA Methylation in Mouse Placenta under a High-Fat Diet. *PLOS ONE* **5**, e14398.

Ginhoux, F., Schultze, J. L., Murray, P. J., Ochando, J. and Biswas, S. K. (2016). New insights into the multidimensional concept of macrophage ontogeny, activation and function. *Nat Immunol* **17**, 34-40.

Giolli, R. A., Blanks, R. H. and Lui, F. (2006). The accessory optic system: basic organization with an update on connectivity, neurochemistry, and function. *Prog Brain Res* **151**, 407-40.

Go, G.-W. and Mani, A. (2012). Low-density lipoprotein receptor (LDLR) family orchestrates cholesterol homeostasis. *The Yale journal of biology and medicine* **85**, 19-28.

Godin, I. and Cumano, A. (2002). The hare and the tortoise: an embryonic haematopoietic race. *Nature reviews. Immunology* **2**, 593-604.

Goldman, B. D. (2001). Mammalian photoperiodic system: formal properties and neuroendocrine mechanisms of photoperiodic time measurement. *J Biol Rhythms* **16**, 283-301.

Gooley, J. J., Chamberlain, K., Smith, K. A., Khalsa, S. B. S., Rajaratnam, S. M. W., Van Reen, E., Zeitzer, J. M., Czeisler, C. A. and Lockley, S. W. (2011). Exposure to room light before bedtime suppresses melatonin onset and shortens melatonin duration in humans. *The Journal of clinical endocrinology and metabolism* **96**, E463-E472.

Granit, R. (1933). The components of the retinal action potential in mammals and their relation to the discharge in the optic nerve. *J Physiol* **77**, 207-39.

Gray, T. K., Lester, G. E. and Lorenc, R. S. (1979). Evidence for extra-renal 1 alpha-hydroxylation of 25-hydroxyvitamin D3 in pregnancy. *Science (New York, N.Y.)* **204**, 1311-3.

Green, C. B., Takahashi, J. S. and Bass, J. (2008). The meter of metabolism. *Cell* **134**, 728-42.

Griffin, P., Dimitry, J. M., Sheehan, P. W., Lananna, B. V., Guo, C., Robinette, M. L., Hayes, M. E., Cedeño, M. R., Nadarajah, C. J., Ezerskiy, L. A. et al. (2019). Circadian clock protein Rev-erbα regulates neuroinflammation. *Proceedings of the National Academy of Sciences* **116**, 5102-5107.

Grün, F. and Blumberg, B. (2009). Endocrine disrupters as obesogens. *Molecular and Cellular Endocrinology* **304**, 19-29.

Gudapati, K., Singh, A., Clarkson-Townsend, D., Feola, A. J. and Allen, R. S. (2020). Behavioral Assessment of Visual Function via Optomotor Response and Cognitive Function via Y-Maze in Diabetic Rats. *JoVE*, e61806.

Gupta, N., Brown, K. E. and Milam, A. H. (2003). Activated microglia in human retinitis pigmentosa, late-onset retinal degeneration, and age-related macular degeneration. *Exp Eye Res* **76**, 463-71.

Hadadi, E., Taylor, W., Li, X.-M., Aslan, Y., Villote, M., Rivière, J., Duvallet, G., Auriau, C., Dulong, S., Raymond-Letron, I. et al. (2020). Chronic circadian disruption modulates breast cancer stemness and immune microenvironment to drive metastasis in mice. *Nature Communications* **11**, 3193.

Haertle, L., El Hajj, N., Dittrich, M., Müller, T., Nanda, I., Lehnen, H. and Haaf, T. (2017). Epigenetic signatures of gestational diabetes mellitus on cord blood methylation. *Clinical Epigenetics* **9**, 28.

Hall, K. D. (2018). Did the Food Environment Cause the Obesity Epidemic? *Obesity* **26**, 11-13.

Harfmann, B. D., Schroder, E. A., Kachman, M. T., Hodge, B. A., Zhang, X. and Esser, K. A. (2016). Muscle-specific loss of Bmal1 leads to disrupted tissue glucose metabolism and systemic glucose homeostasis. *Skeletal Muscle* **6**, 12.

Hatori, M., Gronfier, C., Van Gelder, R. N., Bernstein, P. S., Carreras, J., Panda, S., Marks, F., Sliney, D., Hunt, C. E., Hirota, T. et al. (2017). Global rise of potential health hazards caused by blue light-induced circadian disruption in modern aging societies. *npj Aging and Mechanisms of Disease* **3**, 9.

Hattar, S., Kumar, M., Park, A., Tong, P., Tung, J., Yau, K. W. and Berson, D. M. (2006). Central projections of melanopsin-expressing retinal ganglion cells in the mouse. *J Comp Neurol* **497**, 326-49.

Haugen, A. C., Schug, T. T., Collman, G. and Heindel, J. J. (2015). Evolution of DOHaD: the impact of environmental health sciences. *Journal of developmental origins of health and disease* **6**, 55-64.

Hedström, A. K., Åkerstedt, T., Hillert, J., Olsson, T. and Alfredsson, L. (2011). Shift work at young age is associated with increased risk for multiple sclerosis. *Annals of Neurology* **70**, 733-741.

Heijmans, B. T., Tobi, E. W., Stein, A. D., Putter, H., Blauw, G. J., Susser, E. S., Slagboom, P. E. and Lumey, L. H. (2008). Persistent epigenetic differences associated with prenatal exposure to famine in humans. *Proceedings of the National Academy of Sciences of the United States of America* **105**, 17046-17049.

Hergenhan, S., Holtkamp, S. and Scheiermann, C. (2020). Molecular Interactions Between Components of the Circadian Clock and the Immune System. *Journal of Molecular Biology* **432**, 3700-3713.

Heydemann, A. (2016). An Overview of Murine High Fat Diet as a Model for Type 2 Diabetes Mellitus. *Journal of Diabetes Research* **2016**, 2902351.

Hirano, A., Fu, Y. H. and Ptáček, L. J. (2016). The intricate dance of post-translational modifications in the rhythm of life. *Nat Struct Mol Biol* **23**, 1053-1060.

Hoch, D., Novakovic, B., Cvitic, S., Saffery, R., Desoye, G. and Majali-Martinez, A. (2020). Sex matters: XIST and DDX3Y gene expression as a tool to determine fetal sex in human first trimester placenta. *Placenta* **97**, 68-70.

Holdcroft, A. (2007). Gender bias in research: how does it affect evidence based medicine? *Journal of the Royal Society of Medicine* **100**, 2-3.

Hong, J., Stubbins, R. E., Smith, R. R., Harvey, A. E. and Núñez, N. P. (2009). Differential susceptibility to obesity between male, female and ovariectomized female mice. *Nutr J* **8**, 11.

Honma, S., Kawamoto, T., Takagi, Y., Fujimoto, K., Sato, F., Noshiro, M., Kato, Y. and Honma, K. (2002). Dec1 and Dec2 are regulators of the mammalian molecular clock. *Nature* **419**, 841-4.

Hood, D. C. and Birch, D. G. (1996). Assessing abnormal rod photoreceptor activity with the a-wave of the electroretinogram: Applications and methods. *Documenta Ophthalmologica* **92**, 253-267.

Horvat, F., Fulka, H., Jankele, R., Malik, R., Jun, M., Solcova, K., Sedlacek, R., Vlahovicek, K., Schultz, R. M. and Svoboda, P. (2018). Role of Cnot6l in maternal mRNA turnover. *Life science alliance* **1**, e201800084-e201800084.

Houseman, E. A., Kile, M. L., Christiani, D. C., Ince, T. A., Kelsey, K. T. and Marsit, C. J. (2016). Reference-free deconvolution of DNA methylation data and mediation by cell composition effects. *BMC Bioinformatics* **17**, 259.

Howie, G. J., Sloboda, D. M. and Vickers, M. H. (2012). Maternal undernutrition during critical windows of development results in differential and sex-specific effects on postnatal adiposity and related metabolic profiles in adult rat offspring. *Br J Nutr* **108**, 298-307.

Hu, F. B., Manson, J. E., Stampfer, M. J., Colditz, G., Liu, S., Solomon, C. G. and Willett, W. C. (2001). Diet, Lifestyle, and the Risk of Type 2 Diabetes Mellitus in Women. *New England Journal of Medicine* **345**, 790-797.

Huang, T., Mariani, S. and Redline, S. (2020). Sleep Irregularity and Risk of Cardiovascular Events: The Multi-Ethnic Study of Atherosclerosis. *J Am Coll Cardiol* **75**, 991-999.

Huang, T. and Redline, S. (2019). Cross-sectional and Prospective Associations of Actigraphy-Assessed Sleep Regularity With Metabolic Abnormalities: The Multi-Ethnic Study of Atherosclerosis. *Diabetes Care* **42**, 1422-1429.

Huang, Y. and Mahley, R. W. (2014). Apolipoprotein E: structure and function in lipid metabolism, neurobiology, and Alzheimer's diseases. *Neurobiol Dis* **72 Pt A**, 3-12.

Hughes, M. E., Hogenesch, J. B. and Kornacker, K. (2010). JTK_CYCLE: an efficient non-parametric algorithm for detecting rhythmic components in genome-scale datasets. *Journal of Biological Rhythms* **25**, 372-380.

IARC. (2010). Painting, firefighting, and shiftwork. *IARC Monogr Eval Carcinog Risks Hum* **98**, 9-764.

IARC. (2019). Carcinogenicity of night shift work. *Lancet Oncol* **20**, 1058-1059.

IARC. (2021). Agents Classified by the IARC Monographs, Volumes 1–128. https://monographs.iarc.who.int/agents-classified-by-the-iarc/.

Ibrahim, A. S., El-Remessy, A. B., Matragoon, S., Zhang, W., Patel, Y., Khan, S., Al-Gayyar, M. M., El-Shishtawy, M. M. and Liou, G. I. (2011). Retinal microglial activation and inflammation induced by amadori-glycated albumin in a rat model of diabetes. *Diabetes* **60**, 1122-1133.

Ietta, F., Wu, Y., Winter, J., Xu, J., Wang, J., Post, M. and Caniggia, I. (2006). Dynamic HIF1A Regulation During Human Placental Development1. *Biology of Reproduction* **75**, 112-121.

Inokawa, H., Umemura, Y., Shimba, A., Kawakami, E., Koike, N., Tsuchiya, Y., Ohashi, M., Minami, Y., Cui, G., Asahi, T. et al. (2020). Chronic circadian misalignment accelerates immune senescence and abbreviates lifespan in mice. *Scientific Reports* **10**, 2569.

Itoh, K., Mochizuki, M., Ishii, Y., Ishii, T., Shibata, T., Kawamoto, Y., Kelly, V., Sekizawa, K., Uchida, K. and Yamamoto, M. (2004). Transcription factor Nrf2 regulates inflammation by mediating the effect of 15-deoxy-Delta(12,14)-prostaglandin j(2). *Molecular and Cellular Biology* **24**, 36-45.

Jackson, C. R., Capozzi, M., Dai, H. and McMahon, D. G. (2014). Circadian Perinatal Photoperiod Has Enduring Effects on Retinal Dopamine and Visual Function. *The Journal of Neuroscience* **34**, 4627.

Jaffe, A. E., Murakami, P., Lee, H., Leek, J. T., Fallin, M. D., Feinberg, A. P. and Irizarry, R. A. (2012). Bump hunting to identify differentially methylated regions in epigenetic epidemiology studies. *Int J Epidemiol* **41**, 200-9.

James, P. T., Leach, R., Kalamara, E. and Shayeghi, M. (2001). The Worldwide Obesity Epidemic. *Obesity Research* **9**, 228S-233S.

Jansson, T. and Powell, T. L. (2007). Role of the placenta in fetal programming: underlying mechanisms and potential interventional approaches. *Clin Sci (Lond)* **113**, 1-13.

Javadi, M.-A. and Zarei-Ghanavati, S. (2008). Cataracts in diabetic patients: a review article. *Journal of ophthalmic & vision research* **3**, 52-65.

Javeed, N. and Matveyenko, A. V. (2018). Circadian Etiology of Type 2 Diabetes Mellitus. *Physiology (Bethesda)* **33**, 138-150.

Jayaratne, S. K., Donaldson, P. J., Vickers, M. H. and Lim, J. C. (2017). The Effects of Maternal Under-Nutrition and a Post-Natal High Fat Diet on Lens Growth, Transparency and Oxidative Defense Systems in Rat Offspring. *Curr Eye Res* **42**, 589-599.

Jehan, S., Zizi, F., Pandi-Perumal, S. R., Myers, A. K., Auguste, E., Jean-Louis, G. and McFarlane, S. I. (2017). Shift Work and Sleep: Medical Implications and Management. *Sleep medicine and disorders : international journal* **1**, 00008.

Ji, Y., Sun, S., Xia, S., Yang, L., Li, X. and Qi, L. (2012). Short term high fat diet challenge promotes alternative macrophage polarization in adipose tissue via natural killer T cells and interleukin-4. *J Biol Chem* **287**, 24378-86.

Jia, G., Fu, Y., Zhao, X., Dai, Q., Zheng, G., Yang, Y., Yi, C., Lindahl, T., Pan, T., Yang, Y.-G. et al. (2011). N(6)-Methyladenosine in Nuclear RNA is a Major Substrate of the Obesity-Associated FTO. *Nature chemical biology* **7**, 885-887.

Jo, D. H., Yun, J. H., Cho, C. S., Kim, J. H., Kim, J. H. and Cho, C. H. (2019). Interaction between microglia and retinal pigment epithelial cells determines the integrity of outer blood-retinal barrier in diabetic retinopathy. *Glia* **67**, 321-331.

Johnson, W. E., Li, C. and Rabinovic, A. (2007). Adjusting batch effects in microarray expression data using empirical Bayes methods. *Biostatistics* **8**, 118-27.

Joyal, J.-S., Sun, Y., Gantner, M. L., Shao, Z., Evans, L. P., Saba, N., Fredrick, T., Burnim, S., Kim, J. S., Patel, G. et al. (2016). Retinal lipid and glucose metabolism dictates angiogenesis through the lipid sensor Ffar1. *Nature Medicine* **22**, 439-445.

Jung, C. M., Khalsa, S. B. S., Scheer, F. A. J. L., Cajochen, C., Lockley, S. W., Czeisler, C. A. and Wright, K. P., Jr. (2010). Acute effects of bright light exposure on cortisol levels. *Journal of Biological Rhythms* **25**, 208-216.

Kalmijn, S., Launer, L. J., Ott, A., Witteman, J. C. M., Hofman, A. and Breteler, M. M. B. (1997). Dietary fat intake and the risk of incident dementia in the Rotterdam study. *Annals of Neurology* **42**, 776-782.

Karatsoreos, I. N., Bhagat, S., Bloss, E. B., Morrison, J. H. and McEwen, B. S. (2011). Disruption of circadian clocks has ramifications for metabolism, brain, and behavior. *Proceedings of the National Academy of Sciences* **108**, 1657-1662.

Karlsson, B., Knutsson, A. and Lindahl, B. (2001). Is there an association between shift work and having a metabolic syndrome? Results from a population based study of 27 485 people. *Occupational and Environmental Medicine* **58**, 747-752.

Kato, Y., Kawamoto, T., Fujimoto, K. and Noshiro, M. (2014). Chapter Ten - DEC1/STRA13/SHARP2 and DEC2/SHARP1 Coordinate Physiological Processes, Including Circadian Rhythms in Response to Environmental Stimuli. In *Current Topics in Developmental Biology*, vol. 110 (ed. R. Taneja), pp. 339-372: Academic Press.

Katsumata, K. (1970). The disturbance of the carbohydrate metabolism and the specific retinal lesions of rats fed with a high fat, and high calory diet. *Nagoya J Med Sci* **32**, 407-16.

Kawai, M. and Rosen, C. J. (2010). PPARγ: a circadian transcription factor in adipogenesis and osteogenesis. *Nature reviews. Endocrinology* **6**, 629-636.

Kecklund, G. and Axelsson, J. (2016). Health consequences of shift work and insufficient sleep. *BMJ* **355**, i5210.

Kevany, B. M. and Palczewski, K. (2010). Phagocytosis of retinal rod and cone photoreceptors. *Physiology (Bethesda, Md.)* **25**, 8-15.

Khazen, T., Hatoum, O. A., Ferreira, G. and Maroun, M. (2019). Acute exposure to a high-fat diet in juvenile male rats disrupts hippocampal-dependent memory and plasticity through glucocorticoids. *Scientific Reports* **9**, 12270.

Kim, A. J., Chang, J. Y., Shi, L., Chang, R. C., Ko, M. L. and Ko, G. Y. (2017). The Effects of Metformin on Obesity-Induced Dysfunctional Retinas. *Invest Ophthalmol Vis Sci* **58**, 106-118.

Kim, S. H., Wang, D., Park, Y. Y., Katoh, H., Margalit, O., Sheffer, M., Wu, H., Holla, V. R., Lee, J. S. and DuBois, R. N. (2013). HIG2 promotes colorectal cancer progression via hypoxia-dependent and independent pathways. *Cancer Lett* **341**, 159-65.

Kim, Y. H., Marhon, S. A., Zhang, Y., Steger, D. J., Won, K.-J. and Lazar, M. A. (2018). Rev-erbα dynamically modulates chromatin looping to control circadian gene transcription. *Science (New York, N.Y.)* **359**, 1274-1277.

Kinnunen, K., Heinonen, S. E., Kalesnykas, G., Laidinen, S., Uusitalo-Jarvinen, H., Uusitalo, H. and Yla-Herttuala, S. (2013). LDLR(-/-)ApoB(100/100) mice with insulin-like growth factor II overexpression reveal a novel form of retinopathy with photoreceptor atrophy and altered morphology of the retina. *Molecular Vision* **19**, 1723-1733.

Klein, R. J., Zeiss, C., Chew, E. Y., Tsai, J.-Y., Sackler, R. S., Haynes, C., Henning, A. K., SanGiovanni, J. P., Mane, S. M., Mayne, S. T. et al. (2005). Complement factor H polymorphism in age-related macular degeneration. *Science (New York, N.Y.)* **308**, 385-389.

Klingberg, E., Oleröd, G., Konar, J., Petzold, M. and Hammarsten, O. (2015). Seasonal variations in serum 25-hydroxy vitamin D levels in a Swedish cohort. *Endocrine* **49**, 800-808.

Klingenspor, M., Dickopp, A., Heldmaier, G. and Klaus, S. (1996). Short photoperiod reduces leptin gene expression in white and brown adipose tissue of Djungarian hamsters. *Febs Letters* **399**, 290-294.

Kneer, K., Green, M. B., Meyer, J., Rich, C. B., Minns, M. S. and Trinkaus-Randall, V. (2018). High fat diet induces pre-type 2 diabetes with regional changes in corneal sensory nerves and altered P2X7 expression and localization. *Exp Eye Res* **175**, 44-55.

Knutsson, A., Jonsson, B., Akerstedt, T. and Orth-Gomer, K. (1986). INCREASED RISK OF ISCHAEMIC HEART DISEASE IN SHIFT WORKERS. *The Lancet* **328**, 89-92.

Kolb, H. (1987). Mouse models of insulin dependent diabetes: low-dose streptozocin-induced diabetes and nonobese diabetic (NOD) mice. *Diabetes Metab Rev* **3**, 751-78.

Könner, A. C. and Brüning, J. C. (2011). Toll-like receptors: linking inflammation to metabolism. *Trends in Endocrinology & Metabolism* **22**, 16-23.

Kothari, V., Luo, Y., Tornabene, T., O'Neill, A. M., Greene, M. W., Geetha, T. and Babu, J. R. (2017). High fat diet induces brain insulin resistance and cognitive impairment in mice. *Biochimica et Biophysica Acta (BBA) - Molecular Basis of Disease* **1863**, 499-508.

Kowluru, R. A. and Chan, P.-S. (2007). Oxidative stress and diabetic retinopathy. *Experimental diabetes research* **2007**, 43603-43603.

Krady, J. K., Basu, A., Allen, C. M., Xu, Y., LaNoue, K. F., Gardner, T. W. and Levison, S. W. (2005). Minocycline reduces proinflammatory cytokine expression, microglial activation, and caspase-3 activation in a rodent model of diabetic retinopathy. *Diabetes* **54**, 1559-65.

Kriegsfeld, L. J., LeSauter, J. and Silver, R. (2004). Targeted microlesions reveal novel organization of the hamster suprachiasmatic nucleus. *J Neurosci* **24**, 2449-57.

Kuleshov, M. V., Jones, M. R., Rouillard, A. D., Fernandez, N. F., Duan, Q., Wang, Z., Koplev, S., Jenkins, S. L., Jagodnik, K. M., Lachmann, A. et al. (2016). Enrichr: a comprehensive gene set enrichment analysis web server 2016 update. *Nucleic acids research* **44**, W90-W97.

Kunert, S. (2014). The role of neuron navigator 1 in vascular development: Humboldt-Universität zu Berlin, Mathematisch-Naturwissenschaftliche Fakultät I.

Kwan, C. C., Lee, H. E., Schwartz, G. and Fawzi, A. A. (2020). Acute Hyperglycemia Reverses Neurovascular Coupling During Dark to Light Adaptation in Healthy Subjects on Optical Coherence Tomography Angiography. *Investigative Ophthalmology & Visual Science* **61**, 38-38.

Lam, L. L., Emberly, E., Fraser, H. B., Neumann, S. M., Chen, E., Miller, G. E. and Kobor, M. S. (2012). Factors underlying variable DNA methylation in a human community cohort. *Proceedings of the National Academy of Sciences of the United States of America* **109**, 17253-17260.

Lamb, T. D. (2013). Evolution of phototransduction, vertebrate photoreceptors and retina. *Prog Retin Eye Res* **36**, 52-119.

Landowski, M., Kelly, U., Klingeborn, M., Groelle, M., Ding, J. D., Grigsby, D. and Bowes Rickman, C. (2019). Human complement factor H Y402H polymorphism causes an age-related macular degeneration phenotype and lipoprotein dysregulation in mice. *Proc Natl Acad Sci U S A* **116**, 3703-3711.

Lanoix, D., Beghdadi, H., Lafond, J. and Vaillancourt, C. (2008). Human placental trophoblasts synthesize melatonin and express its receptors. *Journal of Pineal Research* **45**, 50-60.

Lanoix, D., Guérin, P. and Vaillancourt, C. (2012). Placental melatonin production and melatonin receptor expression are altered in preeclampsia: new insights into the role of this hormone in pregnancy. *Journal of Pineal Research* **53**, 417-425.

Lassi, G., Ball, S. T., Maggi, S., Colonna, G., Nieus, T., Cero, C., Bartolomucci, A., Peters, J. and Tucci, V. (2012). Loss of Gnas Imprinting Differentially Affects REM/NREM Sleep and Cognition in Mice. *PLOS Genetics* **8**, e1002706.

Lawrence, T. (2009). The nuclear factor NF-kappaB pathway in inflammation. *Cold Spring Harbor perspectives in biology* **1**, a001651-a001651.

Le May, C., Chu, K., Hu, M., Ortega, C. S., Simpson, E. R., Korach, K. S., Tsai, M. J. and Mauvais-Jarvis, F. (2006). Estrogens protect pancreatic beta-cells from apoptosis and prevent insulin-deficient diabetes mellitus in mice. *Proc Natl Acad Sci U S A* **103**, 9232-7.

Lee, J.-Y., Yun, H. J., Kim, C. Y., Cho, Y. W., Lee, Y. and Kim, M. H. (2017). Prenatal exposure to dexamethasone in the mouse induces sex-specific differences in placental gene expression. *Development, Growth & Differentiation* **59**, 515-525.

Lee, J. J., Wang, P. W., Yang, I. H., Huang, H. M., Chang, C. S., Wu, C. L. and Chuang, J. H. (2015). High-Fat Diet Induces Toll-Like Receptor 4-Dependent Macrophage/Microglial Cell Activation and Retinal Impairment. *Investigative Ophthalmology & Visual Science* **56**, 3041-3050.

Lee, S. J., Kim, J. H., Kim, J. H., Chung, M. J., Wen, Q., Chung, H., Kim, K. W. and Yu, Y. S. (2007). Human apolipoprotein E2 transgenic mice show lipid accumulation in retinal pigment epithelium and altered expression of VEGF and bFGF in the eyes. *Journal of Microbiology and Biotechnology* **17**, 1024-1030.

Lee, S. K. (2018). Sex as an important biological variable in biomedical research. *BMB Rep* **51**, 167-173.

Leek, J. T. (2014). svaseq: removing batch effects and other unwanted noise from sequencing data. *Nucleic acids research* **42**, e161-e161.

Leek, J. T., Johnson, W. E., Parker, H. S., Jaffe, A. E. and Storey, J. D. (2012). The sva package for removing batch effects and other unwanted variation in high-throughput experiments. *Bioinformatics* **28**, 882-3.

Leek, J. T. and Storey, J. D. (2007). Capturing Heterogeneity in Gene Expression Studies by Surrogate Variable Analysis. *PLOS Genetics* **3**, e161.

Lehman, M. N., Silver, R., Gladstone, W. R., Kahn, R. M., Gibson, M. and Bittman, E. L. (1987). Circadian rhythmicity restored by neural transplant. Immunocytochemical characterization of the graft and its integration with the host brain. *J Neurosci* **7**, 1626-38.

Leproult, R., Holmbäck, U. and Van Cauter, E. (2014). Circadian Misalignment Augments Markers of Insulin Resistance and Inflammation, Independently of Sleep Loss. *Diabetes* **63**, 1860-1869.

LeSauter, J. and Silver, R. (1999). Localization of a suprachiasmatic nucleus subregion regulating locomotor rhythmicity. *J Neurosci* **19**, 5574-85.

Li, W.-Q., Qureshi, A. A., Schernhammer, E. S. and Han, J. (2013). Rotating night-shift work and risk of psoriasis in US women. *The Journal of investigative dermatology* **133**, 565-567.

Liao, Y., Smyth, G. K. and Shi, W. (2013). The Subread aligner: fast, accurate and scalable read mapping by seed-and-vote. *Nucleic acids research* **41**, e108.

Lim, A. S. P., Klein, H.-U., Yu, L., Chibnik, L. B., Ali, S., Xu, J., Bennett, D. A. and De Jager, P. L. (2017). Diurnal and seasonal molecular rhythms in human neocortex and their relation to Alzheimer's disease. *Nature Communications* **8**, 14931.

Lin, Y.-J., Huang, L.-T., Tsai, C.-C., Sheen, J.-M., Tiao, M.-M., Yu, H.-R., Lin, I. C. and Tain, Y.-L. (2019). Maternal high-fat diet sex-specifically alters placental morphology and transcriptome in rats: Assessment by next-generation sequencing. *Placenta* **78**, 44-53.

Lin, Y. C., Hsiao, T. J. and Chen, P. C. (2009). Persistent rotating shift-work exposure accelerates development of metabolic syndrome among middle-aged female employees: a five-year follow-up. *Chronobiol Int* **26**, 740-55.

Liu, C.-H., Sun, Y., Li, J., Gong, Y., Tian, K. T., Evans, L. P., Morss, P. C., Fredrick, T. W., Saba, N. J. and Chen, J. (2015). Endothelial microRNA-150 is an intrinsic suppressor of pathologic ocular neovascularization. *Proceedings of the National Academy of Sciences* **112**, 12163-12168.

Lo Giudice, Q., Leleu, M., La Manno, G. and Fabre, P. J. (2019). Single-cell transcriptional logic of cell-fate specification and axon guidance in early-born retinal neurons. *Development* **146**, dev178103.

Lockett, G. A., Soto-Ramírez, N., Ray, M. A., Everson, T. M., Xu, C. J., Patil, V. K., Terry, W., Kaushal, A., Rezwan, F. I., Ewart, S. L. et al. (2016). Association of season of birth with DNA methylation and allergic disease. *Allergy* **71**, 1314-1324.

Loef, B., Nanlohy, N. M., Jacobi, R. H. J., van de Ven, C., Mariman, R., van der Beek, A. J., Proper, K. I. and van Baarle, D. (2019). Immunological effects of shift work in healthcare workers. *Scientific Reports* **9**, 18220.

Loef, B., van Baarle, D., van der Beek, A. J., Sanders, E. A. M., Bruijning-Verhagen, P. and Proper, K. I. (2018). Shift Work and Respiratory Infections in Health-Care Workers. *American Journal of Epidemiology* **188**, 509-517.

Lofgren, E., Fefferman, N. H., Naumov, Y. N., Gorski, J. and Naumova, E. N. (2007). Influenza Seasonality: Underlying Causes and Modeling Theories. *Journal of Virology* **81**, 5429-5436.

London, A., Benhar, I. and Schwartz, M. (2013). The retina as a window to the brain-from eye research to CNS disorders. *Nature Reviews Neurology* **9**, 44-53.

London, E., Nesterova, M. and Stratakis, C. A. (2017). Acute vs chronic exposure to high fat diet leads to distinct regulation of PKA. *J Mol Endocrinol* **59**, 1-12.

Love, M. I., Huber, W. and Anders, S. (2014). Moderated estimation of fold change and dispersion for RNA-seq data with DESeq2. *Genome Biology* **15**, 550.

Ludwig, N., Hecksteden, A., Kahraman, M., Fehlmann, T., Laufer, T., Kern, F., Meyer, T., Meese, E., Keller, A. and Backes, C. (2019). Spring is in the air: seasonal profiles indicate vernal change of miRNA activity. *Rna Biology* **16**, 1034-1043.

Lunn, R. M., Blask, D. E., Coogan, A. N., Figueiro, M. G., Gorman, M. R., Hall, J. E., Hansen, J., Nelson, R. J., Panda, S., Smolensky, M. H. et al. (2017). Health consequences of electric lighting practices in the modern world: A report on the National Toxicology Program's workshop on shift work at night, artificial light at night, and circadian disruption. *The Science of the total environment* **607-608**, 1073-1084.

Lunshof, S., Boer, K., van Hoffen, G., Wolf, H. and Mirmiran, M. (1997). The diurnal rhythm in fetal heart rate in a twin pregnancy with discordant anencephaly: comparison with three normal twin pregnancies. *Early Hum Dev* **48**, 47-57.

Lynch, S. K. and Abràmoff, M. D. (2017). Diabetic retinopathy is a neurodegenerative disorder. *Vision Res* **139**, 101-107.

MacArthur, J., Bowler, E., Cerezo, M., Gil, L., Hall, P., Hastings, E., Junkins, H., McMahon, A., Milano, A., Morales, J. et al. (2017). The new NHGRI-EBI Catalog of published genome-wide association studies (GWAS Catalog). *Nucleic acids research* **45**, D896-D901.

Maccani, J. Z., Koestler, D. C., Lester, B., Houseman, E. A., Armstrong, D. A., Kelsey, K. T. and Marsit, C. J. (2015). Placental DNA Methylation Related to Both Infant Toenail Mercury and Adverse Neurobehavioral Outcomes. *Environ Health Perspect* **123**, 723-9.

Maes, T., Barcelo, A. and Buesa, C. (2002). Neuron navigator: a human gene family with homology to unc-53, a cell guidance gene from Caenorhabditis elegans. *Genomics* **80**, 21-30.

Malek, G., Johnson, L. V., Mace, B. E., Saloupis, P., Schmechel, D. E., Rickman, D. W., Toth, C. A., Sullivan, P. M. and Rickman, C. B. (2005). Apolipoprotein E allele-dependent pathogenesis: A model for age-related retinal degeneration. *Proceedings of the National Academy of Sciences of the United States of America* **102**, 11900-11905.

Maltepe, E. and Fisher, S. J. (2015). Placenta: the forgotten organ. *Annu Rev Cell Dev Biol* **31**, 523-52.

Mancini, J. E., Ortiz, G., Croxatto, J. O. and Gallo, J. E. (2013). Retinal upregulation of inflammatory and proangiogenic markers in a model of neonatal diabetic rats fed on a high-fat-diet. *Bmc Ophthalmology* **13**.

Mandel, Y., Grotto, I., El-Yaniv, R., Belkin, M., Israeli, E., Polat, U. and Bartov, E. (2008). Season of Birth, Natural Light, and Myopia. *Ophthalmology* **115**, 686-692.

Maniu, A., Aberdeen, G. W., Lynch, T. J., Nadler, J. L., Kim, S. O. K., Quon, M. J., Pepe, G. J. and Albrecht, E. D. (2016). Estrogen deprivation in primate pregnancy leads to insulin resistance in offspring. *J Endocrinol* **230**, 171-183.

Mao, J., Zhang, X., Sieli, P. T., Falduto, M. T., Torres, K. E. and Rosenfeld, C. S. (2010). Contrasting effects of different maternal diets on sexually dimorphic gene expression in the murine placenta. *Proc Natl Acad Sci U S A* **107**, 5557-62.

Marcal, A. C., Leonelli, M., Fiamoncini, J., Deschamps, F. C., Rodrigues, M. A., Curi, R., Carpinelli, A. R., Britto, L. R. and Carvalho, C. R. (2013). Diet-induced obesity impairs AKT signalling in the retina and causes retinal degeneration. *Cell Biochem Funct* **31**, 65-74.

Marchant, E. G. and Mistlberger, R. E. (1997). Anticipation and entrainment to feeding time in intact and SCN-ablated C57BL/6j mice. *Brain Res* **765**, 273-82.

Marcheva, B., Ramsey, K. M., Buhr, E. D., Kobayashi, Y., Su, H., Ko, C. H., Ivanova, G., Omura, C., Mo, S., Vitaterna, M. H. et al. (2010). Disruption of the clock components CLOCK and BMAL1 leads to hypoinsulinaemia and diabetes. *Nature* **466**, 627.

Marei, W. F. A., Smits, A., Mohey-Elsaeed, O., Pintelon, I., Ginneberge, D., Bols, P. E. J., Moerloose, K. and Leroy, J. L. M. R. (2020). Differential effects of high fat diet-induced obesity on oocyte mitochondrial functions in inbred and outbred mice. *Scientific Reports* **10**, 9806.

Mark, P. J., Crew, R. C., Wharfe, M. D. and Waddell, B. J. (2017). Rhythmic Three-Part Harmony: The Complex Interaction of Maternal, Placental and Fetal Circadian Systems. *J Biol Rhythms* **32**, 534-549.

Marquié, J.-C., Tucker, P., Folkard, S., Gentil, C. and Ansiau, D. (2015). Chronic effects of shift work on cognition: findings from the VISAT longitudinal study. *Occupational and environmental medicine* **72**, 258-264.

Martin, E. M. and Fry, R. C. (2016). A cross-study analysis of prenatal exposures to environmental contaminants and the epigenome: support for stress-responsive transcription factor occupancy as a mediator of gene-specific CpG methylation patterning. *Environ Epigenet* **2**.

Martinez-Lopez, M. J., Alcantara, S., Mascaro, C., Perez-Branguli, F., Ruiz-Lozano, P., Maes, T., Soriano, E. and Buesa, C. (2005). Mouse neuron navigator 1, a novel microtubule-associated protein involved in neuronal migration. *Mol Cell Neurosci* **28**, 599-612.

McMahon, D. G., Iuvone, P. M. and Tosini, G. (2014). Circadian organization of the mammalian retina: from gene regulation to physiology and diseases. *Progress in Retinal and Eye Research* **39**, 58-76.

McMenamin, T. M. (2007). A time to work: recent trends in shift work and flexible schedules. *Monthly Labor Review* **130**, 3-15.

McMillen, I. C. and Robinson, J. S. (2005). Developmental origins of the metabolic syndrome: prediction, plasticity, and programming. *Physiol Rev* **85**, 571-633.

Mendez, N., Halabi, D., Spichiger, C., Salazar, E. R., Vergara, K., Alonso-Vasquez, P., Carmona, P., Sarmiento, J. M., Richter, H. G., Seron-Ferre, M. et al. (2016). Gestational Chronodisruption Impairs Circadian Physiology in Rat Male Offspring, Increasing the Risk of Chronic Disease. *Endocrinology* **157**, 4654-4668.

Mendez, N., Torres-Farfan, C., Salazar, E., Bascur, P., Bastidas, C., Vergara, K., Spichiger, C., Halabi, D., Vio, C. P. and Richter, H. G. (2019). Fetal Programming of Renal Dysfunction and High Blood Pressure by Chronodisruption. *Frontiers in endocrinology* **10**, 362-362.

Menet, J. S., Pescatore, S. and Rosbash, M. (2014). CLOCK:BMAL1 is a pioneer-like transcription factor. *Genes Dev* **28**, 8-13.

Merle, B. M., Silver, R. E., Rosner, B. and Seddon, J. M. (2015). Adherence to a Mediterranean diet, genetic susceptibility, and progression to advanced macular degeneration: a prospective cohort study. *Am J Clin Nutr* **102**, 1196-206.

Meyer-Bernstein, E. L., Jetton, A. E., Matsumoto, S. I., Markuns, J. F., Lehman, M. N. and Bittman, E. L. (1999). Effects of suprachiasmatic transplants on circadian rhythms of neuroendocrine function in golden hamsters. *Endocrinology* **140**, 207-18.

Miceli, M. V., Newsome, D. A., Tate, D. J. and Sarphie, T. G. (2000). Pathologic changes in the retinal pigment epithelium and Bruch's membrane of fat-fed atherogenic mice. *Current Eye Research* **20**, 8-16.

Miller, W. P., Ravi, S., Martin, T. D., Kimball, S. R. and Dennis, M. D. (2017). Activation of the Stress Response Kinase JNK (c-Jun N-terminal Kinase) Attenuates Insulin Action in Retina through a p70S6K1-dependent Mechanism. *Journal of Biological Chemistry* **292**, 1591-1602.

Mitchell, P., Liew, G., Gopinath, B. and Wong, T. Y. (2018). Age-related macular degeneration. *Lancet* **392**, 1147-1159.

Mohamed, I. N., Hafez, S. S., Fairaq, A., Ergul, A., Imig, J. D. and El-Remessy, A. B. (2014). Thioredoxin-interacting protein is required for endothelial NLRP3 inflammasome activation and cell death in a rat model of high-fat diet. *Diabetologia* **57**, 413-23.

Mohamed, I. N., Sheibani, N. and El-Remessy, A. B. (2020). Deletion of Thioredoxin-Interacting Protein (TXNIP) Abrogates High Fat Diet-induced Retinal Leukostasis, Barrier Dysfunction and Microvascular Degeneration in a Mouse Obesity Model. *Int J Mol Sci* **21**.

Mohawk, J. A., Green, C. B. and Takahashi, J. S. (2012). Central and peripheral circadian clocks in mammals. *Annual review of neuroscience* **35**, 445-462.

Mohren, D. C., Jansen, N. W., Kant, I. J., Galama, J., van den Brandt, P. A. and Swaen, G. M. (2002). Prevalence of common infections among employees in different work schedules. *J Occup Environ Med* **44**, 1003-11.

Molday, R. S. and Moritz, O. L. (2015). Photoreceptors at a glance. *J Cell Sci* **128**, 4039-4045.

Moore, R. Y. and Eichler, V. B. (1972). Loss of a circadian adrenal corticosterone rhythm following suprachiasmatic lesions in the rat. *Brain Res* **42**, 201-6.

Morey, J. S., Neely, M. G., Lunardi, D., Anderson, P. E., Schwacke, L. H., Campbell, M. and Van Dolah, F. M. (2016). RNA-Seq analysis of seasonal and individual variation in blood transcriptomes of healthy managed bottlenose dolphins. *BMC Genomics* **17**, 720.

Morikawa, Y., Nakagawa, H., Miura, K., Soyama, Y., Ishizaki, M., Kido, T., Naruse, Y., Suwazono, Y. and Nogawa, K. (2007). Effect of shift work on body mass index and metabolic parameters. *Scandinavian Journal of Work Environment & Health* **33**, 45-50.

Morris, C. J., Yang, J. N., Garcia, J. I., Myers, S., Bozzi, I., Wang, W., Buxton, O. M., Shea, S. A. and Scheer, F. A. J. L. (2015). Endogenous circadian system and circadian misalignment impact glucose tolerance via separate mechanisms in humans. *Proceedings of the National Academy of Sciences* **112**, E2225-E2234.

Motz, C. T., Chesler, K. C., Allen, R. S., Bales, K. L., Mees, L. M., Feola, A. J., Maa, A. Y., Olson, D. E., Thule, P. M., Iuvone, P. M. et al. (2020). Novel Detection and Restorative Levodopa Treatment for Preclinical Diabetic Retinopathy. *Diabetes* **69**, 1518-1527.

Muhammad, F. Y., Peters, K., Wang, D. and Lee, D. J. (2019). Exacerbation of autoimmune uveitis by obesity occurs through the melanocortin 5 receptor. *J Leukoc Biol* **106**, 879-887.

Mui, A. M., Yang, V., Aung, M. H., Fu, J., Adekunle, A. N., Prall, B. C., Sidhu, C. S., Park, H. N., Boatright, J. H., Iuvone, P. M. et al. (2018). Daily visual stimulation in the critical period enhances multiple aspects of vision through BDNF-mediated pathways in the mouse retina. *PLoS One* **13**, e0192435.

Mure, L. S., Le, H. D., Benegiamo, G., Chang, M. W., Rios, L., Jillani, N., Ngotho, M., Kariuki, T., Dkhissi-Benyahya, O., Cooper, H. M. et al. (2018). Diurnal transcriptome atlas of a primate across major neural and peripheral tissues. *Science (New York, N.Y.)* **359**, eaao0318.

Murphy, E. A., Velazquez, K. T. and Herbert, K. M. (2015). Influence of high-fat diet on gut microbiota: a driving force for chronic disease risk. *Current opinion in clinical nutrition and metabolic care* **18**, 515-520.

Musiek, E. S., Lim, M. M., Yang, G., Bauer, A. Q., Qi, L., Lee, Y., Roh, J. H., Ortiz-Gonzalez, X., Dearborn, J. T., Culver, J. P. et al. (2013). Circadian clock proteins regulate neuronal redox homeostasis and neurodegeneration. *J Clin Invest* **123**, 5389-400.

Mykkanen, O. T., Kalesnykas, G., Adriaens, M., Evelo, C. T., Torronen, R. and Kaarniranta, K. (2012). Bilberries potentially alleviate stress-related retinal gene expression induced by a high-fat diet in mice. *Molecular Vision* **18**, 2338-2351.

Myung, J., Hong, S., Hatanaka, F., Nakajima, Y., De Schutter, E. and Takumi, T. (2012). Period coding of Bmal1 oscillators in the suprachiasmatic nucleus. *J Neurosci* **32**, 8900-18.

Nakazato, R., Kawabe, K., Yamada, D., Ikeno, S., Mieda, M., Shimba, S., Hinoi, E., Yoneda, Y. and Takarada, T. (2017). Disruption of Bmal1 Impairs Blood-Brain Barrier Integrity via Pericyte Dysfunction. *J Neurosci* **37**, 10052-10062.

Nakazawa, Y., Ishimori, N., Oguchi, J., Nagai, N., Kimura, M., Funakoshi-Tago, M. and Tamura, H. (2019). Coffee brew intake can prevent the reduction of lens glutathione and ascorbic acid levels in HFD-fed animals. *Experimental and Therapeutic Medicine* **17**, 1420-1425.

Nam, K. N., Mounier, A., Wolfe, C. M., Fitz, N. F., Carter, A. Y., Castranio, E. L., Kamboh, H. I., Reeves, V. L., Wang, J., Han, X. et al. (2017). Effect of high fat diet on phenotype, brain transcriptome and lipidome in Alzheimer's model mice. *Scientific Reports* **7**, 4307.

Nguyen, L. T., Chen, H., Pollock, C. and Saad, S. (2017). SIRT1 reduction is associated with sex-specific dysregulation of renal lipid metabolism and stress responses in offspring by maternal high-fat diet. *Sci Rep* **7**, 8982.

Nickla, D. L. and Wallman, J. (2010). The multifunctional choroid. *Prog Retin Eye Res* **29**, 144-68.

Noack Watt, K. E., Achilleos, A., Neben, C. L., Merrill, A. E. and Trainor, P. A. (2016). The Roles of RNA Polymerase I and III Subunits Polr1c and Polr1d in Craniofacial Development and in Zebrafish Models of Treacher Collins Syndrome. *PLOS Genetics* **12**, e1006187.

Noda, M., Iwamoto, I., Tabata, H., Yamagata, T., Ito, H. and Nagata, K.-i. (2019). Role of Per3, a circadian clock gene, in embryonic development of mouse cerebral cortex. *Scientific Reports* **9**, 5874.

Oishi, Y., Hayashi, S., Isagawa, T., Oshima, M., Iwama, A., Shimba, S., Okamura, H. and Manabe, I. (2017). Bmal1 regulates inflammatory responses in macrophages by modulating enhancer RNA transcription. *Sci Rep* **7**, 7086.

Olofsson, S.-O. and Borén, J. (2005). Apolipoprotein B: a clinically important apolipoprotein which assembles atherogenic lipoproteins and promotes the development of atherosclerosis. *Journal of Internal Medicine* **258**, 395-410.

Opperhuizen, A. L., van Kerkhof, L. W., Proper, K. I., Rodenburg, W. and Kalsbeek, A. (2015). Rodent models to study the metabolic effects of shiftwork in humans. *Front Pharmacol* **6**, 50.

Orozco-Solis, R. and Aguilar-Arnal, L. (2020). Circadian Regulation of Immunity Through Epigenetic Mechanisms. *Front Cell Infect Microbiol* **10**, 96.

Osmond, C., Barker, D. J., Winter, P. D., Fall, C. H. and Simmonds, S. J. (1993). Early growth and death from cardiovascular disease in women. *BMJ* **307**, 1519-24.

Ospri, L. L., Prusky, G. and Hattar, S. (2017). Mood, the Circadian System, and Melanopsin Retinal Ganglion Cells. *Annual review of neuroscience* **40**, 539-556.

Owen, C. G., Jarrar, Z., Wormald, R., Cook, D. G., Fletcher, A. E. and Rudnicka, A. R. (2012). The estimated prevalence and incidence of late stage age related macular degeneration in the UK. *British Journal of Ophthalmology* **96**, 752-756.

Ozawa, G. Y., Bearse, M. A. and Adams, A. J. (2015). Male–Female Differences in Diabetic Retinopathy? *Current Eye Research* **40**, 234-246.

Painter, R., Osmond, C., Gluckman, P., Hanson, M., Phillips, D. and Roseboom, T. (2008). Transgenerational effects of prenatal exposure to the Dutch famine on neonatal adiposity and health in later life. *BJOG: An International Journal of Obstetrics & Gynaecology* **115**, 1243-1249.

Palmer, K. T., Bonzini, M., Harris, E. C., Linaker, C. and Bonde, J. P. (2013). Work activities and risk of prematurity, low birthweight and pre-eclampsia: an updated review with meta-analysis. *Occupational and environmental medicine* **70**, 213-222.

Pan, A., Schernhammer, E. S., Sun, Q. and Hu, F. B. (2011). Rotating Night Shift Work and Risk of Type 2 Diabetes: Two Prospective Cohort Studies in Women. *Plos Medicine* **8**.

Panda, S. (2016). Circadian physiology of metabolism. *Science (New York, N.Y.)* **354**, 1008-1015.

Panda, S., Antoch, M. P., Miller, B. H., Su, A. I., Schook, A. B., Straume, M., Schultz, P. G., Kay, S. A., Takahashi, J. S. and Hogenesch, J. B. (2002). Coordinated Transcription of Key Pathways in the Mouse by the Circadian Clock. *Cell* **109**, 307-320.

Paquette, A. G., Houseman, E. A., Green, B. B., Lesseur, C., Armstrong, D. A., Lester, B. and Marsit, C. J. (2016). Regions of variable DNA methylation in human placenta associated with newborn neurobehavior. *Epigenetics* **11**, 603-613.

Pardue, M. T., Barnes, C. S., Kim, M. K., Aung, M. H., Amarnath, R., Olson, D. E. and Thulé, P. M. (2014). Rodent Hyperglycemia-Induced Inner Retinal Deficits are Mirrored in Human Diabetes. *Translational Vision Science & Technology* **3**, 6-6.

Parisi, V. (2003). Correlation between morphological and functional retinal impairment in patients affected by ocular hypertension, glaucoma, demyelinating optic neuritis and Alzheimer's disease. *Seminars in Ophthalmology* **18**, 50-57.

Parks, B. W., Sallam, T., Mehrabian, M., Psychogios, N., Hui, S. T., Norheim, F., Castellani, L. W., Rau, C. D., Pan, C., Phun, J. et al. (2015). Genetic architecture of insulin resistance in the mouse. *Cell Metab* **21**, 334-347.

Patton, A. P. and Hastings, M. H. (2018). The suprachiasmatic nucleus. *Curr Biol* **28**, R816-r822.

Peek, C. B., Levine, D. C., Cedernaes, J., Taguchi, A., Kobayashi, Y., Tsai, S. J., Bonar, N. A., McNulty, M. R., Ramsey, K. M. and Bass, J. (2017). Circadian Clock Interaction with HIF1alpha Mediates Oxygenic Metabolism and Anaerobic Glycolysis in Skeletal Muscle. *Cell Metab* **25**, 86-92.

Peek, C. B., Ramsey, K. M., Marcheva, B. and Bass, J. (2012). Nutrient sensing and the circadian clock. *Trends in endocrinology and metabolism: TEM* **23**, 312-318.

Peirson, S. and Foster, R. G. (2006). Melanopsin: another way of signaling light. *Neuron* **49**, 331-9.

Peirson, S. N., Oster, H., Jones, S. L., Leitges, M., Hankins, M. W. and Foster, R. G. (2007). Microarray analysis and functional genomics identify novel components of melanopsin signaling. *Curr Biol* **17**, 1363-72.

Peng, R. D., Dominici, F., Pastor-Barriuso, R., Zeger, S. L. and Samet, J. M. (2005). Seasonal Analyses of Air Pollution and Mortality in 100 US Cities. *American Journal of Epidemiology* **161**, 585-594.

Penn, R. D. and Hagins, W. A. (1969). Signal Transmission along Retinal Rods and the Origin of the Electroretinographic a-Wave. *Nature* **223**, 201-205.

Pennesi, M. E., Neuringer, M. and Courtney, R. J. (2012). Animal models of age related macular degeneration. *Molecular aspects of medicine* **33**, 487-509.

Perelis, M., Marcheva, B., Moynihan Ramsey, K., Schipma, M. J., Hutchison, A. L., Taguchi, A., Peek, C. B., Hong, H., Huang, W., Omura, C. et al. (2015). Pancreatic β cell enhancers regulate rhythmic transcription of genes controlling insulin secretion. *Science* **350**.

Pérez, S., Murias, L., Fernández-Plaza, C., Díaz, I., González, C., Otero, J. and Díaz, E. (2015). Evidence for clock genes circadian rhythms in human full-term placenta. *Syst Biol Reprod Med* **61**, 360-6.

Phillips, M. C. (2018). Is ABCA1 a lipid transfer protein? *Journal of Lipid Research* **59**, 749-763.

Phipson, B., Maksimovic, J. and Oshlack, A. (2016). missMethyl: an R package for analyzing data from Illumina's HumanMethylation450 platform. *Bioinformatics* **32**, 286-288.

Picard, E., Houssier, M., Bujold, K., Sapieha, P., Lubell, W., Dorfman, A., Racine, J., Hardy, P., Febbraio, M., Lachapelle, P. et al. (2010). CD36 plays an important role in the clearance of oxLDL and associated age-dependent sub-retinal deposits. *Aging (Albany NY)* **2**, 981-9.

Pizarro, A., Hayer, K., Lahens, N. F. and Hogenesch, J. B. (2013). CircaDB: a database of mammalian circadian gene expression profiles. *Nucleic acids research* **41**, D1009-13.

Prendergast, B. J., Onishi, K. G. and Zucker, I. (2014). Female mice liberated for inclusion in neuroscience and biomedical research. *Neurosci Biobehav Rev* **40**, 1-5.

Prins, J. R., Eskandar, S., Eggen, B. J. L. and Scherjon, S. A. (2018). Microglia, the missing link in maternal immune activation and fetal neurodevelopment; and a possible link in preeclampsia and disturbed neurodevelopment? *J Reprod Immunol* **126**, 18-22.

Provost, A. C., Vede, L., Bigot, K., Keller, N., Tailleux, A., Jais, J. P., Savoldelli, M., Ameqrane, I., Lacassagne, E., Legeais, J. M. et al. (2009). Morphologic and Electroretinographic Phenotype of SR-BI Knockout Mice after a Long-Term Atherogenic Diet. *Investigative Ophthalmology & Visual Science* **50**, 3931-3942.

Prusky, G. T., Alam, N. M., Beekman, S. and Douglas, R. M. (2004). Rapid quantification of adult and developing mouse spatial vision using a virtual optomotor system. *Invest Ophthalmol Vis Sci* **45**, 4611-6.

Prusky, G. T., Alam, N. M. and Douglas, R. M. (2006). Enhancement of vision by monocular deprivation in adult mice. *J Neurosci* **26**, 11554-61.

Puttonen, S., Viitasalo, K. and Härmä, M. (2011). Effect of shiftwork on systemic markers of inflammation. *Chronobiol Int* **28**, 528-35.

Qiu, C., Gelaye, B., Denis, M., Tadesse, M. G., Enquobahrie, D. A., Ananth, C. V., Pacora, P. N., Salazar, M., Sanchez, S. E. and Williams, M. A. (2016). Placental genetic variations in circadian clock-related genes increase the risk of placental abruption. *International journal of molecular epidemiology and genetics* **7**, 32-40.

Qu, B., Wu, S., Jiao, G., Zou, X., Li, Z., Guo, L., Sun, X., Huang, C., Sun, Z., Zhang, Y. et al. (2020). Treating Bietti crystalline dystrophy in a high-fat diet-exacerbated murine model using gene therapy. *Gene Ther* **27**, 370-382.

Rajagopal, R., Bligard, G. W., Zhang, S., Yin, L., Lukasiewicz, P. and Semenkovich, C. F. (2016). Functional Deficits Precede Structural Lesions in Mice With High-Fat Diet-Induced Diabetic Retinopathy. *Diabetes* **65**, 1072-1084.

Rakshit, K., Qian, J., Colwell, C. S. and Matveyenko, A. V. (2015). The Islet Circadian Clock: Entrainment Mechanisms, Function and Role in Glucose Homeostasis. *Diabetes, obesity & metabolism* **17**, 115-122.

Ramsey, A. M., Stowie, A., Castanon-Cervantes, O. and Davidson, A. J. (2020). Environmental Circadian Disruption Increases Stroke Severity and Dysregulates Immune Response. *J Biol Rhythms* **35**, 368-376.

Rao, S., Chun, C., Fan, J., Kofron, J. M., Yang, M. B., Hegde, R. S., Ferrara, N., Copenhagen, D. R. and Lang, R. A. (2013). A direct and melanopsin-dependent fetal light response regulates mouse eye development. *Nature* **494**, 243-246.

Rashid, H., Kagami, M., Ferdous, F., Ma, E., Terao, T., Hayashi, T. and Wagatsuma, Y. (2016). Temperature during pregnancy influences the fetal growth and birth size. *Tropical medicine and health* **45**, 1-1.

Rashid, K., Akhtar-Schaefer, I. and Langmann, T. (2019). Microglia in Retinal Degeneration. *Frontiers in immunology* **10**, 1975.

Reik, W. (2007). Stability and flexibility of epigenetic gene regulation in mammalian development. *Nature* **447**, 425.

Reis, F. M., Florio, P., Cobellis, L., Luisi, S., Severi, F. M., Bocchi, C., Picciolini, E., Centini, G. and Petraglia, F. (2001). Human placenta as a source of neuroendocrine factors. *Biol Neonate* **79**, 150-6.

Reutrakul, S. and Knutson, K. L. (2015). Consequences of Circadian Disruption on Cardiometabolic Health. *Sleep medicine clinics* **10**, 455-468.

Rhainds, D. and Brissette, L. (2004). The role of scavenger receptor class B type I (SR-BI) in lipid trafficking. defining the rules for lipid traders. *Int J Biochem Cell Biol* **36**, 39-77.

Rich-Edwards, J. W., Stampfer, M. J., Manson, J. E., Rosner, B., Hankinson, S. E., Colditz, G. A., Willett, W. C. and Hennekens, C. H. (1997). Birth weight and risk of cardiovascular disease in a cohort of women followed up since 1976. *BMJ* **315**, 396-400.

Risérus, U., Willett, W. C. and Hu, F. B. (2009). Dietary fats and prevention of type 2 diabetes. *Progress in lipid research* **48**, 44-51.

Robinson, R., Barathi, V. A., Chaurasia, S. S., Wong, T. Y. and Kern, T. S. (2012). Update on animal models of diabetic retinopathy: from molecular approaches to mice and higher mammals. *Disease Models &amp; Mechanisms* **5**, 444-456.

Robson, J. G. and Frishman, L. J. (1995). Response linearity and kinetics of the cat retina: the bipolar cell component of the dark-adapted electroretinogram. *Vis Neurosci* **12**, 837-50.

Robson, J. G. and Frishman, L. J. (1996). Photoreceptor and bipolar-cell contributions to the cat electroretinogram: a kinetic model for the early part of the flash response. *Journal of the Optical Society of America A* **13**, 613-622.

Roddy, G. W., Rosa, R. H., Viker, K. B., Holman, B. H., Hann, C. R., Krishnan, A., Gores, G. J., Bakri, S. J. and Fautsch, M. P. (2019). Diet Mimicking "Fast Food" Causes Structural Changes to the Retina Relevant to Age-Related Macular Degeneration. *Curr Eye Res*, 1-7.

Rosenfeld, C. S. (2021). The placenta-brain-axis. *J Neurosci Res* **99**, 271-283.

Rouch, I., Wild, P., Ansiau, D. and Marquié, J. C. (2005). Shiftwork experience, age and cognitive performance. *Ergonomics* **48**, 1282-93.

Ruben, M. D., Wu, G., Smith, D. F., Schmidt, R. E., Francey, L. J., Lee, Y. Y., Anafi, R. C. and Hogenesch, J. B. (2018). A database of tissue-specific rhythmically expressed human genes has potential applications in circadian medicine. *Sci Transl Med* **10**, eaat8806.

Rudolf, M., Winkler, B., Aherrahou, Z., Doehring, L. C., Kaczmarek, P. and Schmidt-Erfurth, U. (2005). Increased expression of vascular endothelial growth factor associated with accumulation of lipids in Bruch's membrane of LDL receptor knockout mice. *British Journal of Ophthalmology* **89**, 1627-1630.

Russart, K. L. G. and Nelson, R. J. (2018). Light at night as an environmental endocrine disruptor. *Physiology & Behavior* **190**, 82-89.

Rytkonen, K. T., Heinosalo, T., Mahmoudian, M., Ma, X., Perheentupa, A., Elo, L. L., Poutanen, M. and Wagner, G. P. (2020). Transcriptomic responses to hypoxia in endometrial and decidual stromal cells. *Reproduction*.

Saccà, S. C., Cutolo, C. A., Ferrari, D., Corazza, P. and Traverso, C. E. (2018). The Eye, Oxidative Damage and Polyunsaturated Fatty Acids. *Nutrients* **10**, 668.

Sachs, M. (2014). cosinor: Tools for estimating and predicting the cosinor model version 1.1.

Saeedi, P., Petersohn, I., Salpea, P., Malanda, B., Karuranga, S., Unwin, N., Colagiuri, S., Guariguata, L., Motala, A. A., Ogurtsova, K. et al. (2019). Global and regional diabetes prevalence estimates for 2019 and projections for 2030 and 2045: Results from the International Diabetes Federation Diabetes Atlas, 9th edition. *Diabetes Research and Clinical Practice* **157**, 107843.

Safi, H., Safi, S., Hafezi-Moghadam, A. and Ahmadieh, H. (2018). Early detection of diabetic retinopathy. *Survey of Ophthalmology* **63**, 601-608.

Sakaguchi, K., Takeda, K., Maeda, M., Ogawa, W., Sato, T., Okada, S., Ohnishi, Y., Nakajima, H. and Kashiwagi, A. (2015). Glucose area under the curve during oral glucose tolerance test as an index of glucose intolerance. *Diabetology international* **7**, 53-58.

Samuels, L. T., Reinecke, R. M. and Ball, H. A. (1942). Effect of diet on glucose tolerance and liver and muscle glycogen of hypophysectomized and normal rats1,2. *Endocrinology* **31**, 42-45.

Sanmiguel, C., Gupta, A. and Mayer, E. A. (2015). Gut Microbiome and Obesity: A Plausible Explanation for Obesity. *Current obesity reports* **4**, 250-261.

Saper, C. B. (2013). The Central Circadian Timing System. *Current opinion in neurobiology* **23**, 747-751.

Sarks, S., Cherepanoff, S., Killingsworth, M. and Sarks, J. (2007). Relationship of Basal laminar deposit and membranous debris to the clinical presentation of early age-related macular degeneration. *Invest Ophthalmol Vis Sci* **48**, 968-77.

Sasaki, M., Kawasaki, R., Rogers, S., Man, R. E. K., Itakura, K., Xie, J., Flood, V., Tsubota, K., Lamoureux, E. and Wang, J. J. (2015). The Associations of Dietary Intake of Polyunsaturated Fatty Acids With Diabetic Retinopathy in Well-Controlled Diabetes. *Investigative Ophthalmology & Visual Science* **56**, 7473-7479.

Sawant, O. B., Horton, A. M., Zucaro, O. F., Chan, R., Bonilha, V. L., Samuels, I. S. and Rao, S. (2017). The Circadian Clock Gene Bmal1 Controls Thyroid Hormone-Mediated Spectral Identity and Cone Photoreceptor Function. *Cell Reports* **21**, 692-706.

Sawant, O. B., Jidigam, V. K., Fuller, R. D., Zucaro, O. F., Kpegba, C., Yu, M., Peachey, N. S. and Rao, S. (2019). The circadian clock gene Bmal1 is required to control the timing of retinal neurogenesis and lamination of Müller glia in the mouse retina. *The FASEB Journal* **33**, 8745-8758.

Sayles, G. D. (2002). Environmental Engineering and Endocrine Disrupting Chemicals. *Journal of Environmental Engineering* **128**, 1-2.

Scheer, F., Hilton, M. F., Mantzoros, C. S. and Shea, S. A. (2009). Adverse metabolic and cardiovascular consequences of circadian misalignment. *Proceedings of the National Academy of Sciences of the United States of America* **106**, 4453-4458.

Scheiermann, C., Gibbs, J., Ince, L. and Loudon, A. (2018). Clocking in to immunity. *Nature reviews. Immunology* **18**, 423-437.

Schiller, P. H. (2010). Parallel information processing channels created in the retina. *Proc Natl Acad Sci U S A* **107**, 17087-94.

Schmid, B., Helfrich-Förster, C. and Yoshii, T. (2011). A New ImageJ Plug-in “ActogramJ” for Chronobiological Analyses. *Journal of Biological Rhythms* **26**, 464-467.

Schmidt-Erfurth, U., Rudolf, M., Funk, M., Hofmann-Rummelt, C., Franz-Haas, N. S., Aherrahrou, Z. and Schlotzer-Schrehardt, U. (2008). Ultrastructural changes in a murine model of graded Bruch membrane lipoidal degeneration and corresponding VEGF(164) detection. *Investigative Ophthalmology & Visual Science* **49**, 390-398.

Schmidt, T. M., Chen, S.-K. and Hattar, S. (2011). Intrinsically photosensitive retinal ganglion cells: many subtypes, diverse functions. *Trends in neurosciences* **34**, 572-580.

Schug, T. T., Janesick, A., Blumberg, B. and Heindel, J. J. (2011). Endocrine Disrupting Chemicals and Disease Susceptibility. *The Journal of steroid biochemistry and molecular biology* **127**, 204-215.

Seagle, B.-L. L., Rezai, K. A., Kobori, Y., Gasyna, E. M., Rezaei, K. A. and Norris, J. R. (2005). Melanin photoprotection in the human retinal pigment epithelium and its correlation with light-induced cell apoptosis. *Proceedings of the National Academy of Sciences of the United States of America* **102**, 8978-8983.

Sedov, I. D., Cameron, E. E., Madigan, S. and Tomfohr-Madsen, L. M. (2018). Sleep quality during pregnancy: A meta-analysis. *Sleep Med Rev* **38**, 168-176.

Shaito, A., Hasan, H., Habashy, K. J., Fakih, W., Abdelhady, S., Ahmad, F., Zibara, K., Eid, A. H., El-Yazbi, A. F. and Kobeissy, F. H. (2020). Western diet aggravates neuronal insult in post-traumatic brain injury: Proposed pathways for interplay. *EBioMedicine* **57**.

Shanab, A. Y., Nakazawa, T., Ryu, M., Tanaka, Y., Himori, N., Taguchi, K., Yasuda, M., Watanabe, R., Takano, J., Saido, T. et al. (2012). Metabolic stress response implicated in diabetic retinopathy: The role of calpain, and the therapeutic impact of calpain inhibitor. *Neurobiology of Disease* **48**, 556-567.

Shi, G., Xing, L., Wu, D., Bhattacharyya, B. J., Jones, C. R., McMahon, T., Chong, S. Y. C., Chen, J. A., Coppola, G., Geschwind, D. et al. (2019). A Rare Mutation of β1-Adrenergic Receptor Affects Sleep/Wake Behaviors. *Neuron* **103**, 1044-1055.e7.

Shi, L., Kim, A. J., Chang, R. C., Chang, J. Y., Ying, W., Ko, M. L., Zhou, B. and Ko, G. Y. (2016). Deletion of miR-150 Exacerbates Retinal Vascular Overgrowth in High-Fat-Diet Induced Diabetic Mice. *PLoS One* **11**, e0157543.

Shim, J.-S., Oh, K. and Kim, H. C. (2014). Dietary assessment methods in epidemiologic studies. *Epidemiology and health* **36**, e2014009-e2014009.

Shimba, S., Ogawa, T., Hitosugi, S., Ichihashi, Y., Nakadaira, Y., Kobayashi, M., Tezuka, M., Kosuge, Y., Ishige, K., Ito, Y. et al. (2011). Deficient of a Clock Gene, Brain and Muscle Arnt-Like Protein-1 (BMAL1), Induces Dyslipidemia and Ectopic Fat Formation. *PLoS One* **6**, e25231.

Shirao, Y. and Kawasaki, K. (1998). Electrical responses from diabetic retina. *Prog Retin Eye Res* **17**, 59-76.

Shu, X., Zhang, Y., Li, M., Huang, X., Yang, Y., Zeng, J., Zhao, Y., Wang, X., Zhang, W. and Ying, Y. (2019). Topical ocular administration of the GLP-1 receptor agonist liraglutide arrests hyperphosphorylated tau-triggered diabetic retinal neurodegeneration via activation of GLP-1R/Akt/GSK3beta signaling. *Neuropharmacology* **153**, 1-12.

Sieving, P. A., Murayama, K. and Naarendorp, F. (1994). Push–pull model of the primate photopic electroretinogram: A role for hyperpolarizing neurons in shaping the b-wave. *Visual Neuroscience* **11**, 519-532.

Sieweke, M. H. and Allen, J. E. (2013). Beyond stem cells: self-renewal of differentiated macrophages. *Science (New York, N.Y.)* **342**, 1242974.

Silver, R., LeSauter, J., Tresco, P. A. and Lehman, M. N. (1996). A diffusible coupling signal from the transplanted suprachiasmatic nucleus controlling circadian locomotor rhythms. *Nature* **382**, 810-3.

Silvestri, R. and Aricò, I. (2019). Sleep disorders in pregnancy. *Sleep science (Sao Paulo, Brazil)* **12**, 232-239.

Simó, R., Stitt, A. W. and Gardner, T. W. (2018). Neurodegeneration in diabetic retinopathy: does it really matter? *Diabetologia* **61**, 1902-1912.

Simón, M. V., Prado Spalm, F. H., Vera, M. S. and Rotstein, N. P. (2019). Sphingolipids as Emerging Mediators in Retina Degeneration. *Frontiers in Cellular Neuroscience* **13**.

Smarr, B. L., Grant, A. D., Perez, L., Zucker, I. and Kriegsfeld, L. J. (2017a). Maternal and Early-Life Circadian Disruption Have Long-Lasting Negative Consequences on Offspring Development and Adult Behavior in Mice. *Sci Rep* **7**, 3326.

Smarr, B. L., Grant, A. D., Perez, L., Zucker, I. and Kriegsfeld, L. J. (2017b). Maternal and Early-Life Circadian Disruption Have Long-Lasting Negative Consequences on Offspring Development and Adult Behavior in Mice. *Scientific Reports* **7**, 3326.

Song, M.-S. and Rossi, J. J. (2017). Molecular mechanisms of Dicer: endonuclease and enzymatic activity. *Biochem J* **474**, 1603-1618.

Sparrow, J. R., Hicks, D. and Hamel, C. P. (2010). The retinal pigment epithelium in health and disease. *Current molecular medicine* **10**, 802-823.

Speakman, J. R. (2019). Use of high-fat diets to study rodent obesity as a model of human obesity. *International Journal of Obesity* **43**, 1491-1492.

Spector, T. D. and Gardner, C. D. (2020). Challenges and opportunities for better nutrition science—an essay by Tim Spector and Christopher Gardner. *BMJ* **369**, m2470.

Stanton, J. B., Marmorstein, A. D., Zhang, Y. and Marmorstein, L. Y. (2017). Deletion of Efemp1 Is Protective Against the Development of Sub-RPE Deposits in Mouse Eyes. *Invest Ophthalmol Vis Sci* **58**, 1455-1461.

Stephan, F. K. and Zucker, I. (1972). Circadian rhythms in drinking behavior and locomotor activity of rats are eliminated by hypothalamic lesions. *Proc Natl Acad Sci U S A* **69**, 1583-6.

Stevenson, T. J., Visser, M. E., Arnold, W., Barrett, P., Biello, S., Dawson, A., Denlinger, D. L., Dominoni, D., Ebling, F. J., Elton, S. et al. (2015). Disrupted seasonal biology impacts health, food security and ecosystems. *Proc Biol Sci* **282**, 20151453.

Stone, W. L., Farnsworth, C. C. and Dratz, E. A. (1979). A reinvestigation of the fatty acid content of bovine, rat and frog retinal rod outer segments. *Experimental Eye Research* **28**, 387-397.

Storti, F., Klee, K., Todorova, V., Steiner, R., Othman, A., van der Velde-Visser, S., Samardzija, M., Meneau, I., Barben, M., Karademir, D. et al. (2019). Impaired ABCA1/ABCG1-mediated lipid efflux in the mouse retinal pigment epithelium (RPE) leads to retinal degeneration. *Elife* **8**.

Straif, K., Baan, R., Grosse, Y., Secretan, B., El Ghissassi, F., Bouvard, V., Altieri, A., Benbrahim-Tallaa, L. and Cogliano, V. (2007). Carcinogenicity of shift-work, painting, and fire-fighting. *Lancet Oncol* **8**, 1065-6.

Stremmel, C., Schuchert, R., Wagner, F., Thaler, R., Weinberger, T., Pick, R., Mass, E., Ishikawa-Ankerhold, H. C., Margraf, A., Hutter, S. et al. (2018). Yolk sac macrophage progenitors traffic to the embryo during defined stages of development. *Nature Communications* **9**, 75.

Stumvoll, M., Goldstein, B. J. and van Haeften, T. W. (2005). Type 2 diabetes: principles of pathogenesis and therapy. *The Lancet* **365**, 1333-1346.

Su, S., Leng, F., Guan, L., Zhang, L., Ge, J., Wang, C., Chen, S. and Liu, P. (2014). Differential Proteomic Analyses of Cataracts From Rat Models of Type 1 and 2 Diabetes. *Investigative Ophthalmology & Visual Science* **55**, 7848-7861.

Sun, Y. and Smith, L. E. H. (2018). Retinal Vasculature in Development and Diseases. *Annual review of vision science* **4**, 101-122.

Sura, A. A., Chen, L., Messinger, J. D., Swain, T. A., McGwin, G., Jr., Freund, K. B. and Curcio, C. A. (2020). Measuring the Contributions of Basal Laminar Deposit and Bruch's Membrane in Age-Related Macular Degeneration. *Invest Ophthalmol Vis Sci* **61**, 19.

Suwazono, Y., Dochi, M., Oishi, M., Tanaka, K., Kobayashi, E. and Sakata, K. (2009). Shiftwork and impaired glucose metabolism: a 14-year cohort study on 7104 male workers. *Chronobiol Int* **26**, 926-41.

Tackenberg, M. C. and McMahon, D. G. (2018). Photoperiodic Programming of the SCN and Its Role in Photoperiodic Output. *Neural plasticity* **2018**, 8217345-8217345.

Takahashi, J. S. (2016). Transcriptional architecture of the mammalian circadian clock. *Nature Reviews Genetics* **18**, 164.

Tannenbaum, C., Ellis, R. P., Eyssel, F., Zou, J. and Schiebinger, L. (2019). Sex and gender analysis improves science and engineering. *Nature* **575**, 137-146.

Taylor, R. (2013). Type 2 Diabetes. *Etiology and reversibility* **36**, 1047-1055.

Teschendorff, A. E. and Zheng, S. C. (2017). Cell-type deconvolution in epigenome-wide association studies: a review and recommendations. *Epigenomics* **9**, 757-768.

Thigpen, J. E., Setchell, K. D. R., Saunders, H. E., Haseman, J. K., Grant, M. G. and Forsythe, D. B. (2004). Selecting the Appropriate Rodent Diet for Endocrine Disruptor Research and Testing Studies. *ILAR Journal* **45**, 401-416.

Tian, J., Qiu, M., Li, Y., Zhang, X. e., Wang, H., Sun, S., Sharp, N. S., Tong, W., Zeng, H., Zheng, S. et al. (2017). Contribution of birth weight and adult waist circumference to cardiovascular disease risk in a longitudinal study. *Scientific Reports* **7**, 9768.

Tikidji-Hamburyan, A., Reinhard, K., Storchi, R., Dietter, J., Seitter, H., Davis, K. E., Idrees, S., Mutter, M., Walmsley, L., Bedford, R. A. et al. (2017). Rods progressively escape saturation to drive visual responses in daylight conditions. *Nature Communications* **8**, 1813.

Tomita, T. (1950). STUDIES ON THE INTRARETINAL ACTION POTENTIAL PART I. RELATION BETWEEN THE LOCALIZATION OF MICRO-PIPETTE IN THE RETINA AND THE SHAPE OF THE INTRARETINAL ACTION POTENTIAL. *The Japanese Journal of Physiology* **1**, 110-117.

Tong, Y. L. (1976). Parameter estimation in studying circadian rhythms. *Biometrics* **32**, 85-94.

Toomey, C. B., Kelly, U., Saban, D. R. and Rickman, C. B. (2015). Regulation of age-related macular degeneration-like pathology by complement factor H. *Proceedings of the National Academy of Sciences of the United States of America* **112**, E3040-E3049.

Toomey, C. B., Landowski, M., Klingeborn, M., Kelly, U., Deans, J., Dong, H., Harrabi, O., Van Blarcom, T., Yeung, Y. A., Grishanin, R. et al. (2018). Effect of Anti-C5a Therapy in a Murine Model of Early/Intermediate Dry Age-Related Macular Degeneration. *Investigative Ophthalmology & Visual Science* **59**, 662-673.

Tosini, G., Pozdeyev, N., Sakamoto, K. and Iuvone, P. M. (2008). The circadian clock system in the mammalian retina. *BioEssays : news and reviews in molecular, cellular and developmental biology* **30**, 624-633.

Tüchsen, F., Hannerz, H. and Burr, H. (2006). A 12 year prospective study of circulatory disease among Danish shift workers. *Occupational and Environmental Medicine* **63**, 451-455.

Turner, P. V. and Albassam, M. A. (2005). Susceptibility of rats to corneal lesions after injectable anesthesia. *Comp Med* **55**, 175-82.

Tuzcu, M., Orhan, C., Muz, O. E., Sahin, N., Juturu, V. and Sahin, K. (2017). Lutein and zeaxanthin isomers modulates lipid metabolism and the inflammatory state of retina in obesity-induced high-fat diet rodent model. *Bmc Ophthalmology* **17**.

Ueda, H. R. (2007). Systems biology of mammalian circadian clocks. *Cold Spring Harb Symp Quant Biol* **72**, 365-80.

van Alphen, B., Winkelman, B. H. J. and Frens, M. A. (2009). Age- and Sex-Related Differences in Contrast Sensitivity in C57Bl/6 Mice. *Investigative Ophthalmology & Visual Science* **50**, 2451-2458.

Van den Bergh, B. R. H., van den Heuvel, M. I., Lahti, M., Braeken, M., de Rooij, S. R., Entringer, S., Hoyer, D., Roseboom, T., Räikkönen, K., King, S. et al. (2020). Prenatal developmental origins of behavior and mental health: The influence of maternal stress in pregnancy. *Neurosci Biobehav Rev* **117**, 26-64.

van Haren, J., Draegestein, K., Keijzer, N., Abrahams, J. P., Grosveld, F., Peeters, P. J., Moechars, D. and Galjart, N. (2009). Mammalian Navigators are microtubule plus-end tracking proteins that can reorganize the cytoskeleton to induce neurite-like extensions. *Cell Motil Cytoskeleton* **66**, 824-38.

van Leeuwen, E. M., Emri, E., Merle, B. M. J., Colijn, J. M., Kersten, E., Cougnard-Gregoire, A., Dammeier, S., Meester-Smoor, M., Pool, F. M., de Jong, E. K. et al. (2018). A new perspective on lipid research in age-related macular degeneration. *Progress in Retinal and Eye Research* **67**, 56-86.

van Lookeren Campagne, M., LeCouter, J., Yaspan, B. L. and Ye, W. (2014). Mechanisms of age-related macular degeneration and therapeutic opportunities. *J Pathol* **232**, 151-64.

Varcoe, T. J. (2018). Timing is everything: maternal circadian rhythms and the developmental origins of health and disease. *The Journal of Physiology* **596**, 5493-5494.

Varcoe, T. J., Boden, M. J., Voultsios, A., Salkeld, M. D., Rattanatray, L. and Kennaway, D. J. (2013). Characterisation of the Maternal Response to Chronic Phase Shifts during Gestation in the Rat: Implications for Fetal Metabolic Programming. *PLoS One* **8**, e53800.

Varcoe, T. J., Gatford, K. L. and Kennaway, D. J. (2018). Maternal circadian rhythms and the programming of adult health and disease. *Am J Physiol Regul Integr Comp Physiol* **314**, R231-r241.

Varcoe, T. J., Wight, N., Voultsios, A., Salkeld, M. D. and Kennaway, D. J. (2011). Chronic Phase Shifts of the Photoperiod throughout Pregnancy Programs Glucose Intolerance and Insulin Resistance in the Rat. *PLoS One* **6**, e18504.

Voellenkle, C., Garcia-Manteiga, J. M., Pedrotti, S., Perfetti, A., De Toma, I., Da Silva, D., Maimone, B., Greco, S., Fasanaro, P., Creo, P. et al. (2016). Implication of Long noncoding RNAs in the endothelial cell response to hypoxia revealed by RNA-sequencing. *Scientific Reports* **6**, 24141.

Wachtmeister, L. (1998a). Oscillatory potentials in the retina: what do they reveal. *Progress in Retinal and Eye Research* **17**, 485-521.

Wachtmeister, L. (1998b). Oscillatory potentials in the retina: what do they reveal. *Prog Retin Eye Res* **17**, 485-521.

Wachtmeister, L. and Dowling, J. E. (1978). The oscillatory potentials of the mudpuppy retina. *Invest Ophthalmol Vis Sci* **17**, 1176-88.

Waddell, B. J., Wharfe, M. D., Crew, R. C. and Mark, P. J. (2012). A rhythmic placenta? Circadian variation, clock genes and placental function. *Placenta* **33**, 533-9.

Walton, J. C., Weil, Z. M. and Nelson, R. J. (2011). Influence of photoperiod on hormones, behavior, and immune function. *Frontiers in neuroendocrinology* **32**, 303-319.

Wang, T., Tang, Z., Yu, X., Gao, Y., Guan, F., Li, C., Huang, S., Zheng, J. and Zeng, P. (2020). Birth Weight and Stroke in Adult Life: Genetic Correlation and Causal Inference With Genome-Wide Association Data Sets. *Frontiers in Neuroscience* **14**.

Warden, C. H. and Fisler, J. S. (2008). Comparisons of diets used in animal models of high-fat feeding. *Cell metabolism* **7**, 277-277.

Watson, P. E. and McDonald, B. W. (2007). Seasonal variation of nutrient intake in pregnancy: effects on infant measures and possible influence on diseases related to season of birth. *European Journal of Clinical Nutrition* **61**, 1271-1280.

Wehr, T. A. (1997). Melatonin and seasonal rhythms. *J Biol Rhythms* **12**, 518-27.

Welsh, D. K., Takahashi, J. S. and Kay, S. A. (2010). Suprachiasmatic nucleus: cell autonomy and network properties. *Annual review of physiology* **72**, 551-577.

Wild, S., Roglic, G., Green, A., Sicree, R. and King, H. (2004). Global Prevalence of Diabetes. *Estimates for the year 2000 and projections for 2030* **27**, 1047-1053.

Williams, L. M., Campbell, F. M., Drew, J. E., Koch, C., Hoggard, N., Rees, W. D., Kamolrat, T., Thi Ngo, H., Steffensen, I. L., Gray, S. R. et al. (2014). The development of diet-induced obesity and glucose intolerance in C57BL/6 mice on a high-fat diet consists of distinct phases. *PLoS One* **9**, e106159.

Winett, L., Wallack, L., Richardson, D., Boone-Heinonen, J. and Messer, L. (2016). A Framework to Address Challenges in Communicating the Developmental Origins of Health and Disease. *Current environmental health reports* **3**, 169-177.

Woon, P. Y., Kaisaki, P. J., Bragança, J., Bihoreau, M.-T., Levy, J. C., Farrall, M. and Gauguier, D. (2007). Aryl hydrocarbon receptor nuclear translocator-like (BMAL1) is associated with susceptibility to hypertension and type 2 diabetes. *Proceedings of the National Academy of Sciences* **104**, 14412-14417.

Wu, Y., Wu, J., Bu, J., Tang, L., Yang, Y., Ouyang, W., Lin, X., Liu, Z., Huang, C., Quantock, A. J. et al. (2020). High-fat diet induces dry eye-like ocular surface damages in murine. *Ocul Surf* **18**, 267-276.

Wymann, M. P. and Schneiter, R. (2008). Lipid signalling in disease. *Nature Reviews Molecular Cell Biology* **9**, 162-176.

Yang, Y., Smith, D. L., Jr., Keating, K. D., Allison, D. B. and Nagy, T. R. (2014). Variations in body weight, food intake and body composition after long-term high-fat diet feeding in C57BL/6J mice. *Obesity (Silver Spring, Md.)* **22**, 2147-2155.

Yorek, M. S., Obrosov, A., Shevalye, H., Holmes, A., Harper, M. M., Kardon, R. H. and Yorek, M. A. (2015). Effect of diet-induced obesity or type 1 or type 2 diabetes on corneal nerves and peripheral neuropathy in C57Bl/6J mice. *J Peripher Nerv Syst* **20**, 24-31.

Zamiri, P., Masli, S., Streilein, J. W. and Taylor, A. W. (2006). Pigment Epithelial Growth Factor Suppresses Inflammation by Modulating Macrophage Activation. *Investigative Ophthalmology & Visual Science* **47**, 3912-3918.

Zeng, H. Y., Green, W. R. and Tso, M. O. (2008). Microglial activation in human diabetic retinopathy. *Arch Ophthalmol* **126**, 227-32.

Zhang, M., Chu, Y., Mowery, J., Konkel, B., Galli, S., Theos, A. C. and Golestaneh, N. (2018). Pgc-1 alpha repression and high-fat diet induce age-related macular degeneration-like phenotypes in mice. *Disease Models & Mechanisms* **11**.

Zhang, R., Lahens, N. F., Ballance, H. I., Hughes, M. E. and Hogenesch, J. B. (2014). A circadian gene expression atlas in mammals: implications for biology and medicine. *Proc Natl Acad Sci U S A* **111**, 16219-24.

Zhang, Y.-W. and Vande Woude, G. F. (2007). Mig-6, Signal Transduction, Stress Response and Cancer. *Cell Cycle* **6**, 507-513.

Zhang, Y., Castellani, L. W., Sinal, C. J., Gonzalez, F. J. and Edwards, P. A. (2004). Peroxisome proliferator-activated receptor-gamma coactivator 1alpha (PGC-1alpha) regulates triglyceride metabolism by activation of the nuclear receptor FXR. *Genes & development* **18**, 157-169.

Zhao, I., Bogossian, F. and Turner, C. (2012). Does Maintaining or Changing Shift Types Affect BMI? A Longitudinal Study. *Journal of Occupational and Environmental Medicine* **54**, 525-531.

Zhao, L., Zabel, M. K., Wang, X., Ma, W., Shah, P., Fariss, R. N., Qian, H., Parkhurst, C. N., Gan, W. B. and Wong, W. T. (2015). Microglial phagocytosis of living photoreceptors contributes to inherited retinal degeneration. *EMBO Mol Med* **7**, 1179-97.

Zhao, Z. Y., Xu, P., Jie, Z. L., Zuo, Y. Q., Yu, B., Soong, L., Sun, J. R., Chen, Y. and Cai, J. Y. (2014). gamma delta T Cells as a Major Source of IL-17 Production During Age-Dependent RPE Degeneration. *Investigative Ophthalmology & Visual Science* **55**.

Zhu, H. Z., Zhang, W. Z., Zhao, Y. Y., Shu, X. S., Wang, W. C., Wang, D. D., Yang, Y. F., He, Z. J., Wang, X. M. and Ying, Y. (2018). GSK3-mediated tau hyperphosphorylation triggers diabetic retinal neurodegeneration by disrupting synaptic and mitochondrial functions. *Molecular Neurodegeneration* **13**.

Zhu, L., Zou, F., Yang, Y., Xu, P., Saito, K., Othrell Hinton, A., Jr., Yan, X., Ding, H., Wu, Q., Fukuda, M. et al. (2015). Estrogens Prevent Metabolic Dysfunctions Induced by Circadian Disruptions in Female Mice. *Endocrinology* **156**, 2114-2123.